FC

CORNELL AERONAUTICAL LABORATORY, INC.

HELICOPTER HANDLING QUALITIES INVESTIGATION

PHASE II

ANALYSIS OF HELICOPTER STABILIZATION AND CONTROL PROBLEMS

PART C

CHARACTERISTICS AND COMPARISON OF EXISTING HELICOPTER STABILIZING DEVICES

REPORT NO. TB-707-S-2

BUFFALO NEW YORK

CORNELL AERONAUTICAL LABORATORY, INC.
Buffalo 21, New York

REPORT NO. TB-707-S-2

HELICOPTER HANDLING QUALITIES INVESTIGATION

PHASE II

ANALYSIS OF HELICOPTER STABILIZATION AND CONTROL PROBLEMS

Part C

Characteristics and Comparison of Existing Helicopter Stabilizing Devices

BY H. Daughaday
H. Daughaday

F. A. DuWaldt
F. A. DuWaldt

APPROVED H. Daughaday
H. Daughaday, Head
Helicopter Section

A. F. Donovan
A. F. Donovan, Head
Aero-Mechanics Department

DATE June 1955

ABSTRACT

Under Navy Contract NOa(S) 12151, Cornell Aeronautical Laboratory has been conducting a research program aimed at evolving concepts of artificial stabilization and control devices which will improve the flight and handling characteristics of the helicopter. The over-all program was conducted in four phases: (I) consideration of operational problems, (II) analysis of stabilization and control problems, (III) flight test instrumentation and data analysis, and (IV) study of new devices.

This is Part C of a report of three parts (A, B, and C) covering the work accomplished in Phase II. Part C includes a description of various existing stabilizing devices and a physical explanation of how each one affects helicopter flying qualities. Also, an attempt is made to give a unified treatment of these devices by considering them as special cases of a generalized autopilot.

Quantitative data on the influence of the devices considered is obtained by determining how they would modify the handling qualities of a sample helicopter. Response time histories for the sample helicopter with the various devices were obtained on an analogue computer and used in evaluating the devices.

TABLE OF CONTENTS

Page No.

LIST OF FIGURES

LIST OF TABLES

INTRODUCTION

Navy Contract NOa(S) 12151 authorizes studies and tests aimed at evolving means and methods of developing artificial stabilization and control devices which will improve the flight and handling characteristics of the helicopter. This program, which provides for theoretical study, instrumented flight test measurements and design investigations consistent with the program objectives is divided into four phases. Phase I is a general study of the influence of stability characteristics on helicopter operations, Phase II is a detailed analysis of helicopter stabilization and control problems, Phase III is concerned with flight test instrumentation and data analysis for obtaining experimental stability data, and Phase IV is a study of new devices for improving helicopter handling qualities.

The report presenting the results of the Phase II investigation is submitted in three parts. Part A, includes the results of a survey of literature on helicopter stability and presents the equations of motion which are the basis for the analytical and computer studies made during the program. Existing derivations of the equations of motion for the helicopter and various stabilizing devices are reviewed, combined, modified, and extended in Part A in accordance with the project objectives. Part B presents a physical description of handling qualities of the unstabilized helicopter and a comparison with corresponding airplane characteristics. In addition, deficiencies in helicopter stability characteristics are pointed out and desirable handling characteristics formulated which can be used in evaluating the relative advantages of different stabilizing devices. This is Part C, the concluding third of the Phase II report. A physical description and comparison of various existing helicopter stabilizing devices are presented in Part C and their effects on the stability characteristics of a sample helicopter are indicated.

Chapter I discusses the notation and axes systems used in the report and the form of the equations of motion derived in Part A. Equations of motion are tabulated which describe the longitudinal stability of the single rotor helicopter in hovering and in forward flight. The longitudinal hovering equations can also be used in analyzing the initial roll response by replacing the longitudinal parameters and variables by the analogous lateral quantities. Since the initial roll response which can be determined in this manner is the lateral handling quality of most interest, the complete lateral equations of motion are not presented.

Chapter 2 reviews the stability and control characteristics of the unstabilized helicopter which are taken up in greater detail in Part B. The more important stability derivatives are explained and a description of helicopter flying qualities is given including a discussion of static speed and maneuver stability, initial response in hovering flight, initial response in forward flight, and long period response. Section 2.3, the last section of

Chapter 2 summarizes helicopter handling qualities which are believed to be acceptable on the basis of the Part B studies and indicates the deficiencies of the unstabilized helicopter in meeting these requirements.

An attempt is made in Chapter 3 to give a unified treatment of existing stabilizing devices by considering them as special cases of a generalized autopilot for controlling cyclic pitch. The direct cyclic pitch feedbacks which can be introduced by each device are summarized. A method is indicated for determining effective autopilot feedback constants which are convenient in many applications. The effective feedbacks due to changes in forward speed, pitching rate, etc. include the effect of a direct blade flapping feedback. In the last section of Chapter 3 the existing stabilizing devices considered are classified into groups with similar basic characteristics for convenience in discussing them in following chapters.

The influences of existing stabilizing devices are shown in Chapters 4 and 5 by somewhat different approaches. Chapter 4 gives a general evaluation of the effect of different cyclic feedbacks on helicopter handling qualities and the possibility of improving helicopter stability and control characteristics with existing stabilizing devices. Chapter 5 presents a separate discussion of each individual device describing its mechanism, giving a physical description of its action, and indicating how it affects stability and control. Some repetition of data and discussion is included in the treatment of individual devices but is believed desirable for the sake of clarity.

In order to obtain quantitative data as an aid in the evaluation of the devices considered, their effects on the flying qualities of a sample helicopter were determined. The XH03S-2 helicopter was selected for this study and its properties are given in Appendix A. The response characteristics of the helicopter are believed to give the best indication of its handling qualities and a number of response time histories for the sample helicopter are presented which were obtained in analogue computer solutions.

It can be seen from the relations obtained in Part A that allowable values for the generalized autopilot constants used to represent a given device must some times be in definite ratios, or of limited magnitude. These relations have been kept in mind in the discussion of stabilizing devices and in the simulation of different devices in order that a realistic evaluation of their potentialities might be obtained.

4. DISCUSSION OF NOTATION AND EQUATIONS USED IN ANALYSIS

The longitudinal equations of motion summarized in this section form the basis of the analytical and analogue computer studies presented in Sections 4 and 5. As discussed in the introduction of this report, the longitudinal control problem was selected as the case to receive analytical emphasis in determining the characteristics of various stabilizing devices. The detailed derivation of the equations of motion is presented in the Part A volume of this report including both the basic helicopter equations and the equations for several stabilizing devices which are represented mathematically as special cases of a generalized autopilot. Expressions for generalized autopilot constants representing the following devices are given in Part A.

1. Conventional helicopter auto pilot
2. Gyroscopic stabilizer bar (Bell)
3. Double gyroscopic stabilizer bar
4. Control rotor (Hiller)
5. Swash plate spring damper stabilizer
6. Aerodynamic servo control flap (Kaman)
7. Biased cyclic pitch control
8. Doman-Frasier Rotor Head
9. Floating vane stabilizer (Erickson)

In addition, the effects on stability of fixed tail surfaces, offset flapping hinges, and Hohenemser's pitch-cone coupling linkage are taken into account.

The following sections discuss the mathematical representation of the helicopter, the control input systems, and the stabilizing systems as well as the form of the helicopter longitudinal stability and control equations. These equations are summarized for two axis systems, one referenced to horizontal and vertical axes and the other referenced to axes moving with the helicopter.

Figure 1 shows a schematic diagram of a helicopter longitudinal control system of sufficient generality to be applicable to all systems considered, and an analogous diagram might be drawn for the lateral case. The functions of some of the components shown in Fig. 1 are indicated by giving typical transfer functions and the interrelation between different elements in the system can be seen by an examination of the inputs to and outputs from the various boxes.

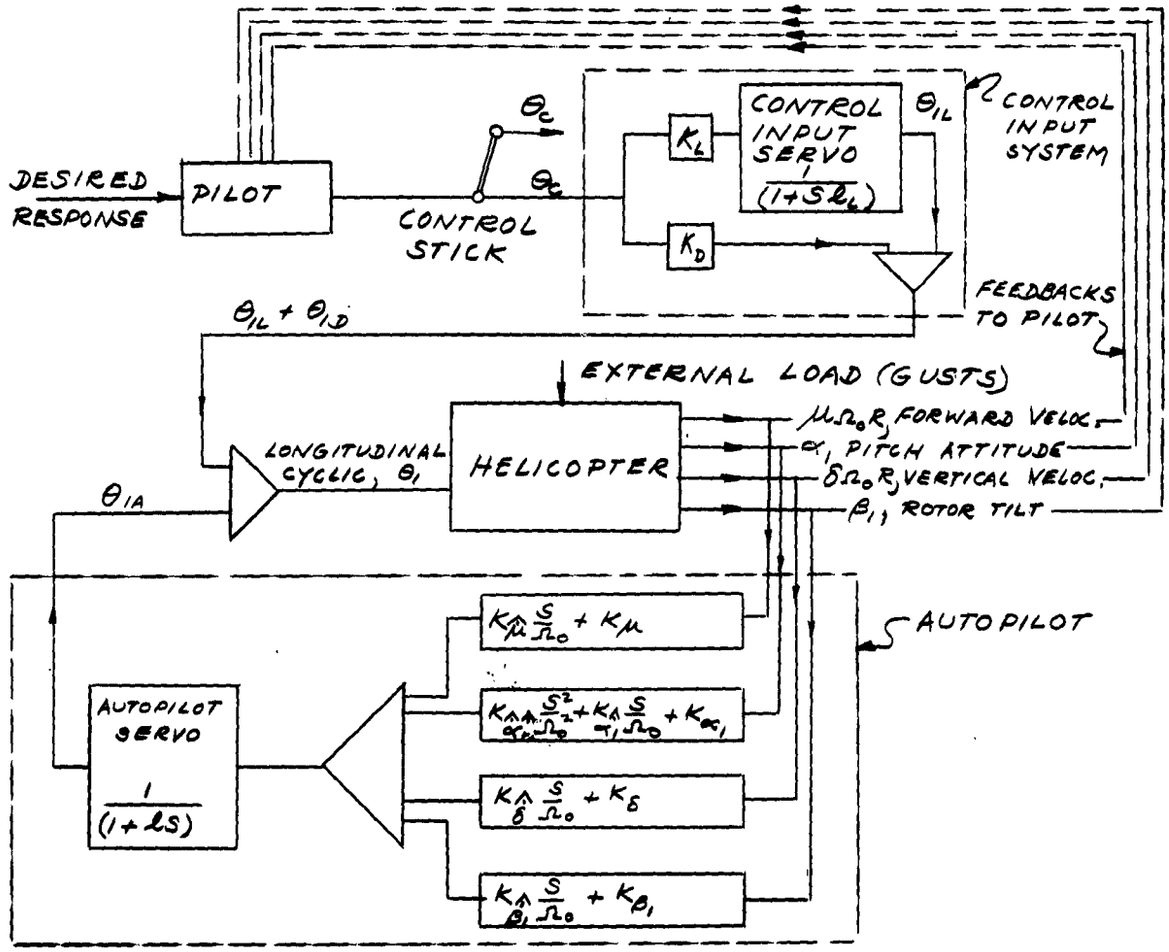

Fig. 1. Schematic Diagram of Pilot Controlling a Helicopter Equipped with a Generalized Auto pilot

1.1 Representation of Helicopter (Horizontal and Vertical Axes)

The box marked "helicopter" represents the inherent characteristics of the helicopter which depend on the initial flight conditions existing at the time a control input is applied, as well as the configuration of the helicopter under consideration. It will be noted that the control input to the helicopter which is indicated is the longitudinal cyclic pitch, θ_1 . While most helicopter stabilizing systems operate by control of the cyclic pitch, the addition of a

fixed tail surface, pitch cone coupling linkage, or flapping hinge offset will also affect stability. A separate box is not shown for these devices, however, and they are considered to change the basic configuration of the helicopter and are thus included in the helicopter transfer function.

In addition, since longitudinal cyclic pitch is the only input indicated, the case shown should be considered as a flight condition in which the pilot does not move the collective pitch stick and the effect of any lateral cyclic movements required to compensate for small couplings between the longitudinal and lateral degrees of freedom is included in the helicopter transfer function. Four output variables are shown coming from the helicopter box; forward velocity ($\mu\Omega_0 R$), vertical velocity ($\delta\Omega_0 R$), fuselage pitch angle (α_1), and longitudinal tilt of the rotor tip path plane (β_1). The normal acceleration and other quantities depending on derivatives of the output variables are also output variables but are not shown explicitly on the diagram. The longitudinal equations of motion of the helicopter provide relationships between the dimensionless variables μ, α_1, δ, β_1 and θ_1 and are derived in Part A in the form shown on Table 1. The control equation discussed in the next section is also included for completeness. In order to utilize these equations in the study of stability and control problems, it is necessary to assign values to the stability derivatives (i.e. $x_\mu, m_\mu, z_\mu, \beta_{1\mu}, x_{\alpha_1}$, etc.). Part A presents analytical methods which can be used to compute these derivatives for any initial forward speed condition, and derivatives computed by this procedure for the sample helicopter studied are given in Appendix A.

Insufficient experimental data are available at present to determine if the expressions given in Part A predict the derivatives with sufficient accuracy and it would be preferable to make use of experimentally determined stability derivatives. In fact, there is still some question concerning the number of degrees of freedom required to obtain a satisfactory representation of the motion of the helicopter. Many analyses of helicopter longitudinal stability have used a quasi-static treatment of blade motion which makes it unnecessary to retain longitudinal blade flapping as a degree of freedom. This procedure simplifies the equations of motion making it easier to obtain analytic solutions but is of doubtful validity for some ranges of parameters.

It was decided to retain the longitudinal flapping degree of freedom in obtaining computer solutions since it did not introduce a large increase in labor and avoided questions concerning the validity of the results. However, a quasi-static treatment of lateral blade flapping was used in the computer solution and is believed to provide sufficient accuracy in the study of longitudinal stability. If additional rotor degrees of freedom had been included, the problem would have become so complicated that it could not have been solved with the available computing equipment.

Part A includes a derivation of the quasi-static equations which are obtained by eliminating longitudinal flapping from the first three equations appearing in Table 1, and they are arranged in the same form as the Table 1 equations with the β_1 terms set equal to zero. Symbols similar to those in Table 1 are used to denote quasi-static derivatives but are distinguished by the addition of primes (e.g. x'_μ, x'_{α_1}).

TABLE 1

SUMMARY OF LONGITUDINAL STABILITY EQUATIONS
REFERRED TO HORIZONTAL AND VERTICAL AXES

$$\left(\frac{s}{\Omega_0}+x_\mu\right)\mu + \left(\quad x_\delta \quad\right)\delta + \left(-\frac{s^2}{\Omega_0^2}\frac{f_1}{R}+\frac{s}{\Omega_0}x_{\alpha_1}+x_{\alpha_1}\right)\alpha_1 + \left(\frac{s}{\Omega_0}x_{\beta_1}+x_{\beta_1}\right)\beta_1 + \left(\quad x_{\theta_1}\right)\theta_1 = (0.46) \quad \text{(A.46)}^*$$

$$\left(\quad z_\mu \quad\right)\mu + \left(\frac{s}{\Omega_0}+z_\delta\right)\delta + \left(\qquad z_{\alpha_1} \qquad\right)\alpha_1 + \left(\frac{s}{\Omega_0}z_{\beta_1}+z_{\beta_1}\right)\beta_1 + \left(\quad z_{\theta_1}\right)\theta_1 = (0.47) \quad \text{(A.47)}$$

$$\left(\quad m_\mu \quad\right)\mu + \left(\quad m_\delta \quad\right)\delta + \left(\frac{s^2}{\Omega_0^2}+\frac{s}{\Omega_0}m_{\dot\alpha_1}+m_{\alpha_1}\right)\alpha_1 + \left(\frac{s}{\Omega_0}m_{\dot\beta_1}+m_{\beta_1}\right)\beta_1 + \left(\quad m_{\theta_1}\right)\theta_1 = (0.48) \quad \text{(A.48)}$$

$$\left(\quad \beta_{1_\mu} \quad\right)\mu + \left(\quad \beta_{1_\delta} \quad\right)\delta + \left(\qquad \beta_{1_{\alpha_1}} \qquad\right)\alpha_1 + \left(\frac{s}{\Omega_0}\beta_{1_{\dot\beta_1}}-1\right)\beta_1 + \left(\quad \beta_{1_{\theta_1}}\right)\theta_1 = (0.49) \quad \text{(A.49)}$$

$$\left(\quad K_\mu \quad\right)\mu + \left(\quad K_\delta \quad\right)\delta + \left(\quad \frac{s}{\Omega_0}K_{\dot\alpha_1} + K_{\alpha_1}\right)\alpha_1 + \left(\frac{s}{\Omega_0}K_{\dot\beta_1}+K_{\beta_1}\right)\beta_1 + (\ell s-1)\theta_1 =$$

$$-\left[K_L\theta_c + K_b(\ell s\theta_c + \theta_c)\right] \quad \text{(B.6)}$$

(A.46) and (A.47) give equilibrium of horizontal and vertical forces.
(A.48) gives the equilibrium of moments about the c.g.
(A.49) gives longitudinal rotor tilt relative to a horizontal plane and
(B.6) is the control equation discussed in Section 1.2

μ = forward advance ratio of hub, δ = vertical advance ratio, α_1 = forward tilt of shaft, β_1 = forward tilt of tip path plane relative to horizontal, θ_1 = aft tilt of control plane θ_c = control input.

Number of Roots

	Unstabilized Helicopter or Stabilized Helicopter $\ell = 0$	Stabilized Helicopter Auto-pilot With Time Lag (ℓ)
Hovering (Vertical motion omitted)		
- For equations listed above	4	5
- Quasi-static equations	3	4
Forward Flight		
- For equations listed above	5	6
- Quasi-static equations	4	5

* The equation numbers refer to those used in the Part A derivation.

The number of roots obtained from the equations of motion for various conditions are listed in Table 1. The unstabilized hovering helicopter has four roots when the uncoupled vertical degree of freedom is omitted. Two of these roots correspond to the long period mode of oscillation; the other two roots correspond to either motions which are primarily subsidences of the pitching and longitudinal rotor plane tilt degrees of freedom or to a highly damped short period mode. In forward flight the vertical degree of freedom must be included in studying dynamic longitudinal stability of the helicopter. This adds a root which corresponds to a subsidence of vertical motion at low advance ratios, and at high forward speeds the vertical and pitching motions couple together to give an oscillatory short period mode.

The same number of roots is obtained for the case of the autopilot with zero time lag as for the unstabilized helicopter since it does not effectively add a degree of freedom. It is possible to arrange the equations of motion of a helicopter stabilized by a zero time lag autopilot in the same form as the equations of the unstabilized helicopter. This "equivalent helicopter" approach is discussed in Section 1.4.

One root is added to each of the cases listed in Table 1 when there is a finite autopilot time lag. Under many considerations the added root corresponds to a mode primarily involving a subsidence of control plane motion with the associated tip path plane tilt. However, in some ranges of parameters the longitudinal control plane tilt root couples with fuselage pitching or tip path plane roots to give an oscillatory mode.

1.2 Representation of Autopilot and Control Input Systems (Horizontal and Vertical Axes)

The longitudinal cyclic input (θ_1) shown on Fig. 1 is the sum of three components, one determined by the autopilot feedbacks and the other two by the fore and aft motion of the pilot's cyclic control stick. Equation B.1 of Part A expresses this relation as follows:

$$\theta_1 = \theta_{1A} + \theta_{1L} + \theta_{1D}$$

The component $\theta_{1D} = K_D \theta_c$ is the input produced by stick motion due to a direct mechanical linkage from the pilot through the swash plate to the blade horn. However, lags can occur in systems using mechanical or aerodynamic servos to change blade pitch (e.g. the control rotor stabilizer) and for such systems movement of the effective control plane is not exactly proportional to stick motion at all times. The component of the pilot's input which is affected by servo lags is denoted by θ_{1L} and is approximated by a simple time lag system in Eq. B.5:

$$\ell \dot{\theta}_{1L} + \theta_{1L} = K_L \theta_c$$

In most practical cases the pilot's control is applied directly or through a servo, but not in combination, so that either K_D or K_L will be equal to zero.

The generalized autopilot is defined as that part of the system which modifies the cyclic pitch in accordance with changes in the helicopter outputs (e.g. μ, α_1, δ, β_1 and their derivatives), and is represented by Eq. B.4 which is rewritten below:

$$\ell\dot{\theta}_{1A} + \theta_{1A} = \frac{K_{\hat{\mu}}}{\Omega_0}\dot{\mu} + K_\mu \mu + \frac{K_{\hat{\alpha}_1}}{\Omega_0^2}\ddot{\alpha}_1 + \frac{K_{\dot{\alpha}_1}}{\Omega_0}\dot{\alpha}_1 + K_{\alpha_1}\alpha_1 + \frac{K_{\hat{\delta}}}{\Omega_0}\dot{\delta} + K_\delta \delta + \frac{K_{\hat{\beta}_1}}{\Omega_0}\dot{\beta}_1 + K_{\beta_1}\beta$$

For convenience the diagram (Fig. 1) indicates that derivative feedbacks are obtained by networks which modify measured values of μ, α_1, δ and β_1. However, derivative feedbacks are generated directly in most actual stabilizing devices. All the feedback constants (K's) in the above equation are defined in such a manner that they are dimensionless and appropriate Ω_0's are introduced to make the equation dimensionless. It will be noted that all autopilot lags shown on Fig. 1 are assumed concentrated in the autopilot pitch change servo and are approximated by a simple time lag. It is believed that a satisfactory representation of the stabilizing devices considered can be obtained using this assumption. Furthermore, all the devices considered which have time lags in the pilot's input system have generalized autopilot time lags of the same magnitude. Equation B.6 which is rewritten below, gives the combined control equation for the case of equal time lags and includes the inputs of the generalized autopilot and both types of pilot inputs (θ_{1L}, θ_{1D}).

$$\ell\dot{\theta}_1 + \theta_1 = \frac{K_{\hat{\mu}}}{\Omega_0}\dot{\mu} + K_\mu \mu + \frac{K_{\hat{\alpha}_1}}{\Omega_0^2}\ddot{\alpha}_1 + \frac{K_{\dot{\alpha}_1}}{\Omega_0}\dot{\alpha}_1 + K_{\alpha_1}\alpha_1 + \frac{K_{\hat{\delta}}}{\Omega_0}\dot{\delta} + K_\delta \delta + \frac{K_{\hat{\beta}}}{\Omega_0}\dot{\beta}_1 + K_{\beta_1}\beta_1 + [K_L\theta_c + K_D(\ell\dot{\theta}_c + \theta_c)]$$

The usual pilot input system associated with a conventional autopilot is shown in Fig. 1. With this system a change in stick position tends to cause a proportional change in swash plate tilt. Other systems might be preferable for some applications. For example, the rate of change of swash plate tilt might be made proportional to stick position. Special input systems of this type have not been analyzed in Part A but the equations presented are easily modified to handle them.

Finally, it should be pointed out that the pilot must be considered in the over-all control problem and a pilot feedback loop has been shown on the diagram. The pilot senses normal acceleration, helicopter attitude, pitching velocity, etc. and moves the stick in accordance with these feedbacks as well as the desired response. The part played by the pilot is taken up in Part B and kept in mind in evaluating the stabilizing devices.

1.3 Equations Referred to Moving Axes

The equations of motion are first derived in Part A referring the motion of the helicopter and longitudinal tilt of the tip path plane to horizontal and vertical axes and this form was used in simulating the complete longitudinal control problem on an analogue computer. In some applications, it is found more convenient to refer the tip path plane tilt to the shaft or swash plate and appropriate transformations of the equations are easily made. Although the choice of a horizontal and vertical axis system is attractive in the derivation and for analyzing the hovering case, axes moving with the helicopter are preferable in considering some forward flight conditions.

The discussion of stability characteristics given in this volume of the Phase II report is primarily in terms of the moving axis equations. Recorder records of computer solutions which were based on the Table 1 equations are also labeled in terms of the moving axes variables making it possible to discuss the responses shown using either set of notation.

Figure 2 indicates the application of a moving axes system frequently used for fixed wing analysis to the case of helicopter stability. The $\bar{x}$ axis is approximately along the longitudinal axis of the helicopter and is initially aligned with the directional of flight. The $\bar{z}$ axis is perpendicular to the $\bar{x}$ axis and is taken positive downward.

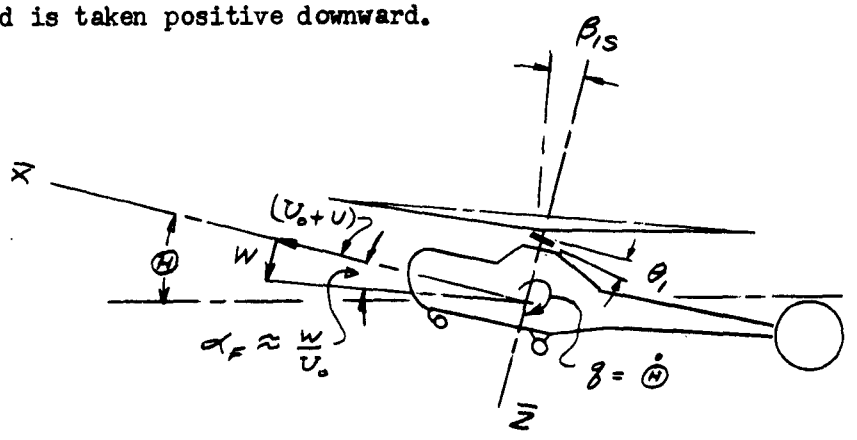

Fig. 2. Notation Used with Moving Axes System

Changes in velocity from the initial equilibrium condition are resolved into a forward component, u, along the $\bar{x}$ axis and a normal component, w, along the $\bar{z}$ axis. The dimensional form of the equations of motion that are obtained using the axis system shown on Fig. 2 is given in Table 2. Conversion formulas are derived in Part A for computing the derivatives and feedback constants referred to moving axes from those referred to horizontal and vertical axes.

TABLE 2

SUMMARY OF LONGITUDINAL STABILITY EQUATIONS
REFERRED TO MOVING AXES

$$m\dot{u} = \bar{X}_u u + \bar{X}_w w + \bar{X}_q q - mg\Theta + \bar{X}_{\dot{\beta}_{1s}}\dot{\beta}_{1s} + \bar{X}_{\beta_{1s}}\beta_{1s} + \bar{X}_{\theta_1}\theta_1 \quad (A.78)$$

$$m(\dot{w} - U_0 q) = \bar{Z}_u u + \bar{Z}_w w + \bar{Z}_q q + \bar{Z}_{\dot{\beta}_{1s}}\dot{\beta}_{1s} + \bar{Z}_{\beta_{1s}}\beta_{1s} + \bar{Z}_{\theta_1}\theta_1 \quad (A.79)$$

$$I\dot{q} = \bar{M}_u u + \bar{M}_w w + \bar{M}_q q + \bar{M}_{\dot{\beta}_{1s}}\dot{\beta}_{1s} + \bar{M}_{\beta_{1s}}\beta_{1s} + \bar{M}_{\theta_1}\theta_1 \quad (A.80)$$

$$\beta_{1s} = (\beta_{1s})_u u + (\beta_{1s})_w w + (\beta_{1s})_q q + (\beta_{1s})_{\dot{\beta}_{1s}}\dot{\beta}_{1s} + (\beta_{1s})_{\theta_1}\theta_1 \quad (A.81)$$

$$\lambda\dot{\theta}_1 + \theta_1 = K_u u + K_w w + K_q q + K_\Theta \Theta + K_{\dot{\beta}_{1s}}\dot{\beta}_{1s} + K_{\beta_{1s}}\beta_{1s} + [K_C\theta_C + K_D(\lambda\dot{\theta}_C + \theta_C)] \quad (B.67)$$

(A.78) and (A.79) give equilibrium of forces in $\bar{x}$ and $\bar{z}$ directions. (A.80) gives the equilibrium of moments about the c.g. (A.81) gives the longitudinal flapping relative to the shaft, and (B.67) the longitudinal cyclic pitch control equation.

u and w are increments in velocity in $\bar{x}$ and $\bar{z}$ directions. q = pitching velocity, Θ = pitch attitude, β_{1s} = forward tilt of tip path plane relative to shaft, θ_1 = aft tilt of control plane.

Effective Derivative Form of (A.78), (A.79), (A.80) and (B.67):

$$m\dot{u} = \bar{X}'_u u + \bar{X}'_w w + \bar{X}'_q q - mg\Theta + \bar{X}'_{\dot{\beta}_{1s}}\dot{\beta}_{1s} + \bar{X}'_{\theta_1}\theta_1$$

$$m(\dot{w} - U_0 q) = \bar{Z}'_u u + \bar{Z}'_w w + \bar{Z}'_q q + \bar{Z}'_{\dot{\beta}_{1s}}\dot{\beta}_{1s} + \bar{Z}'_{\theta_1}\theta_1$$

$$I\dot{q} = \bar{M}'_u u + \bar{M}'_w w + \bar{M}'_q q + \bar{M}'_{\dot{\beta}_{1s}}\dot{\beta}_{1s} + \bar{M}'_{\theta_1}\theta_1$$

$$\frac{\lambda\dot{\theta}_1}{1 - K_{\beta_{1s}}(\beta_{1s})_{\theta_1}} + \theta_1 = K'_u u + K'_w w + K'_q q + K'_\Theta \Theta + K'_{\dot{\beta}_{1s}}\dot{\beta}_{1s} + \frac{[K_C\theta_C + K_D(\lambda\dot{\theta}_C + \theta_C)]}{1 - K_{\beta_{1s}}(\beta_{1s})_{\theta_1}}$$

* The equation numbers refer to those used in the Part A derivation.

Two forms of the stability equations are shown on Table 2 which differ in the treatment of longitudinal flapping. The derivatives in the upper set give the increments in forces and pitching moments due to changes in u, w, etc., without considering that changes in these variables also produce changes in blade flapping which in turn produces even larger force and moment increments. The lower set of equations makes use of effective coefficients obtained by using (A.81) to eliminate blade flapping from the other equations.

Quasi-static equations which do not involve longitudinal flapping or flapping rate readily follow from the effective derivative form by making appropriate assumptions regarding $\dot{\beta}_{1S}$. For example, in Part A quasi-static equations are obtained by assuming the longitudinal tilting rate of the rotor equal to the longitudinal tilting velocity of swash plate due to autopilot feedbacks (i.e., $\dot{\beta}_{1S} = -\dot{\theta}_{1A}$).

1.4 Equivalent Helicopter Equations

In studying how a given stabilizing device affects stability and control, equivalent helicopter equations are sometimes useful which do not explicitly contain either blade flapping or longitudinal cyclic pitch due to the device as variables. Equivalent helicopter equations referred to axes moving with the helicopter were derived in Part A by eliminating autopilot cyclic pitch (θ_{1A}) from the quasi-static equations of motion and then defining new stability equations which include the effect of the autopilot feedbacks. The resulting equations were as follows:

TABLE 3

EQUIVALENT HELICOPTER EQUATIONS

$$m\dot{u} = \overline{\overline{X}}_u u + \overline{\overline{X}}_w w + \overline{\overline{X}}_q q + [\overline{\overline{X}}_\Theta - W]\Theta + \overline{\overline{X}}_{\theta_1}(K_c \theta_c) \quad \text{(B.71)}$$

$$m(\dot{w} - U_0 q) = \overline{\overline{Z}}_u u + \overline{\overline{Z}}_w w + \overline{\overline{Z}}_q q + \overline{\overline{Z}}_\Theta \Theta + \overline{\overline{Z}}_{\theta_1}(K_c \theta_c) \quad \text{(B.72)}$$

$$\overline{\overline{I}}\,\dot{q} = \overline{\overline{M}}_u u + \overline{\overline{M}}_w w + \overline{\overline{M}}_q q + \overline{\overline{M}}_\Theta \Theta + \overline{\overline{M}}_{\theta_1}(K_c \theta_c) \quad \text{(B.73)}$$

The equivalent helicopter derivatives are indicated by double bars and expressions for them in terms of the feedback constants are given in Appendix A.

In general, it would not be expected that the results obtained with the equivalent helicopter equations would be as accurate as with the more complete equations given in earlier sections of the report. The chief purpose for deriving expressions for equivalent helicopter stability derivatives is to obtain a relatively simple indication of the effect of various stabilizing devices, and several assumptions are made which appreciably simplified the equations at some sacrifice in accuracy. The principal assumption made was that the effective autopilot time lag is zero.

The equivalent helicopter derivatives reduce to the quasi-static derivatives of the unstabilized helicopter when the autopilot feedbacks are zero. For this reason the double bar notation can be used in discussing stability derivatives of the unstabilized helicopter in the following section.

2. SUMMARY OF STABILITY AND CONTROL CHARACTERISTICS OF THE UNSTABILIZED HELICOPTER

This section presents a summary of the stability characteristics of the unstabilized helicopter which are discussed in more detail in Part B. Also the desired flying qualities discussed in Part B are indicated to serve as a basis for evaluating the various stabilizing devices studied.

2.1 Explanation of the More Important Stability and Control Derivatives of the Helicopter

The control and stability characteristics of the helicopter are determined to a large extent in both hovering and forward flight by the following derivatives:

Control power ($\overline{\overline{M}}_{\theta_1}$) = control moment about c.g. per radian swash plate tilt.

Speed stability derivative ($\overline{\overline{M}}_{u}$) = rate of change of moment about c.g. with forward velocity.

Damping in pitch ($\overline{\overline{M}}_{q}$) = rate of change of moment about c.g. with pitching velocity.

In addition, the following derivatives are of considerable importance in forward flight:

Vertical control force ($\overline{\overline{Z}}_{\theta_1}$) = vertical force due to one radian swash plate tilt.

Vertical damping ($\overline{\overline{Z}}_{w}$) = rate of change of vertical force with normal velocity.

Normal velocity stability ($\overline{\overline{M}}_{w}$) = rate of change of moment about c.g. with normal velocity.

Although the magnitudes of the first set of derivatives indicated above change with initial forward speed, their essential characteristics can be seen from the hovering case.

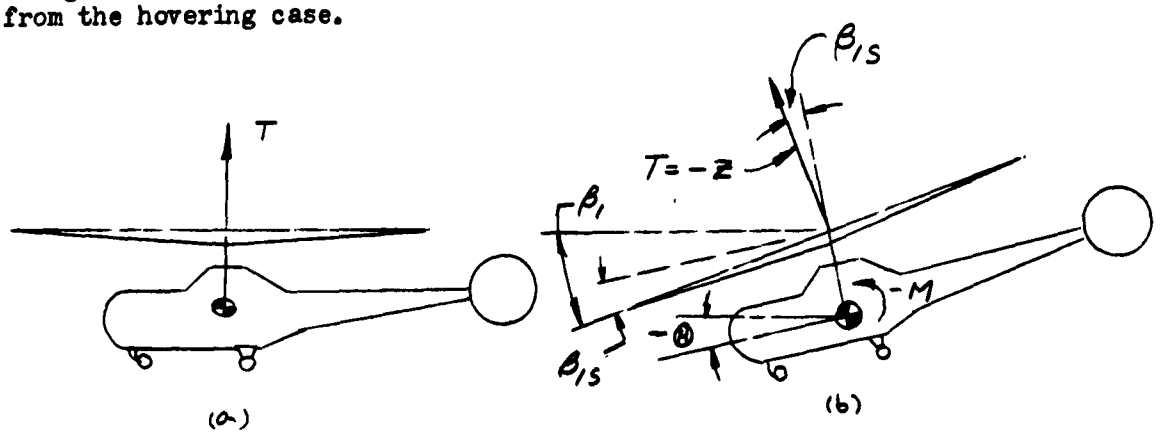

Fig. 3. Approximate Treatment of Rotor Forces

Figure 3 indicates an approximate treatment of rotor forces which has been frequently used in helicopter literature. In diagram (a) the helicopter is shown hovering in an equilibrium position with the rotor thrust exactly balanced by the helicopter's weight. Diagram (b) shows the helicopter slightly disturbed from the hovering condition. The fuselage is pitched through an angle $-\Theta$, the tip path plane is tilted through an angle β_1, and the thrust vector (assumed perpendicular to the tip path plane for this part of the discussion) tends to produce a horizontal acceleration of the helicopter.

Both articulated and seesaw type rotors exert moments about the c.g. of the helicopter when the tip path plane and rotor thrust tilt relative to the rotor shaft. The tilt, β_{1s}, shown in Fig. 3 would produce a negative pitching moment, $-M$, or one tending to make the helicopter pitch forward. An additional pitching moment is obtained with an articulated rotor design incorporating offset flapping hinges. In this case the blade centrifugal forces in combination with hinge offset introduce a couple as discussed in Part A.

It is apparent that the position of the tip path plane must be known to find the horizontal force component and the pitching moment produced by the rotor. Thus the primary factors determining tip path plane tilt must be taken up in discussing rotor stability and control derivatives, and have been indicated on Fig. 4 for small perturbations from hovering.

At zero airspeed the equilibrium position of the rotor is parallel to the control plane which is assumed parallel to the swash plate for purposes of the present discussion. It can be readily observed in a ground run up that when the pilot moves the swash plate to a new position the tip path plane moves to a parallel position, Fig. 4(a). When the swash plane is inclined relative to the mast by an angle Θ_1, a control moment ($\bar{M}_{\Theta_1}\Theta_1$) results due to the combined effect of the tilt of the thrust vector and the offset hinge moment. It is apparent from the diagram that the control moment derivative $\bar{M}_{\Theta_1}$ is positive.

A more difficult experiment to perform with a full-scale ship, although easily demonstrated with a model, is to keep the swash plate fixed relative to the shaft but tilt the swash plate relative to fixed axes by inclining the shaft (Fig. 4b). Again the tip path plane is found to assume a position parallel to the swash plate which requires it to remain perpendicular to the shaft. The change in attitude does not produce a moment about the c.g. because the thrust vector does not tilt relative to the shaft. It can be seen that the hovering helicopter has neutral attitude stability ($\bar{M}_\Theta = 0$). The rotor characteristics shown in diagrams (a) and (b) are, of course, due to the aerodynamic flapping moments which act on the blade when the blade is feathering relative to the tip path plane. The kinematics of the control mechanism are such that when the rotor plane is parallel to the control plane there is no feathering relative to the tip path plane, and no tendency for the rotor plane to move to a new position at zero forward speed.

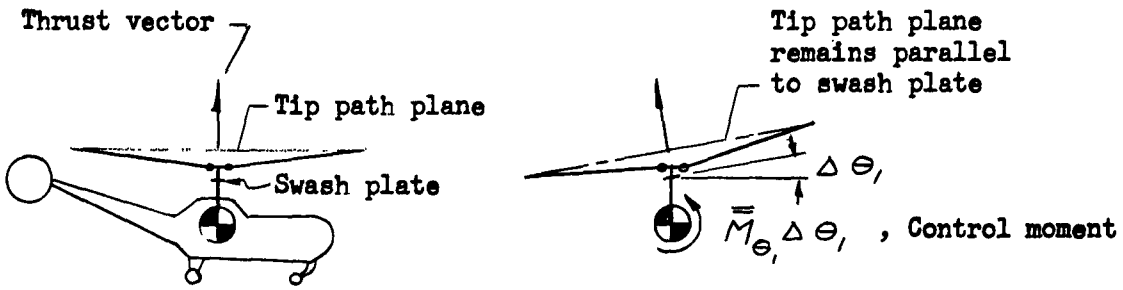

a) Control Moment due to Swash Plate Tilt

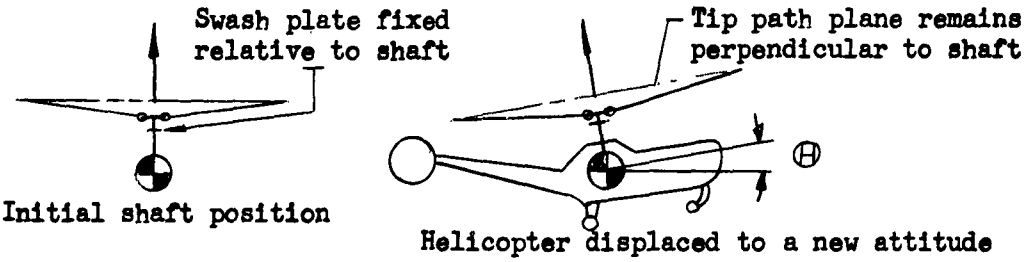

b) Diagram Showing Hovering Helicopter's Neutral Attitude Stability

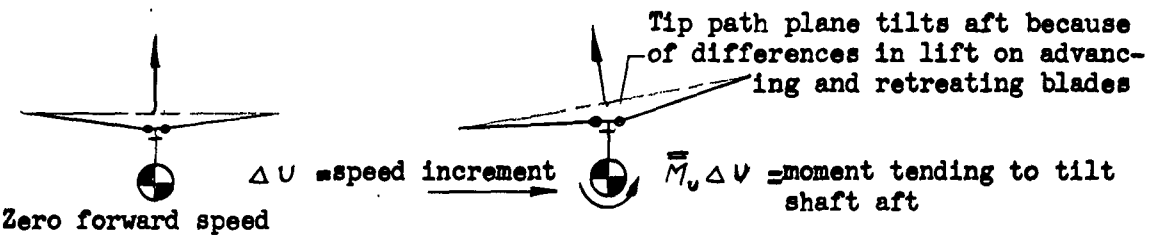

c) Diagram Explaining Positive Speed Stability Derivative of Helicopter

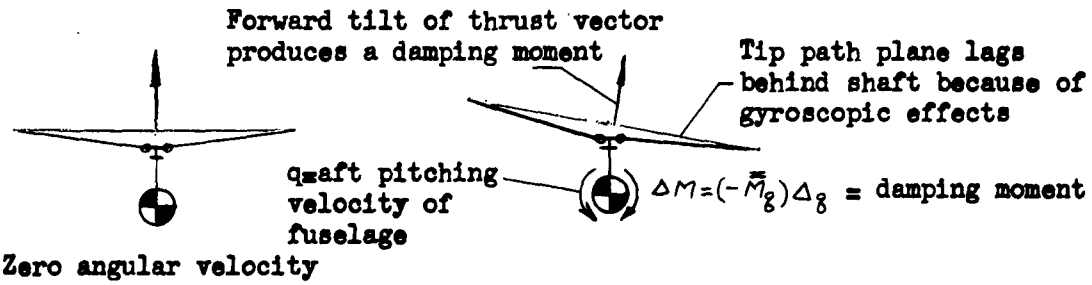

d) Diagram Indicating Damping in Pitch Due to Gyroscopic Effects

Fig. 4. Explanation of Hovering Flight Stability Derivatives in Terms of Rotor Characteristics

Other factors influencing the position of the tip path plane are the aerodynamic forces produced by a change in forward velocity, and the gyroscopic forces resulting from a pitching or rolling velocity of the tip path plane. The increase in lift on the advancing blade and the decrease in lift on the retreating blade cause the tip path plane and thrust vector to tilt aft relative to the swash plate in forward flight (Fig. 4(c)). Although the maximum increment in lift occurs when the blade is in the cross wind position, an aft tilt rather than a side tilt results because of the characteristic 90 degree lag in blade response. It can be seen that the helicopter rotor is inherently stable with respect to speed changes producing an aft force and pitching moment when the speed is increased (i.e., the rotor makes a positive contribution to the speed derivative $\bar{M}_u$).

Figure 4(d) illustrates how the moment due to the inclination of the thrust vector and the offset hinge moment provide the helicopter with inherent damping in pitch and roll. These moments exist because the tip path plane lags behind the shaft when the helicopter has a constant pitching or rolling velocity. The lag is primarily due to the gyroscopic blade moments discussed in Part B. A pitching or rolling velocity about the c.g. of the helicopter produces a linear velocity at the hub resulting in an additional tip path plane inclination of the type indicated on Fig. 4(c) which increases the damping in pitch. Positive damping is obtained when $\bar{M}_q$ is negative with the sign convention used.

In the preceding discussion helicopter stability characteristics have been explained assuming that the thrust vector acts perpendicular to the tip path plane. The convenience of this assumption is obvious and justifies its use in a qualitative discussion of helicopter stability. However, it has been found using more exact methods of analysis that in some cases gross errors result if the force acting in the plane of the rotor is neglected. Perhaps the most important correction which must be made to the simple theory, which assumes the resultant rotor force perpendicular to the tip path plane, is the effect of the induced drag on the rotor damping in pitch and roll. This effect is included in the equations of motion and is discussed in Part B.

Figure 4 has indicated the source of the stability derivatives which are most important in hovering flight. In forward flight the force and moment derivatives associated with changes in normal velocity (w) or fuselage angle of attack ($\alpha_f = w/v_o$) are also found to have an important effect on helicopter longitudinal stability. Figure 5 indicates the nature of these normal velocity derivatives and compares them with the control force and moment derivatives obtained in forward flight.

Diagram (a) of Fig. 5 shows a case in which the helicopter is moved with a constant horizontal velocity v_o. The initial swash plate tilt is assumed zero but the rotor plane has an aft tilt relative to the swash plate due to the velocity v_o. In diagram (b) at the right of the figure, the swash plate is tilted aft relative to the shaft by an angle $\Delta\theta_1$. Thus the swash plate is given an angle of attack and the average angle of attack of the rotor blades is increased. A thrust increment, ($\Delta T = -\Delta Z = -Z_{\theta_1} \Delta\theta_1$), is indicated which

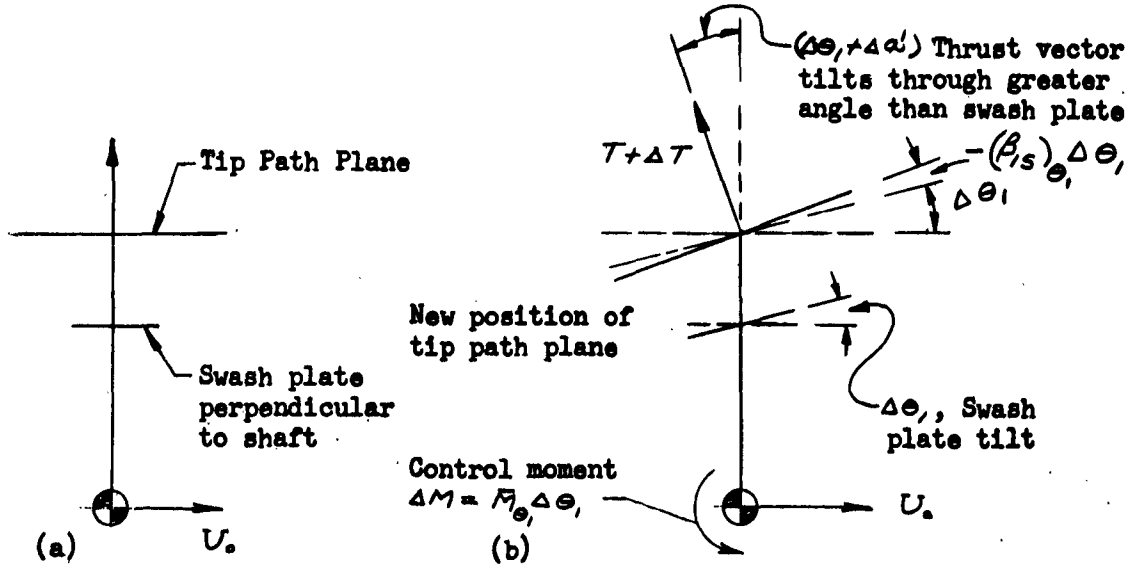

Control Force and Control Moment Derivatives

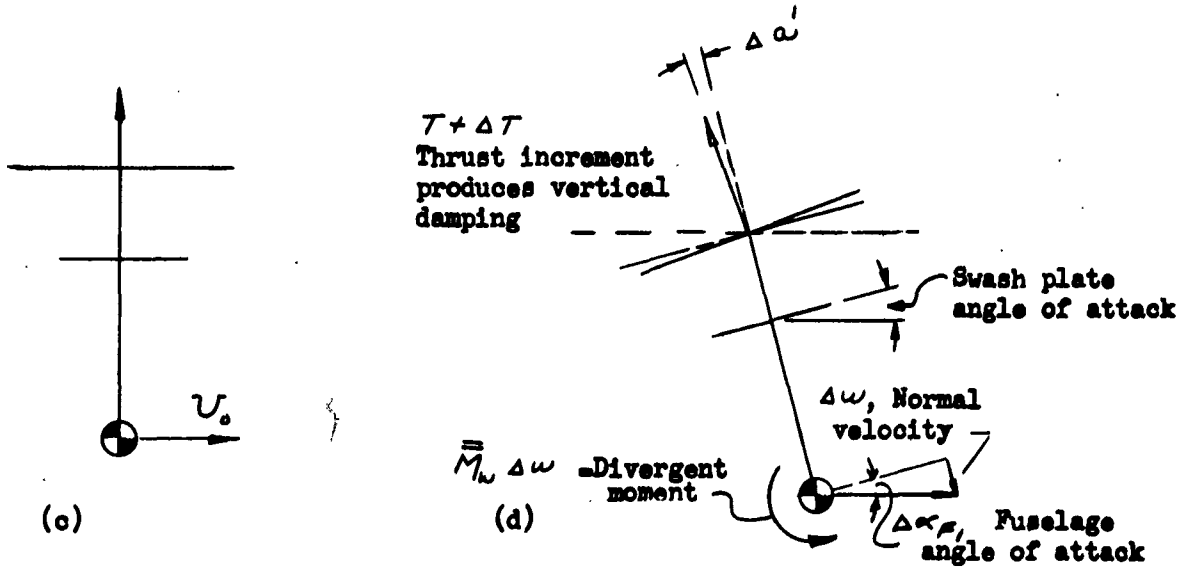

Diagrams indicating vertical damping and angle of attack instability

Fig. 5. Explanation of Some Important Derivatives in Forward Flight

results from the higher angles of attack. Also the aft flapping of the rotor relative to the swash plate is larger by an increment, $-(\beta_{1s})_{\theta_1} \Delta\theta_1$, shown on the diagram. It will be noted that the aft tilt of the thrust vector exceeds the aft tilt of the swash plate by the increment $\Delta\alpha'$ which is largely due to the greater tip path plane tilt. The control moment increment $\bar{M}_{\theta_1} \Delta\theta_1$ is readily seen to be greater in forward flight than in hovering since the swash plate tilt results in a thrust increment as well as a greater tilt of the tip path plane and thrust vector.

Diagrams (c) and (d) indicate the nature of the derivatives associated with changes in normal velocity and fuselage angle of attack. In the case shown increments in the normal velocity and fuselage angle of attack are produced by changing the attitude of the helicopter assuming the direction of motion unchanged. A similar change in normal velocity component could be obtained with the fuselage attitude unchanged if the c.g. were given a downward translation.

In order to indicate the relationships between the forces and moments due to a fuselage angle of attack change ($\Delta\alpha_F$) and a swash plate tilt relative to the shaft ($\Delta\theta_1$), diagrams (c) and (d) are drawn making $\Delta\alpha_F$, and $\Delta\theta_1$ equal in magnitude. The positions of the thrust vector and tip path plane are identical in the two diagrams since the swash plate angles of attack are the same in the two cases. It can be seen that the thrust vector increment ($\Delta T = -\Delta Z = -\bar{Z}_w \Delta w$) opposes the normal velocity change and thus provides vertical damping. However, the $\bar{Z}_w$ derivative is negative because the $\bar{Z}$ axis is defined positive downward. A smaller aft pitching moment is obtained in diagram (d) than in diagram (b) due to the change in attitude of the fuselage. In hovering no pitching moment results for a similar change in attitude, the tip path plane remaining parallel to the swash plate and perpendicular to the shaft. However, the larger tilt of the tip path plane and thrust vector obtained in forward flight gives rise to a divergent moment, $\bar{M}_w \Delta w$. A positive $\bar{M}_w$ derivative represents an unstable variation in pitching moment with normal velocity with the notation used.

2.2 Discussion of Helicopter Flying Qualities

The handling qualities of the helicopter can be conveniently expressed in terms of speed stability, maneuver stability, initial response, and long period response characteristics.

(a) Stick Position Speed Stability

Both speed stability and maneuver stability can be defined in terms of stick position (stick fixed stability) or stick forces (stick free stability). Since irreversible boost systems are now in common usage in helicopters, the stick force characteristics can be adjusted by installation of springs and weights on the stick and will not be considered in the following discussion. Speed stability (stick fixed) refers to the relationship between a change in the cyclic stick position from trim and the final speed increment achieved

as a result of the deflection. It is desirable that a forward stick increment ($-\Delta\theta_c$) result in a final unaccelerated flight condition at a speed greater than the initial trim speed. The requirement that there be positive speed stability can be written as follows by solving the equations* on p. 9 after setting all time derivatives equal to zero:

$$-\frac{\Delta U}{\Delta \theta_c}\Big|_{\dot{U}=\dot{w}=q=0} = \text{Stick position speed stability}$$

$$= K_c \frac{\bar{M}_{\theta_1}\bar{Z}_w - \bar{Z}_{\theta_1}\bar{M}_w}{\bar{M}_u\bar{Z}_w - \bar{Z}_u\bar{M}_w} \approx K_c \frac{\bar{M}_{\theta_1}}{\bar{M}_u} > 0$$

The use of the approximate form given above can be justified in the case of the sample helicopter by referring to the tabulated derivatives in Appendix A. Since the linkage ratio, K_c , and the control moment derivative, $\bar{M}_\theta$, are positive, it is seen that (positive) speed stability exists if the moment speed derivative, $\bar{M}_u$, is positive. The stick position variation with speed is generally found to be stable because of the aft tilting of the rotor with increasing speed making M_u positive as discussed previously. If the fuselage is sufficiently unstable to overcome the positive contribution of the rotor to the speed stability derivative, some device such as a tail can be used to correct the difficulty.

(b) Stick Position Maneuver Stability

The term "maneuver stability" has been used with various connotations in discussing helicopter stability. For example, Ref. 1 uses this term in describing the shape of the normal acceleration response obtained in a pull-up maneuver. In the present study the shape characteristics are taken up in the discussion of the initial response in forward flight. The term maneuver stability has also been applied to the variation in stick position in changing the curvature of the flight path (or normal acceleration) and this definition will be used here. In particular, to tighten a steady turn should require aft stick displacement ($+\Delta\theta_c$). The following expression is obtained for the normal acceleration increment (Δn) produced by an aft stick motion ($\Delta\theta_c$) using the equations on p. 9 .

$$\frac{\Delta n}{\Delta \theta_c}\Big|_{U_o=\text{CONST}} = \text{Stick position maneuver stability}$$

$$= K_c U_o \frac{\Delta q}{\Delta \theta_c} = K_c U_o \frac{\bar{Z}_{\theta_1}\bar{M}_w - \bar{M}_{\theta_1}\bar{Z}_w}{\bar{Z}_w\bar{M}_q - \bar{M}_w(\bar{Z}_q + m U_o)}$$

$$\approx K_c U_o \frac{(-\bar{M}_{\theta_1}\bar{Z}_w)}{\bar{Z}_w\bar{M}_q - \bar{M}_w m U_o} \quad \text{(positive for stability)}$$

*$\bar{M}_\theta$, $\bar{Z}_\theta$, $\bar{X}_\theta$ have been neglected since the basic helicopter has no attitude stability. The special cases of the conventional autopilot and double bar which introduce attitude stability are considered in a subsequent section.

The above expression was obtained assuming the forward velocity remains constant and $\Delta\eta$ is the acceleration increment existing after short period oscillations have damped out. Again the approximate form which is shown can be justified by referring to the derivatives in Appendix A.

Since the vertical damping derivative ($\bar{\bar{Z}}_w$) is negative, the control moment derivative ($\bar{M}_\theta$) positive, and the damping in pitch derivative ($\bar{\bar{M}}_q$) negative, the numerator ($-\bar{M}_{\theta_1}\bar{\bar{Z}}_w$) and first term in the denominator ($\bar{\bar{Z}}_w \bar{\bar{M}}_q$) are positive. The pitching moment of the unstabilized helicopter increases with normal velocity and angle of attack (i.e., $\bar{M}_w$ is positive) and, as a result, the second term in the denominator tends to make the denominator negative. Thus it can be seen the stick position maneuver stability of the unstabilized helicopter is negative unless the damping in pitch derivative is large enough to overcome the adverse effect of the instability with normal velocity.

(c) Initial Response in Hovering Flight

A good approximation for the hovering pitch response of the helicopter for the first two or three seconds following a fore or aft step displacement of the stick is obtained by treating fuselage pitching as a separate degree of freedom. The pitching motion is little affected by the small speed changes occurring in this period and in hovering flight vertical motion is decoupled from the other degrees of freedom. Since, in addition, the unstabilized helicopter has no attitude derivatives, the pitch equation given on p. 9 reduces to the following form for the case under consideration.

$$I\dot{q} = \bar{\bar{M}}_q q + \bar{\bar{M}}_{\theta_1}(K_c \theta_c)$$

where the effect of blade motion is included in the $\bar{\bar{M}}_q$ and $\bar{\bar{M}}_{\theta_1}$ derivatives. The solution of the above equation is,

$$q(t) = \frac{\bar{\bar{M}}_{\theta_1}}{(-\bar{\bar{M}}_q)} K_c \theta_c \left[1 - e^{\frac{\bar{\bar{M}}_q}{I} t}\right]$$

and a typical plot is given on Fig. 6.

It can be seen from the form of the solution and from the plot that the pitching rate builds up exponentially in the initial motion. Some of the quantities defining this response are of sufficient importance to enjoy special names in the literature on helicopter stability. $\bar{\bar{M}}_{\theta_1}/(-\bar{\bar{M}}_q)$ is referred to as the sensitivity and is the final pitch rate in the initial response per radian cyclic pitch change produced by the pilot. The sensitivity is often defined including the constant K_c (i.e. $K_c\bar{\bar{M}}_{\theta_1}/(-\bar{\bar{M}}_q)$) in which case it is the final pitching rate per unit stick motion. $\bar{\bar{M}}_q/I$ has been called the "damping rate" and is the inverse of the time required for the exponential term in the solution to decay to 1/e times its initial value. In the present report a response time (τ_R) is used in discussing the initial motion and is defined as the time required to reach 90% of the maximum pitching rate. The response time is related to the damping rate by:

$$\tau_R = 2.31/(-\bar{\bar{M}}_q/I)$$

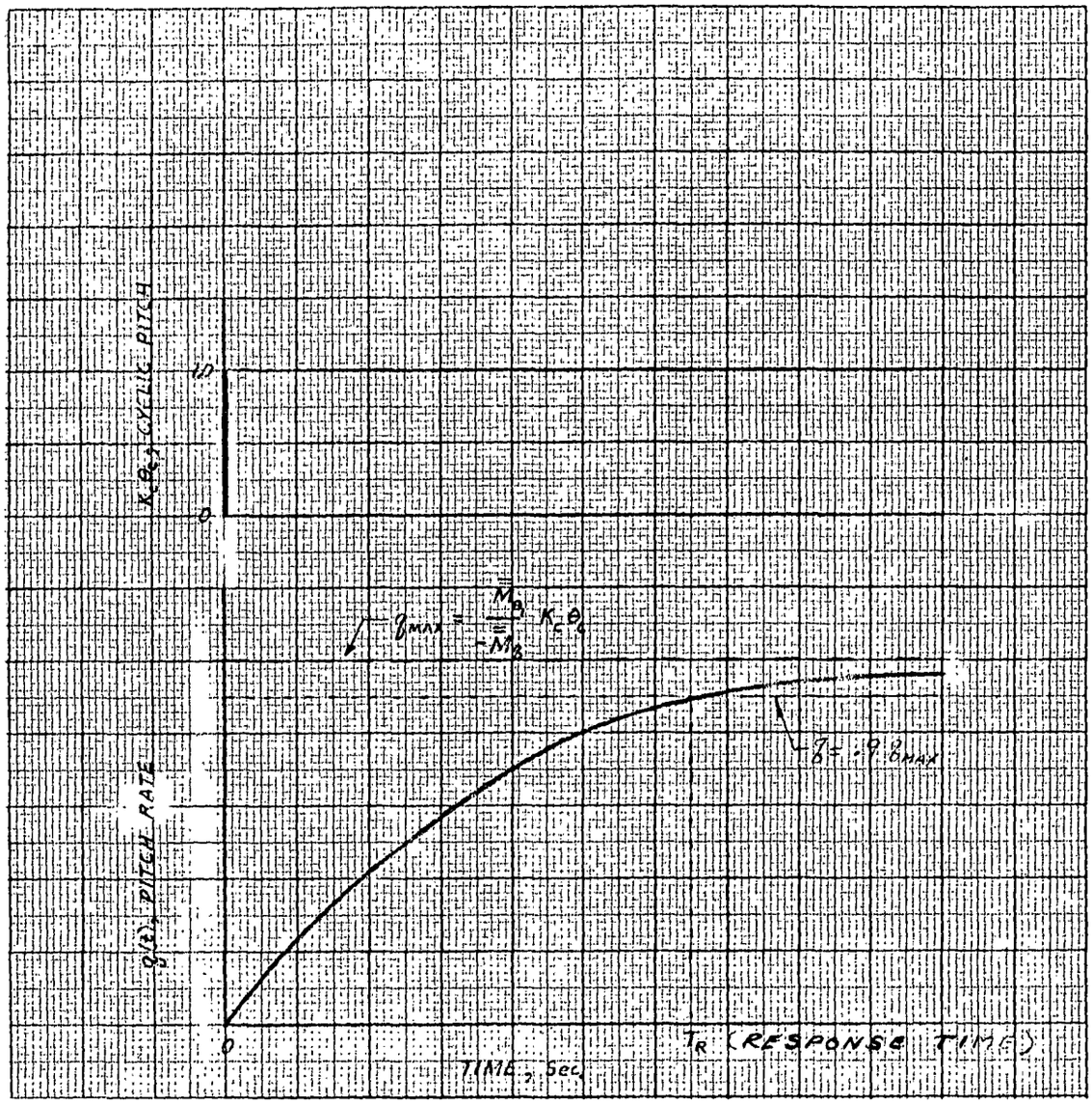

FIG. 6. INITIAL RESPONSE TO CYCLIC PITCH STEP IN HOVERING FLIGHT

in the one degree of freedom case discussed above. It can be seen that increasing the damping in pitch ($-\bar{M}_q$) decreases the response time and the final pitching velocity while increasing the control power derivative ($\bar{M}_{\theta_1}$) increases the sensitivity and maximum pitching rate.

The simplified approach to the initial response characteristics in hovering flight given above must be treated with caution if the flapping inertia of the blades is very high or the pitch inertia of the fuselage is very low. Also, the introduction of a device which effectively changes the blade inertia or introduces a fuselage attitude feedback modifies the initial response. When the blade inertia is large (or is effectively increased by a stabilizing device), there exists a possibility that the initial response will be oscillatory rather than of the exponential form discussed above. Also the above analysis is not valid when there is an attitude autopilot feedback since the motion tends to approach an attitude rather than a pitch rate. These points will be amplified in the discussion of the devices (Section 5).

(d) Initial Response in Forward Flight

In forward flight as in hovering the initial response to a cyclic control input is little affected by changes in velocity along the flight path. However, the normal velocity degree of freedom is not decoupled since the fuselage angle of attack changes which result from pitching motion introduce coupling forces and moments. It is no longer permissible to treat pitching motion as an isolated degree of freedom and the normal velocity degree of freedom must also be included to obtain a satisfactory approximation of the initial motion.

The following characteristics of the initial response in forward flight are considered to be important from the handling qualities standpoint:

1) Pitch rate sensitivity

2) Pitch rate response time

3) Normal acceleration sensitivity

4) Normal acceleration response time

5) Shape of normal acceleration time history

Figures 7(a) and 7(b) present forward flight time histories on which the significance of the above quantities are noted. Items (1) and (2) have already been discussed in regard to the hovering response, and the normal acceleration sensitivity and normal acceleration response times are defined in a similar manner. The normal acceleration does not change significantly in the initial hovering response, but appreciable normal acceleration changes do occur in forward flight since the fuselage and swash plate angles of attack vary as discussed on p. 14 .

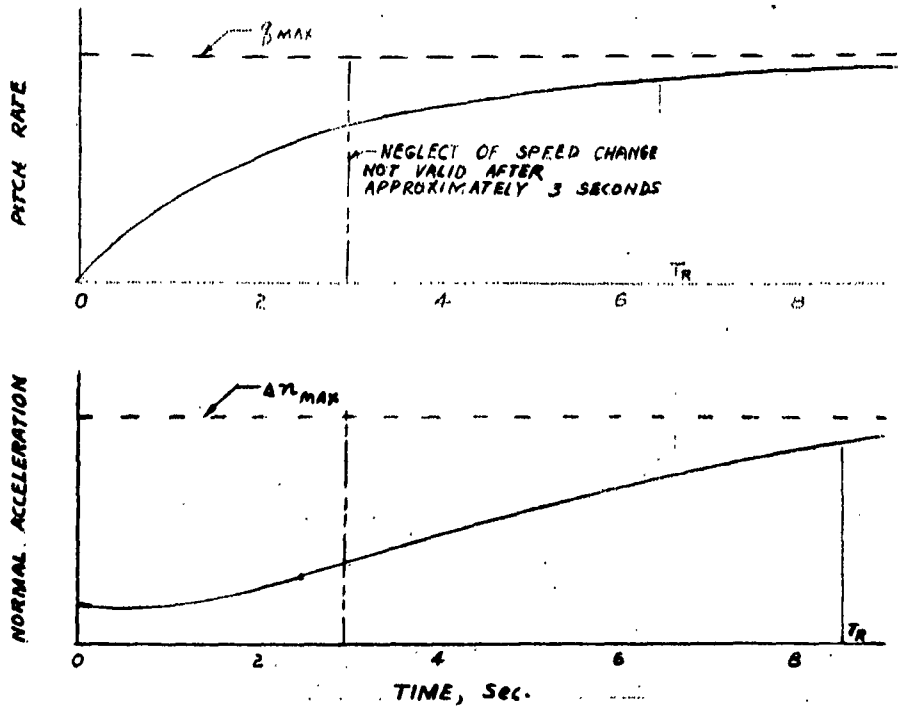

FIG. 7(a). LONGITUDINAL RESPONSES OF AN UNSTABILIZED HELICOPTER IN FORWARD FLIGHT

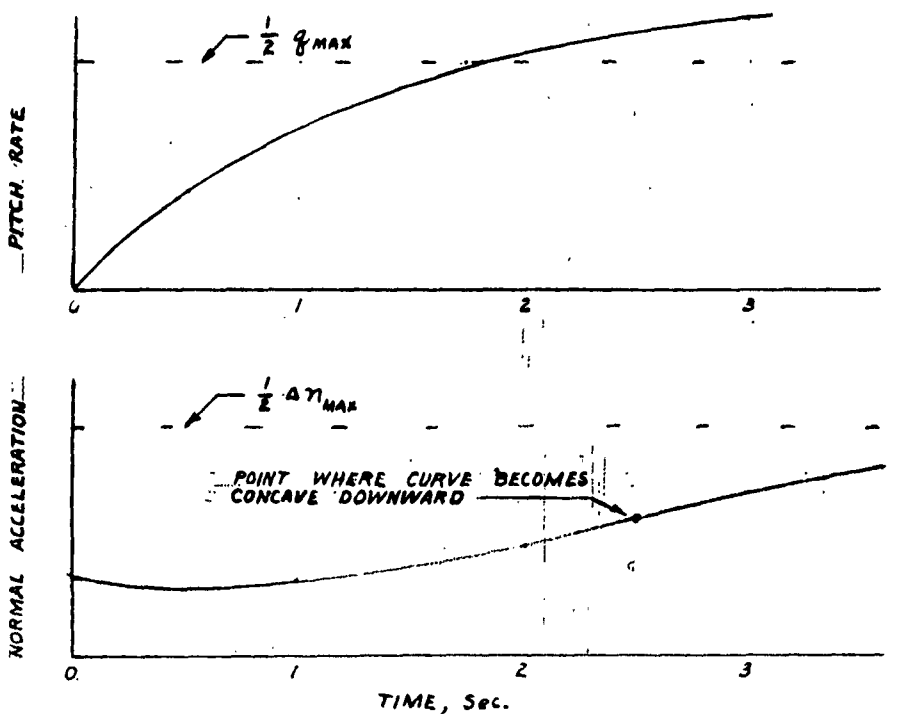

FIG. 7(b). LONGITUDINAL RESPONSES DURING FIRST THREE SECONDS

Figure 7 indicates that the pitching rate and normal acceleration reach steady values at some time after a step change in cyclic pitch. This is only true if the stick position maneuver stability is positive and the forward speed is assumed constant. The steady state change in normal acceleration is given by

$$\Delta n = K_c U_o \frac{\bar{\bar{Z}}_{\theta_1} \bar{\bar{M}}_w - \bar{\bar{M}}_{\theta_1} \bar{\bar{Z}}_w}{\bar{\bar{Z}}_w \bar{\bar{M}}_q - M_w (Z_q + m U_o)} \Delta \theta_c$$

which is seen to be the same expression given in discussing stick position maneuver stability.

In many cases, the equilibrium condition would not be reached within the first two or three seconds during which the constant speed assumption is reasonably good. Nevertheless, an approximate solution using pitching and normal velocity for degrees of freedom gives a good description of the motion of the unstabilized helicopter for this period. There are two roots involved which can be of different importance in the pitch rate and normal acceleration responses, making one or the other appear to approach a steady value more rapidly.

The initial pitch rate response in forward flight is usually quite similar to that shown for the hovering case indicating that the same derivatives, ($\bar{\bar{M}}_q$ AND $\bar{\bar{M}}_{\theta_1}$) are important. However, the normal velocity derivative ($\bar{\bar{M}}_w$) can tend to make the pitch response oscillatory or divergent depending on its sign. The initial response can also become oscillatory if the effective blade inertia is increased as discussed for the hovering case. The normal acceleration response is to a large extent dependent on the normal velocity damping derivative ($\bar{\bar{Z}}_w$) and is usually quite slow due to the low lift curve slope-weight ratio of the helicopter.

Figure 7(b) is presented to indicate details of the normal acceleration time history which have been found to have an important bearing on pilot's evaluation of handling qualities. Characteristics that are undesirable are a dip appearing immediately after the control input or too long a time elapsing before the curve becomes concave downward. It was determined (Ref. 2) that the presence of the dip was disturbing to pilots because they could not anticipate the further build up of the acceleration after the dip. It was also found that when the normal acceleration is not concave downward within two seconds the pilot gets the impression that the motion is divergent. It is possible, of course, for the motion to be divergent and this occurs when the maneuver stability is negative.

(e) Long Period Response

The long period response characteristics of the unstabilized helicopter are somewhat similar to the phugoid of the airplane. The long period mode shows an inherent unstability but its period is sufficiently long to enable the pilot to control it.

The gravitational forces which are necessary for the existence of an airplane phugoid do not play as important a role in the case of the helicopter long period mode (see Part B). The speed stability derivative ($\bar{M}_u$) and damping in pitch derivative ($\bar{M}_q$) are the most important parameters in determining the period of oscillation which is approximately given by :

$$P \approx 2\pi \sqrt{\frac{-\bar{M}_q}{g\bar{M}_u}} \quad \text{AT} \quad \mu_o = 0$$

$$P \approx 2\pi \sqrt{\frac{-\bar{M}_q + m U_o \bar{M}_w/\bar{Z}_w}{g\bar{M}_u}} \quad \text{AT} \quad \mu_o \neq 0$$

The approximate time to double amplitude is given by:

$$T_{2A} \approx 1.386 \frac{M_q}{g I M_u} \qquad \text{in hovering}$$

The above approximations correspond to those given by Hohenemser in several papers. The formulae are convenient for making rapid estimates, but the accuracy deteriorates when the system is rapidly convergent or divergent, when other roots of about the same size are present, or when the radius of gyration is high (i.e., neglected terms are of the same order as the moment derivatives).

2.3 Desirable Handling Qualities and Deficiencies of Unstabilized Helicopter

The deficiencies of the unstabilized helicopter and the handling qualities that are desirable are discussed in Part B in detail. Characteristics found acceptable in Part B are compared to those of the sample helicopter in the following table.

TABLE 4

ACCEPTABLE HELICOPTER HANDLING CHARACTERISTICS

	Acceptable Value	Sample Helicopter* (without stabilizing device)
1. Speed Stability = $\frac{\Delta u}{-\Delta \theta_c}$	> 0	> 0
2. Maneuver Stability = $\frac{\Delta n}{\Delta \theta_c}$	> 0	< 0 at High Speed
3. Short Period		
a. Hovering		
(1) Maximum equilibrium pitch rate, q_{max}	> .5 rad/sec.	1.8 rad/sec.
(2) Pitch rate response time	< 1 sec.	7.5 sec.
(3) Damping in pitch	> .7 critical	> .7 critical
(4) Maximum equilibrium roll rate, p_{MAX}	> .5 rad/sec.	1.6 rad/sec.
(5) Roll rate response time	< 1 sec.	1.5 sec.
(6) Damping in roll	> .7 critical	> .7 critical
b. Forward Flight (μ = .2)		
(1) Maximum equilibrium pitch rate, q_{max}	> .5 rad/sec.	
(2) Pitch rate response time	< 1 sec.	
(3) Proper shape of g vs t	see section 2.2	marginal
(4) Normal velocity stability derivative, $\bar{M}_w$	< 0	+37.8
(5) Damping	> .7 critical	> .7 critical
4. Long Period Damping $e^{\lambda t}$	λ < 0	λ > 0

* Assuming no blade stall limitation - see Part B.

From Table 4 it can be seen that the unstabilized sample helicopter should be improved in the following ways:

1. The pitch response time in both hovering and forward flight should be reduced. This implies that the damping should be increased considerably. It must be noted, however, that if the damping is increased the control power, $\bar{M}_{\theta_1}$, must be increased if the pitch rate is to be maintained.

2. The shape of the normal acceleration curve should be improved.

3. The normal velocity stability derivative, $\bar{M}_w$, should be made a stabilizing quantity.

4. The long period damping should be increased.

In seeking ways to achieve the above improvements care must be exercised to maintain the existing satisfactory qualities. In Table 4 only regions of values are given for some handling qualities because there are insufficient data to fix limits.

In Section 4 approximate analyses are made to formulate some of these handling qualities in terms of the feedback constants of the generalized autopilot.

3. GENERALIZED AUTOPILOT TREATMENT OF EXISTING STABILIZING DEVICES

3.1 Summary of Autopilot Constants Corresponding to Various Stabilizing Devices

It was indicated in Section 1.2 that most of the stabilizing devices considered in this report can be represented mathematically as special cases of a generalized autopilot. Tables 5 and 6 summarize the autopilot constants which are required to represent those devices that operate on cyclic pitch. The control equation and the generalized autopilot constants shown on Table 5 are based on the formulation of the equations of motion in which the motion of the helicopter and the longitudinal tilt of the tip path plane are referred to horizontal and vertical axes. Expressions for these constants in terms of device parameters are derived in Appendix B of Part A of this report.

Table 6 gives the form of the control equation and the required feedback constants when the tilt of the tip path plane is referred to the shaft and the equations of motion are referred to axes moving with the helicopter. As previously mentioned, the discussion in this part of the report is primarily in terms of the moving axis system indicated on Table 6. The relationships between the feedback constants obtained with the two axes systems are given on Table 6.

It can be seen from an examination of Table 6 that a single set of feedback constants is given in the case of the conventional helicopter autopilot, gyroscopic bar, biased cyclic, Doman head, and tip path plane rate feedback systems and these constants apply both in hovering and in forward flight. The floating vane stabilizer is only effective in forward flight. While the other devices considered are effective in hovering, their constants are functions of initial forward flight speed. A brief indication of the source of the various feedback constants is given below and this subject is taken up in greater detail in Section 5.

The magnitude of the speed feedback constants obtained with each device depends on the selection of design parameters. For example, it depends on the collective pitch angle of the control rotor, the camber of the blades used with the swash plate spring damper, the initial servo flap angle, and the initial floating vane angle.

The conventional helicopter autopilot and the idealized approximation for the double bar stabilizer are the only devices shown which have true pitch attitude feedbacks that are not associated with changes in fuselage angle of attack. The pitching rate feedbacks (κ_q) are primarily due to gyroscopic effects except in the case of the floating vane stabilizer where a vane angle of attack change proportional to the pitching velocity occurs when the vane is displaced aft of the c.g. Since the rotor hub is in general located above the c.g., a pitching velocity about the c.g. implies a linear velocity at the rotor. This linear velocity of the hub should be considered in computing the pitching rate feedback κ_q, but its effect is generally found to be small.

The K_w feedbacks in Table 6 give the changes in cyclic pitch due to increments in normal velocity, w, measured relative to axes moving with the helicopter. Since changes in normal velocity produce proportional changes in fuselage angle of attack

$$\alpha_F \approx \frac{w}{U_o}$$

the angle of attack feedback is proportional to the normal velocity feedback and can be written as $U_o K_{\dot{\alpha}}$. The control rotor, swash plate spring damper, servo flap, and floating vane stabilizers all have K_w feedbacks and thus affect the angle of attack stability of the helicopter. The control rotor response to an angle of attack change is similar to that of the main rotor and the corresponding angle of attack feedback is destabilizing. On the other hand, the inherent angle of attack feedback obtained with the servo flap is stabilizing, and considerable control over the angle of attack stability is possible in the case of the floating vane stabilizer.

Both the swash plate spring damper and the servo flap have feedbacks arising from gyroscopic forces. The gyroscopic forces which produce control movements in these devices are proportional to the rate of tilting of the rotor tip path plane relative to fixed coordinates which can be thought of as a combination of fuselage pitching velocity (q) and rate of change of longitudinal flapping relative to the shaft ($\dot{\beta}_{1s}$). Part of these gyroscopic effects are taken into account in the K_q feedback as previously discussed, and the second part which depends on the rate of change of longitudinal flapping is included in the $K_{\dot{\beta}_{1s}}$ feedback. In quasi-static conditions when the rate of tilting of the tip path plane relative to the shaft is zero the gyroscopic feedbacks of the swash plate spring damper mechanism and servo flap are the same as those produced by a rate gyro mounted in the fuselage. The tip path plane rate device which is studied is assumed to give longitudinal and lateral cyclic feedbacks proportional to the pitching and rolling rates of the tip path plane.

$K_{\beta_{1s}}$, the cyclic pitch feedback due to flapping relative to the shaft, is the only feedback constant needed to represent the Doman Head and biased cyclic stabilizers, and this feedback can also be obtained with the control rotor, swash plate spring damper, and servo flap devices. It is shown in Section 5.6 that flapping relative to the shaft is amplified or attenuated depending on the sign of the $K_{\beta_{1s}}$ feedback. Thus it is evident that both the basic rotor derivatives and the effect of all other autopilot feedbacks are modified by the presence of a $K_{\beta_{1s}}$ feedback.

In studying various stabilizing devices in Part A, it is found that the generalized autopilot constants for each device cannot always be varied arbitrarily and some of these limitations have been indicated on Table 6. For example, the kinematics of the gyroscopic bar stabilizer are such that the rate constant and time lag (ℓ) are related by:

$$-K_q = p\ell$$

Although some of the limitations on the selection of feedback constants for the representation of various stabilizing devices have been noted other limitations which exist are too complicated to be given in such a condensed form. Thus it is necessary to refer to the additional relations and limitations given in Part A in order to make a realistic study of the helicopter stability and control characteristics obtainable with a given device.

TABLE 5

GENERALIZED AUTOPILOT CONSTANTS FOR REPRESENTING VARIOUS STABILIZING DEVICES
(Horizontal and Vertical Axes)

	Time Lag	Forward Velocity Feedback	α_1, Forward Pitch Change About Hub		Vertical Velocity Feedback	β_1, Forward Long. Flapping Relative to Horizontal Plane		Control Input	
			Rate Feedback	Attitude Feedback		Rate Feedback	Position Feedback	Direct	Through Servo
Gyroscopic Stabilizer Bar (Bell)	ℓ	0	$K_{\dot{\alpha}_1} = (P\Omega_0)\ell$	0	0	0	0	$K_D\theta_c$	0
Control Rotor (Hiller) $\mu_0 = 0$	ℓ	K_μ	$K_{\dot{\alpha}_1} = (P\Omega_0)\ell$	$K_{\alpha_1} = -K_{\beta_1}$	0	0	K_{β_1}	0	$K_L\theta_c$
$\mu_0 \neq 0$	ℓ	K_μ	$K_{\dot{\alpha}_1} = (P\Omega_0)\ell$	$K_{\alpha_1} = \mu_0 K_\delta - K_{\beta_1}$	K_δ	0	K_{β_1}	0	$K_L\theta_c$
Conventional Helicopter Autopilot	$\ell \approx 0$	0	$K_{\dot{\alpha}_1}$	K_{α_1}	0	0	0	$K_D\theta_c$	0
Double Gyroscopic Bar (Approx. Form)	ℓ	0	$K_{\dot{\alpha}_1}$	K_{α_1}	0	0	0	$K_D\theta_c$	0
Tip Path Plane Rate Autopilot	0	0	0	0	0	$K_{\dot{\beta}_1}$	0	$K_D\theta_c$	0
Biased Cyclic	0	0	0	$K_{\alpha_1} = -K_{\beta_1}$	0	0	K_{β_1}	$K_D\theta_c$	0
Doman Head	0	0	0	$K_{\alpha_1} = -K_{\beta_1}$	0	0	K_{β_1}	$K_D\theta_c$	0
Servo Flap (Kaman) $\mu_0 = 0$	$\ell \approx 0$	K_μ	0	$K_{\alpha_1} = -K_{\beta_1}$	0	$K_{\dot{\beta}_1}$	K_{β_1}	0	$K_L\theta_c$
$\mu_0 \neq 0$	$\ell \approx 0$	K_μ	0	$K_{\alpha_1} = \mu_0 K_\delta - K_{\beta_1}$	K_δ	$K_{\dot{\beta}_1}$	K_{β_1}	0	$K_L\theta_c$
Swash Plate Spring Damper Stabilizer $\mu_0 = 0$	ℓ	K_μ	$K_{\dot{\alpha}_1}$	$K_{\alpha_1} = -K_{\beta_1}$	0	$K_{\dot{\beta}_1}$	K_{β_1}	$K_D\theta_c$	$K_L\theta_c$
$\mu_0 \neq 0$	ℓ	K_μ	$K_{\dot{\alpha}_1}$	$K_{\alpha_1} = \mu_0 K_\delta - K_{\beta_1}$	K_δ	$K_{\dot{\beta}_1}$	K_{β_1}	$K_D\theta_c$	$K_L\theta_c$
Floating Vane Stabilizer* (Erickson) $\mu_0 \neq 0$	$\ell \approx 0$	K_μ	$K_{\dot{\alpha}_1}$	$K_{\alpha_1} = \mu_0 K_\delta$	K_δ	0	0	$K_D\theta_c$	0

Control Equation (Referred to horizontal and vertical axes):

$$\ell\dot{\theta}_1 + \theta_1 - K_\mu\mu + \frac{K_{\dot{\alpha}_1}}{\Omega}\dot{\alpha}_1 + K_{\alpha_1}\alpha_1 + K_\delta\delta + \frac{K_{\dot{\beta}_1}}{\Omega}\dot{\beta}_1 + K_{\beta_1}\beta_1 + [K_L\theta_c + K_D(\ell\dot{\theta}_c + \theta_c)]$$

$$K_c = K_L + K_D$$

*Basic helicopter derivatives must be corrected for the tail effectivity of the vane in the stabilizing device.

TABLE 6

GENERALIZED AUTOPILOT CONSTANTS FOR REPRESENTING VARIOUS STABILIZING DEVICES
(Moving Axes System)

	Time Lag	Forward Speed Feedback	Ⓗ, Aft Pitch Change about c.g.		Feedback Due to Normal Velocity Component, w	β_{1s}, Long. Flapping Relative to Shaft		Control Input	
			Rate Feedback	Attitude Feedback		Rate Feedback	Position Feedback	Direct	Through Servo
Gyroscopic Stabilizer Bar (Bell)	ℓ	0	$K_\beta = -P\ell$	0	0	0	0	$K_D\theta_c$	
Control Rotor $\mu_o = 0$ (Hiller) $\mu_o \neq 0$	ℓ	K_U	K_β	0	0	0	$K_{\beta_{1s}}$	0	$K_L\theta_c$
	ℓ	K_U	K_β	0	K_W	0	$K_{\beta_{1s}}$	0	$K_L\theta_c$
Conventional Helicopter Autopilot	$\ell \approx 0$	0	K_β	$K_Ⓗ$	0	0	0	$K_D\theta_c$	0
Double Gyroscopic Bar (Approx. Form)	ℓ	0	K_β	$K_Ⓗ$	0	0	0	$K_D\theta_c$	0
Tip Path Plane Rate Autopilot	0	0	$K_\beta = -K_{\dot\beta_{1s}}$	0	0	$K_{\dot\beta_{1s}}$	0	$K_D\theta_c$	0
Biased Cyclic	0	0	0	0	0	0	$K_{\beta_{1s}}$	$K_D\theta_c$	0
Doman Head	0	0	0	0	0	0	$K_{\beta_{1s}}$	$K_D\theta_c$	0
Servo Flap $\mu_o = 0$ (Kaman) $\mu_o \neq 0$	$\ell \approx 0$	K_U	$K_\beta = -K_{\dot\beta_{1s}} - h K_U$	0	0	$K_{\dot\beta_{1s}}$	$K_{\beta_{1s}}$	0	$K_L\theta_c$
	$\ell \approx 0$	K_U	$K_\beta = -K_{\dot\beta_{1s}} - h K_U$	0	K_W	$K_{\dot\beta_{1s}}$	$K_{\beta_{1s}}$	0	$K_L\theta_c$
Swash Plate Spring $\mu = 0$ Damper Stab. $\mu_o \neq 0$	ℓ	K_U	K_β	0	0	$K_{\dot\beta_{1s}}$	$K_{\beta_{1s}}$	$K_D\theta_c$	$K_L\theta_c$
	ℓ	K_U	K_β	0	K_W	$K_{\dot\beta_{1s}}$	$K_{\beta_{1s}}$	$K_D\theta_c$	$K_L\theta_c$
Floating Vane (Erickson) $\mu_o \neq 0$	$\ell \approx 0$	K_U	K_β	0	K_W	0	0	$K_D\theta_c$	0

Control equation (Referred to coordinates moving with helicopter):

$$\ell\dot\theta_1 + \theta_1 = K_U U + K_W w + K_\beta \beta + K_Ⓗ Ⓗ + K_{\dot\beta_{1s}}\dot\beta_{1s} + K_{\beta_{1s}}\beta_{1s} + [K_L\theta_c + K_D(\ell\dot\theta_c + \theta_c)]$$

Relation of feedback constants in Tables 3 and 4:

$$K_U = \frac{K_\mu}{\Omega_o R}\,,\quad K_W = -\frac{K_\delta}{\Omega_o R}\,,\quad K_\beta = -\frac{1}{\Omega_o}\left[K_{\dot\alpha_1} + K_{\dot\beta_1} + \frac{h}{R}K_\mu\right],\quad K_Ⓗ = [\mu_o K_\delta - K_{\alpha_1} - K_{\beta_1}],\quad K_{\dot\beta_{1s}} = \frac{K_{\dot\beta_1}}{\Omega_o},\quad K_{\beta_{1s}} = K_{\beta_1}$$

3.2 Effective Autopilot Feedback Constants

It is mentioned in Section 3.1 that a flapping feedback not only modifies the basic rotor characteristics of the unstabilized helicopter but also changes the effect of other feedbacks which are present. This makes it difficult to predict by physical intuition how some of the devices listed in Table 6 affect helicopter stability.

In the summary of equations on Table 2 (p. 8) another form of the generalized autopilot equation is given which does not include blade flapping explicitly although including the effect of a flapping feedback by the use of effective feedback constants for the other variables. This effective form of the autopilot equation is often helpful in obtaining a direct indication of how a given device affects stability.

Longitudinal flapping, β_{1s} , which appears as a variable in the autopilot equation (A.81),

$$\ell\dot{\theta}_1 + \theta_1 = K_u u + K_w w + K_q q + K_{\dot{w}}\dot{w} + K_{\dot{\beta}_{1s}}\dot{\beta}_{1s} + K_{\beta_{1s}}\beta_{1s} + [K_c\theta_c + K_d(\ell\dot{\theta}_c + \theta_c)]$$

is determined by the rotor response to forward speed, pitching velocity, etc. and thus could be eliminated by the longitudinal flapping equation (B.67),

$$\beta_{1s} = (\beta_{1s})_u u + (\beta_{1s})_w w + (\beta_{1s})_q q + (\beta_{1s})_{\dot{\beta}_{1s}}\dot{\beta}_{1s} + (\beta_{1s})_{\theta_1}\theta_1 ,$$

giving the following effective autopilot equation:

$$\frac{\ell\dot{\theta}_1}{1-K_{\beta_{1s}}(\beta_{1s})_{\theta_1}} + \theta_1 = K_u' u + K_w' w + K_q' q + K_{\dot{w}}'\dot{w} + K_{\dot{\beta}_{1s}}'\dot{\beta}_{1s} + \frac{[K_c\theta_c + K_d(\ell\dot{\theta}_c + \theta_c)]}{1-K_{\beta_{1s}}(\beta_{1s})_{\theta_1}}$$

Effective autopilot constants are denoted by primes.

It will be observed that there is a flapping rate feedback in the effective autopilot equation although the longitudinal flapping feedback has been eliminated. The flapping rate feedback produces a delay in the application of cyclic pitch but is not found to have much effect on initial response characteristics (see Section 4.3).

Expressions for the effective feedback constant are listed below and numerical parameters are inserted for the sample helicopter.

$$K'_w = \frac{K_w + (\beta_{1s})_w K_{\beta_{1s}}}{1 - K_{\beta_{1s}}(\beta_{1s})_{\theta_1}} = 0 \qquad (\mu_0 = 0)$$

$$= \frac{K_w - .000831 K_{\beta_{1s}}}{1 + 1.08 K_{\beta_{1s}}} \qquad (\mu_0 = .2)$$

$$K'_q = \frac{K_q + ((\beta_{1s})_q K_{\beta_{1s}}}{1 - K_{\beta_{1s}}(\beta_{1s})_{\theta_1}} = \frac{K_q + .0958 K_{\beta_{1s}}}{1 + K_{\beta_{1s}}} \qquad (\mu_0 = 0)$$

$$= \frac{K_q + .0964 K_{\beta_{1s}}}{1 + 1.08 K_{\beta_{1s}}} \qquad (\mu_0 = .2)$$

$$K'_{\theta_0} = \frac{K_{\theta_0}}{1 - K_{\beta_{1s}}(\beta_{1s})_{\theta_1}} = \frac{K_{\theta_0}}{1 + K_{\beta_{1s}}} \qquad (\mu_0 = 0)$$

$$\frac{K_{\theta_0}}{1 + 1.08 K_{\beta_{1s}}} \qquad (\mu_0 = .2)$$

$$K'_{\dot{\beta}_{1s}} = \frac{K_{\dot{\beta}_{1s}} + K_{\beta_{1s}}(\beta_{1s})_{\dot{\beta}_s}}{1 - K_{\beta_{1s}}(\beta_{1s})_{\theta_1}} = \frac{K_{\dot{\beta}_{1s}} - .0907 K_{\beta_{1s}}}{1 + K_{\beta_{1s}}} \qquad (\mu_0 = 0)$$

$$= \frac{K_{\dot{\beta}_{1s}} - .0925 K_{\beta_{1s}}}{1 + 1.08 K_{\beta_{1s}}} \qquad (\mu_0 = .2)$$

$$\frac{1}{1 - K_{\beta_{1s}}(\beta_{1s})_{\theta_1}} = \frac{1}{1 + K_{\beta_{1s}}} \qquad (\mu_0 = 0)$$

$$= \frac{1}{1 + 1.08 K_{\beta_{1s}}} \qquad (\mu_0 = .2)$$

3.3 Classification of Devices

For convenience in discussing and comparing the various stabilizing devices considered in this report they are classified into groups in Table 7. The devices placed in each group have certain basic characteristics in common but may differ in some minor respects as noted.

The horizontal tail and the pitch-cone coupling linkage stabilizers do not operate by varying the cyclic pitch, the former applying moments directly to the fuselage and the latter modifying rotor characteristics by changing the

collective pitch. The other devices considered function by changing the cyclic pitch and were classified using the data given in Table 6 and the expressions for effective feedback constants given in Section 3.2. Devices with K_u feedback constants modify the speed stability, those with $K_{(\alpha)}$ feedbacks modify the attitude stability, and those with K_w feedbacks modify the normal velocity stability and angle of attack stability. When there is a K_q feedback coefficient and no $K_{\dot{\beta}_{1s}}$ feedback constant, the damping with respect to fuselage motions is modified. Devices which introduce cyclic pitch proportional to the absolute velocity of the tip path plane relative to fixed axes are indicated by the combined presence of $K_{\dot{\beta}_{1s}}$ and K_q feedbacks. For such devices the $K_{\dot{\beta}_{1s}}$ feedback results in a slowing down of the tip path plane response to control movement while the K_q feedback again results in an increase in the pitch and roll damping of fuselage motions.

One does not ordinarily have an intuitive understanding of how helicopter stability is affected by a flapping feedback ($K_{\beta_{1s}}$) as such. However, when it is remembered that blade flapping depends on changes in forward velocity, angle of attack, and tilting velocity of the tip path plane, it can be seen that the damping with respect to tip path plane motion, speed stability, and angle of attack stability are all influenced by the presence of a $K_{\beta_{1s}}$ feedback constant. Devices with $K_{\beta_{1s}}$ feedbacks were classified making use of the definitions of effective feedback coefficients given in Section 3.2. In particular, it should be noted that the effective normal velocity feedback K'_w is often made destabilizing by a negative $K_{\beta_{1s}}$ feedback although the K_w feedback tends to reduce the normal velocity instability.

Group I includes devices whose primary characteristic is to increase the pitch and roll damping of fuselage motions. Both the gyroscopic bar and the control rotor stabilizers are classed in Group I and have time lags which cause them to introduce small cyclic pitch components proportional to helicopter attitude which help to stabilize the long period mode. However, the Group II devices are the only ones listed which provide the helicopter with substantial attitude stability. These devices also increase the damping of pitching and rolling motions.

The devices classed in Group III all provide cyclic pitch feedbacks proportional to the rate of tilting of the tip path plane and thus slow down blade response and increase pitch and roll damping of fuselage motions. The Group III devices have varied effects on the angle of attack stability of the helicopter. The biased cyclic and Doman Frasier head system considerably increase the angle of attack instability, the servo flap at 75% of span has a slightly unfavorable effect, the tip path plane rate autopilot has no normal velocity feedback, and the swash plate spring damper can produce a decrease in the angle of attack instability when the aerodynamic center is offset from the pitching axis.

The swash plate spring damper differs from the other devices of Group III in that it has a time lag whose magnitude is proportional to the swash plate damping. Furthermore, some swash plate damper configurations have been proposed which speed up rather than slow down the blade response.

The devices listed in Group IV are the only ones which provide appreciable improvement in the angle of attack instability. However, they do not give suitable damping and are only effective in forward flight.

TABLE 7

CLASSIFICATION OF DEVICES INTO GROUPS

GROUP	BASIC CHARACTERISTICS OF THE DEVICES IN GROUP	DEVICE	REMARKS
I	1) Increase pitch and roll damping of fuselage motions 2) Have time lags tending to improve stability of long period mode	a) Gyroscopic Stabilizer Bar (Bell)	
		b) Control rotor stabilizer (Hiller)	Increases angle of attack instability, can affect speed stability, introduces lag in pilot's input
II	1) Increase pitch and roll damping of fuselage motion 2) Introduce pitch and roll attitude stability	a) Conventional helicopter autopilot b) Double bar stabilizer	
III	1) Increase pitch and roll damping of fuselage motion 2) Slow down blade response 3) Have little effect on or increase effective angle of attack instability	a) Tip path plane rate autopilot	
		b) Biased cyclic c) Doman Frasier Rotor Head	Increase angle of attack instability, increase speed stability
		d) Servo flap (Kaman)	Can affect speed stability
		e) Swash plate spring damper	Can affect speed stability, can use time lag to speed up blade response
IV	1) Introduce angle of attack stability 2) Only effective in forward flight	a) Horizontal tail b) Floating vane stabilizer (Erickson)	
		c) Pitch cone linkage (Hohenemser)	Decreases vertical damping

4. GENERAL EVALUATION OF EXISTING STABILIZING DEVICES

4.1 Consideration of Methods for Studying the Effect of a Generalized Autopilot on Helicopter Control Characteristics

The main purpose of this report is to show how the stability and control characteristics of a helicopter are modified by a generalized autopilot and thereby investigate the effect of a number of stabilizing devices. Several methods which were considered for evaluating the helicopter handling characteristics obtained with various combinations of feedback constants are discussed below.

(a) Transfer Function Approach:

In recent years, considerable emphasis has been placed on the application of the transfer function servomechanism techniques in the study of helicopter autopilots. The transfer function approach is best suited for use in the stabilization of a particular mechanism and the first step in applying it is to obtain an approximation for the transfer function of the helicopter to be controlled. The stability of the system can be determined from the transfer function and servomechanism theory provides information concerning the forms of transfer functions which can be expected to give desirable response characteristics. The design procedure would involve selecting autopilot feedback constants which would make the closed loop transfer function of the helicopter plus autopilot have the desired form. Although the transfer function procedure has been applied successfully in cases where there is a pitch attitude and rate feedback, the procedure becomes considerably more complicated when feedbacks depending on more than one output variable are present. For example, when both attitude and forward speed feedbacks are present, it would be necessary to work with a combination of the speed and attitude transfer functions of the helicopter. It was concluded that the transfer function approach would not be suitable for the present study because it was necessary to determine the effect of multiple feedbacks.

(b) Root Locus Technique:

Reference 3 demonstrated that the Evans root locus method provides a useful tool for studying the control of a helicopter. A plot is made on the complex plane of all the stability roots of the combined helicopter autopilot system and the locus of each root is found when the feedback constants are varied. The locus plot is particularly helpful in indicating some of the compromises which must be made in adjusting feedbacks since in many cases feedback changes which improve the stability of some of the roots make other roots less stable.

(c) Helicopter Transient Response:

The final test of the handling characteristics of a stabilized helicopter is the manner in which it responds to a control input. Although the transfer function and root locus techniques show whether the system is stable

they do not indicate directly many of the details of the response which must be considered in evaluating handling characteristics. This is particularly true when there are a number of roots present. For this reason, it is believed that the best method of indicating the characteristics of the stabilizing devices considered in this report is to study how they influence helicopter responses. In the following sections, helicopter responses are presented which were obtained by direct computation and by simulation using an analogue computer. Step or impulse functions have been most commonly used as test functions in computer studies. An abrupt cyclic pitch change was used to initiate the responses presented in Sections 4 and 5.

Several questions had to be settled once it was decided to study the characteristics of various stabilizing devices by finding how they affected the response of a typical helicopter. Since there were too many combinations of autopilot time lags and feedback constants to make a systematic study of all possible settings feasible, it was necessary to decide what range of values should be assigned to the equivalent autopilot constants required to represent each device. Should they be typical of constants used in actual applications of the device or would other constants prove more desirable in the case of the sample helicopter considered? In general, constants were selected keeping in mind the limitations imposed by the various mechanisms. In some instances, constants were investigated which are considerably different from those ordinarily used when the device is mounted on the helicopter for which it was designed.

4.2 Effect of Stabilizing Devices on Speed and Maneuver Stability

In Section 2.2 a discussion is given of the unstabilized helicopter's speed and maneuver stability (i.e., the variations in forward speed and normal acceleration with stick position respectively). Expressions for these quantities were given in terms of equivalent helicopter derivatives which are applicable to the stabilized helicopter as well as the basic helicopter although requiring different values for the derivatives in the two cases.

The following expression for the speed stability at $\mu_o = .2$ in terms of effective feedback constants is obtained using the equivalent helicopter derivatives for the sample helicopter given in Appendix A:

$$\frac{\Delta u}{-\Delta \theta_c} = \frac{\text{Speed Change}}{\text{Forward Stick Movement}} = \frac{\bar{M}_{\theta_1} \bar{\bar{Z}}_w - \bar{Z}_{\theta_1}' \bar{M}_w}{\bar{M}_u \bar{\bar{Z}}_w - \bar{\bar{Z}}_u \bar{M}_w} \left[\frac{K_c}{1 - K_{\beta_{1s}} (\beta_{1s})_{\theta_1}} \right] *$$

$$= \frac{21.8}{1 + 168 K_w' + 1245 K_u'} \left[\frac{K_c}{1 + 1.08 K_{\beta_{1s}}} \right] \frac{(\text{FT./SEC.})}{(\text{DEG.})}$$

---

* The relatively small effect of an attitude feedback has been omitted. For the sample helicopter the complete expression is:

$$\frac{\Delta u}{-\Delta \theta_c} = \frac{21.8}{1 + 168 K_w' + 1245 (K_u' - .000834 K_\theta')} \left[\frac{K_c}{1 + 1.08 K_{\beta_{1s}}} \right]$$

The changes in speed stability with the effective speed feedback, K'_u, and effective normal velocity feedback, K'_w, are shown on Fig. 8. In plotting this expression, the bracketed expression was taken equal to unity which is equivalent to assuming that the linkage ratio, K_c, is varied in such a manner that the effective cyclic input due to the pilot's stick motion is the same with different flapping feedback constants.

It should be emphasized that Fig. 8 indicates the static speed stability characteristics of the stabilized helicopter and does not imply that the helicopter has been made dynamically stable with the feedback constants shown. It is found as might be expected that the speed feedback, K'_u, has a much larger effect on the speed stability than the normal velocity or attitude feedbacks. Appreciable changes in speed stability result from the large variations in K'_w shown but the static speed stability remains finite unless negative K'_u feedbacks are used when $K_w' > -.003$.

The maneuver stability at $\mu_o = .2$ is shown on Fig. 9 as a function of the effective pitching rate feedback, K'_q, and effective normal velocity feedback, K'_w. This figure like Fig. 8 is based on the equivalent helicopter derivatives for the sample helicopter given in Appendix A. These derivatives lead to the following expression for maneuver stability:

$$\frac{\Delta n}{\Delta \theta_c} = \frac{\text{Normal Acceleration}}{\text{Aft Stick Deflect}} = \frac{v_o}{(57.3)(32.2)} \frac{\bar{Z}'_{\theta_1} \bar{M}_w - \bar{M}'_{\theta_1} \bar{Z}_w}{\bar{Z}_w \bar{M}_q - \bar{M}_w (\bar{I}_y + m v_o)} \left[\frac{K_c}{1 - K_{\theta_{1s}} (\theta_{1s})_{\theta_1}} \right]$$

$$= \frac{.496}{.198 - 9.34 K'_q - 937 K'_w} \left[\frac{K_c}{1 + 1.08 K_{\theta_{1s}}} \right]$$

The bracketed term was taken equal to unity in plotting the maneuver stability as was done in the case of speed stability.

It will be remembered that the normal acceleration change predicted by the maneuver stability expression is the steady state change which would occur if there were no changes in forward speed. In most cases where $\Delta n/\Delta \theta_c$ is large, speed changes become important before a quasi-static equilibrium is reached.

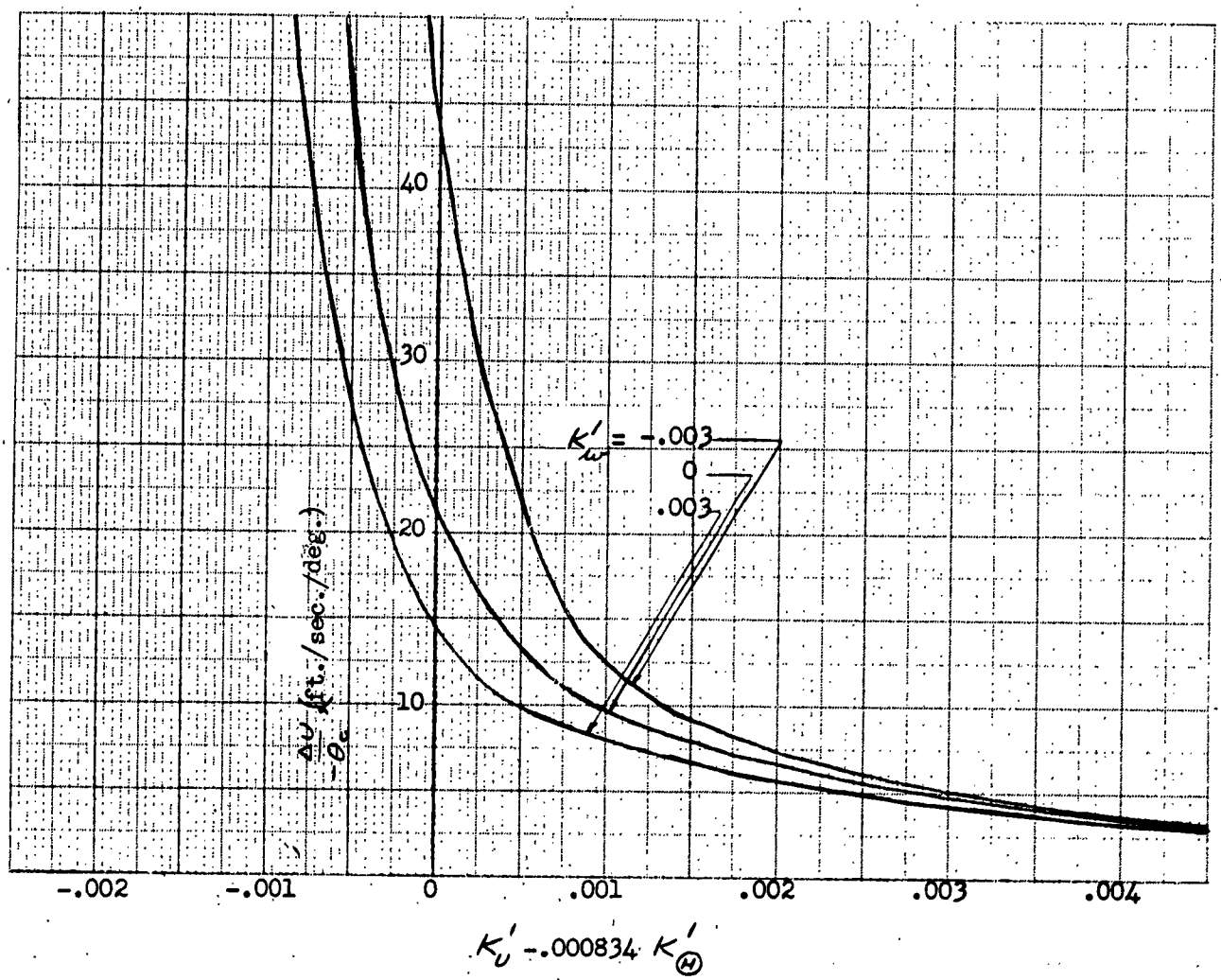

FIG. 8. INFLUENCE OF AUTOPILOT FEEDBACKS ON SPEED STABILITY; $\mu_0 = .2$

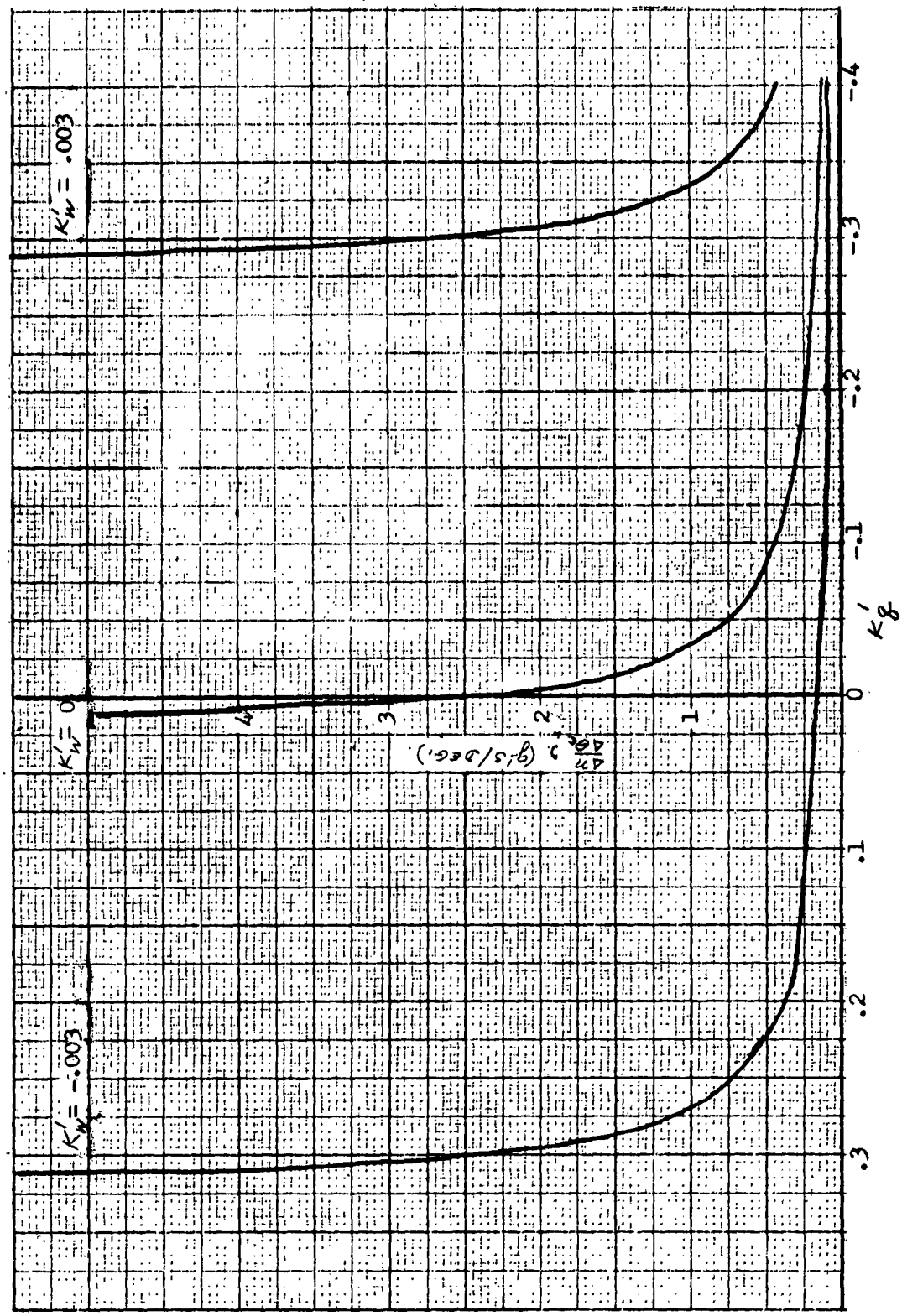

FIG. 9. INFLUENCE OF AUTOPILOT FEEDBACKS ON MANEUVER STABILITY; $\mu_\delta = .2$

4.3 Effect of Stabilizing Devices on Initial Response in Hovering Flight

The effect of a zero time lag generalized autopilot on initial hovering response characteristics is discussed in this section since consideration of this case is helpful in obtaining a general evaluation of a number of stabilizing devices. It is noted on Table 6 that the time lags of several stabilizing devices are negligible, and, in addition, it is found that study of the comparatively simple zero time lag case gives physical intuition into the effect of various feedbacks which is valid for the finite time lag case.

The analysis of initial response characteristics with a zero time lag stabilizing device is approached in two steps. First, equivalent helicopter equations are used which are based on a quasi-static treatment of blade motion and, secondly, initial response time histories are presented that were obtained including blade flapping as a separate degree of freedom.

(a) Prediction of Pitch and Roll Rates and Response Times by Equivalent Helicopter Equations

The equivalent helicopter equations discussed in Section 1.4 made use of derivatives that included the effect of a zero time lag generalized autopilot. Methods of treating the initial response characteristics of the stabilized helicopter with these equations are similar to those used for the unstabilized helicopter. However, if there are attitude feedbacks present there are attitude derivatives in the equivalent helicopter equations which do not exist in the case of the unstabilized helicopter. A different type of initial response is obtained in this case as explained in the discussion of the conventional helicopter autopilot (p. 93). In this section the treatment is simplified by assuming that there is no attitude feedback.

The equivalent control moment, $\bar{\bar{M}}_{\theta_1} K_c \theta_c$, equivalent damping in pitch derivative, $\bar{M}_q$, and equivalent fuselage pitching moment of inertia, $\bar{\bar{I}}$, which are the most important parameters in determining initial response characteristics in hovering flight are all functions of the generalized autopilot feedbacks. They can be expressed as follows for the sample helicopter by making use of the data given in Appendix A .

$$\bar{M}_{\theta_1} K_c \theta_c = \frac{\bar{M}'_{\theta_1} K_c \theta_c}{1 - K_{\beta_{1S}} (\beta_{1S})_{\theta_1}} = 58416 \left[\frac{K_c \theta_c \, (RAD)}{1 + K_{\beta_{1S}}} \right] \quad (FT.\ LBS)$$

$$\bar{M}_q = \bar{M}'_q + \bar{M}_{\theta_1} K'_q = -4433 + 58416 K'_q \quad (FT.\ LBS/RAD./SEC.)$$

$$= \frac{-4433 + 58416 K_q + 1160 K_{\beta_{1S}}}{1 + K_{\beta_{1S}}}$$

$$\bar{\bar{I}} = I - \bar{\bar{M}}'_{\dot{\theta}_1} K'_q = [15000 + 4074 K'_q] \quad (SLUG\ FT^2)$$

$$= \frac{[15000 + 15390 K_{\beta_{1S}} + 4074 K_q]}{1 + K_{\beta_{1S}}}$$

It can be seen that the control moment is proportional to $K_c \theta_c / (1 + K_{\beta_{1s}})$, the effective cyclic input of the pilot, and depends on the amplification produced by the flapping feedback constant, $K_{\beta_{1s}}$. The desired magnitude for the pilot's effective input will, in most cases, be determined by clearance considerations which are not affected by the addition of a stabilizing device. Consequently, it is assumed in this section that whenever a $K_{\beta_{1s}}$ feedback is used, a compensating change is made in the linkage ratio, K_c, such that the maximum cyclic pitch obtained with full stick deflection will be unchanged. The maximum longitudinal cyclic pitch of the sample helicopter is approximately 8 degrees and the maximum lateral cyclic pitch is approximately 6.8 degrees.

The equivalent damping in pitch derivative and equivalent moment of inertia are given in terms of the K_q and $K_{\beta_{1s}}$ feedbacks and also in terms of the effective rate feedback constant K_q'. The damping in pitch derivative $\bar{M}_q$ increases with $-K_q$ and is approximately inversely proportional to $(1 + K_{\beta_{1s}})$ since the $K_{\beta_{1s}}$ term in the numerator is relatively small. The equivalent pitching moment of inertia is nearly equal to the pitching moment of inertia of the sample helicopter for the ordinary range of feedbacks but larger differences exist in the analogous roll quantities. Although it would be expected that a pitching rate feedback would influence the damping in pitch derivative it is not as evident why the moment of inertia is also changed. The explanation for the effective increment in pitching moment of inertia can be seen by considering a case where the helicopter has a nose-up pitching acceleration and linearly increasing pitching velocity. The swash plate will then have a nose-down tilting velocity relative to the fuselage if there is a negative K_q' feedback. There is an aft tilt of the tip path plane relative to the swash plate associated with this swash plate tilting because of rotor gyroscopic effects. This aft tilt results in a thrust component tending to increase the pitching acceleration of the fuselage and effectively reduces the helicopter's pitching moment of inertia.

In the discussion of the initial response of the unstabilized helicopter to a step stick displacement (Section 2.2), it is pointed out that the pitching rate builds up exponentially with time. A similar time history is obtained with a zero time lag autopilot and the pitch rate response time and maximum pitching rate for an 8 degree swash plate tilt are given by the following expressions in the case of the sample helicopter:

$$T_R = 2.31 \left(\frac{\bar{I}}{\bar{M}_q}\right) = \text{Pitch rate response time}$$

$$= 2.31 \frac{(15000 + 4074 K_q')}{(4433 - 58416 K_q')}$$

$$= \frac{34600 + 35500 K_{\beta_{1s}} + 9440 K_q}{4433 - 58416 K_q - 1160 K_{\beta_{1s}}}$$

$$q_{MAX} = \frac{M_{\theta_1}}{(-\bar{M}_q)} \frac{K_c (\theta_c)_{MAX.}}{} = \text{Maximum pitching rate (assuming no speed change)}$$

$$= \frac{58416 (8/57.3)}{4433 - 58416 K_q'} \quad (\text{RAD./SEC.})$$

The above results are presented graphically on Fig. 10.

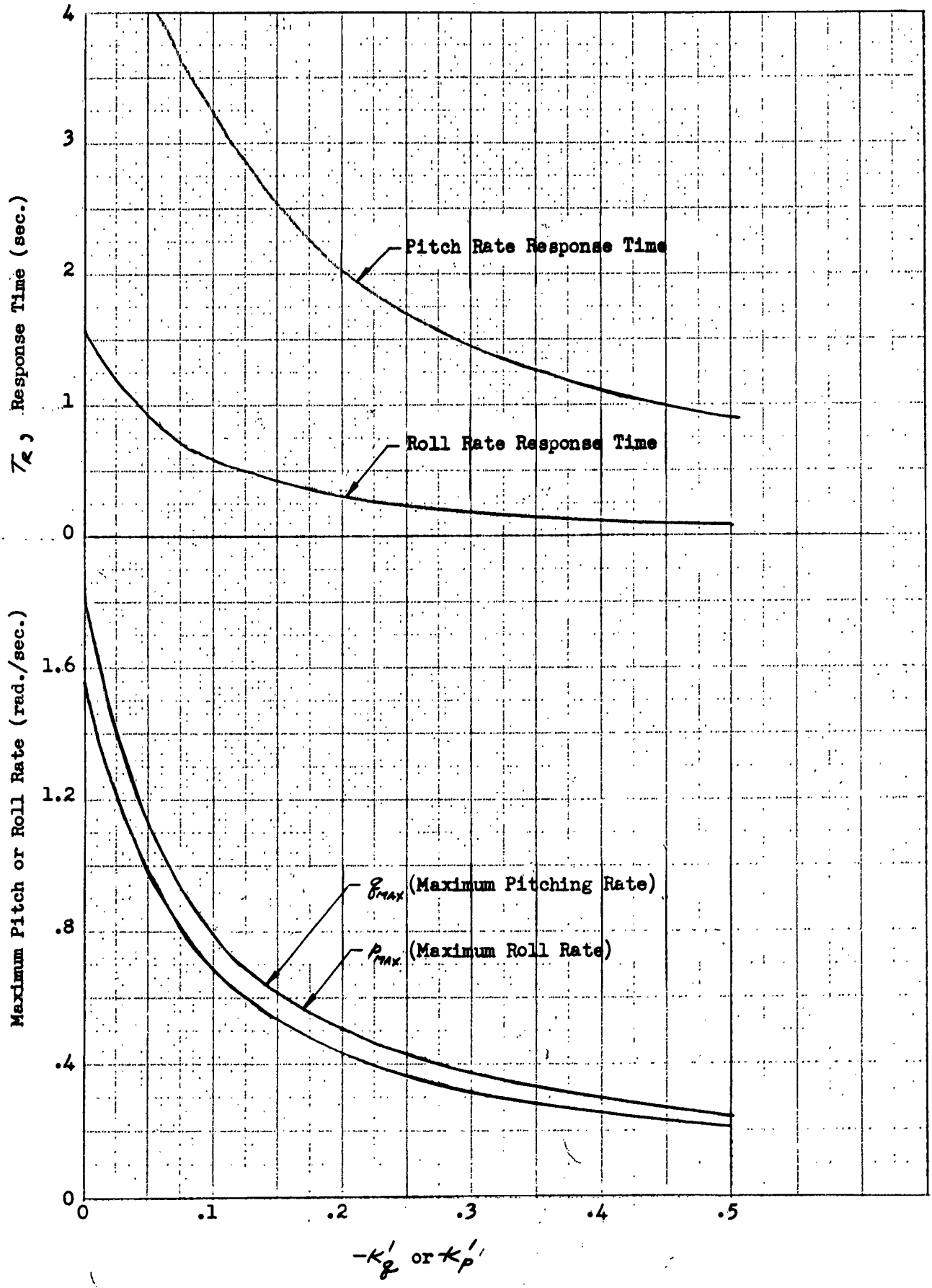

FIG. 10. MAXIMUM PITCH AND ROLL RATES AND RESPONSE TIMES AS FUNCTIONS OF AUTOPILOT FEEDBACKS; HOVERING

Although equations of motion for the roll case are not derived in this report, the initial roll response in hovering can be predicted by applying the longitudinal equations with appropriate roll parameters. This procedure was carried out for the sample helicopter parameters given in Appendix A and resulted in the following expressions for roll response time and maximum roll rate due to a 6.8 degree swash plate deflection.

$$\text{Roll rate response time} = 2.31 \frac{(3000 + 4074 K_p')}{(4433 - 58416 K_p')}$$

$$P_{max} = \text{Maximum roll rate} = \frac{58416 (6.8/57.3)}{(4433 - 58416 K_p')}$$

In the above expressions the effective roll rate feedback constant, K_p', replaces K_q' used in the corresponding pitch expressions. Figure 10 presents plots of the roll rate response times and maximum rolling rates as functions of the feedback constants. The effects of feedback changes on the roll response properties are similar to those found for the pitch case.

(b) Treatment of Blade Flapping

It was pointed out previously that the initial response data given on Fig. 10 was computed using equivalent helicopter derivatives based on a quasi-static treatment of blade motion. The validity of this treatment of blade motion can be investigated by referring to the initial response time histories presented on Fig. 11. These responses were obtained in an analogue computer solution which included longitudinal flapping as a separate degree of freedom in finding the pitch response and considered lateral flapping as a separate degree of freedom in finding the roll response. Forward speed changes were neglected as was done in the equivalent helicopter analysis of initial response.

Solutions based on quasi-static and separate degree of freedom treatments of blade motion give the same equilibrium pitch and roll rates in the initial response. However, it will be noted on Fig. 11, that when the blade flapping degree of freedom is included, the roll rate responses for higher feedback gains overshoot the equilibrium rolling rate instead of having the simple exponential build-ups predicted with a quasi-static treatment of blade motion. The same definition of response time is used in considering these cases of relatively small overshoots as with an exponential response. For example, the $K_p' = -.2$ curve of Fig. 11 gives

Equilibrium roll rate = .44 rad/sec.

Response time = .40 sec. (Time at which roll rate reaches 90% of equilibrium value.)

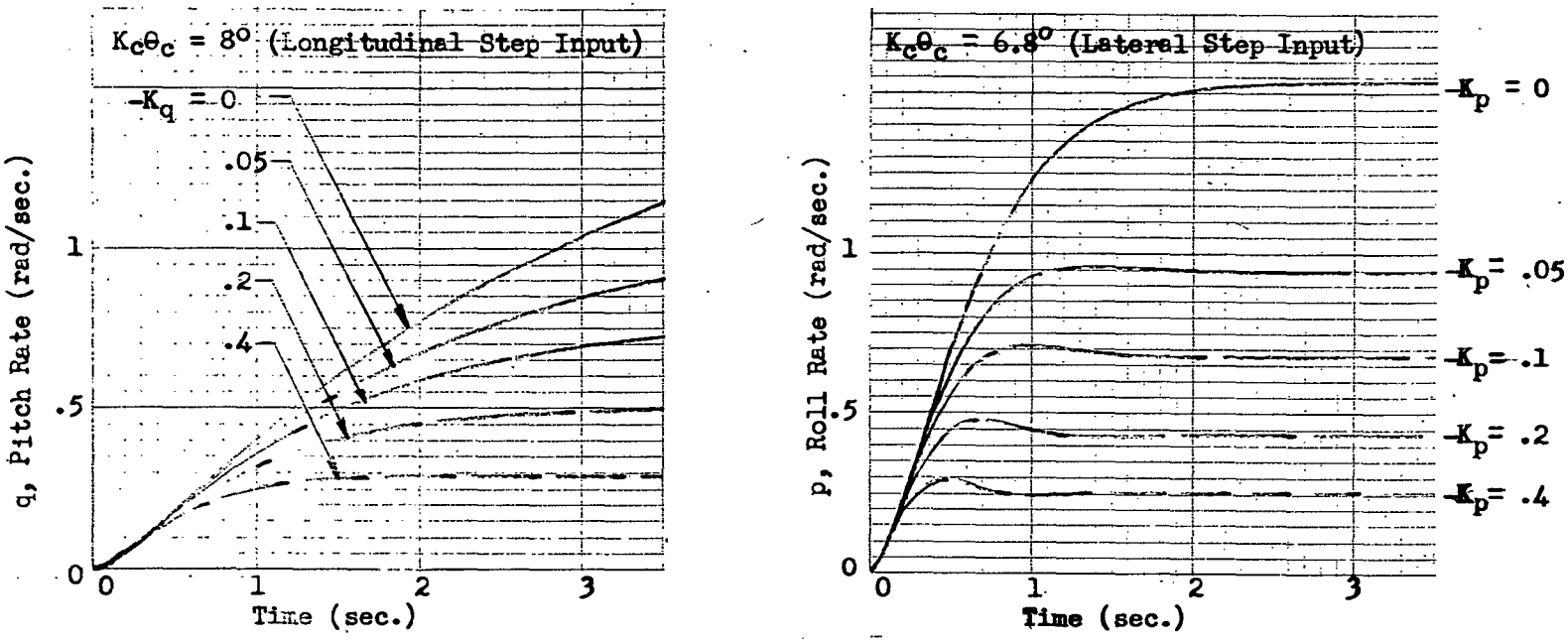

FIG.11 INITIAL RESPONSES TO LONGITUDINAL AND LATERAL STEP CYCLIC PITCH INPUTS; EFFECT OF FUSELAGE RATE FEEDBACKS; HOVERING

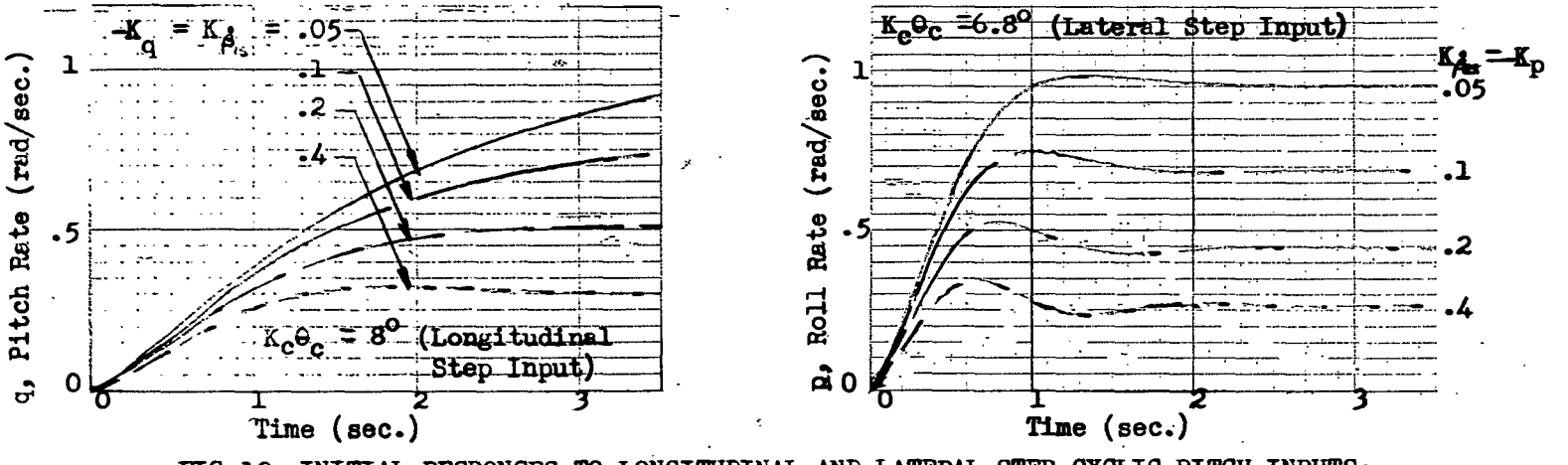

FIG.12 INITIAL RESPONSES TO LONGITUDINAL AND LATERAL STEP CYCLIC PITCH INPUTS; EFFECT OF TIP PATH PLANE RATE FEEDBACKS; HOVERING

The equivalent helicopter approximation for the roll rate response time shown on Fig. 10 gives a value of .31 sec. for the same condition. It is found that at the higher feedback gains the response times given on Fig. 10 are lower than those measured on the responses on Fig. 11 but are only in error by approximately .1 sec.

The initial response time histories presented on Fig. 11 show the effect of a cyclic pitch feedback proportional to the pitching or rolling velocity of the fuselage and for comparison Fig. 12 shows responses obtained with feedbacks proportional to the rate of tilting of the tip path plane relative to fixed axes. As discussed previously, a pitching velocity of the tip path plane relative to fixed axes can be described as the combination of a fuselage pitching velocity and a pitching velocity of the tip path plane relative to the shaft (i.e., a rate of change of the longitudinal flapping of the rotor). A similar breakdown can be made of the tip path plane rolling velocity. Thus flapping rate feedbacks, $K_{\dot{\beta}_{1s}}$ and $K_{\dot{\beta}_{2s}}$ were used in simulating the Fig. 12 case as well as the K_q and K_p feedbacks used in Fig. 11. These flapping feedbacks introduce an effective lag in the cyclic pitch introduced by the autopilot as discussed in Section 3.2. However, comparison of Fig. 11 and Fig. 12 indicates that the flapping rate response feedbacks are not having an important effect on the initial response time histories. The flapping rate feedbacks do not affect the equilibrium pitching and rolling rates because the rotor does not have a tilting velocity relative to the shaft at equilibrium. The time histories including the $K_{\dot{\beta}_{1s}}$ and $K_{\dot{\beta}_{2s}}$ feedbacks are slightly more oscillatory but their presence does not cause a significant change in the response times. Thus the initial response characteristics for the Fig. 12 case can also be approximated by the data given on Fig. 10.

(c) Possibility of Improving Initial Hovering Response

The previous discussion indicates that a general evaluation of the effects of a number of stabilizing devices on initial response characteristics can be obtained from Fig. 10 which shows the variations of the maximum pitch and roll rates and response times in the initial response with effective pitch and roll rate feedback constants. The response time curves only apply rigorously for the case of zero generalized autopilot time lag, but the steady state rate data are equally applicable with and without time lags. When time lags are present large overshoots and oscillatory responses are sometimes obtained which precludes the use of certain feedback gains. These restrictions are taken up in the discussion of individual stabilizing devices. However, for time lag configurations which do not have undesirable oscillatory characteristics, the response time data given on Fig. 10 gives a good indication of the rapidity of the response. Thus Fig. 10 can be used to estimate the initial response characteristics obtainable with a fuselage pitch and roll rate autopilot, a tip path plane pitch and roll rate autopilot, a gyroscopic stabilizer bar, a control rotor, a swash plate spring damper, an aerodynamic servo control flap, the Doman Head, and a biased cyclic system.

Approximately the same initial hovering response could be obtained with any one of these devices if they were not restricted due to oscillatory characteristics. The response time of the control rotor would be somewhat slower than those of the other devices for the same feedback gains due to a lag in the pilot's input system.

Acceptable initial response handling characteristics were summarized in Section 2.3 which included maximum pitch and roll rates of .5 rad/sec. and pitch and roll rate response times less than one second. It is evident from Fig. 10 that it is impossible to select feedback gains for the sample helicopter which will satisfy all of these requirements. An effective roll rate feedback of $K'_p = -.05$ would give a satisfactory roll response. However, it would require a pitch rate feedback $K'_q = -.45$ to reduce the pitch rate response time to one second and at this feedback the maximum pitching rate is only .25 rad/sec. Thus it is impossible to select a pitch rate feedback which will give the desired response and compromises would have to be made in stabilizing the sample helicopter with any stabilizing device. Further compromises are required with many devices which must have equal pitch rate and roll rate feedbacks.

The slow pitch response of the Appendix A helicopter is due to a deficiency in control power and cannot be remedied by any stabilizing device. The pitch and roll rate response times are proportional to the pitch and roll moments of inertia which, of course, explains why the pitch response time is so much longer. In the case of configurations where the pitching and rolling moments of inertia are more nearly equal (e.g., syncropters, coaxial, or jet-driven helicopters), this difference in response would not exist and the desired response times and rolling rates might be obtained in hovering with any of the devices listed.

The ratio of pitch rate response time to maximum equilibrium pitching rate is

$$\frac{T_R}{q_{MAX}} = \frac{2.31\ \bar{I}}{M_{\theta_1} K_c(\theta_c)_{MAX}}$$

and is little affected by the addition of a stabilizing device. Thus a change in the basic helicopter configuration is required if desired pitch rate characteristics are to be obtained.

4.4 Effect of Stabilizing Devices on Initial Longitudinal Response in Forward Flight

A general discussion is given in this section of the effect of existing stabilizing devices on the initial longitudinal response of the helicopter in forward flight. The initial roll response of the stabilized helicopter in forward flight is not discussed since it is essentially the same as in hovering. However, a separate treatment is required of the longitudinal response due to the importance of normal velocity changes in this case.

Forward speed changes are neglected in analyzing initial response characteristics and for this case the effective form of the control equation reduces to

$$\frac{\ell}{1-K_{\beta_{1s}}(\beta_{1s})_{\theta_1}}\dot{\theta}_1 + \theta_1 = K'_w w + K'_q q + K'_\theta \theta + K'_{\beta_{1s}}\dot{\beta}_{1s} + \frac{[K'_\ell \theta_c + K'_\delta(\ell\dot{\theta}_c + \theta_c)]}{1-K_{\beta_{1s}}(\beta_{1s})_{\theta_1}}$$

The attitude feedback, K'_θ, is assumed zero in this section since it is not required to represent most of the stabilizing devices considered. The effect of an attitude feedback is taken up in the discussion of the conventional autopilot on p. 93 . It is appropriate to make two additional approximations in this section which are not made in Section 5 in order to make it easier to see the principal effects of several stabilizing devices. These are that the autopilot time lag ℓ and the effective longitudinal flapping rate feedback, $K'_{\beta_{1s}}$, are both zero. In the analysis of individual devices in Section 5, it is found that when these parameters are small (which is usually the case) they do not have much effect on the over-all initial response time histories. However, even comparatively small values of ℓ and $K_{\beta_{1s}}$ can influence the normal acceleration response in the first .5 seconds following a step stick deflection.

(a) Pitch Rate Response Time and Maximum Pitching Rate

Figure 13* shows how the initial response to a step aft stick deflection at $\mu_o = .2$ is affected by changes in the rate feedback K'_q. The initial pitching rate response at hovering is also given for comparison. It is found that the pitching rate responses are very similar at hovering and $\mu_o = .2$ for the first second, but the curves for the latter case do not tend to level off to an equilibrium pitching rate as rapidly because of the unstable normal velocity derivative which is present in forward flight. Since the moments due to the normal velocity instability of the sample helicopter at $\mu_o = .2$ are comparatively weak, it is not surprising that exponential type pitching rate responses are found on Fig. 13 of the type expected with a single pitch degree of freedom.

Figure 14 shows how the initial response time histories of the sample helicopter at $\mu_o = .2$ are varied by a normal velocity feedback, K'_w, in conjunction with a pitching rate feedback, K'_q. The introduction of the normal velocity feedback does not produce an appreciable change in the pitch rate responses for 1.1 sec. following a step displacement of the cyclic pitch stick. It takes this long for the helicopter to pitch through an angle which will result in a large enough normal velocity component to give pitching moments which are appreciable compared to the control and damping moments.

---

* The initial responses for the forward flight case were obtained on an analogue computer using normal velocity, pitching rate, and longitudinal blade flapping as degrees of freedom.

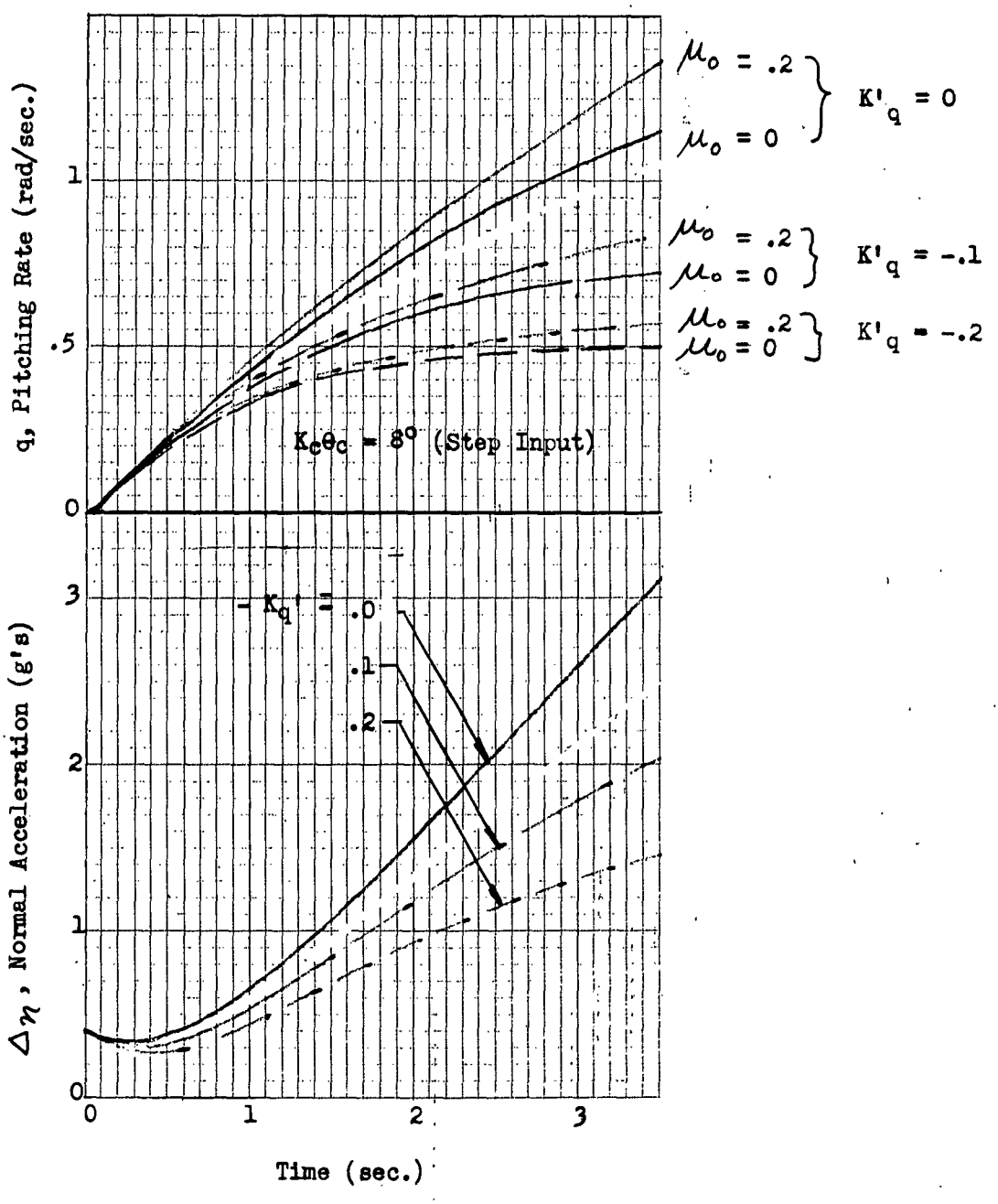

FIG. 13 INITIAL LONGITUDINAL RESPONSES TO STEP CYCLIC PITCH INPUTS; EFFECT OF K'q FEEDBACK; COMPARISON OF RESULTS FOR HOVERING AND μ_o = .2

It is found that negative normal velocity feedbacks which tend to eliminate the normal velocity instability of the basic helicopter cause the pitching rate curves to level off more rapidly and thus tend to reduce the pitch rate response time. For relatively low values of K'_w the pitching rate time histories increase monotonically to a steady state value. At still higher feedbacks the coupling between the pitching and normal velocity degrees of freedom results in an oscillatory response.

Figure 15 represents a plot of the equilibrium pitching rate which is reached in the initial response neglecting changes in forward speed and the pitching rate response time as functions of the pitching rate and normal velocity feedbacks. The response times were measured on the computer records and are the times at which the pitching rate first reaches 90% of its equilibrium value. It can be seen that appreciable reductions in response time can be obtained with a normal velocity feedback.

(b) Normal Acceleration Time History in a Pull-Up

The effect of pitching rate and normal velocity feedbacks on the normal acceleration time histories in a pull-up at $\mu_o = .2$ can be seen on Figs. 13 and 14. The time histories tend to become concave downward at an earlier time as K'_q and K'_w increase negatively.

In Fig. 14 it can be seen that large changes in normal acceleration occur after an essentially constant pitching rate is obtained, and during this time the angle of attack continues to increase to its equilibrium value (computed neglecting speed change).

It was indicated earlier that a pitch rate response time of the desired rapidity might be obtained if the control and damping moments were greatly increased by the use of large flapping hinge offset. Since it was of interest to determine how this modification would affect the normal acceleration curve, the initial response of the typical helicopter was computed assuming a feedback $K'_q = -.2$ and arbitrarily increasing all pitching moments by a factor of 3 (see Fig. 16). The predicted rapid pitch response was achieved, but the normal acceleration was again found to increase for several seconds after the pitching rate had reached a nearly constant value. This response is of the form that would be expected since the increase in moment does not modify the low lift curve slope-weight ratio of the helicopter which is the basic cause of the slow normal acceleration response. However, the rapid pitch response indicated on Fig. 16 is responsible for the normal acceleration curve becoming concave downward in approximately .8 sec. after the step input which is considerably less than the 2 sec. requirement of Ref. 4 .

An effort was made to determine methods by which an initial normal acceleration response time comparable to the pitch rate response time might be obtained. It was noted that this objective might be accomplished by

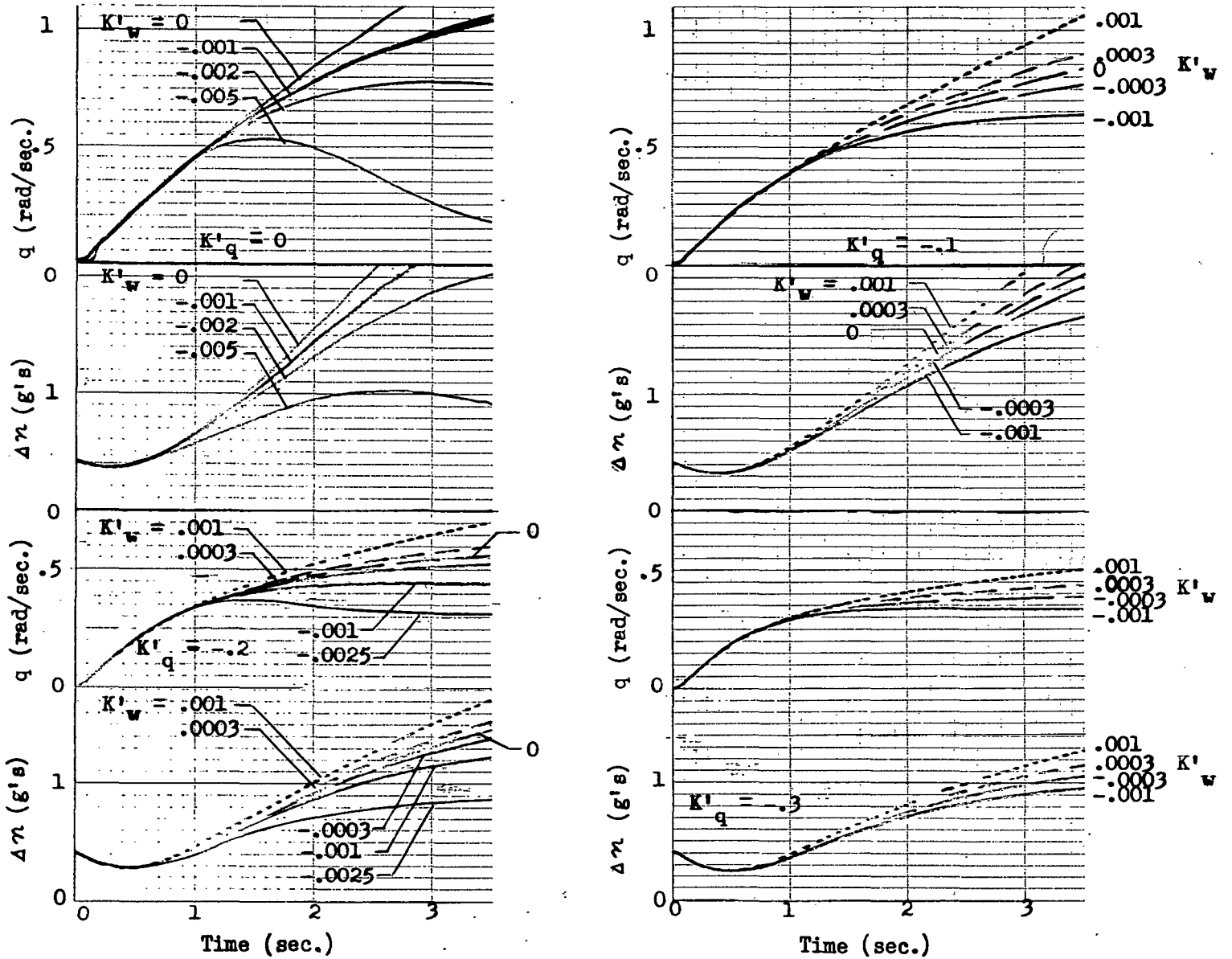

FIG.14 INITIAL LONGITUDINAL RESPONSES TO STEP CYCLIC PITCH INPUTS; EFFECT OF K'_q AND K'_w FEEDBACKS; $\mu_o = .2$; $K_c\theta_c = 8^o$

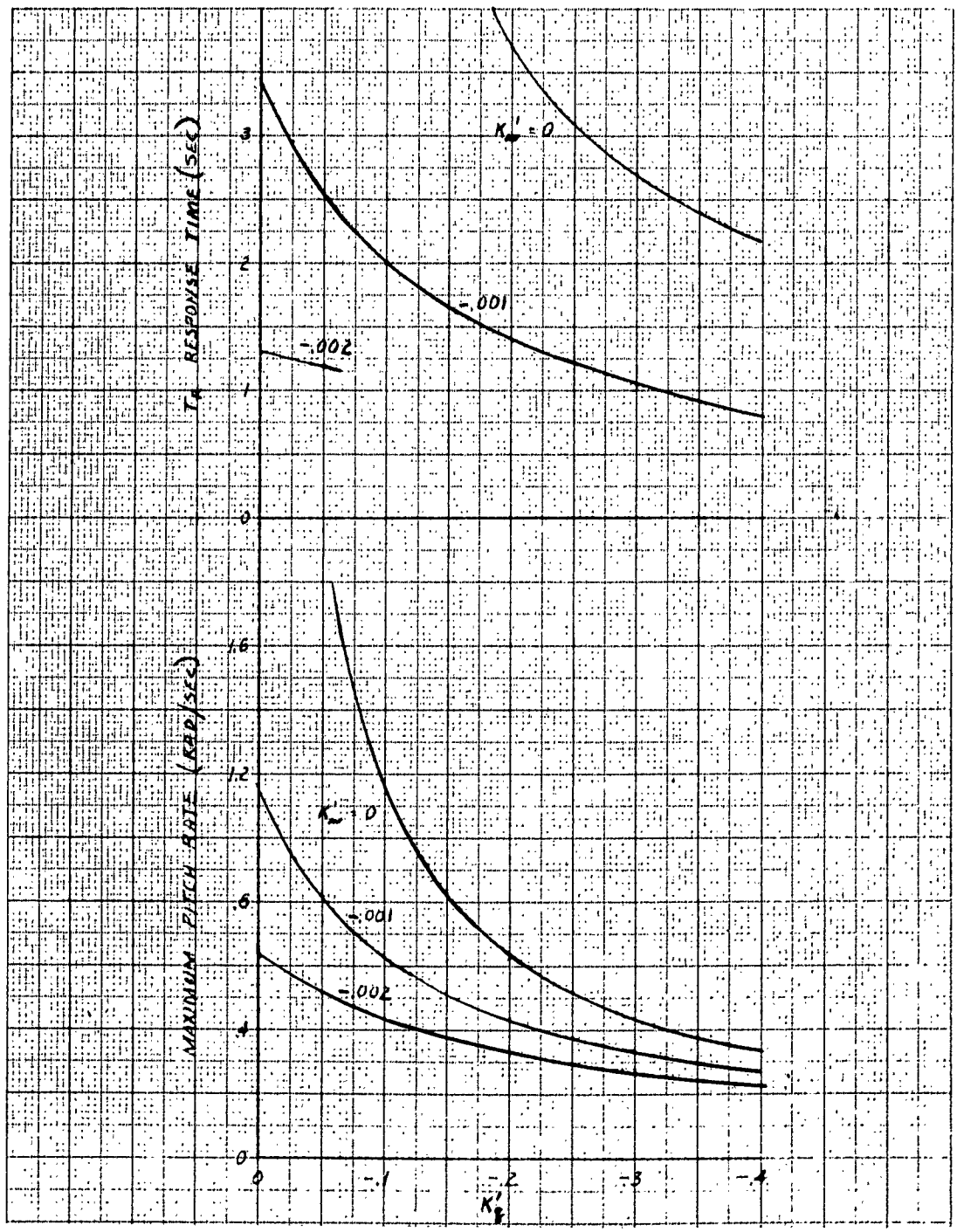

FIG. 15. MAXIMUM PITCH RATE AND RESPONSE TIME AS FUNCTIONS OF EFFECTIVE RATE AND NORMAL VELOCITY FEEDBACKS $\mu_0 = .2$

a stabilizing device which controlled both collective and cyclic pitch, but analysis of such a device was considered beyond the scope of the present report. The only device discussed in this report which makes use of collective control is the pitch-cone coupling stabilizer and in this case the uncoupled normal velocity response time is increased because of a decrease in vertical damping.

When large negative K'_w feedbacks are used the initial response is oscillatory and a pitching rate overshoot is obtained which helps to make the fuselage angle of attack and normal acceleration build up more rapidly. Figure 14 shows the effect of combining an angle of attack feedback $K'_w = -.0025$ and a rate feedback $K'_q = -.2$. It is found that the initial pitching rate response reaches an approximately constant magnitude between one and two seconds and then decreases in magnitude approaching a final value at the same time as the normal acceleration.

Another way of looking at this response is that initially the angle of attack feedback is ineffective since there is a comparatively small angle of attack change, but when an appreciable angle of attack develops, the resulting feedback decreases the pitching rate already built up.

The presence of two modes of motion in the initial response can introduce deceptive dips in the normal acceleration which are objectionable to the pilot. In unstabilized helicopters with slow pitch responses objectionable dips are due to the more rapid normal velocity build up. The initial cyclic pitch application produces an immediate increment in normal acceleration, and the resulting normal velocity reduces the fuselage angle of attack. A corresponding reduction in normal acceleration occurs introducing a dip in the response curve. Finally, the increase in fuselage angle of attack due to a change in pitch attitude reverses this trend and causes a build up in normal acceleration.

The dips in the normal acceleration responses which appear on Figures 13 and 14 are primarily due to cyclic pitch changes resulting from the various feedbacks. For example, as soon as appreciable pitching rates develop on 13, the pitch rate feedbacks produce rapid reductions in cyclic pitch and normal acceleration. The resulting dips obtained with feedback gains of $K_q = -.2$ and $-.3$ reach minimums at approximately .5 sec. and would probably be objectionable to a pilot.

It is difficult to eliminate dips in the normal acceleration response of the Appendix A helicopter in conjunction with any of the stabilizing devices discussed in Section 3 without penalizing the performance of the stabilizing device. Appreciable generalized autopilot time lags or the incorporation of a pilot's input system which make it impossible for the pilot to apply control rapidly can eliminate dips but also make it difficult to obtain short response times. It will be noted that normal velocity feedbacks of the magnitude used in obtaining Fig. 14 did not have an appreciable effect on the dip. Larger normal velocity feedbacks might have a beneficial effect on the dip but would give an observable short period oscillation in the response.

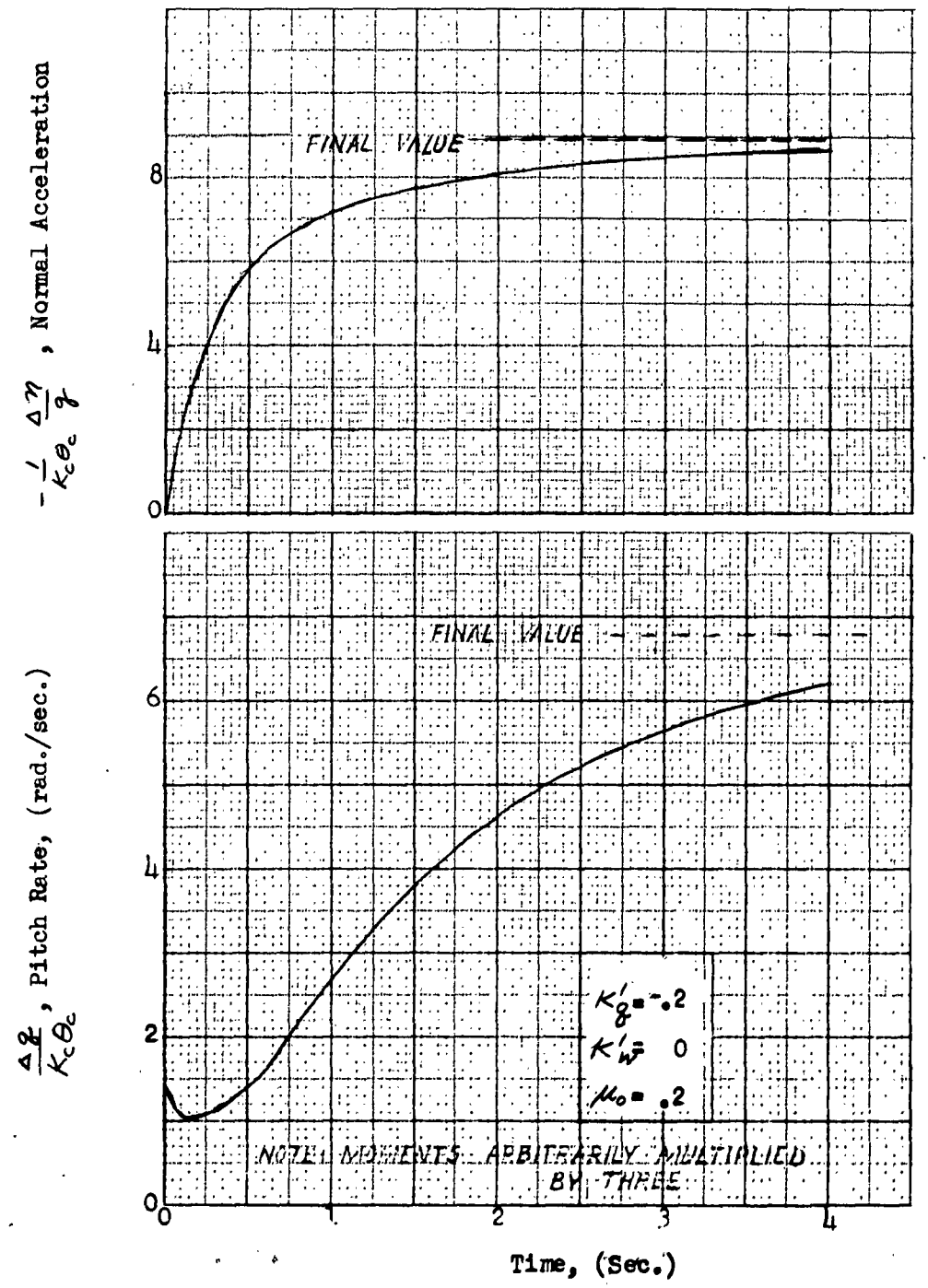

FIG. 16. INITIAL RESPONSE AT $\mu_0 = .2$; PITCHING MOMENTS ARBITRARILY MULTIPLIED BY THREE

(c) Improvement of Initial Response Characteristics in Forward Flight

In forward flight as in hovering, it is believed that the helicopter should have a short pitching rate response time. However, referring to Fig. 15, it is noted in the case of the sample helicopter that low pitch rate response times can only be obtained by accepting low maximum pitching rates. This deficiency in forward flight response as in the hovering case results from the large ratio of pitching moment of inertia of the sample helicopter to control and damping moments. A considerable decrease in the pitch rate response time for the same maximum pitching rate can be obtained by using a negative normal velocity feedback K'_w in conjunction with a K'_q feedback. However, it is found that none of the devices listed in Table 6 can combine pitching rate and normal velocity feedbacks in the required proportions to obtain the best responses shown on Fig. 14. The gyroscopic bar stabilizer had no K'_w feedback nor does the swash plate spring damper with zero aerodynamic offset. The control rotor, servo flap (at 75% span), Doman head and biased cyclic system introduce positive K'_w feedbacks. Only the floating vane stabilizer introduces a negative K'_w feedback which tends to make the pitching moment variation with normal velocity stable. A stable variation of pitching moment with normal velocity can also be obtained with a horizontal tail and to a lesser extent with a pitch cone coupling device. However, the floating vane, horizontal tail, and pitch cone linkage stabilizers do not provide sufficient change in damping in pitch. Thus it is indicated that optimum improvements in initial response characteristics in forward flight might be obtained with a combination of devices.

A short normal acceleration response time in forward flight would be a highly desirable characteristic. Although the Ref. 4 requirement that the normal acceleration curve become concave downward within two seconds insures that the helicopter will have safe maneuvering stability, it provides for obtaining minimum rather than optimum handling characteristics. More desirable control characteristics would exist if the normal acceleration could be made to level off at an earlier time.

A rapid normal acceleration response in the initial transient is more difficult to achieve than a rapid pitching rate response. This difficulty arises from the fact that the normal acceleration not only depends on the pitching of the helicopter but also on the fuselage angle of attack change due to vertical motion. The normal velocity response is inherently slow because of the low lift curve slope-weight ratio of the helicopter. The only possible method of reducing the normal acceleration response time with existing stabilizing devices is to permit an overshoot in the pitching rate response (e.g., the $K'_q = -.2$ $K'_w = -.0025$ curve on Fig. 14).

4.5 Long Period Responses

The long period responses obtained with individual stabilizing devices can be best seen in the curves given in the next section. The usefulness of approximate formulae for long period characteristics is limited because the relative importance of the equivalent helicopter derivatives depends on the type and magnitude of the feedbacks. Also there are feedbacks which tend to couple the short and long period modes more closely and hence reduce the separation of the roots and impair the validity of approximate formulae.

It can be observed in the next Chapter that the long period responses obtained with the devices which are effective in both hovering and forward flight are not much different for the two conditions. The normal velocity feedbacks obtained in forward flight have a considerable influence on the period of oscillation. However, the devices that produce the largest changes in the normal velocity stability (i.e., the fixed horizontal tail and the floating vane) are effective only in forward flight.

Figure 17 shows the effects of equivalent speed and pitch rate feedback constants and an equivalent autopilot time lag on the longitudinal long period frequency and damping in hovering flight. The real part of the long period root (δ) is inversely proportional to the time to double amplitude (or half amplitude if δ is negative). The imaginary part, ν , is the frequency in radians/second.

From Fig. 17 it is seen that for constant values of the speed feedback gain and time lag the frequency and amplification of the long period are reduced as the rate gain, K'_q , is made more negative. For constant values of the rate gain and time lag the frequency and amplification are increased as the speed feedback gain, K'_u , is made more positive. The effect of introducing a time lag depends on the values of the feedbacks. In general, it is seen that for the range of useful gains and small time lags, the longitudinal long period mode can be made approximately neutrally stable at best.

The ranges of rate feedbacks and time lags shown on Fig. 17 are limited to those found useful in improving the initial response characteristics of the sample helicopter. The positive value of the effective speed feedback constant, $K'_u = .003068$, corresponds to the one obtained with $K_u = 0$ and $K_{\beta_{1_s}} = -.8$. The negative value, $K'_u = -.0004625$, corresponds to halving the stick position speed stability of the sample helicopter.

The effect of an attitude feedback constant, K'_θ , is not shown explicitly, but will be discussed in the next section under "Conventional Autopilot". However, combination of a time lag and a K'_q feedback introduces a small effective attitude feedback as previously mentioned. The effect of a K_w feedback can be seen in the section on the floating vane stabilizer.

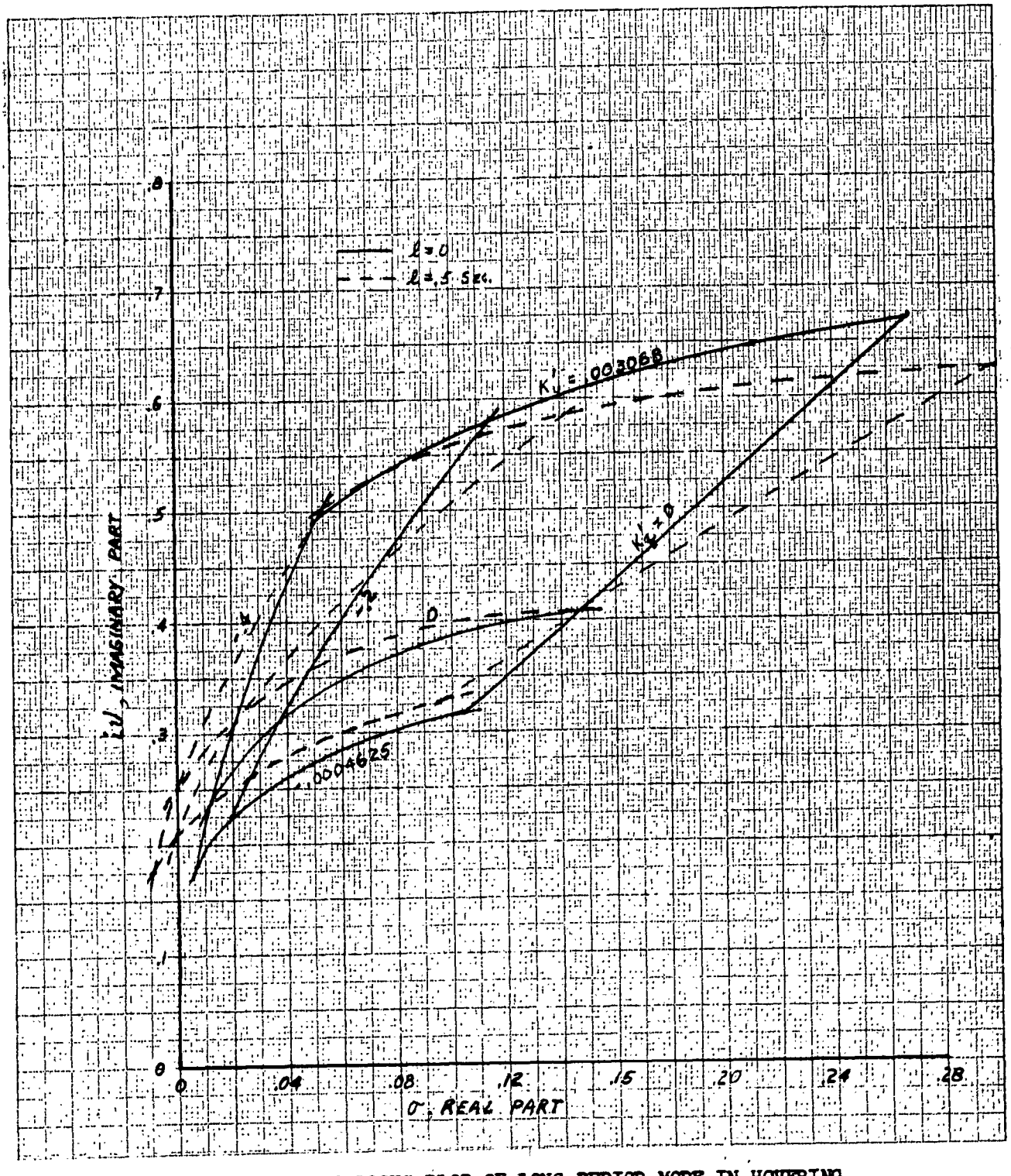

FIG. 17. ROOT LOCUS PLOT OF LONG PERIOD MODE IN HOVERING

5. DISCUSSION OF INDIVIDUAL DEVICES

Sections 4.2 to 4.5 give a general evaluation of existing stabilizing devices without consideration of the specific characteristics of each individual device. In the following sections, detail discussions are given of each individual device and its effect on helicopter stability and control. Although it would be expected that more desirable characteristics might be obtained with a combination of stabilizing devices than with any single device an investigation of this possibility is beyond the scope of the present study.

The discussion of the individual devices is broken down into the following items in most cases:

a) Representation by generalized autopilot equations.

b) Description of mechanism.

c) Description of how device affects stability and control characteristics.

d) Effect of device on the stability and control characteristics of the sample helicopter.

Under (a) the longitudinal control equations required to represent the device are listed using the moving axes system of Table 2. Equations are not presented for lateral cyclic pitch but they would be similar in form to the longitudinal equations. The total longitudinal cyclic pitch, θ_1, is the sum of θ_{1A}, the cyclic pitch due to autopilot feedbacks, θ_{1D}, the direct cyclic pitch due to the stick motion, and θ_{1L}, the cyclic pitch due to stick motion which is affected by a time lag. Control equation (B.67) which is given on Table 2, can be broken down into three equations:

Cyclic due to autopilot feedbacks:

$$\ell \dot{\theta}_{1A} + \theta_{1A} = K_u u + K_w w + K_q q + K_{\dot{w}} \dot{w} + K_{a_{1s}} \beta_{1s} + K_{q_s} \beta_{1s}$$

Cyclic due to stick motion:

Component introduced by direct mechanical linkage:

$$\theta_{1D} = K_D \theta_c$$

Component affected by time lag:

$$\ell \dot{\theta}_{1L} + \theta_{1L} = K_L \theta_L$$

The total steady state cyclic input due to stick motion is:

$$K_D \theta_c + K_L \theta_c = K_c \theta_c$$

The equations listed at the beginning of each section on a particular device indicate which feedbacks the device can provide and this information is also summarized in Table 6. Relations existing between the feedback constants are given in the discussion where applicable.

Physical characteristics of each device are taken up under (b). The stabilizing devices are illustrated, in general, for the configurations presently in use. That is, the pictorial representation of the gyroscopic stabilizing bar is that associated with the Bell two-bladed rotor, the Doman-Frasier Rotor Head is associated with the Doman four-bladed rotor, etc. The helicopter used in this study has three articulated blades and, hence, some of the devices would necessarily be altered if a direct application were to be considered. Since the purpose of this study is to obtain insight into the fundamental principles of the devices, no attempt is made to indicate how the particular mechanisms would be adapted to the rotor configuration of the ship studied.

A non-mathematical explanation of the source of the various feedbacks is included in (c) as well as a description of how the device under consideration affects helicopter stability.

In order to obtain a quantitative idea of the effects of the devices on stability and handling characteristics, a particular helicopter configuration was analyzed in conjunction with each device. The helicopter which was selected is the Sikorsky XHO3S-2 and is reasonably typical of single rotor ships in the 3000 to 8000 lbs. class. The physical parameters for this sample ship are given in Appendix A.

The analytical results presented for the individual devices, as well as those given in Sections 4.2 to 4.5, are based on the numerical values for the stability derivatives given in Appendix A. These derivatives for the sample helicopter were determined in accordance with the equations derived in Part A. Case A.I assumptions of Part A, which included constant rotor speed, collective pitch, and coning angle were used in considering all devices except the pitch-cone coupling stabilizing mechanism. Variations in the collective pitch and coning angles obtained with the pitch-cone linkage were not treated as separate degrees of freedom but are accounted for in the Case A.II derivatives used in studying this device.

It was assumed that all the fuselage moment derivatives of the basic helicopter were zero because of the difficulty of predicting them accurately. If the actual fuselage derivatives were not zero, they could presumably be made zero by the addition of a small tail, and the helicopter modified in this manner could be thought of as the basic configuration.

The characteristics of the sample helicopter with various stabilizing devices are indicated by presenting transient responses of the sample helicopter to abrupt cyclic inputs. Transient responses were obtained for small departures from hovering and cruise conditions by simulating the XHO3S-2 helicopter

on a Reeves Analogue Computer. Two types of responses are presented, one showing initial responses and the other long period characteristics. Initial longitudinal responses which neglected changes in forward speed were obtained simulating equations (A.79), (A.80), (A.81), and (B.67) of Table 2 and recording the outputs on an input-output table. The simulation of initial roll responses in hovering flight was based on roll equations which are analogous to those on Table 2 .

A simulation of the motion of the helicopter including speed changes was carried out using equations (A.46), (A.47), (A.48), (A.49) and (B.6) of Table 1 and the results obtained are used in discussing long period response characteristics. These equations are in terms of a horizontal and vertical axes system but the computer outputs are also labeled in terms of moving axes variables. In order to facilitate the comparison of responses, recorder records obtained at different gains have been superimposed in the presentation of the data obtained for each device.

The initial time histories discussed in Chapters 4 and 5 are presented for maximum control deflections of the pilot's stick. In many cases full step deflections could only be held for a short time without obtaining excessive attitude changes or blade stall, and later portions of the time histories would not be possible with the sample helicopter. For example, the maximum normal acceleration increment of the sample helicopter without blade stall is approximately $\Delta n = .5$ g at $\mu_o = .2$.

Responses obtained with smaller control deflections would be similar in shape to those given for full control travel and would be valid for longer periods of time.

DISCUSSION OF INDIVIDUAL DEVICES - GROUP I

The basic characteristics of the Group I devices are that they increase the pitch and roll damping of fuselage motions and have time lags in their generalized autopilot equations. The gyroscopic stabilizer bar and the control rotor which are included in Group I are considered in Sections 5.1 and 5.2 respectively. A comparison of these devices is given on p. 81 .

5.1 Gyroscopic Stabilizer Bar (Bell)

(a) Representation by Generalized Autopilot Equations

Cyclic due to autopilot feedbacks:

$$\ell \dot{\theta}_{1A} + \theta_{1A} = K_g g$$

Cyclic due to pilot's stick motion:

$$\theta_{1D} = K_c \theta_c$$

(b) Description of Mechanism:

Figure 18 presents a schematic diagram of the type of stabilizing bar arrangement which was developed by Arthur M. Young and has been used on Bell helicopters. Kelley described this device and gave the first mathematical analysis of its action in Ref. 5. The two-bladed rotor shown is universally mounted to the shaft and pitches as a unit when cyclic pitch is applied. The method of changing collective pitch has not been indicated on the diagram. The stabilizing bar is mounted to the mast by pivot bearings permitting it to flap and the seesawing or flapping motion is damped by viscous dampers. It can be seen in Fig. 18(b) that the linkage mechanism is arranged in such a manner that the rotor cyclic pitch is equal to the sum of two terms, one proportional to swash plate tilt and the other proportional to the seesaw motion of the stabilizing bar. From a study of the linkage system, it is obvious that the stabilizing bar is only effective for a fixed stick configuration. Thus friction or an irreversible mechanism must be incorporated in the swash plate design to react the loads in the control system produced by bar motion. It is also apparent that the same feedback constants are obtained in pitch as in roll.

(c) Description of How Device Affects Stability and Control Characteristics

It is convenient to make use of the concept of a bar tip path plane in considering the stabilizer bar. The plane of bar rotation can be thought of as a second swash plate and when the actual swash plate remains fixed perpendicular to the shaft the rotor control plane tilts relative to the shaft in accordance with changes in the tilt of the bar tip path plane. The rotor control plane is perpendicular to the no feathering axis and is the plane of an equivalent swash plate linked directly to the rotor which would produce the same cyclic pitch as the combined effect of the actual swash plate and any stabilizing device which is present.

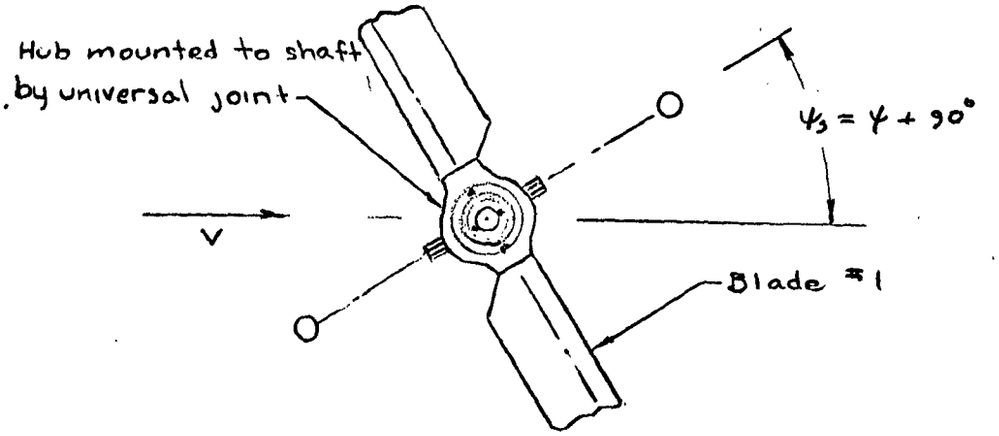

a) Top View of Rotor and Stabilizer Bar

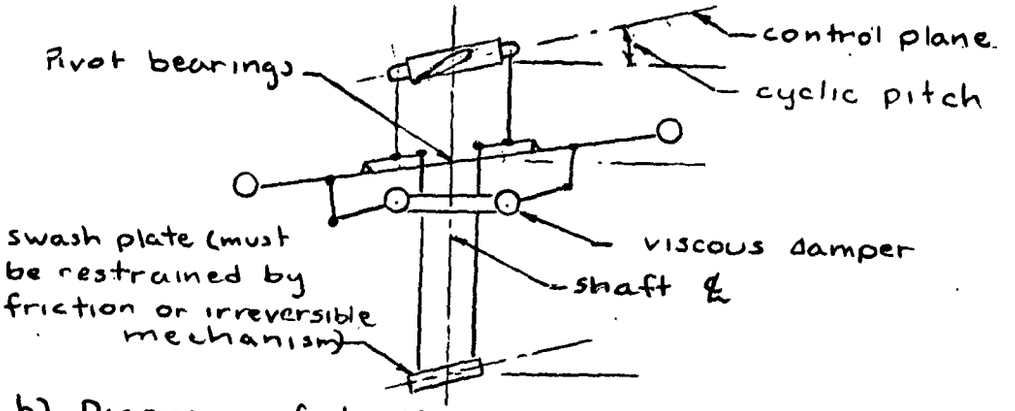

b) Diagram of Linkage Mechanism

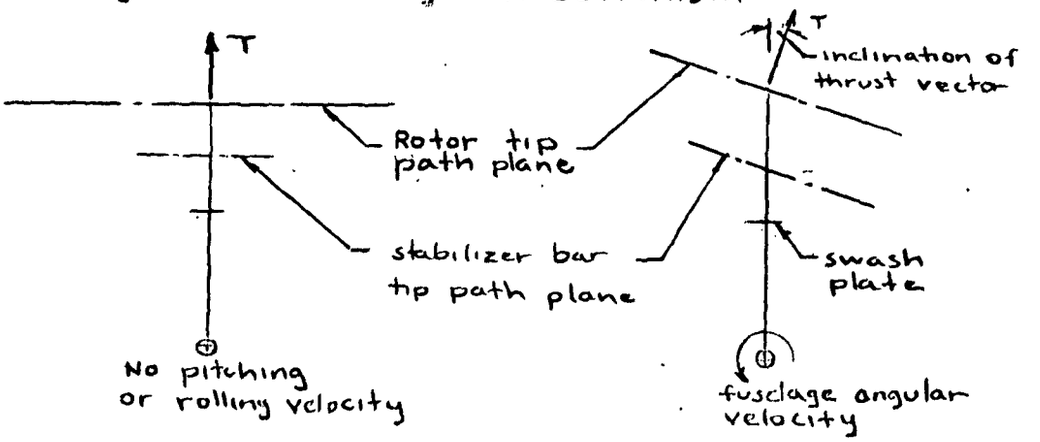

c) Equilibrium Positions of Bar When Bar Dampers are Used

FIG. 18. SCHEMATIC DIAGRAM OF BELL STABILIZER BAR

If there were no bar dampers, and control loads and bearing friction were neglected, tilting the shaft would have no influence on the plane of rotation of the stabilizing bar since no moment would be applied through the bar pivot bearings. In this case, the cyclic pitch feedback introduced by the stabilizing bar would be proportional to the attitude of the helicopter. However, a different cyclic pitch feedback is obtained with bar dampers which is the configuration that has been adopted in successful applications of this device. Then the equilibrium position of the bar tip path plane is perpendicular to the shaft when there is no fuselage angular velocity. If the bar were displaced from this plane and released, the resulting seesawing motion would be damped out by the bar dampers. However, it is important to note that the equilibrium position of the bar tip path plane is not perpendicular to the shaft when the helicopter fuselage and shaft have a constant pitching or rolling velocity. At an equilibrium condition, both the bar plane and shaft must have the same angular velocity but the bar plane is tilted back by a constant angle relative to a plane perpendicular to the shaft (see Fig. 18(c)). This backward tilt results from the fact that a rotating bar has gyroscopic properties, and a constant angular velocity of the bar tip path plane cannot be maintained without an applied moment. The moment necessary to maintain this constant precessional velocity is supplied by the bar dampers. The required moment is proportional in magnitude to the tilting velocity of the bar tip path plane while the moments produced by the bar dampers are proportional to the tilt of the bar plane relative to the shaft. It follows that the aft tilt of the bar plane shown on Fig. 18(c) is proportional to the pitching velocity (q) and is the source of the K_q feedback in the bar control equation. The corresponding tilts of the control plane and thrust vector which are also proportional to angular velocity are indicated on Fig. 18(c). It can be seen that the tilt of the thrust vector produces a moment about the c.g. tending to reduce or damp the fuselage angular velocity. The principal change the stabilizer bar produces in the inherent stability characteristics of the helicopter for conventional bar settings is a considerable increase in the damping in pitch and roll and a corresponding reduction in the pitch and roll rate response times.

When a linkage system of the type shown on Fig. 18(b) is used, neither the pilot's cyclic input nor the control power is altered by the presence of the stabilizing device. Thus the higher damping of pitching and rolling motions decreases the control sensitivity of the helicopter and the equilibrium angular velocity obtained with a given control movement.

It is pointed out in Section 2.2 that the period of the slow mode of oscillation of the helicopter becomes longer when the damping in pitch is increased without changing the speed stability derivative. Since the stabilizer bar does not provide a speed feedback, it would be expected that the increased damping discussed above would lengthen the period of slow mode oscillations, making them less noticeable to the pilot.

The gyroscopic properties of the bar have another important effect on the cyclic pitch feedback. They are responsible for a time lag before the bar plane assumes a new equilibrium position following a sudden change in fuselage

attitude or angular velocity. This characteristic explains the time lag constant (ℓ) in the control equation. During dynamic oscillations, the time lag has the effect of making the cyclic pitch feedback have a small attitude component as well as the rate component which is discussed for the constant angular velocity case. If this attitude component were not present it would not be possible in most cases to stabilize the long period mode of a helicopter by use of a gyroscopic bar alone.

The stabilizer bar has no effect on the angle of attack stability derivative of the helicopter, but the added pitch damping tends to reduce the tendency of the helicopter to diverge in pitch in a pull-up maneuver, (i.e., the maneuver stability is increased). Other effects of the stabilizing bar in pull-up maneuvers are discussed in connection with the REAC studies made for the sample helicopter.

A degree of freedom is added by the stabilizer bar and, consequently, another root appears in the characteristic stability equation of the helicopter. It is found that for certain ranges of parameters the bar root can combine with the basic helicopter roots to give an objectionable high frequency mode. The nature of the oscillation is most easily seen for the hovering case when there is a one-to-one linkage ratio between bar flapping and cyclic pitch change such that the rotor tip path plane tends to remain parallel to the bar plane. When the time lag of the bar is very large, the bar plane remains nearly horizontal in space when the fuselage pitches or rolls. The rotor plane being parallel to the bar plane, remains horizontal and the thrust vector is nearly vertical. Thus when the helicopter pitches or rolls, the thrust vector exerts a restoring moment about the c.g. making an oscillatory mode possible similar to that shown on the diagram below.

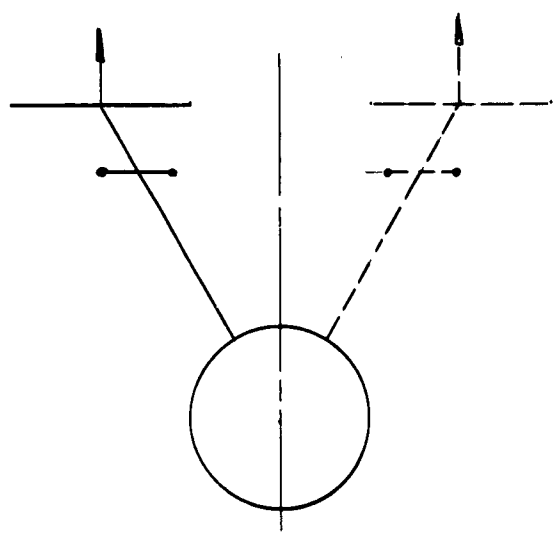

Fig. 19 Short Period Roll Oscillation
Possible with Large Bar Time Lag

(d) Effects of Gyroscopic Bar Stabilizer on the Stability and Control Characteristics of the Sample Helicopter

Although the gyroscopic stabilizer bar as used on two-bladed Bell helicopters could not be applied directly to the three-bladed XH03S-2 helicopter, a number of schemes have been suggested for using stabilizer bars with three-bladed rotors. Also basic helicopter derivatives similar to these obtained for the XH03S-2 could presumably be obtained with a two-bladed rotor which further justifies using the control equation derived for the two-bladed rotor in conjunction with the sample helicopter. It is shown in Part A that the bar time lag and rate constants are related as follows:

$$K_q = -P\ell$$

P = cyclic pitch angle produced by a unit flapping angle of the bar.

Current production models of single-rotor Bell helicopters have used values of P of approximately .9 but the characteristics obtained with a number of different P's were included in the REAC studies. Also responses were obtained for some time lags and rate feedback constants which are in considerable variance with those which are now in use.

Initial Response in Hovering:

Expressions are given on p. 40 for the pitch and roll rate response times and maximum pitching and rolling rates as functions of equivalent autopilot gains. Plots of these quantities for the case of the sample helicopter are given on Fig. 10, p. 41 which show the reduction in the response times and maximum pitching and rolling rates as the magnitude of the rate feedback gains K_q and K_p are increased. Negative feedback constants are required to increase the damping.

These curves can be used to predict the handling qualities obtained with the rate feedback provided by the gyroscopic bar. It is found in the case of the sample helicopter that if a large enough rate feedback is selected to give a pitch response time less than one second, the maximum pitching and rolling rates available are considerably lower than the acceptable minimum of .5 rad/sec. This condition arises from the low ratio of the control power of the sample helicopter to its pitching moment of inertia and is a deficiency that cannot be corrected by increasing the damping in pitch. Thus compromises must be made in applying the stabilizer bar to the sample helicopter.

As previously noted, Fig. 10 was prepared using quasi-static assumptions in treating blade motion, neglecting speed changes, and assuming a zero generalized autopilot time lag. It was realized that the use of a zero autopilot time lag is not a realistic assumption in many stabilizer bar applications and Fig. 20 was prepared to show how the initial response in hovering is modified by the presence of a time lag. Longitudinal flapping was treated as a separate degree

of freedom in obtaining the time histories shown but changes in forward velocity were neglected. Responses are presented for both pitch and roll since the same bar constants must be applied for both cases. Although one set of constants may seem desirable from the pitch response standpoint, it may be precluded by undesirable characteristics found in the roll response for the same feedback gains. All curves shown on Fig. 20 are the responses to a step change in cyclic pitch by the pilot. The values of cyclic pitch change used are the maximum possible for the sample helicopter or $K_c \theta_c = 8^\circ$ in pitch and $K_c \theta_c = 6.8^\circ$ in roll. Since the roll input is slightly lower, the corresponding maximum rolling rate is also lower. It should be noted that the time histories obtained with smaller step inputs would have the same shape as those presented on Fig. 20. Full control deflections could be applied for no longer than one or two seconds without giving excessive pitch or roll angles.

The pitch and roll rate responses obtained with a rate feedback gain of -.1 sec. are given by time histories (a) and (b) respectively while time histories (c) and (d) are the responses obtained with a rate feedback of -.3. Curves for zero time lag are presented for roll as a limiting case although they could not be obtained with an actual stabilizer bar. The introduction of a time lag does not influence the steady state pitching and rolling rates approached but produces some speed up in the initial response. For example, at a feedback gain of $K_g = -.3$ the pitch response time is reduced from 1.5 to .95 seconds in going from a time lag of $\ell = 0$ to $\ell = .5$. However, this improvement in the pitching rate response time is only made possible by accepting some overshoot. In addition, the decidedly oscillatory character of the corresponding roll response would probably preclude the use of the .5 sec. time lag.

The cases shown suggest two possible compromises that might be made in applying a stabilizer bar to the sample helicopter. If a time lag of $\ell = .1$ sec. and rate feedback constant of -.1 sec. were used, the equilibrium pitch and roll rates would be .8 and .7 rad/sec. respectively and the pitch and roll response times would be 3 sec. and .5 sec. Although the maximum rates obtained with this set of parameters are acceptable, the long pitch rate response time is considered a serious deficiency. The $K_g = -.3$ sec. case of time histories (c) and (d) might be selected to obtain better response time characteristics but is probably unacceptable to pilots because of the low maximum angular velocities. A low time lag would be selected in conjunction with the -.3 feedback to avoid poorly damped roll oscillations.

Figure 21 is presented to indicate the magnitudes of the errors which are introduced by neglecting forward speed changes in considering initial response characteristics. Curve (a) is the pitch response for $\ell = .5$ and $K_g = -.3$ previously shown on Fig. 20 and Curve (b) is the result of a computer solution which included speed changes. It can be seen that the responses for the two cases are almost identical for the first two seconds which is the period of primary interest from the initial response standpoint.

Initial Response in Forward Flight:

Figure 22 shows how the initial longitudinal response in forward flight is affected by a gyroscopic stabilizer bar. Pitching rate and normal acceleration time histories are presented which were obtained on the computer including the coupling of normal velocity and pitching motions but neglecting the change in forward velocity from the initial flight condition. It is interesting to note that in the first two seconds following an aft stick displacement, these pitching rate responses for μ_o = .2 are very similar to the corresponding responses for the hovering case given on Fig. 20. The differences which do exist can be explained by changes in the damping in pitch and control moment derivatives in going from hovering to the μ_o = .2 flight condition and by the presence of a normal velocity derivative in the forward flight case. At μ_o = .2 the unstable pitching moment due to normal velocity is not large enough to cause the unstabilized helicopter to diverge in pitch but greatly increases the steady state pitching rate which the helicopter tends to approach neglecting forward speed changes. On the other hand, the steady state pitching rates which the helicopter tends to approach at feedback gains of K_θ = -.1 and -.3 are fairly close to the hovering values.

μ_o	K_θ	q = Steady State Pitching Rate ($K_c \theta_c = 8^\circ$, Speed Change Neglected)
0	0	1.8 rad/sec.
.2	0	5.5
0	-.1	.8
.2	-.1	1.2
0	-.3	.38
.2	-.3	.45

Evidently the rate feedback increases the damping in pitch by such a large factor that the moments due to normal velocity are comparatively unimportant in establishing the equilibrium pitching rate. As in the hovering case, the pitching rate response time is longer than desired but cannot be decreased appreciably without obtaining undesirably low final pitching rates.

The lower section of Fig. 22 again shows that a marked change in the normal acceleration time history is obtained by the addition of a pitching rate feedback constant. However, it is found that the presence of time lags up to ℓ = .5 sec. does not greatly modify the time histories presented from the zero time lag case of Section 4.4. The normal acceleration curves for both K_θ = -.1 and -.3 become concave downward within two sec. after a step stick deflection.

The initial jump in normal acceleration at time t = 0 due to the abrupt increase in swash plate angle of attack produced by an aft stick deflection can be seen on Fig. 22. A further increase in swash plate angle of attack due to pitching of the helicopter produces a gradual build up in normal acceleration in the case of the unstabilized helicopter. However, it is pointed out in Section 4.4 that a rate feedback with zero time lag causes the control plane to tilt forward initially more rapidly than the fuselage pitch angle increases. As a result, the control plane (i.e., effective swash plate) angle of attack is reduced and there is a dip in the normal acceleration response. It can be seen from the time histories on Fig. 22 that this dip can be reduced by using a time lag which delays the initial generalized autopilot cyclic input.

Long Period Response:

The previous discussion has been concerned with the initial response characteristics of the sample helicopter when stabilized by a gyroscopic bar. Next the effect of the stabilizer bar on the long period response is considered making use of the results of analogue computer studies which included speed change. Figures 23 and 24 show time histories obtained with the computer for bar time lags of ℓ = .05 and .5 sec. respectively. As might be expected, the periods of slow mode oscillations are found to increase with rate feedback constant due to the increase in damping in pitch. The period varies approximately as the square root of the damping in pitch as shown on p. 23. Another notable change is that the stability of the long period mode is improved by increasing the rate feedback gain and neutral stability is approached at a feedback of K_ℓ = -.3.

It also can be seen on Fig. 23 that in the first few seconds following a control input, the slope of the pitch attitude curve (i.e., the pitching rate) becomes lower with increasing gain as pointed out in discussing the initial response. It would probably be necessary to choose a feedback constant of K_ℓ = -.3 or lower on the basis of initial response considerations. As a result, a somewhat divergent long period oscillation would exist. A small degree of long period instability has not been found very objectionable in contact operations and would become less noticeable to the pilot with increase in period.

The long period frequency and damping for a given time lag and gain are slightly lower at μ_o = .2 (Figs. 25 and 26) than at μ_o = 0 (Figs. 23 and 24), but, in general, the attitude and speed responses for the hovering and cruise cases are quite similar assuming there is no tail surface present. However, there are changes in normal velocity and altitude during long period oscillations in forward flight which do not exist in hovering.

It is believed, on the basis of the initial response data presented on Fig. 20, that desirable stabilizer bar time lags for the sample helicopter should be below .5 sec. This range includes the .05 to .15 sec. bar time lags which were used in tests of a typical stabilizer bar-helicopter configuration reported in Ref. 6 . However, some references on the gyroscopic bar have

indicated that satisfactory operation might be obtained with bar time lags and rate gains of the order of one sec. Although it would be expected that these bar parameters might lead to undesirable initial handling characteristics in the case of the sample helicopter, it is of interest to see how they affect the long period. Figures 27 and 28 present responses obtained for the XH03S-2 helicopter with a 1 sec. bar time lag and a series of different rate feedback gains. It will be noted that at gains higher than $K_q = -.6$ the helicopter is stable and the periods of slow mode oscillation are very long. As expected, the initial responses for the cases shown have a number of shortcomings. In particular, an oscillatory mode is apparent in the cyclic pitch trace. Although the short period mode produces little distortion of the attitude and speed response, it is believed it could be objectionable to the pilot. This is particularly true in forward flight where the high frequency component is apparent in the normal acceleration response (see Fig. 28).

Several authors have pointed out that the cyclic pitch introduced by a stabilizer bar during sinusoidal oscillations of the fuselage can be represented by a zero time lag autopilot with pitch rate and attitude feedbacks. It is found that the ratio of these equivalent attitude and rate feedbacks is equal to $\omega^2 \ell$ where ω is the frequency of the sinusoidal oscillations ℓ and is the actual time lag of the stabilizer bar.* The frequency of the long period oscillations on Fig. 27 are of the order of $\omega = .3$ rad/sec., and it is evident that the attitude component is very small even with a one sec. time lag. Since it is well known that good stabilization of the long period mode can be obtained with a conventional helicopter autopilot with an appreciable attitude feedback, it is of interest to determine if a similar condition would exist if the attitude feedbacks obtained with the bar were increased in magnitude. Figure 29 indicates time histories for a combination of constants which gives a much higher effective attitude feedback.

In this case, a very long time lag, $\ell = 5$ seconds, is used in conjunction with a fairly high rate gain, $K_q = -.75$. This combination of constants results in a large increase in the period of the short mode which is the dominant oscillation in the time histories. The response for the first three seconds does not differ appreciably from the one obtained for the unstabilized helicopter.

A well-damped long period response is obtained as evidenced by the fairly rapid but nearly critically damped speed response. The maximum steady pitching rate which can be maintained with these settings is very low and, as a result, the steady turn performance of the helicopter would be seriously reduced.

*Substituting $\theta_{1A} = \theta_{1A} e^{j\omega t}$ and $q = j\omega \Theta e^{j\omega t}$ into

$$\ell \theta_{1A} + \theta_{1A} = K_q q$$

gives $\theta_{1A} = \left[\frac{K_q}{1+\omega^2\ell^2}\right] q + \left[\frac{K_q \omega^2 \ell}{1+\omega^2\ell^2}\right] \Theta = [K_q]_{EQUIV.} q + [K_\Theta]_{EQUIV.} \Theta$

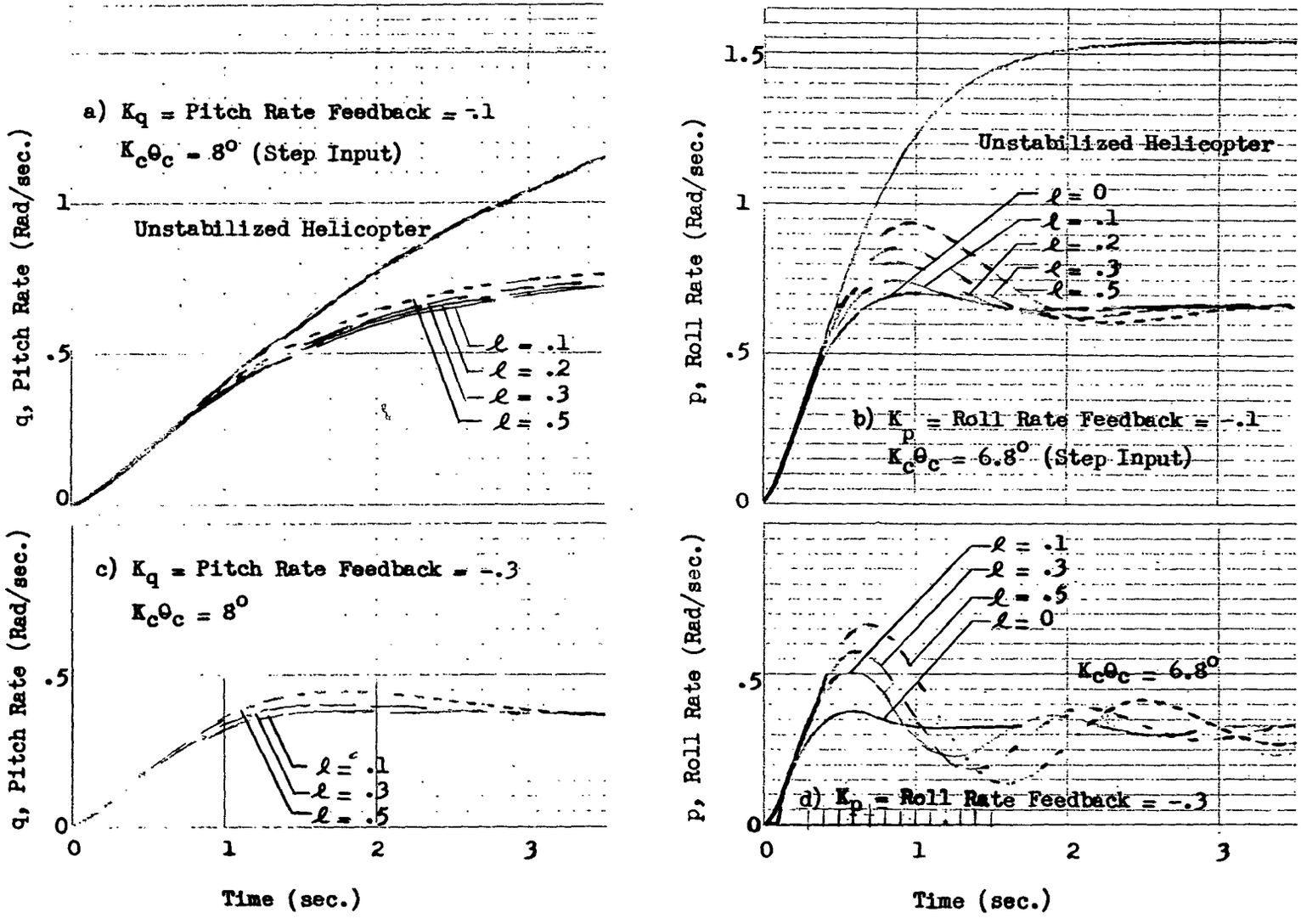

FIG.20 GYROSCOPIC STABILIZER BAR, INITIAL RESPONSES TO LONGITUDINAL AND LATERAL STEP INPUTS; HOVERING.

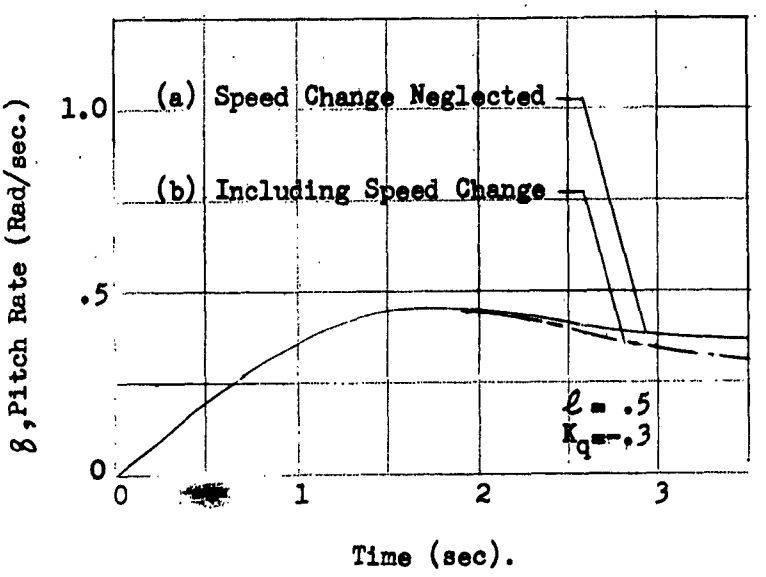

FIG. 21. GYROSCOPIC STABILIZER BAR; EFFECT OF FORWARD SPEED CHANGE ON INITIAL RESPONSE

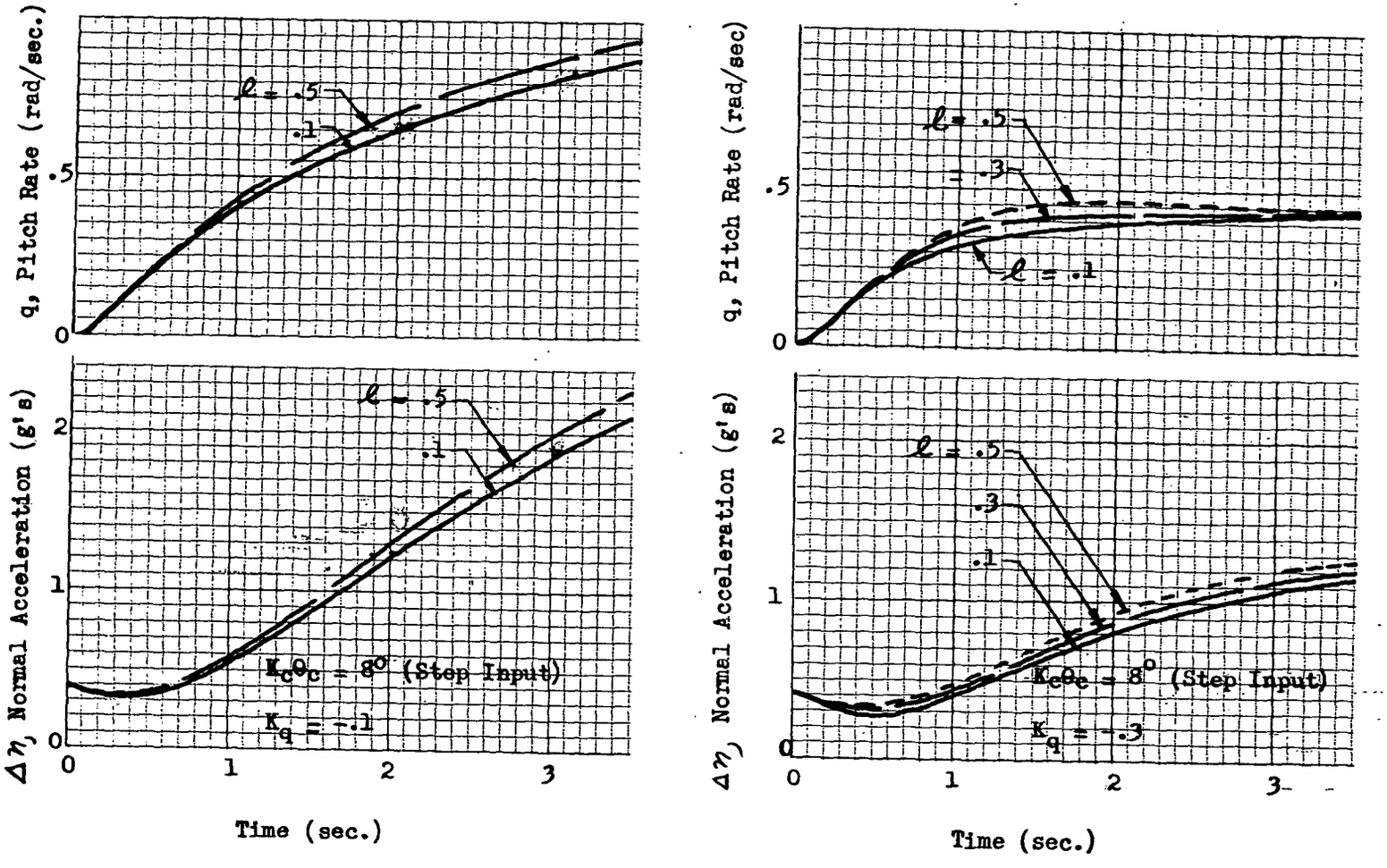

FIG.22 GYROSCOPIC STABILIZER BAR; INITIAL LONGITUDINAL RESPONSES TO STEP CYCLIC PITCH INPUTS; $\mu_o = .2$

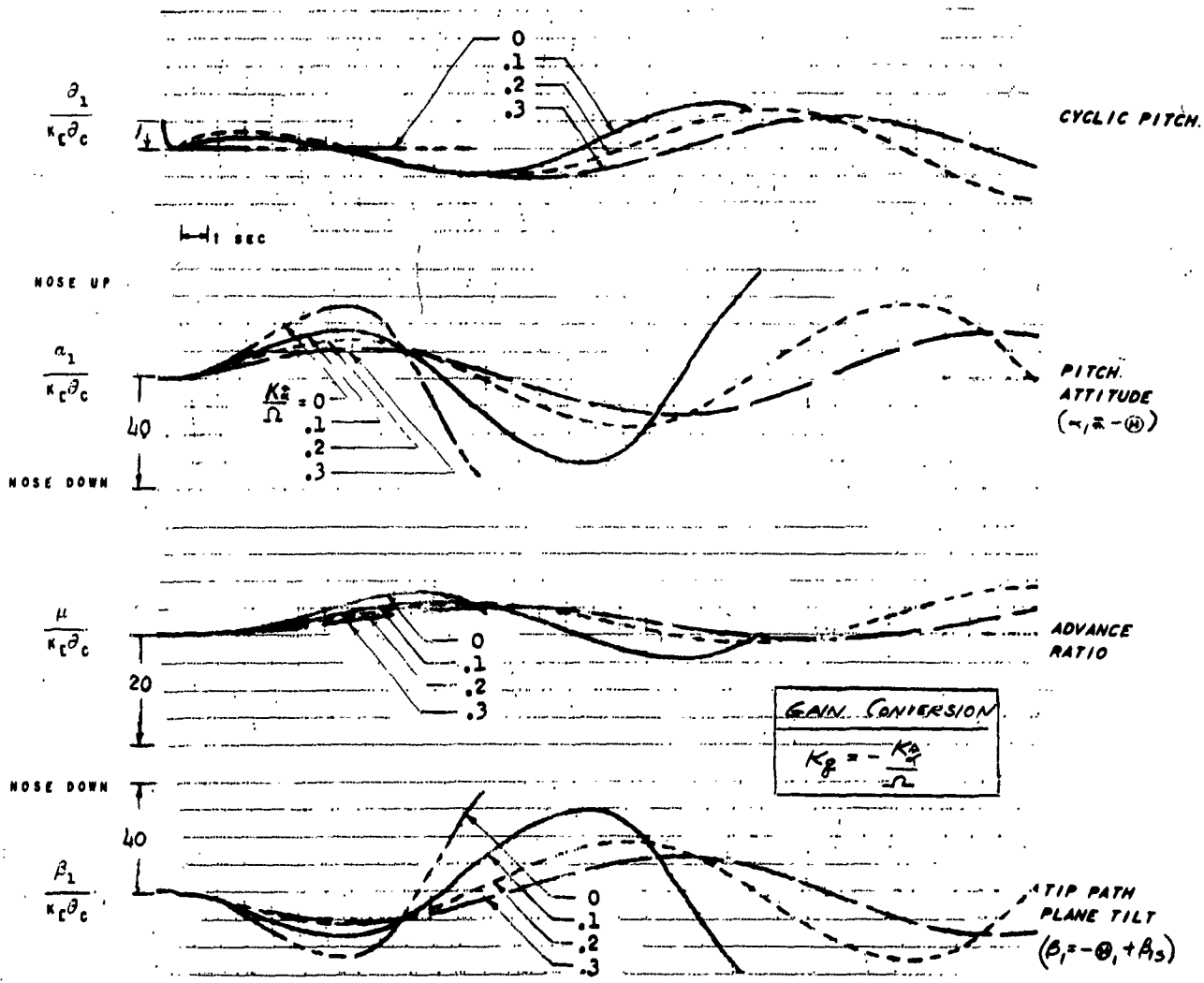

FIG. 23. GYROSCOPIC BAR STABILIZER; HOVERING; ℓ = .05 SECONDS

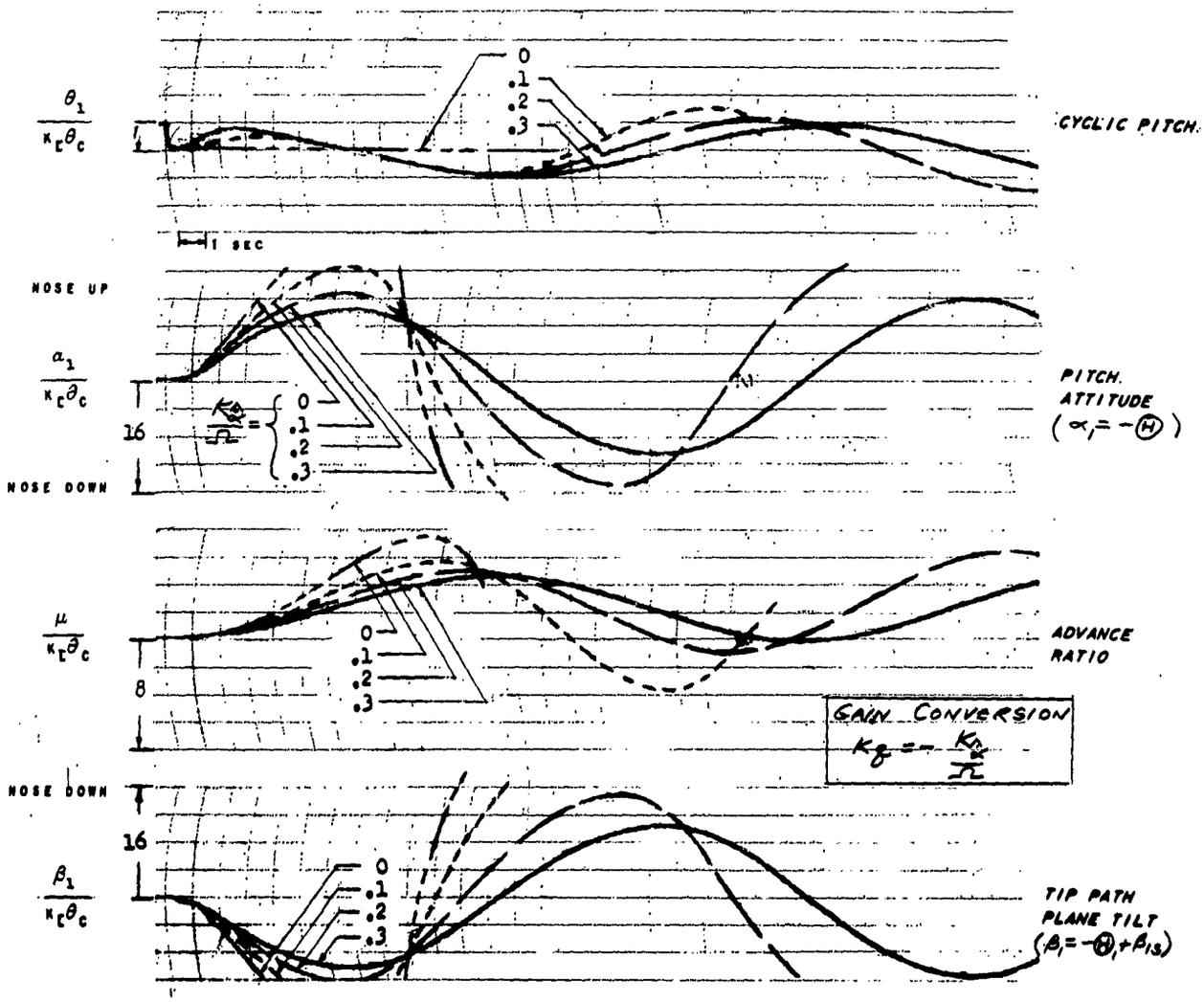

FIG. 24. GYROSCOPIC BAR STABILIZER; HOVERING; ℓ = .5 SECONDS

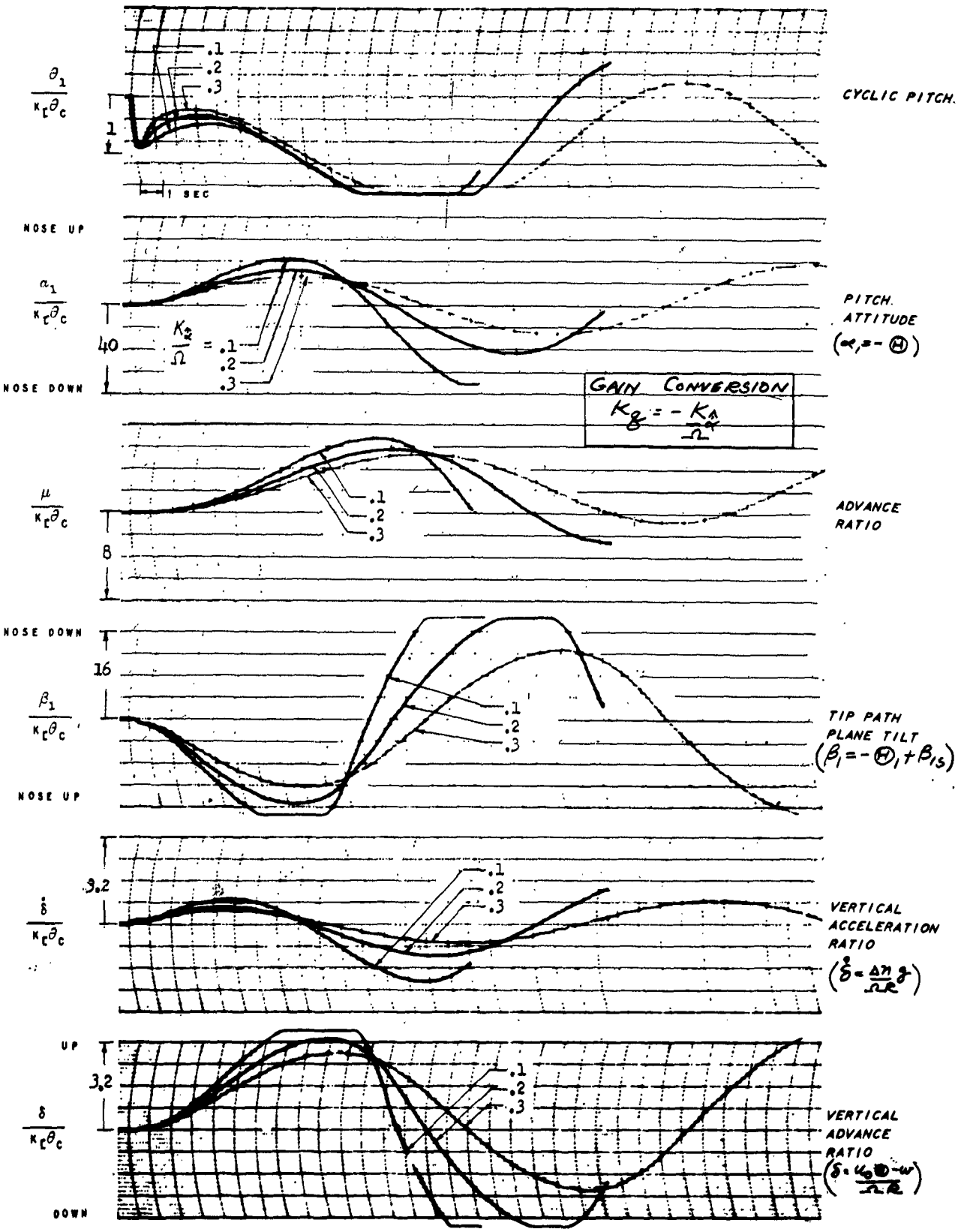

FIG. 25. GYROSCOPIC BAR STABILIZER; $\mu_o = .2$; $\ell = .05$ SECONDS

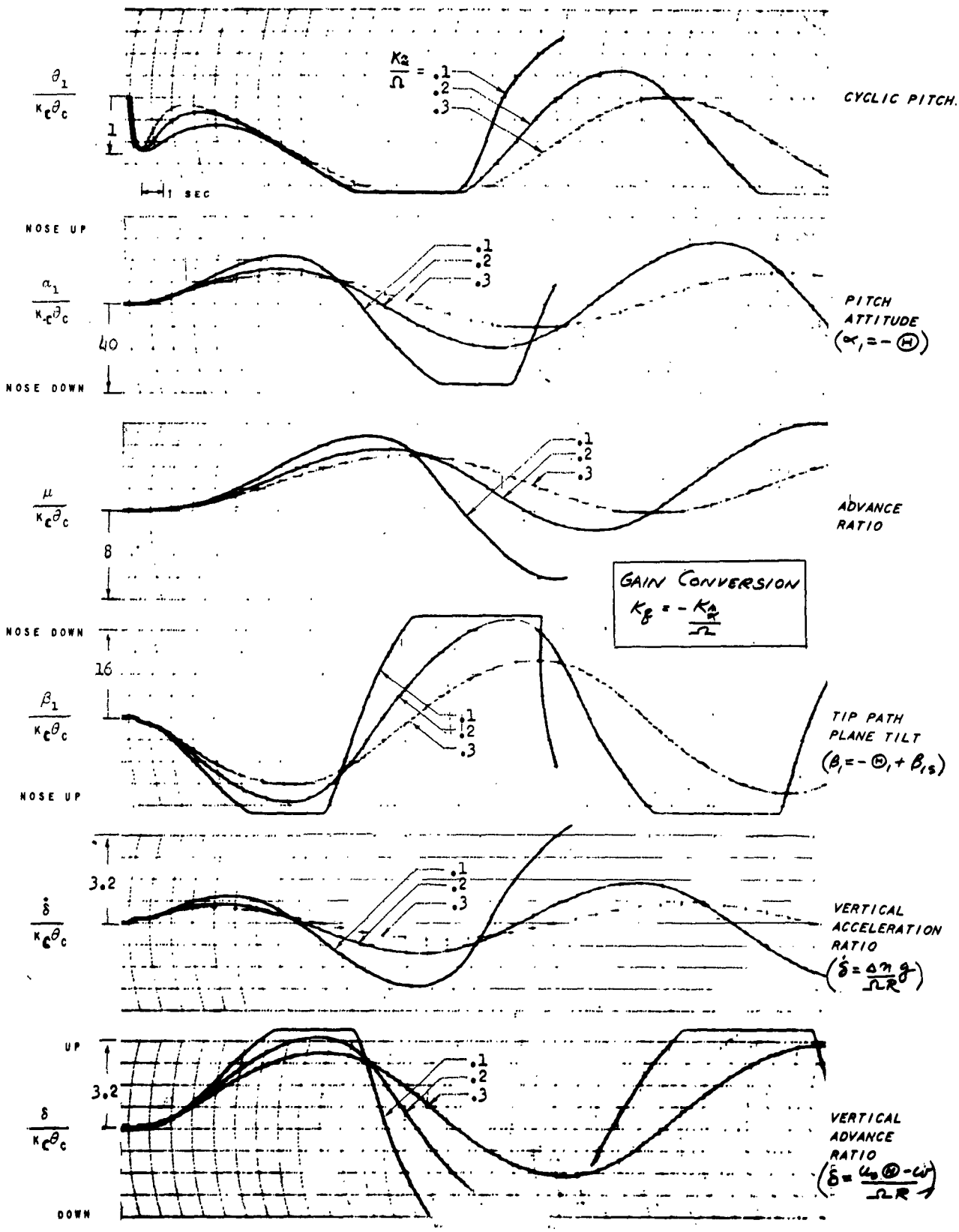

FIG. 26. GYROSCOPIC BAR STABILIZER; $\mu_0 = .2$; $\ell = .5$ SECONDS

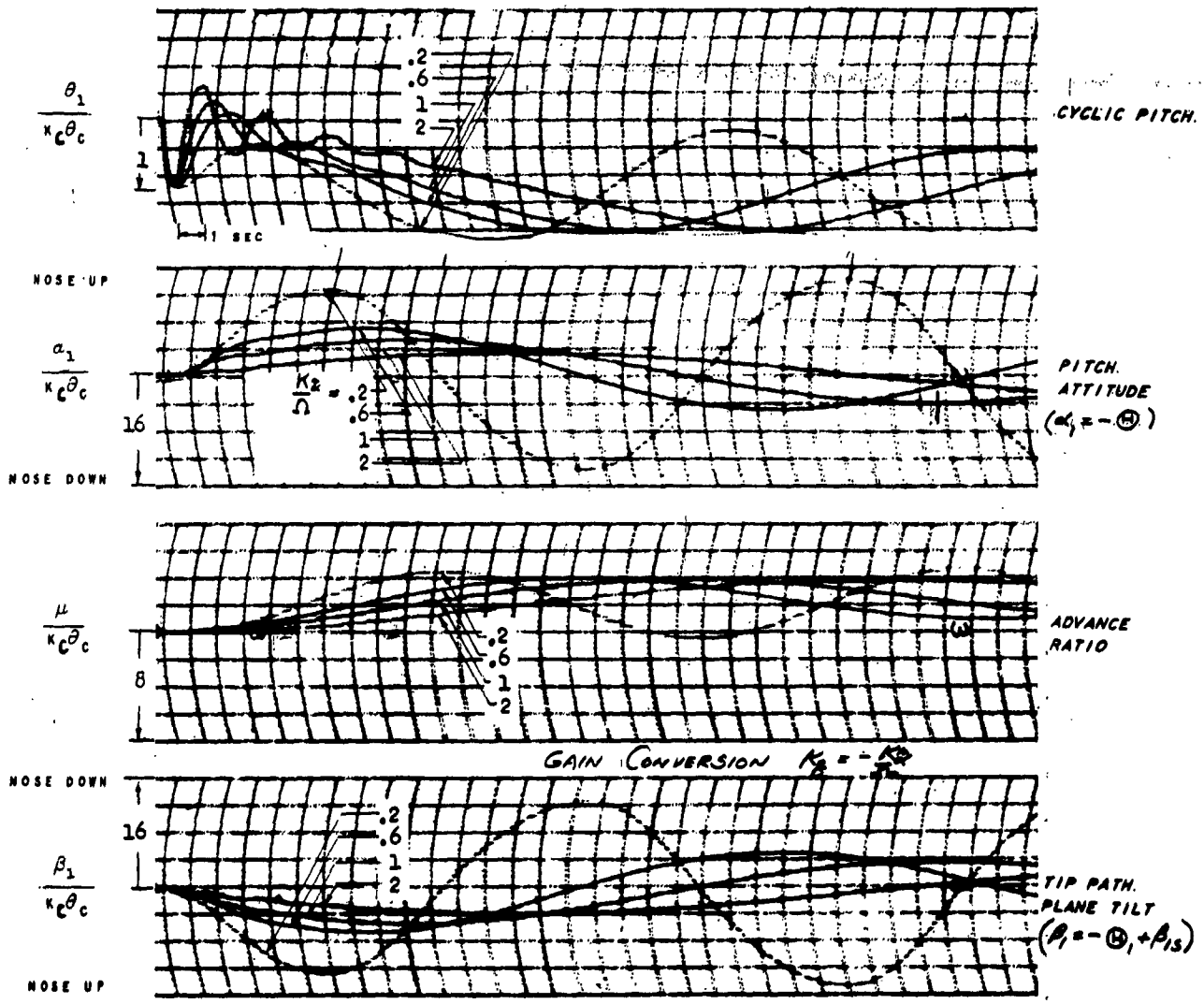

FIG. 27 . GYROSCOPIC BAR STABILIZER; HOVERING; ℓ = 1 SECOND

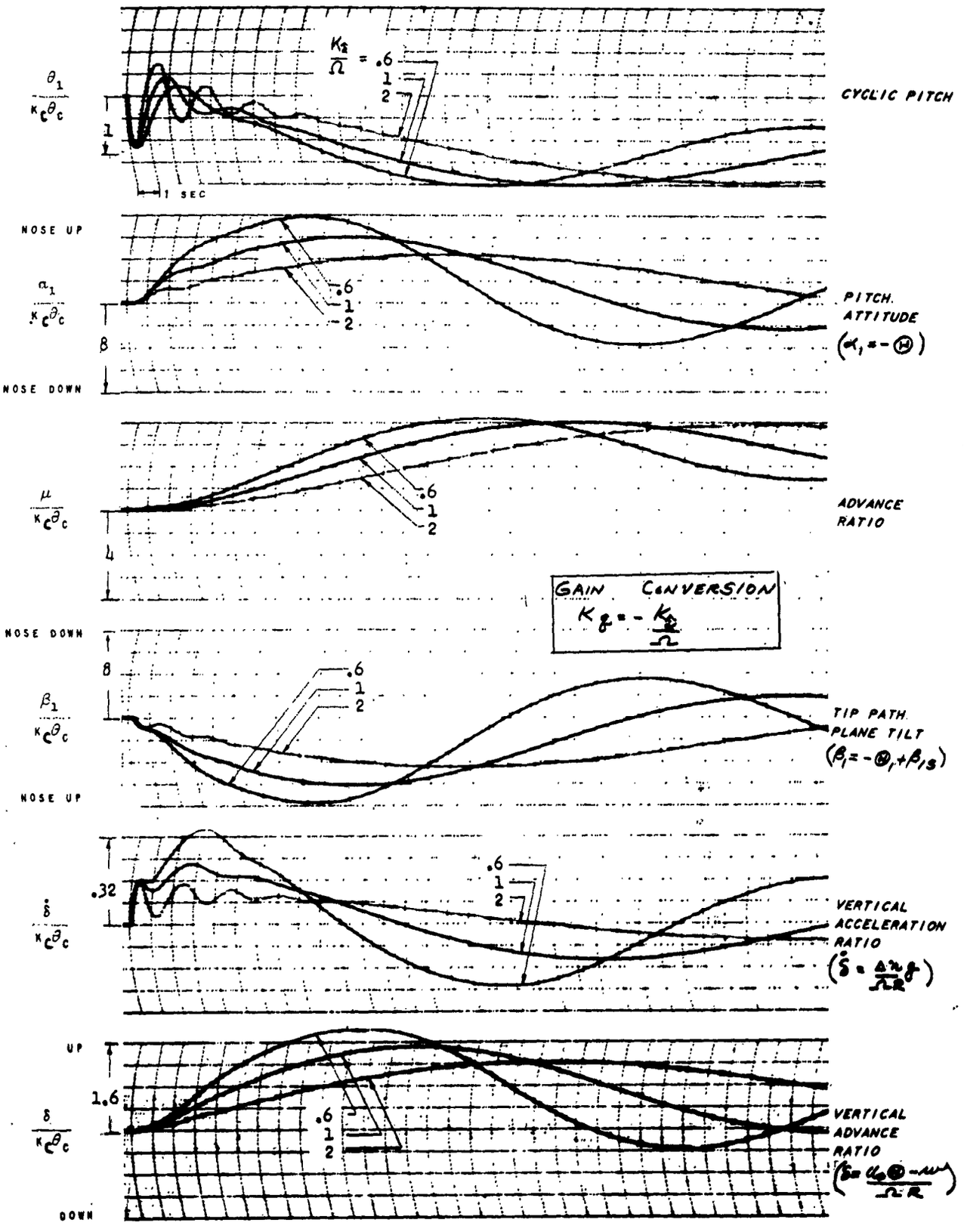

FIG. 28. GYROSCOPIC BAR STABILIZER; $\mu_0 = .2$; $\ell = 1$ SECOND

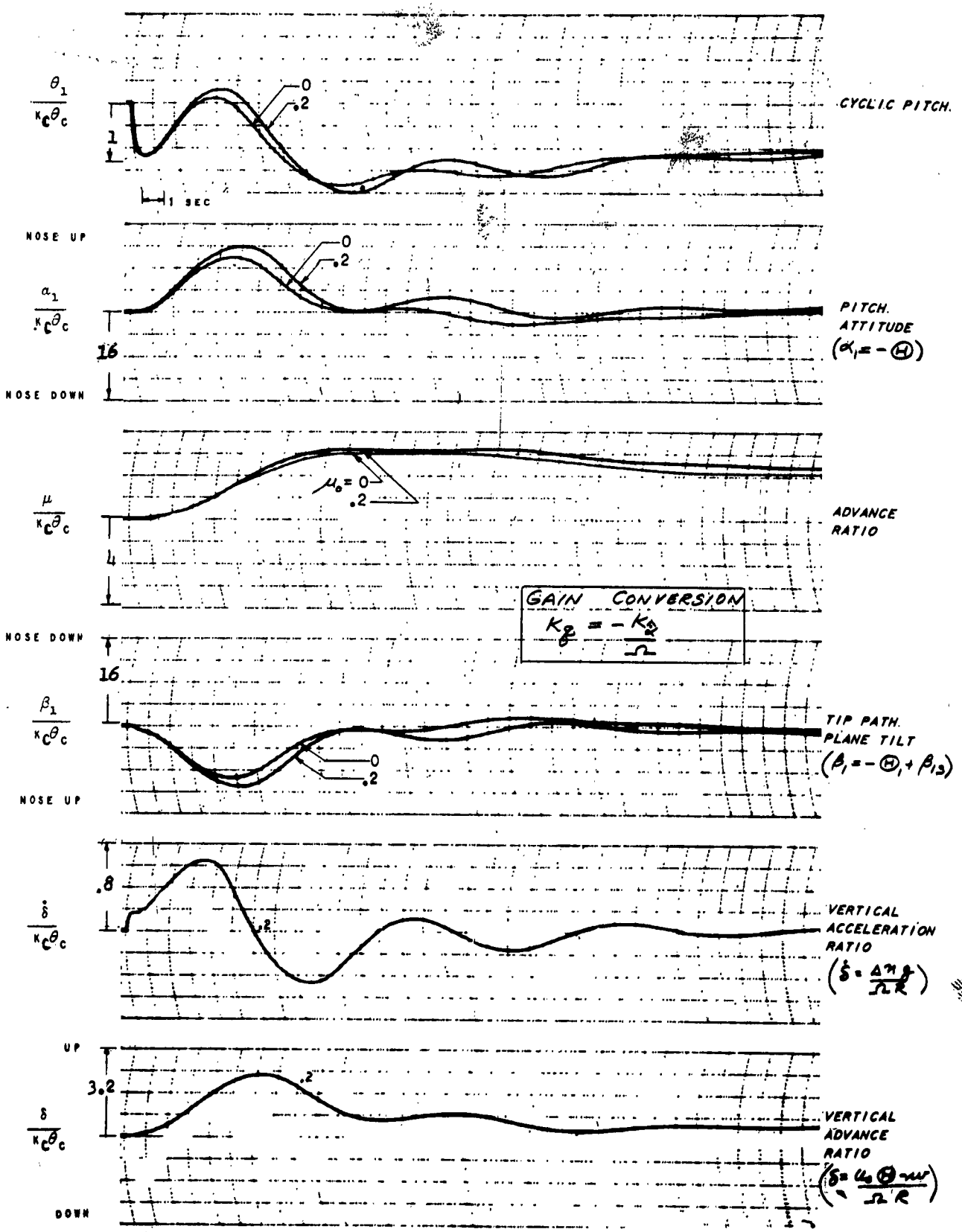

FIG. 29. GYROSCOPIC BAR STABILIZER; l = 1 SECOND; $\frac{K_2}{\Omega}$ = .75

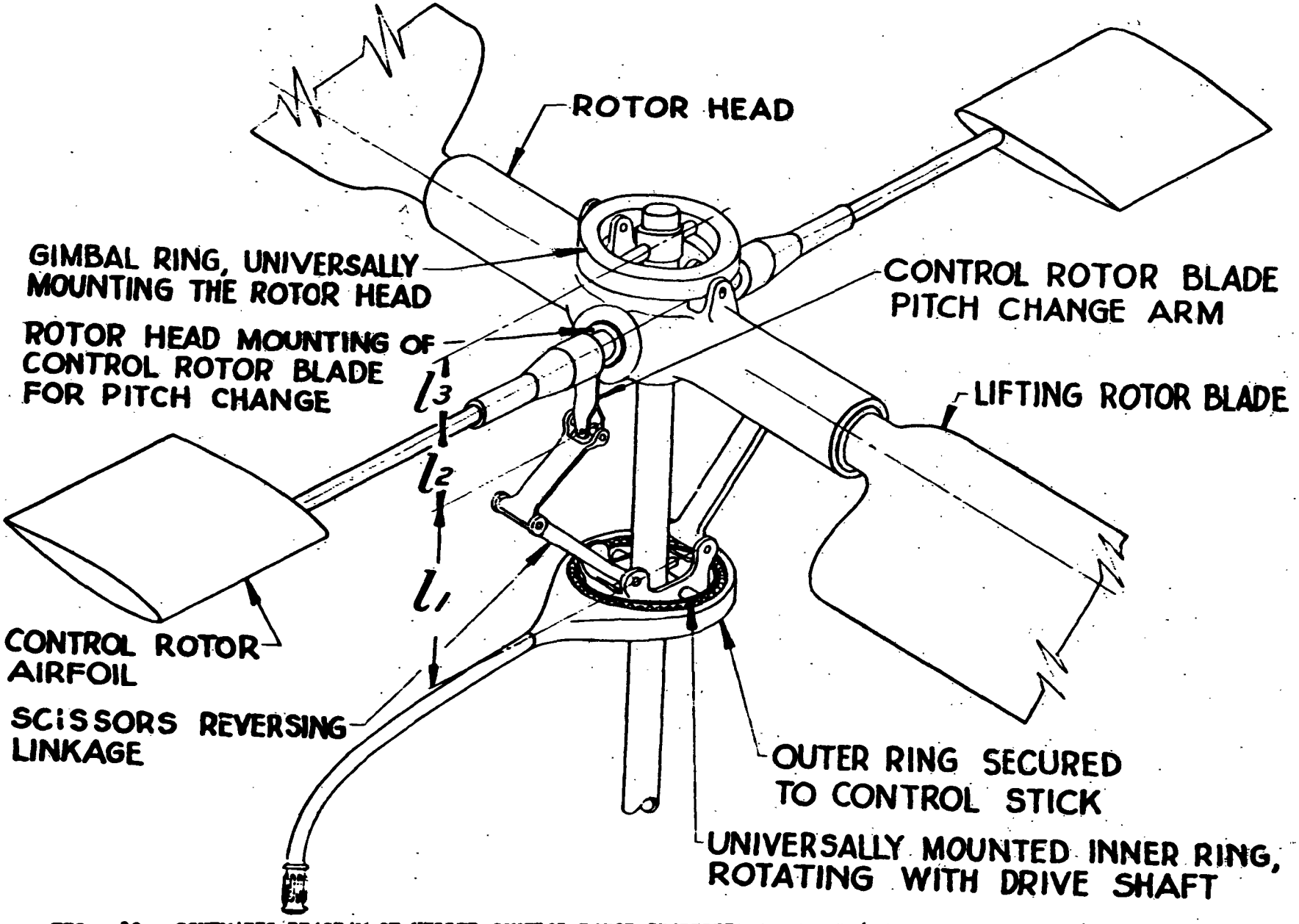

FIG. 30. SCHEMATIC DIAGRAM OF HILLER CONTROL ROTOR STABILIZING DEVICE (TAKEN FROM REF. 7)

5.2 Control Rotor Stabilizer (Hiller)

(a) Representation by Generalized Autopilot Equations

Cyclic due to autopilot feedbacks:

$$\ell \dot{\theta}_{1A} + \theta_{1A} = K_u U + K_w W + K_q q + K_{B_{1S}} B_{1S}$$

Cyclic due to pilot's stick motion:

$$\ell \dot{\theta}_{1L} + \theta_{1L} = K_c \theta_c$$

(b) Description of Mechanism

A schematic diagram of the Hiller control rotor linkage taken from Ref. 7 is presented in Fig. 30 in order to indicate the operation of this mechanism. It will be noted that when the pilot tilts the swash plate he does not directly change the cyclic pitch input to the main lifting rotor but instead puts cyclic pitch into the control rotor. A scissors reversing linkage was adopted in the Hiller configuration to apply cyclic pitch to the control rotor using an approximately vertical pitch change arm instead of the more conventional push-pull rod horizontal pitch change arm arrangement.

The flapping of the control rotor blades in response to the applied cyclic pitch produces an equal main rotor cyclic pitch change when the control rotor is mounted on the main rotor hub. A more general control rotor system than the one shown in Fig. 30 would be possible in which the constant of proportionality between control rotor flapping and main rotor cyclic pitch would be different from unity. A system of this type might be obtained by pivoting the control rotor directly on the shaft similar to the arrangement used with the Bell Stabilizer Bar.

The control rotor shown, on Fig. 30 is mounted a distance ℓ_3 below the flapping axis of the main rotor. Thus when the swash plate is fixed, a flapping of the main rotor causes translation of the control rotor axis and introduces control rotor cyclic pitch.

(c) Description of How Device Affects Stability and Control Characteristics

The characteristics of the control rotor stabilizer were first analyzed by Stuart in Ref. 7 . The principal advantage given for the use of a control rotor was an increase in the rolling and pitching damping of the helicopter. Another advantage for using a servo rotor mentioned in Ref. 7 is that the feedback forces from the main rotor no longer act on the pilot's stick and thus many objectionable stick characteristics of a conventional helicopter without an irreversible boost system are eliminated.

The action of the control rotor can be explained by the main rotor characteristics discussed in Section 2.1. It is pointed out that the damping moment of the unstabilized helicopter in pitch or roll is proportional to the tilt of the main rotor plane relative to the shaft due to a pitching or rolling

velocity of the fuselage. A constant pitching or rolling velocity of the tip path plane of an articulated or seesaw rotor can only be sustained by feathering relative to the tip path plane which produces aerodynamic moments to counteract the gyroscopic blade moments produced by this motion. When the tip path plane is parallel to the control plane (i.e., the effective swash plate), there is no feathering relative to the tip path plane. The required feathering exists, however, when the blades flap relative to the control plane and thus produce an aft tilt of the tip path plane. Stuart defined a "following rate" in this connection as the tilting velocity at which the tip path plane lags behind the control plane by 1 rad. Conventional rotors without tip masses have high "following rates" and remain nearly perpendicular to the control plane at the maximum angular velocities reached by the helicopter.

The control rotor like the main rotor lags behind its control plane in a constant pitching or rolling motion and by so doing produces cyclic pitch of the main rotor. This explains the K_ϕ feedback in the control equation. The plane of rotation of the control rotor may be thought of as the control plane or effective swash plate of the main rotor in the case of the Fig. 30 configuration. Since the control plane of the main rotor is established by the plane of the control rotor, the presence of the control rotor increases the angle the main rotor lags behind the shaft and the damping in pitch and roll. Stuart shows it is practical to obtain high damping with the control rotor by using small low aspect ratio airfoils.

The control rotor responds to changes in forward and normal velocity like any other rotor and these characteristics are accounted for by the K_u and K_w feedbacks in the generalized autopilot representation of this device. The aft tilting of the control rotor with forward speed depends on its collective pitch setting ($\tilde{\tilde{\theta}}_o$) and the magnitude of the K_u feedback can be adjusted by changing $\tilde{\tilde{\theta}}_o$.

The source of the tip path plane tilt or flapping feedback $K_{\beta_{1s}}$ is indicated in the description of the control rotor mechanism. It arises from the control rotor cyclic pitch due to main rotor flapping and is only present when the control rotor is mounted above or below the flapping axis.

The control rotor does not respond instantaneously to changes in μ, w and $\dot{\theta}$. The time lag (ℓ) in the autopilot equation represents the delay in response due to gyroscopic forces. It is also present in the control input equation since the pilot controls the helicopter solely through the control rotor. Reference 7 shows that the cyclic pitch produced by the control rotor during sinusoidal oscillations of the fuselage has a component proportional to fuselage attitude as well as angular velocity because of this time lag. However, at the low frequencies of fuselage oscillations obtained in the long period mode the damping component predominates.

(d) Comparison of Control Rotor and Gyroscopic Stabilizer Bar

In the previous discussion, it has been indicated that the outstanding characteristic of the control rotor similar to the gyroscopic stabilizing bar is to increase the damping of the helicopter in pitch and roll. The planes of rotation of the control rotor and the stabilizing bar tilt relative to the shaft by angles proportional to a steady angular velocity of the fuselage but, in both cases, there is a time lag before this condition is attained. In both cases, the tilt produces moments which balance the gyroscopic moments associated with a constant tilting velocity of the plane of rotation of the control rotor or bar. In the case of the control rotor the required moments are produced by the aerodynamic forces on the control rotor airfoil due to the feathering relative to its plane of rotation. The corresponding moments in the case of the stabilizing bar results from the bar dampers when the bar flaps relative to the mast. A disadvantage of both devices is that the same amount of fuselage damping is added in pitch and roll making it necessary to select system parameters which are usually not optimum for either pitching or rolling.

Since the control rotor acts as a servo, it has the advantage that forces from the main rotor are not transmitted through the control system while in the stabilizing bar system friction or a boost system must be provided below the swash plate to avoid transmitting rotor forces to the pilot. On the other hand, a pilot using a control rotor must put up with a time lag in response to his control movement while the control rotor is changing its plane of rotation. This lag, in response to a control movement applied by the pilot, is avoided with the linkage used on the stabilizing bar shown on Fig. 18.

The operation of the stabilizing bar is essentially the same at all speeds because it does not depend on aerodynamic forces. On the other hand, the K_v and K_w feedback constants of the control rotor will vary with airspeed and can be affected by changes in downwash distribution.

(e) Effect of a Control Rotor on the Stability Characteristics of the Sample Helicopter

The design problems involved in applying the control rotor to the sample helicopter are not considered and it is assumed that the generalized autopilot equations derived for a two-bladed rotor are applicable. In order to limit the number of variables, the following control rotor properties are assumed

$$\frac{2\tilde{R}}{2R} = \frac{\text{control rotor diameter}}{\text{main rotor diameter}} = .4$$

$/-\tilde{B} = .2$ = Span of control rotor paddle in fraction of control rotor radius

When these parameters are substituted into the equations for the control rotor given in Part A, the generalized autopilot constants are found to be related as follows:

$$K_q = -P\ell - hK_v \approx -P\ell$$

$$K_w = 0 \qquad (\mu_o = 0)$$

$$= .00337P \qquad (\mu_o = .2)$$

$$K_{\beta_{1s}} = PX \qquad (\mu_o = 0)$$

$$= 1.33PX \qquad (\mu_o = .2)$$

P is the ratio of main rotor cyclic pitch to control rotor flapping and X is the control rotor cyclic pitch feedback per unit flapping angle of the main rotor. The speed feedback, K_v, depends on the collective pitch angle, trim conditions, downwash, etc. and is difficult to predict theoretically. Values of K_v for several conditions are tabulated below which were computed using the expressions derived in Part A.

Control Rotor Collective Pitch	$\mu_o = 0$ $X = 0$	$\mu_o = .2$ $X = 0$	$\mu_o = 0$ $X = .5$	$\mu_o = .2$ $X = 1$
$\tilde{\theta}_o = 0$	-.00122	-.00117	-.00122	-.00104
$\tilde{\theta}_o = 10^\circ$	+.00122	+.0011	+.00122	+.00122

Initial Response in Hovering Flight:

When it is assumed there is no forward speed increment in the initial response of the helicopter, the speed feedback, K_v, need not be considered. If, in addition, there is no longitudinal flapping feedback, $K_{\beta_{1s}}$, the first autopilot equation for the control rotor on p. 79 reduces to

$$\ell\dot{\theta}_{1A} + \theta_{1A} = K_q q$$

and is identical to the corresponding equation for the gyroscopic stabilizer bar. In this case, the short period response of a helicopter to an external disturbance would be the same with a control rotor or stabilizer bar. However, the responses to a control input would not be the same with the two devices even with identical time lags and rate feedback constants because of differences in the pilot's input. Figure 31 shows the initial response of the sample helicopter stabilized with a control rotor having a time lag $\ell = .3$ sec. and a rate feedback $K_q = -.3$. The corresponding response which was computed for the stabilizer bar is plotted for comparison and two differences between these time histories are apparent. First, the pitching and roll rate build ups obtained with the control rotor are delayed by approximately .3 second which is the magnitude of the time lag in the pilot's input. Secondly, it can be seen that smaller amplitude short period oscillations are

excited with the control rotor probably due to the more gradual application of cyclic pitch. In both cases, the helicopter tends to approach the same steady state angular velocities.

Comparisons of the effects of a control rotor and gyroscopic bar on initial response characteristics at time lags greater than .3 sec. would be similar to those shown on Fig. 31. In particular, a larger delay in the initial response would be noted as the control rotor time lag increased.

It is helpful to refer to the effective autopilot constants discussed in Section 3.2 in studying the influence of a flapping feedback, $K_{\beta_{1s}}$, on the initial hovering response. The positive values of flapping feedback used with the control rotor reduce the pitching and rolling rate feedbacks and effective autopilot time lag. Also the cyclic pitch produced by a given deflection of the pilot's stick is reduced by positive flapping feedback but can be maintained at its original value by changing the linkage constant, K_c.

Referring to the initial responses for the gyroscopic bar in hovering flight shown on Fig. 20, it is seen that they become less oscillatory when the time lag and rate constants are reduced. Time histories for the control rotor would be expected to show similar characteristics although differing somewhat because of the time delay in the pilot's input. Thus it is seen that the use of flapping feedback with the control rotor results in an improvement of the damping of the short period mode.

Initial Response in Forward Flight:

It is pointed out in Section 3.1 that the control rotor contributes to the instability of the helicopter in forward flight with respect to changes in fuselage angle of attack (α_F) and normal velocity ($w = U_o \alpha_F$). At $\mu_o = .2$ the effective normal velocity feedback of the control rotor under consideration is:

$$K'_w = \frac{K_w + (\beta_{1s})_w K_{\beta_{1s}}}{1 - K_{\beta_{1s}} (\beta_{1s})_{\theta_1}} = \frac{.00337 P - .0011 PX}{1 + 1.43 PX}$$

The equivalent normal velocity moment derivative of the sample helicopter including the effect of this feedback is given by

$$\bar{M}_w = 37.8 + 61140 K'_w = \frac{37.8 + 206 P - 13.2 PX}{1 + 1.43 PX}$$

P is equal to one in existing control rotor configurations and various feedback ratios have been tried usually in the range from $X = 0$ to 1. It follows from the above expressions that the addition of such a control rotor to the sample helicopter would considerably increase its unstable normal velocity derivative, $\bar{M}_w$, although by a lesser extent when a positive flapping feedback is present.

Figure 32 shows the initial response of the sample helicopter in forward flight with a control rotor without any flapping feedback. It can be seen that the normal velocity feedback makes curve (a) divergent in spite of a pitch rate feedback $K_q = -.1$. When the pitching rate feedback is increased to $K_q = -.3$, the response is no longer divergent but approaches a quasi-static equilibrium more slowly than in the case of a stabilizer bar. The responses obtained with positive flapping feedbacks would be more favorable than those shown on Fig. 32 but it would be desirable in many cases to use a fixed tail in conjunction with the control rotor to offset its detrimental effects on normal velocity stability.

Although the normal acceleration responses obtained with the control rotor do not become concave downward as rapidly as desired, they do have some desirable characteristics. In particular, it will be noted on Fig. 32 that there is no dip in the normal acceleration time history shortly after the pilot control input.

Long Period Response:

It is found that the time lag in the pilot's input which is obtained with a control rotor has little effect on the long period mode of the helicopter although it is of considerable importance in the initial response. Thus it would be expected that the long period responses of a helicopter stabilized by a control rotor would be very similar to those obtained with bar stabilization for cases with zero speed and flapping feedbacks. Figure 33 indicates long period responses of the sample helicopter with a one sec. time lag, zero flapping feedback, a pitching rate feedback constant ($K_q \approx -1$), and three values of K_u. Although these parameters give an oscillatory short period, the curves shown on Fig. 33 serve to indicate how the long period response is changed by a speed feedback. The time history for $K_u = 0$ is very similar to the corresponding curve for the gyroscopic stabilizer bar. The other two time histories are for feedbacks constants $K_u = -.00122$ and $K_u = +.00122$ which are limits of the constants obtained by using initial control rotor collective pitch angles ranging from 0 to 10°. It is evident that feedback changes of this magnitude have a large effect on the speed stability derivative and long period response. A negative speed feedback $K_u = -.00122$ is obtained at zero collective pitch of the control rotor because of the downwash from the main rotor. The response for $K_u = -.00122$ and $\overline{\theta_o} = 0$ is found to be divergent.

On the other hand, the high speed stability derivative obtained with $\theta_o = 10^\circ$ and $K_u = .00122$ gives a frequency of oscillation which is considerably higher than that obtained with a gyroscopic bar. Similar but smaller changes in long period characteristics would be expected with changes in downwash which would tend to make the long period response characteristics obtained with the control rotor vary with different flight conditions.

Although the long period responses are very different in Fig. 33, it can be seen that the change in K_u has little effect on the response for the first three seconds after the pilot deflects the control stick. As a result, it might

be supposed that the handling characteristics in maneuvers would be unchanged and this conclusion is consistent with test results reported in Ref. 8. In these tests, the pilot found little difference in maneuvering handling qualities when different control rotor collective pitch angles were used. However, a 9 degree control rotor collective gave better speed stability at high speed and thus was more desirable from a stick trim position standpoint.

The initial forward speed is found to have a more important effect on the long period response when a control rotor is used than in the case of the stabilizer bar. Comparing Fig. 34 with Fig. 35, it is found that although the periods of oscillation are not greatly affected in going from $\mu_o = 0$ to .2 the forward flight oscillations are more unstable. This is apparently due to the increase in the angle of attack stability derivative in forward flight.

In the discussion of the initial response it was shown that an improvement in the damping of the short period mode might be obtained by the use of a longitudinal flapping feedback. A comparison of Figs. 35 and 36 show that a change in this parameter produces a comparatively small effect on the long period response.

Positive flapping feedback constants which are necessary to improve the short period response result in a reduction in the flapping due to speed change and pitching velocity. Since a nearly proportional decrease in effective speed and damping in pitch derivatives are obtained by the introduction of the flapping feedback, it is not surprising that the periods of oscillation are little affected by such a change. The introduction of a flapping feedback makes the long period oscillations slightly more unstable probably due to the fact that all derivatives are effectively made smaller compared to the pitching moment of inertia. The trends produced by changes in K_β with the corresponding changes in the damping in pitch are similar for the gyroscopic bar and control rotor stabilizers. At higher K_β's and pitch dampings the expected increase in the period of long period oscillations can be observed on Figs. 34, 35, and 36.

In addition to the figures included in this report, responses were obtained for $P = 5$ and $P = 3$ corresponding to configurations which would be possible if the control rotor were not mounted directly on the hub. It was found that there were no large differences in the long period responses obtained with P's from .5 to 3 for cases where the rate gains (K_β) and speed feedbacks (K_v) were the same. Nevertheless, there are some advantages in going to a greater than 1. It would then be possible to use a short time lag to minimize the time lag due to control input and, at the same time, have a high enough rate feedback to obtain the desired damping in pitch. A disadvantage in using a large P would be a further increase in normal velocity instability.

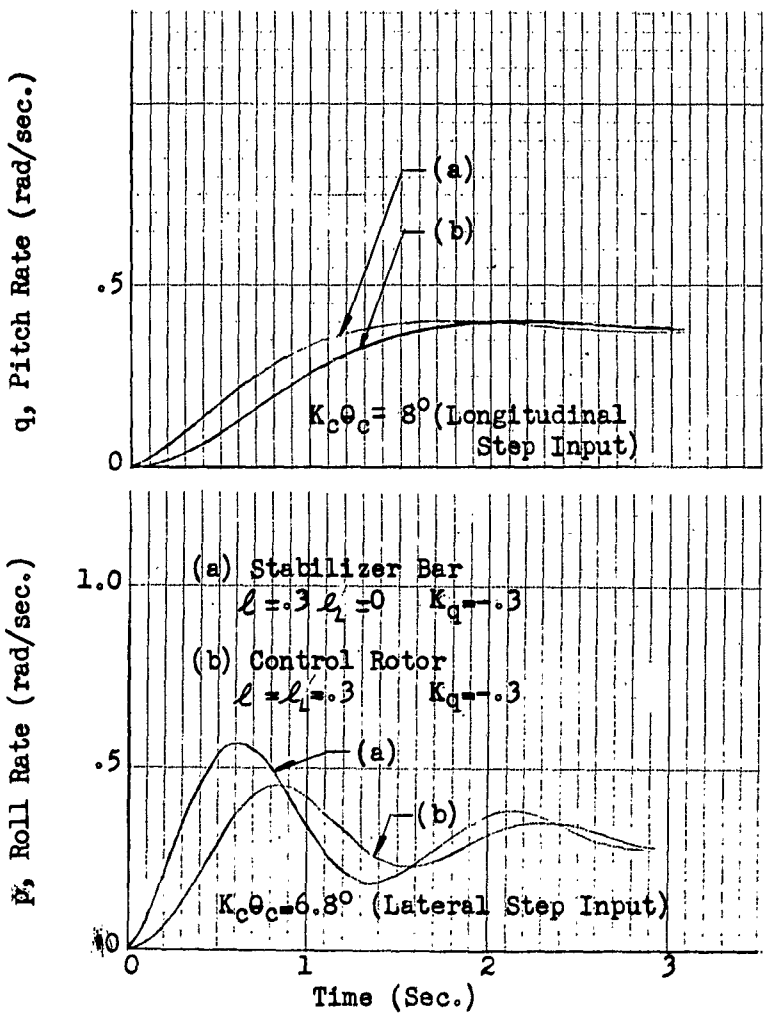

FIG. 31. COMPARISON OF CONTROL ROTOR AND STABILIZER BAR; INITIAL RESPONSES TO LONGITUDINAL AND LATERAL STEP INPUTS; HOVERING

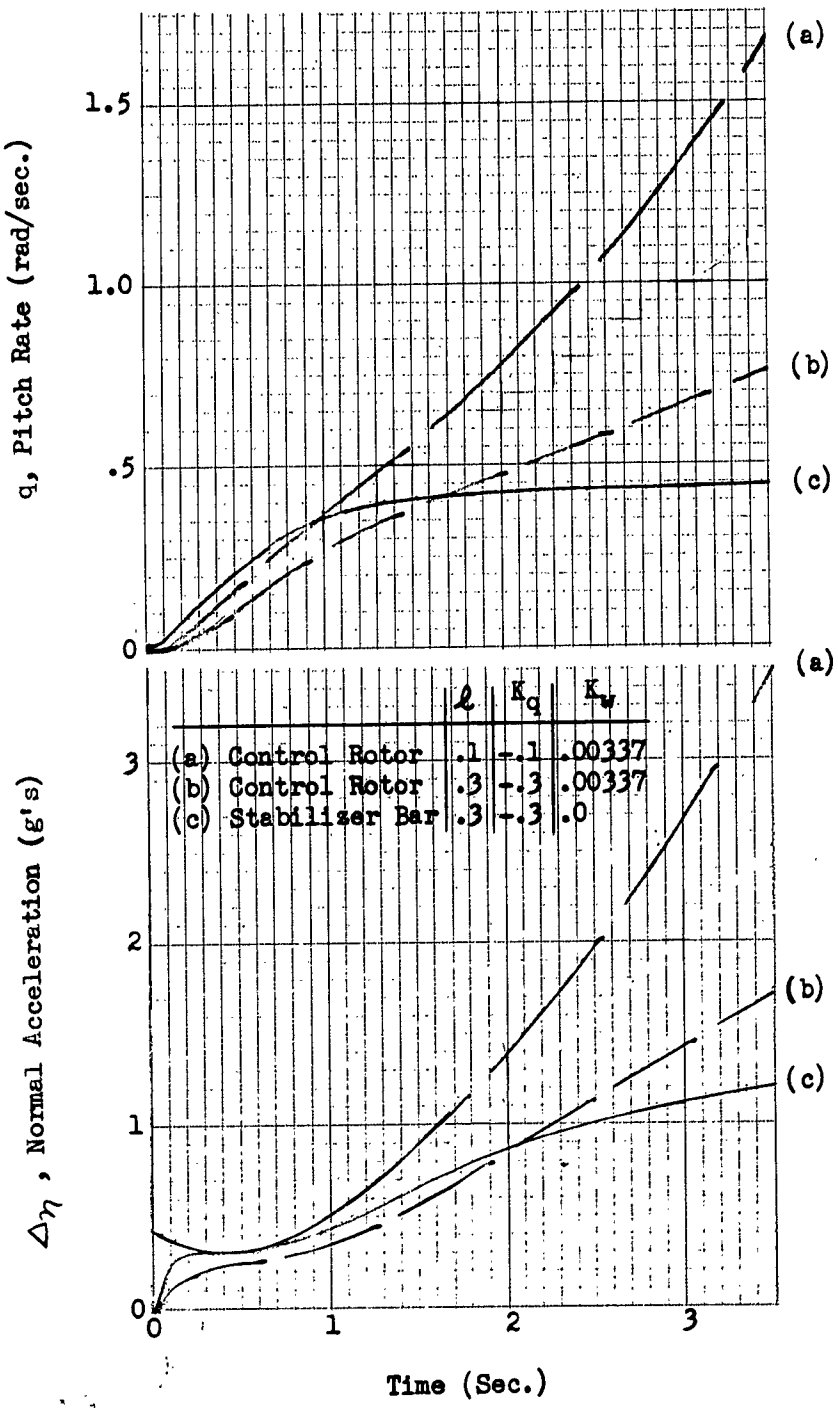

FIG. 32. CONTROL ROTOR; INITIAL LONGITUDINAL RESPONSES TO STEP CYCLIC PITCH INPUTS; $\mu_o = .2$

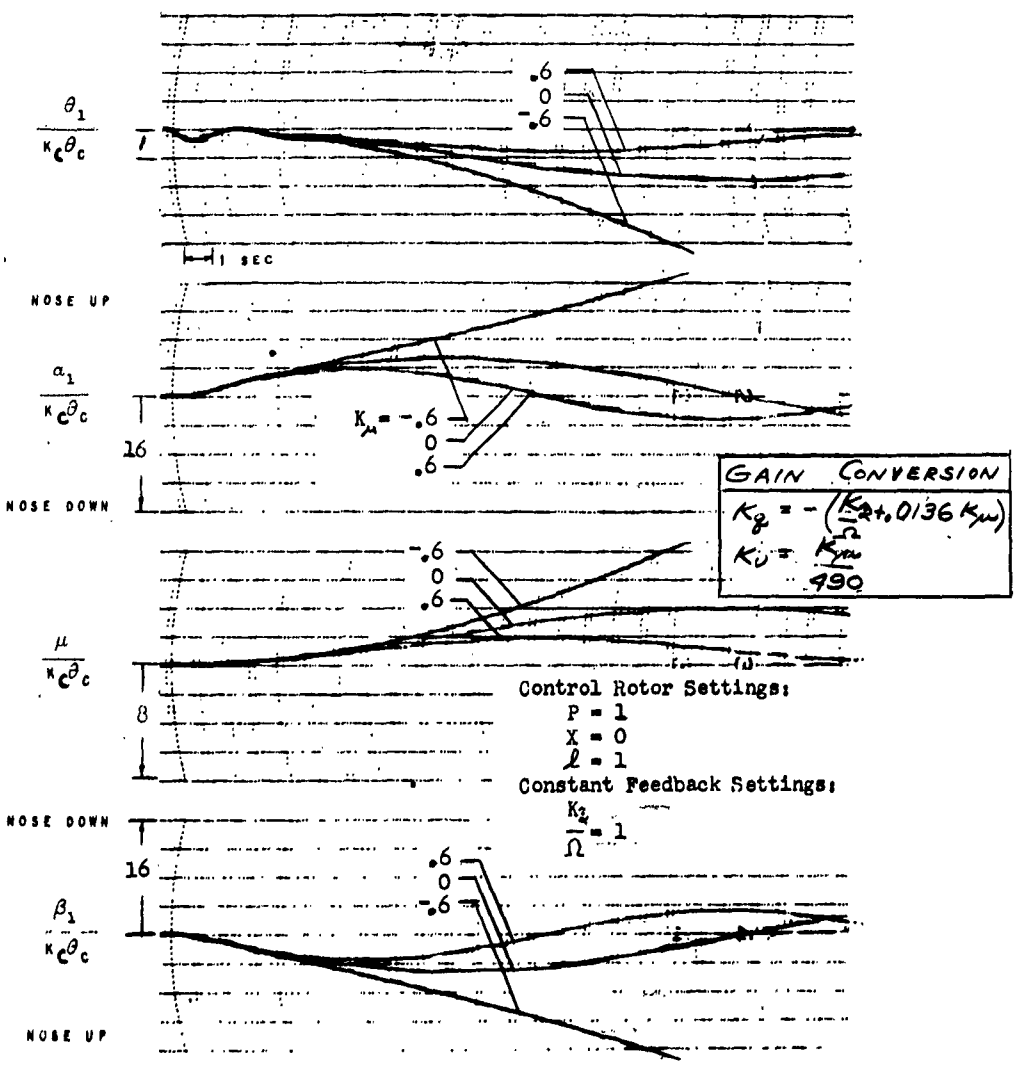

FIG. 33. CONTROL ROTOR STABILIZER; HOVERING

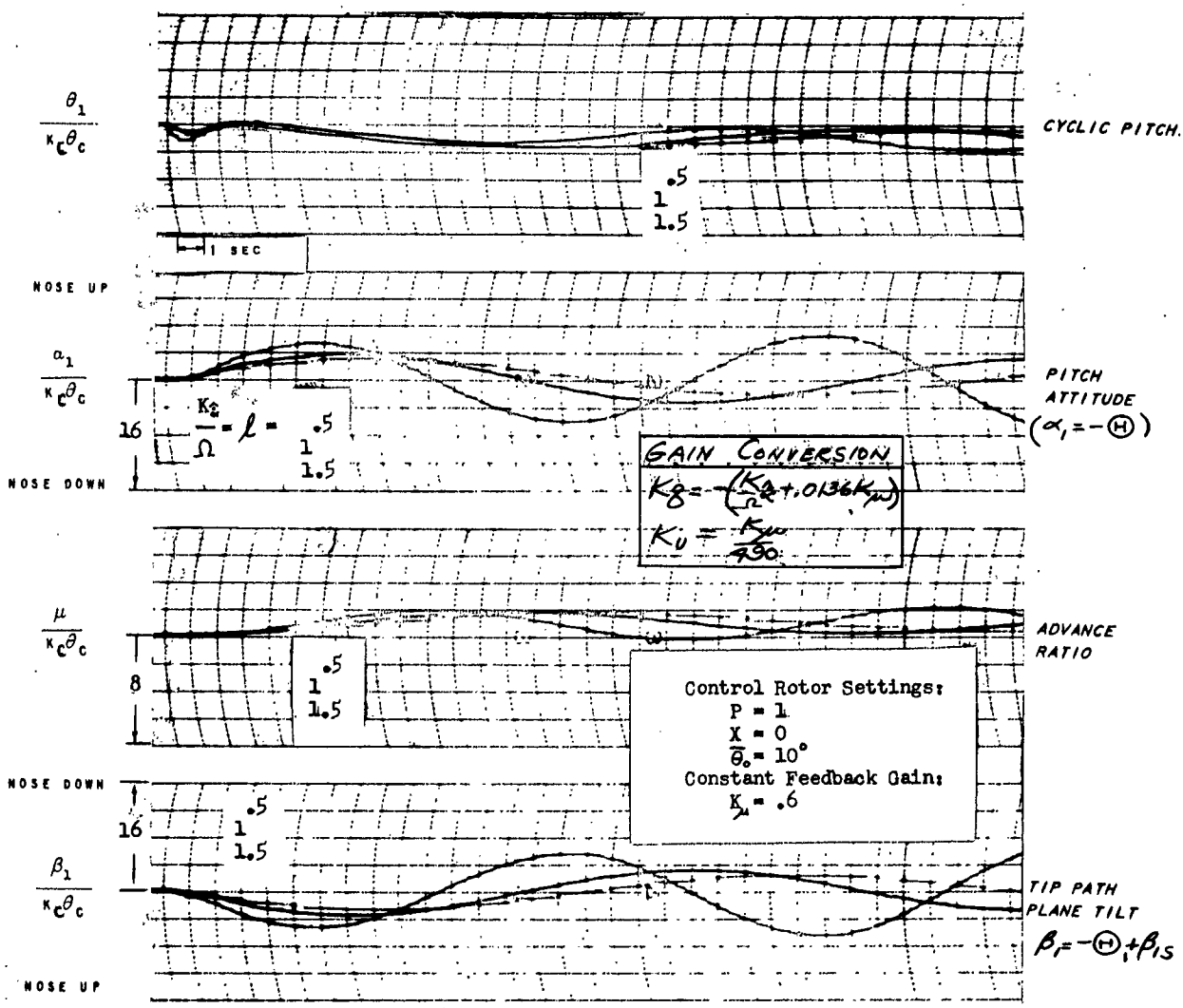

FIG. 34. CONTROL ROTOR STABILIZER; HOVERING

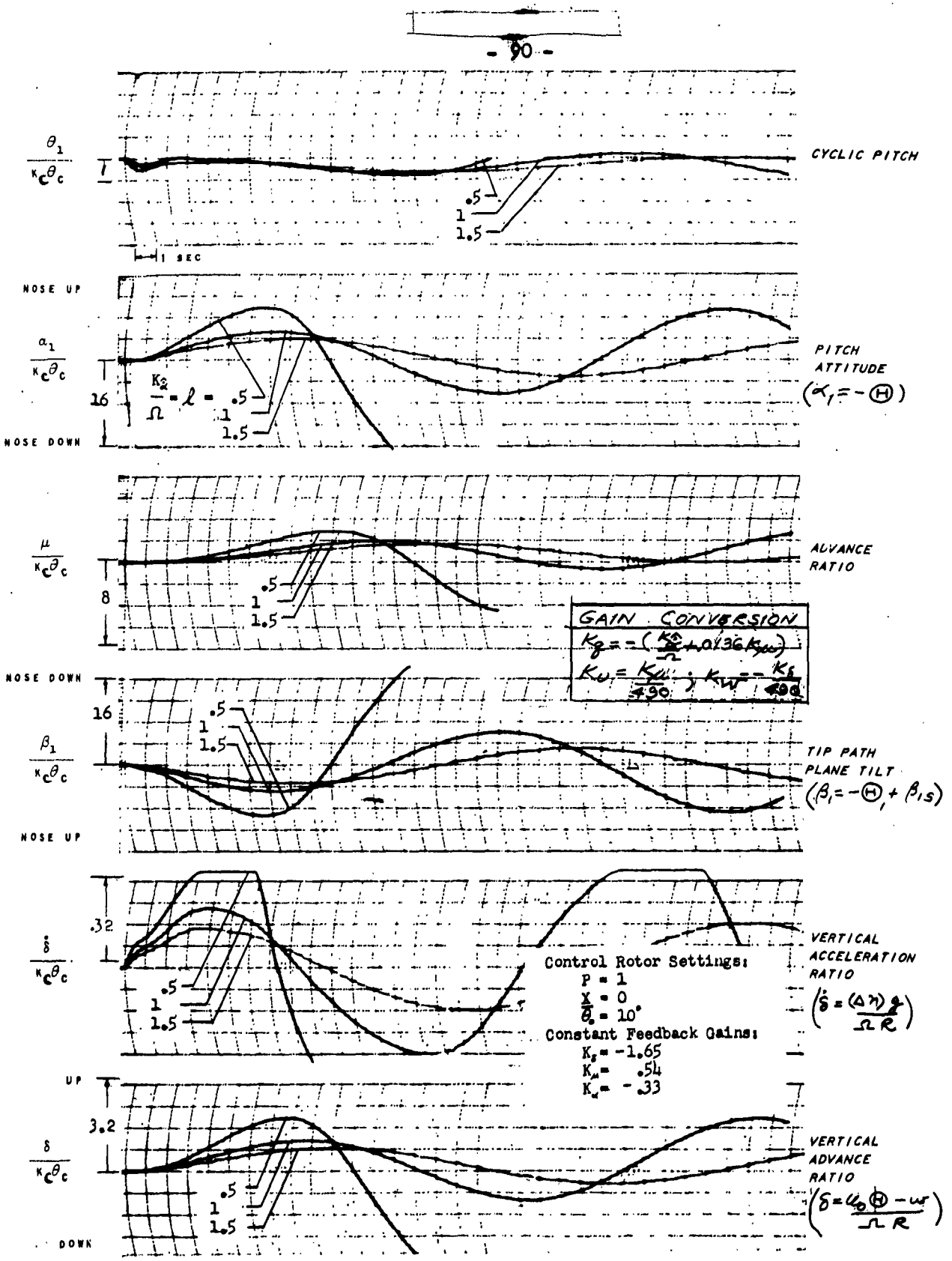

FIG. 35. CONTROL ROTOR STABILIZER; $\mu_o = .2$

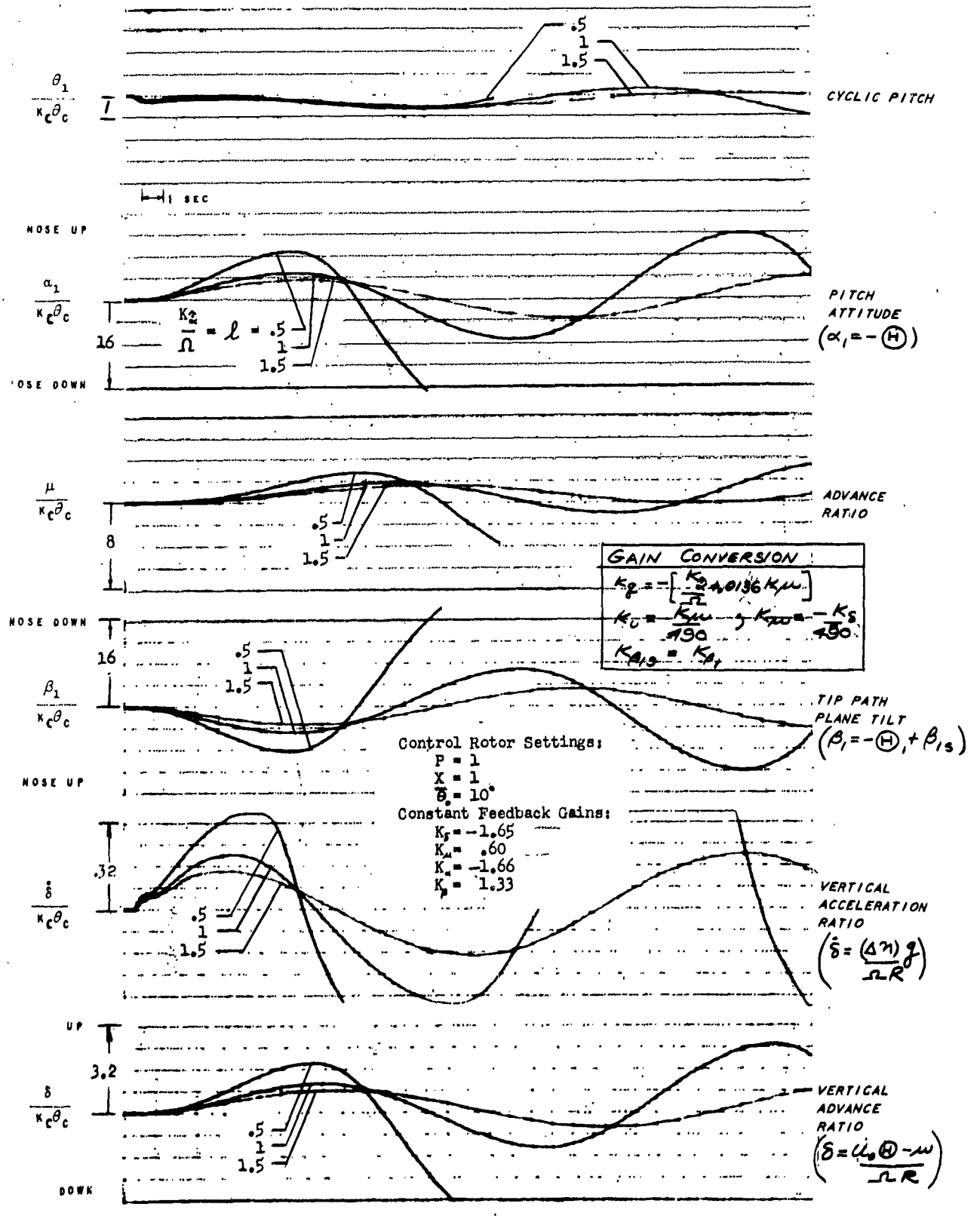

FIG. 36. CONTROL ROTOR STABILIZER; μ_0 = .2

DISCUSSION OF INDIVIDUAL DEVICES - GROUP II

The Group II devices differ from all other stabilizers considered in this report by providing the helicopter with attitude stability. The conventional helicopter autopilot and double bar stabilizers are classified in this group and are discussed in sections 5.3 and 5.4 respectively.

The presence of attitude stability brings about several fundamental changes in stability and handling qualities and makes some of the concepts discussed in preceding sections inapplicable to the Group II devices. In particular it causes the helicopter to tend to approach a constant attitude in the initial response to a cyclic input instead of a constant angular velocity. Similar changes exist in the initial pitch response in hovering and forward flight. Furthermore, if the forward speed is assumed constant in forward flight the helicopter with an attitude feedback would tend to approach a constant climb angle which would result in a zero increment in normal acceleration. Thus the maneuver stability as defined in section 22 would be zero for the Group II devices.

5.3 Conventional Helicopter Autopilot

(a) Representation by Generalized Autopilot Equations

Cyclic due to autopilot feedbacks:

$$\ell \dot{\theta}_{1A} + \theta_{1A} = K_q q + K_{\dot{w}} \dot{w}$$

Cyclic due to pilot's stick motion:

$$\theta_{1D} = K_c \theta_c$$

(b) Description of Mechanism:

Numerous writers have considered the effect of using a conventional autopilot to stabilize the helicopter. The installation of an autopilot designed for fixed wing applications involves linking the "elevator" and "aileron" servos to the two components of cyclic pitch and the "rudder" servo to the tail rotor pitch control. Such an installation is reported, for example, in Ref. 9 . The use of gyroscopes for measurement of fuselage pitch attitude, pitch rate, etc. is now so commonplace as to require no discussion here. The time lags of the (associated) servos and cyclic pitch change mechanisms are of importance in the performance of an autopilot but can be made negligible with good design. In the present study it is assumed that fuselage pitch attitude and/or rate are the only feedbacks provided by a conventional helicopter autopilot although it is not uncommon to have airspeed and altitude feedbacks in fixed wing applications.

(c) Description of How Device Affects Stability and Control Characteristics:

A disturbance of the helicopter from the initial trim condition results in a change of the cyclic pitch by the autopilot which is proportional to the attitude and/or pitching rate. The cyclic pitch change is in the direction to cause the tip path plane (and thrust vector) to tilt in a manner to oppose the motion, and for the zero time lag case the moment due to the rate signal increases the inherent damping in pitch while the moment due to the attitude gyro signal provides the helicopter with attitude stability. The introduction of time lags in the system causes the attitude signal to have an effective negative damping component and the rate signal to have an attitude component. In the discussion that follows it is assumed that the conventional autopilot has a negligible time lag.

As mentioned previously the discussion of the initial response in hovering flight which was given in section 2.2 is no longer applicable when there is an attitude derivative present. When the effect of speed changes is neglected the equivalent helicopter pitch equation for hovering flight (i.e. equation B. 73 in Table 3) can be written as,

$$\bar{\bar{I}}\ddot{\theta} + (-\bar{\bar{M}}_q)\dot{\theta} + (-\bar{\bar{M}}_\theta)\theta = \bar{\bar{M}}_{\theta_1} K_c \theta_c$$

where the helicopter derivatives are functions of the autopilot feedback constants. In the case of the unstabilized helicopter and devices without attitude feedbacks the equivalent attitude derivative, $\bar{\bar{M}}_\theta$, is zero. In this case the previously discussed exponential build up in pitching rate is obtained when a cyclic pitch step is applied (see Fig. 37a). On the other hand when there is an attitude derivative present a quadratic response is obtained with the helicopter approaching a constant pitch attitude as indicated in Fig. 37b. The quadratic response may be monotonic or oscillatory depending on the system parameters. Roll responses similar to those indicated on Fig. 37 for pitch would be obtained for the corresponding roll cases.

In Part B it is concluded that desirable initial response characteristics for helicopters would include the rapid development of pitch and roll rates proportional to the pilots stick deflections. This type of response is particularly desirable in roll since most helicopter pilots are familiar with the rapid roll rate responses of airplanes. Ref. 10 suggests a type of pilots input system which would make the helicopter tend to approach an angular velocity instead of an attitude angle in the initial response in spite of an attitude feedback. The technique involves using an input system that introduces a linear increase in cyclic pitch with time which is proportional to the pilots stick deflection. The required input can be obtained by integrating a signal from the pilots stick and feeding the output to the cyclic pitch servo. Fig. 37c illustrates the type of initial response which might be obtained with the integrated input. It should be pointed out that the same stabilization is obtained with the systems indicated in Fig. 37b and c and the same response would be obtained to an external disturbance acting on the helicopter.

Perhaps the most significant difference in the responses of a helicopter with a conventional helicopter autopilot and those obtained with the other devices considered is the more rapid damping of long mode oscillations. This improvement in the long period response is not due to the presence of the attitude feedback alone. Early attempts to stabilize helicopters with pure attitude autopilots were unsuccessful. Similarly it is seen in the discussion of the other devices considered that the presence of rate or normal velocity feedbacks can change the period of the long mode and give nearly neutrally stable oscillations but good damping of the long mode is not obtained. The explanation is that neither the rate or normal velocity feedbacks are applied with the proper phasing to obtain optimum long period damping. A discussion of the required phase relationships for good damping is not considered in this report since this subject has been taken up in a number of recent papers. One of the advantages of the conventional autopilot is that gains can be selected which give the proper phase relationships for long mode stabilization without adding a time lag which would result in poor initial response characteristics.

(d) Effects of Conventional Autopilot on the Stability and Control Characteristics of the Sample Helicopter

The discussion of the response characteristics of the sample helicopter with a conventional helicopter autopilot is limited to the case of the usual pilot input system which gives a swash plate deflection proportional to the pilots stick deflection.

Initial Response in Hovering Flight:

Fig. 38 shows the pertinent hovering roll attitude response characteristics of the sample helicopter as functions of the rate and attitude gains. These results are based on an analysis made using the equivalent helicopter pitch equation (B.73) and neglecting changes in forward velocity. Fig. 38a shows response shapes of a second order system excited by a step function in terms of amplitude ratio and non-dimensional time; (b) shows the maximum final steady state roll angle achieved by the sample helicopter and is a function of the attitude gain only; (c) indicates the manner in which the undamped natural period, T_n , varies with the autopilot gains; and (d) is a plot of the percent of critical damping as a function of autopilot gains. Fig. 39 shows the roll attitude response times obtainable with various gain combinations. Lines for $K_\rho = K_\phi$ are shown on Fig. 38c and d which correspond to parameters used in the computer solutions. The following points of interest are noted:

(1) The final steady state roll angle is determined by the attitude gain. Hence, if it is required that a minimum roll angle of 30° be achievable the roll attitude gain, K_ϕ , must be less than .225.

(2) The undamped natural period, T_n , decreases as the rate or attitude gain is increased.

(3) The percent of critical damping, ζ , increases as the rate gain increases but decreases as the attitude gain increases.

(4) If it is assumed that the sample helicopter must be able to achieve a 30° roll angle and the damping must be greater than 70% critical the minimum attitude response time is about 1.25 seconds.

Initial pitch attitude responses were analyzed in the same manner indicated for the roll responses and the results obtained are presented on Fig. 39. It is found that very long pitch response times are obtained unless the steady state pitch angle is restricted to a small value. It should be emphasized that the data on Fig. 38 and 39 were obtained neglecting speed changes and would not be expected to give an accurate prediction of response times that are longer than 2 or 3 seconds.

The general characteristics of the attitude responses obtained with a conventional helicopter autopilot have been discussed.

Fig. 40 shows the form of the associated pitch and roll rate time histories when the rate and attitude gains of the autopilot are equal. Since the helicopter approaches a constant attitude, the rate responses are transients which tend to zero as time increases. However, the pitch response times are so long that the pitch rates do not drop off much in the first two seconds. As a result the initial pitch response for the case shown does not show the characteristics expected with a conventional helicopter autopilot and are not much different than some obtained with other devices considered.

Initial Response in Forward Flight:

Fig. 41 shows how the initial longitudinal response in forward flight is affected by a conventional autopilot when $K_q = K_\theta$. Comparison of the pitch rate responses in Figs. 40 and 41 shows that changing the trim speed has relatively little effect on pitch response. Apparently the large effects of the feedbacks overpower the derivative changes of the basic configuration due to change of forward speed.

Fig. 41 shows that the normal acceleration curve becomes concave downward within 2 seconds when $(-K_q)=(-K_\theta) > .\alpha$ but the initial dip becomes greater as the gains are increased.

Long Period Response:

The results of computer studies which included the longitudinal speed change and treated longitudinal tip path plane motion as a separate degree of freedom are presented on Figs. 42 and 43 for the cases $\mu_o = 0$ and $\mu_o = .2$, respectively. It can be seen from these figures that the long period mode can be made quite stable with a conventional helicopter autopilot, a result which is consistent with the finding of other authors.

It will be noted in both figures 42 and 43 that the final pitch attitudes which are achieved after long periods of time are considerably below the quasi-static equilibriums which are reached in three or four seconds. As the forward speed increases the rotor tilts aft and at equilibrium the aft tilting of the rotor due to the speed increment is approximately balanced by the increment in cyclic pitch. A somewhat larger final pitch angle is reached in the $\mu_o = .2$ case due to the greater effect of fuselage drag in forward flight.

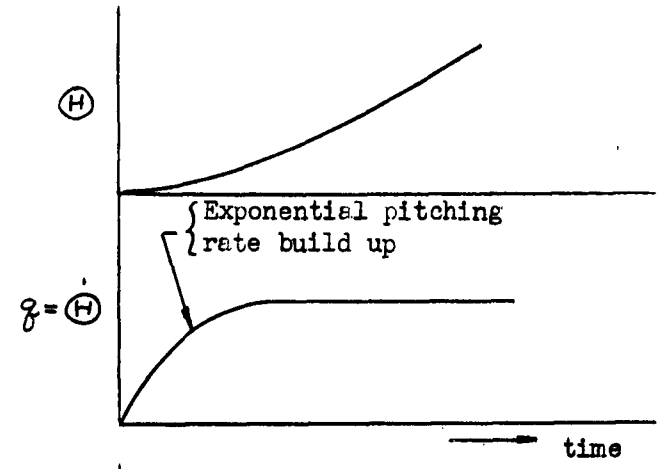

$$\bar{I}\ddot{\Theta} + (-\bar{M}_{\dot{\theta}})\dot{\Theta} = \bar{M}_{\theta_1} K_c \theta_c$$

(a) Zero Attitude Stability ($K_{\dot{\theta}} = 0$)

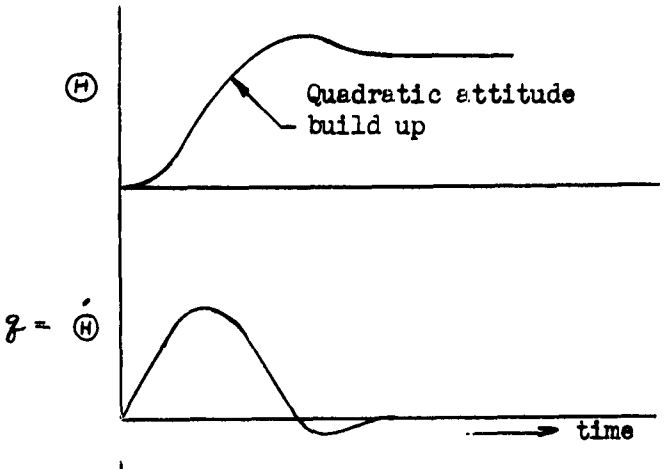

$$\bar{I}\ddot{\Theta} + (-\bar{M}_{\dot{\theta}})\dot{\Theta} + (-M_{\Theta})\Theta = \bar{M}_{\theta_1} K_c \theta_c$$

(b) Attitude Feedback; Usual pilot Input

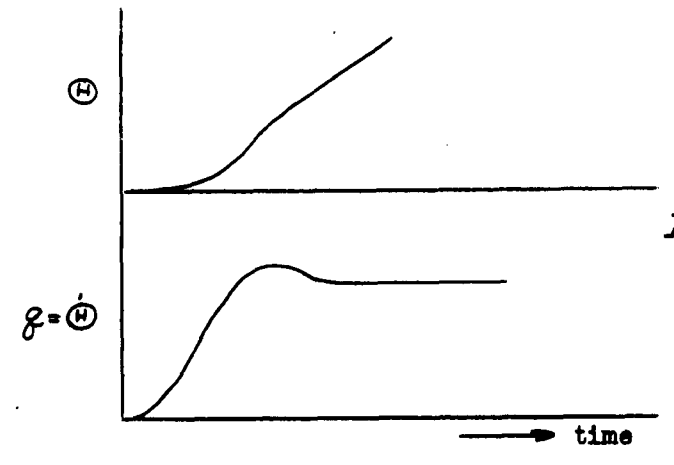

$$I\ddot{\Theta} + (-\bar{M}_{\dot{\theta}})\dot{\Theta} + (-M_{\Theta})\Theta = \bar{M}_{\theta_1} K_c \int \theta_c \, dt$$

(c) Attitude Stability; Integrating Input System

FIG. 37. EFFECT OF AN ATTITUDE FEEDBACK ON INITIAL HOVERING RESPONSE CHARACTERISTICS

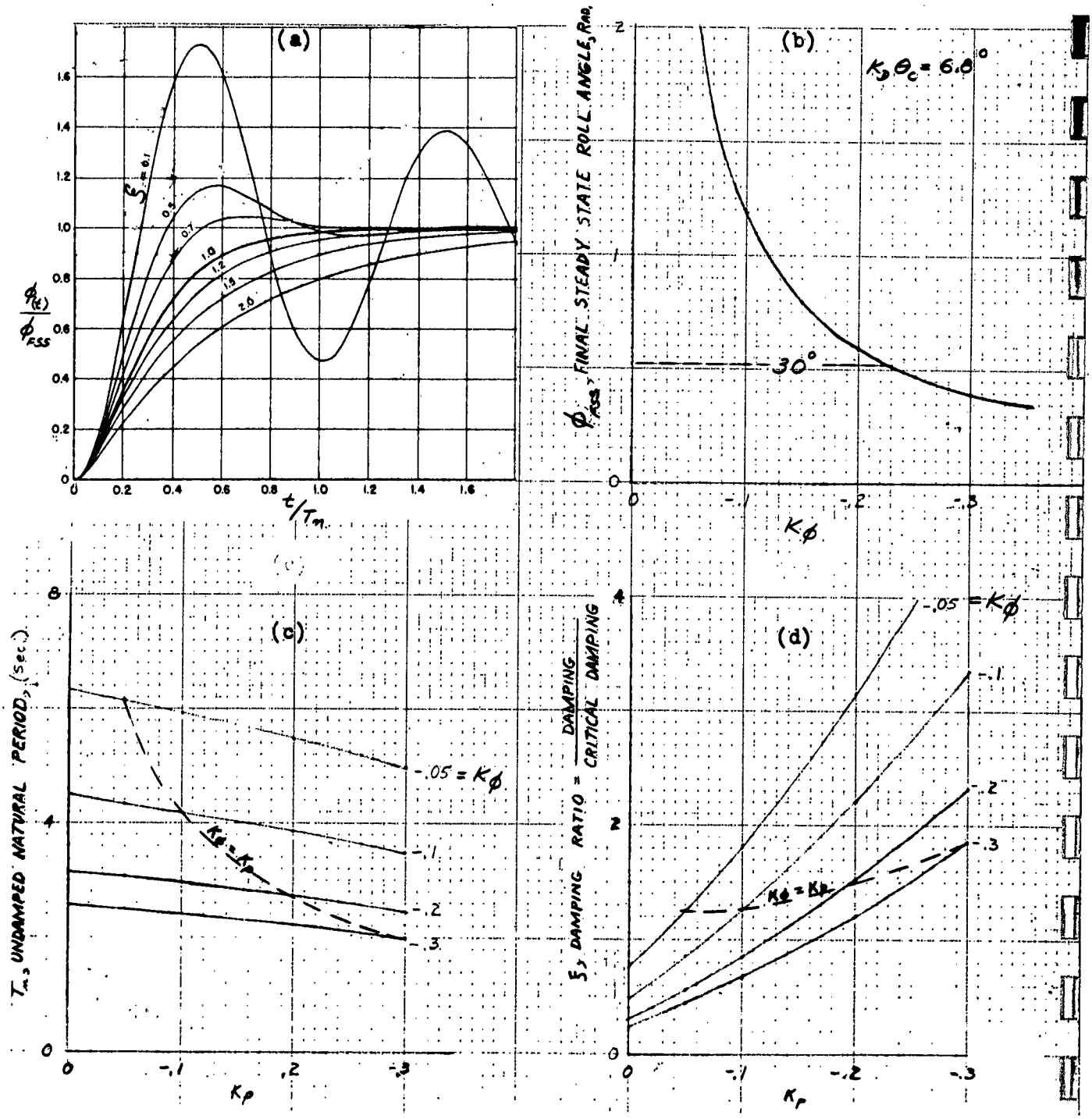

FIG. 38. CONVENTIONAL AUTOPILOT; INITIAL ROLL ATTITUDE RESPONSE CHARACTERISTICS FOR LATERAL CYCLIC PITCH INPUTS; HOVERING

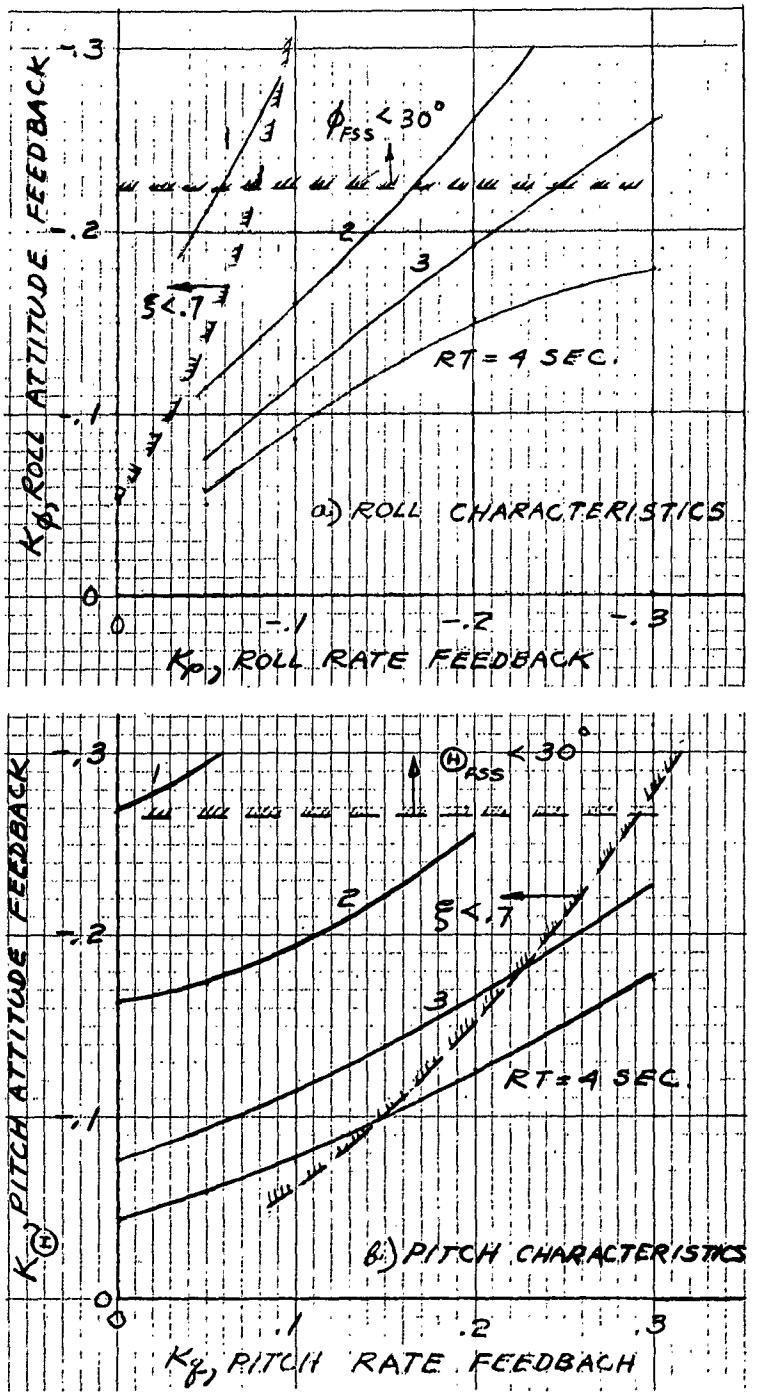

FIG. 39. CONVENTIONAL AUTOPILOT: INITIAL ATTITUDE RESPONSE CHARACTERISTICS: HOVERING

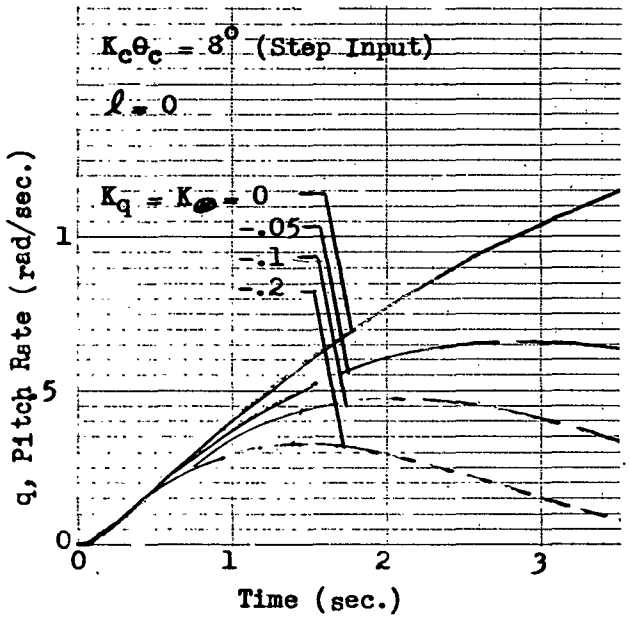

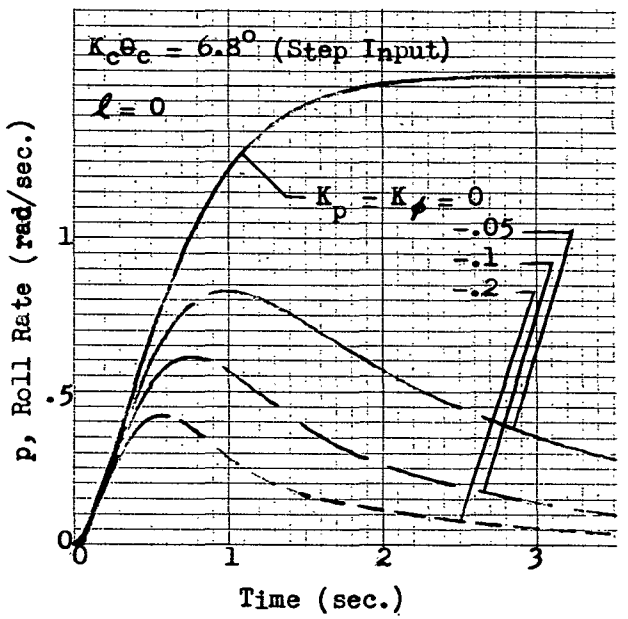

FIG. 40. CONVENTIONAL AUTOPILOT. INITIAL RESPONSES TO LONGITUDINAL AND LATERAL STEP INPUTS IN HOVERING.

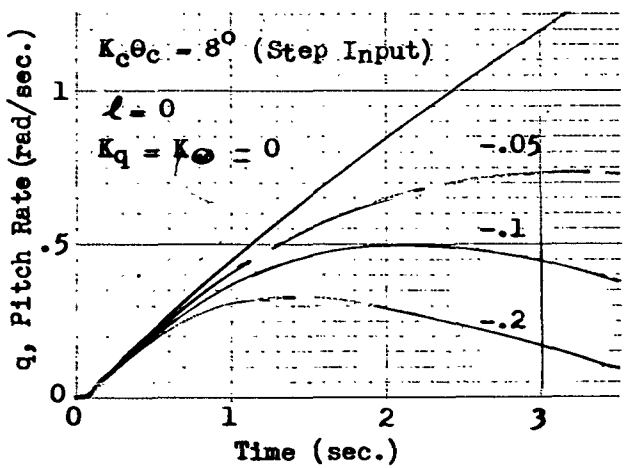

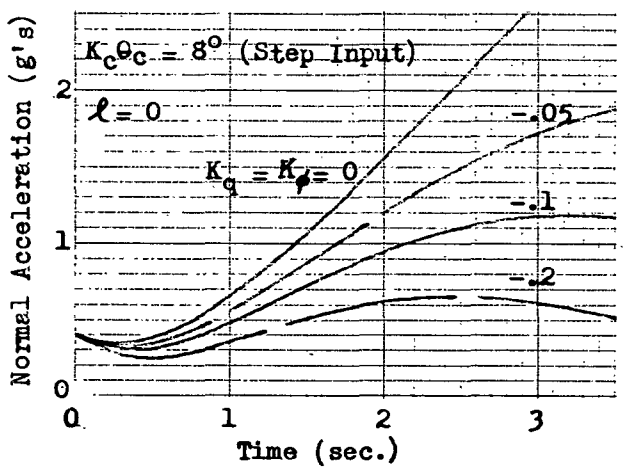

FIG. 41. CONVENTIONAL AUTOPILOT. INITIAL RESPONSES TO LONGITUDINAL CYCLIC STEP INPUT AT $\mu_o = .2$.

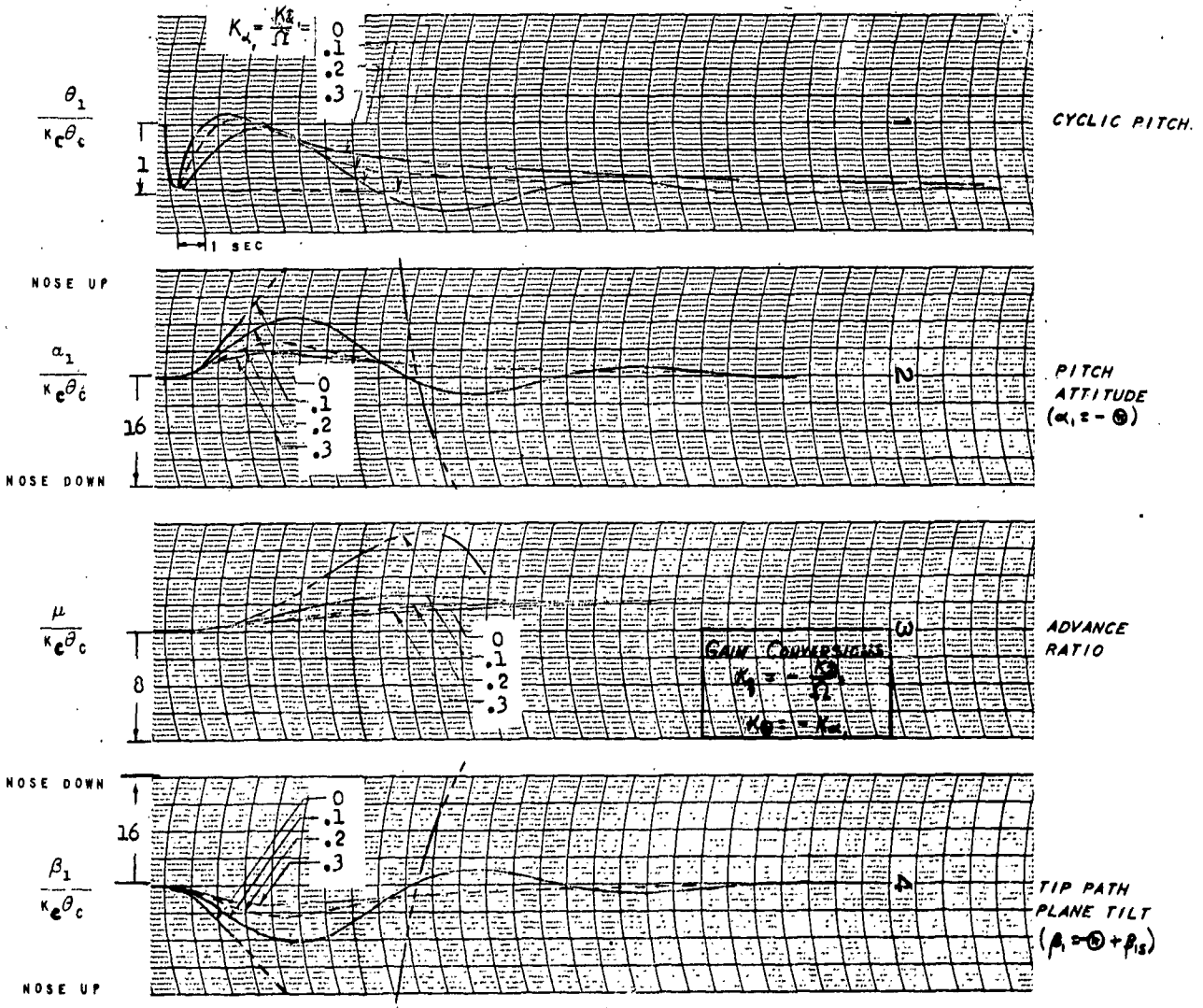

FIG. 42 . CONVENTIONAL AUTOPILOT; HOVERING

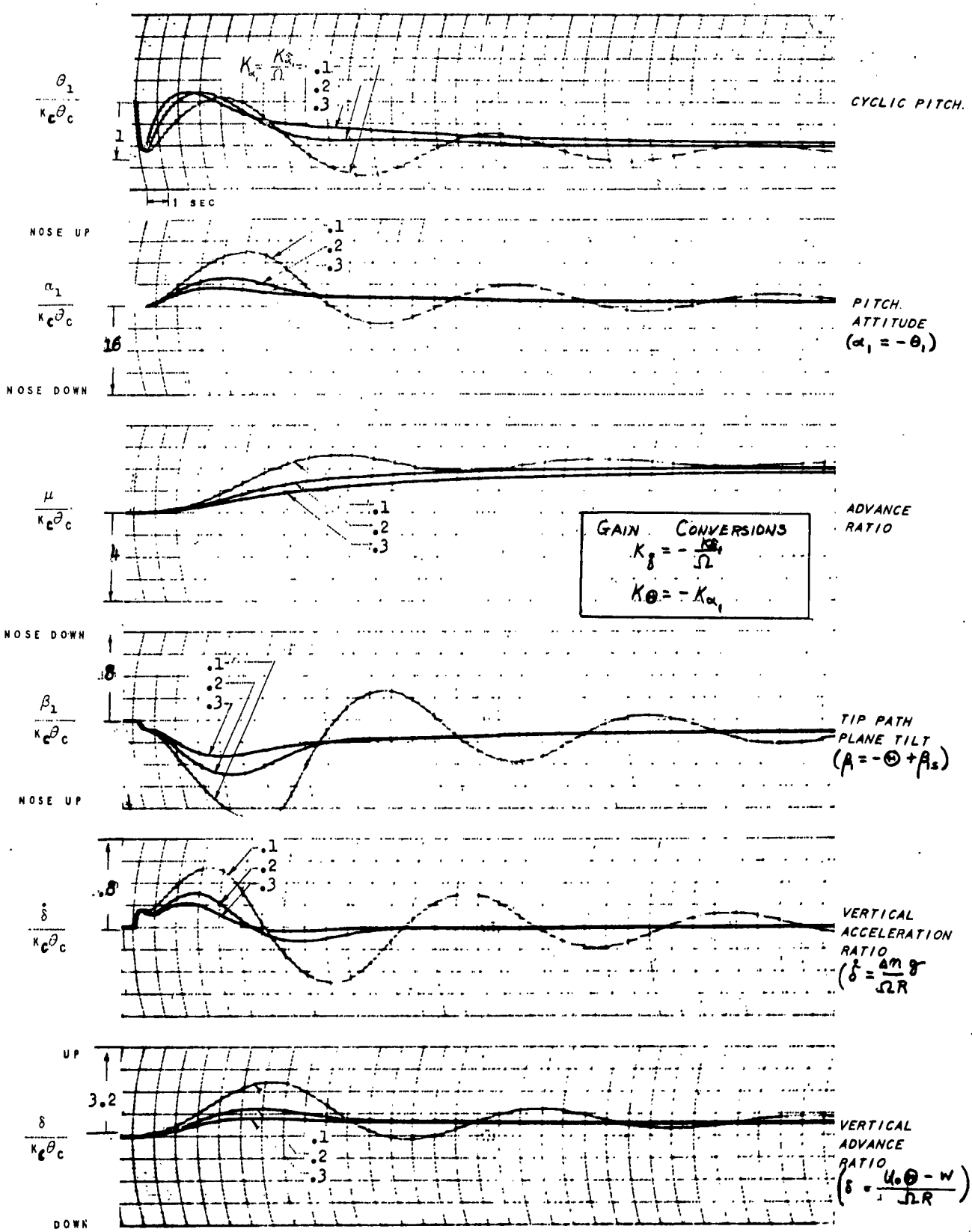

FIG. 43 . CONVENTIONAL AUTOPILOT; $\mu_o = .2$

5.4 Double Bar Stabilizer

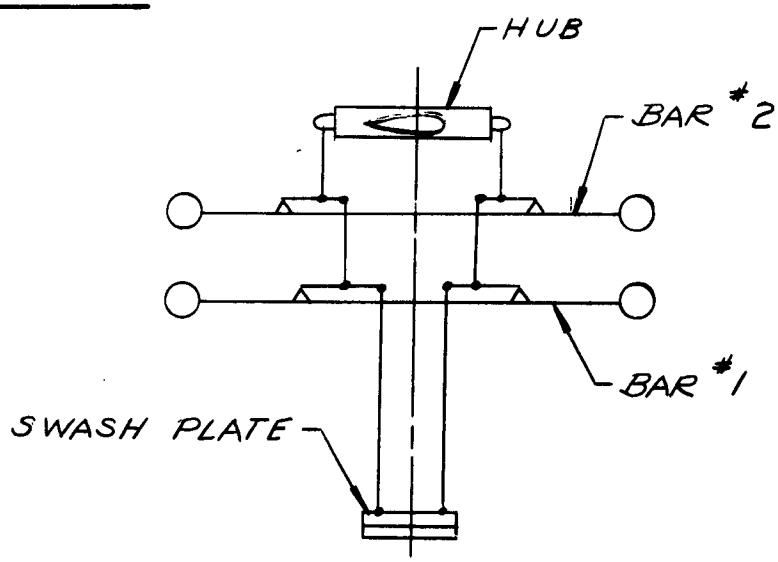

FIG. 44 . SCHEMATIC DIAGRAM OF DOUBLE BAR STABILIZER

(a) Representation by Generalized Autopilot Equations

Cyclic due to autopilot feedbacks:

$$\ell \dot{\theta}_{1A} + \theta_{1A} = K_{\beta}\,\beta + K_{\Omega}\,\Omega$$

Cyclic due to pilots stick motion:

$$\theta_{1D} = K_{D}\,\theta_{C}$$

(b) Description of Mechanism

Ref. 11 suggested the possibility of using the combination of two gyroscopic bars for stabilizing the helicopter. Fig. 44 shows a line diagram of a double bar stabilizer indicating how the cyclic control linkages might be arranged. The total cyclic pitch in this case would be the sum of three terms, one proportional to swash-plate tilt, the second proportional to seesawing motion of bar #1, and the third proportional to seesawing motion of bar #2. Viscous dampers which would be provided for damping the seesawing motion of the bars relative to the shaft have been omitted from the diagram for clarity.

(c) Description of How Device Affects Stability and Control Characteristics

The factors determining the tilt of the tip path plane of each of the bars relative to the shaft are the same as in the case of the single gyroscopic bar stabilizer. It appears desirable to use very little damping of one of the

bars in order that its plane of rotation would not be affected by shaft tilt and its contribution to the cyclic pitch would be an almost pure attitude feedback, K_θ . High damping might be provided for the second bar which would keep it very nearly perpendicular to the shaft at all times. The small tilt of the second bar tip path plane relative to the shaft due to gyroscopic effects would be very nearly proportional to the rate of tilting of the shaft and thus provide a K_q feedback. Since the double bar stabilizer can provide cyclic pitch proportional to fuselage angular velocity and attitude it should be able to provide the same feedbacks obtained with a conventional helicopter autopilot if suitable linkage ratios are used. However, unlike the autopilot the same feedback constants would have to be used for stabilizing pitching and rolling motions.

Some problems might result from the use of very low damping of one of the bars when very violent maneuvers are being made and it might prove desirable to use a non-linear damper. However, this question was not investigated in the present study.

The control equation for the double bar stabilizer which is given above is an approximate form derived in Part A for the case when one of the bars has a very long time lag. It was shown that the cyclic pitch-bar tilt ratios, P_1 and P_2 , bar time lags, τ_1 and τ_2 , and feedback constants were related as follows:

$$K_q = -\tau_1 (P_1 + P_2)$$
$$K_\theta = -\left(\frac{\ell}{\tau_2} P_1 + P_2\right)$$
$$\tau_1 = \ell$$

Here τ_2 is the very long time constant of the bar which generates a nearly pure attitude signal and $\ell = \tau_1$ is the time lag of the bar which primarily generates a rate signal. It was pointed out in Part A that the above approximate form of the double bar equation is identical to the control equation for the conventional helicopter autopilot. Consequently, insofar as the approximation used is valid, the discussion included in section 5.3 on the conventional helicopter autopilot would also apply to the case of the double bar. Of course the integrated pilot's input discussed for the autopilot would not be provided by the double bar mechanism shown.

(d) <u>Effects of Double Bar on the Stability and Control Characteristics of the Sample Helicopter</u>

Responses were obtained on the analogue computer for the same gains that were used in studying the conventional autopilot but with time lags of .5 and 1.5 seconds. These responses were found to be less desirable than the previously discussed time histories obtained with the conventional autopilot

and are not presented. Since a time lag of .05 seconds is known to be obtainable with existing single stabilizer bar configurations the double bar has the potentiality of yielding the same response characteristics as the conventional autopilot.

DISCUSSION OF INDIVIDUAL DEVICES - GROUP III

The principal characteristic of the devices in Group III is a feedback proportional to the rate of tilting of the tip path plane relative to fixed axes. Group III includes the tip path plane rate autopilot, biased cyclic control system, Doman Frasier Rotor Head, aerodynamic servo control flap, and swash plate spring damper stabilizer and these devices are taken up in Sections 5.5, 5.6, 5.7, 5.8, and 5.9 respectively.

5.5 Tip Path Plane Rate Autopilot

(a) Representation by Generalized Autopilot Equations

Cyclic due to autopilot feedback:

$$\theta_{1A} = K_{\beta} \beta + K_{\dot{\beta}_{1S}} \dot{\beta}_{1S} = K_{\dot{\beta}_1} \dot{\beta}_1$$

Cyclic due to pilot's stick motion:

$$\theta_{1D} = K_D \theta_c$$

(b) Description of Mechanism

No device is in use at present which is characterized by a single feedback proportional to the rate of tilting of the tip path plane relative to fixed axes. However, a separate section is devoted to the discussion of such a device since it has often been suggested that better stabilization might be obtained by damping motions of the tip path plane rather than of the fuselage. A possible mechanism for obtaining the feedback in question might consist of the combination of a rate gyro in the fuselage and a device for measuring the rate of change of longitudinal and lateral flapping relative to the shaft. Also some swash plate spring damper configurations approximate a zero time lag tip path plane rate autopilot.

(c) Description of How Device Affects Stability and Control Characteristics

The longitudinal component of cyclic pitch due to the tip path plane rate autopilot can be represented by the combination of a fuselage pitching rate feedback, (K_{β}), and a longitudinal flapping rate feedback, $K_{\dot{\beta}_{1S}}$, as indicated by the generalized autopilot equation above. A similar breakdown can be made of the feedback proportional to the lateral tilting rate of the tip path plane. K_{β} and $K_{\dot{\beta}_{1S}}$ are equal in magnitude but have opposite signs with the sign convention adopted in this report.

An increase in the damping in pitch of the helicopter is obtained with the tip plane rate autopilot as with the fuselage rate autopilot when K_{β} is negative. The tip path plane rate autopilot only differs from the fuselage rate autopilot by the addition of the $K_{\dot{\beta}_{1S}}$ feedback which gives a cyclic pitch component proportional to the rate of change of longitudinal

flapping relative to the shaft. This $K_{\dot{\beta}_{1s}}$ feedback tends to increase the lag in the tip path plane response to a stick movement. However, it is found in the next sub-section that although considerable lag may occur in the tip path plane response the presence of a $K_{\dot{\beta}_{1s}}$ feedback has a comparatively small effect on the over-all response of the helicopter.

(d) Effect of a Tip Path Plane Rate Autopilot on the Stability and Control Characteristics of the Sample Helicopter

Initial Blade Response:

Figure 45 shows the influence of a flapping rate feedback on the initial blade response of the sample helicopter assuming the fuselage is fixed. It can be seen that positive flapping rate feedbacks effectively increase the time lag of blade response. The unstabilized helicopter requires .2 sec. to reach 90% of its final flapping angle while .68 sec. are required with $K_{\dot{\beta}_{1s}} = .2$ and 1.35 sec. with $K_{\dot{\beta}_{1s}} = .5$. Although the flapping response time of the helicopter could be made shorter with the selection of a negative valve for $K_{\dot{\beta}_{1s}}$, such a choice is precluded by the fact that it corresponds to a positive K_q which would decrease the damping of the helicopter in pitch.

Initial Pitch and Roll Rate Response in Hovering Flight:

The effects of a tip path plane rate feedback on the initial response characteristics of the sample helicopter in hovering flight are presented in Section 4.3. It can be seen by comparing Fig. 11 and Fig. 12, p. 43 that at feedbacks gains of $-K_q = +K_{\dot{\beta}_{1s}} = .4$ and lower the initial responses obtained with a tip path plane rate autopilot are quite similar to those obtained with a fuselage rate autopilot. This result is somewhat surprising since a fuselage rate autopilot does not change the blade response to stick motion in contrast to the considerable lag obtained with the tip path plane rate autopilot (Fig. 45). It appears that the tip path plane lag due to the $K_{\dot{\beta}_{1s}}$ and $K_{\dot{\beta}_{1s}}$ feedbacks has a comparatively small effect on the initial pitch and roll response because of the rapid reduction in cyclic pitch and flapping angles due to the fuselage pitch and roll rate feedbacks (see Fig. 46).

Initial Response in Forward Flight

Figure 47 compares the effects of a tip path plane rate autopilot and a fuselage rate autopilot on the longitudinal response of the sample helicopter in forward flight. Curves (a) and (c) are for the fuselage rate autopilot and curves (b) and (d) are for the tip path plane rate autopilot. Very little difference can be seen between the pitching rate responses obtained with these two devices as in the hovering case but it is found that the $K_{\dot{\beta}_{1s}}$ feedback of the tip path plane rate autopilot modifies the normal acceleration time history close to zero time.

The initial normal acceleration increment is due to the increase in swash plate angle of attack produced by the aft stick deflection. Since the

$K_{\beta_{1s}}$ feedback reduces the swash plate angle during the initial motion, a normal acceleration decrement results. It will be noted that this initial reduction in normal acceleration eliminates the dip in the normal acceleration time history which is found in the case of the fuselage rate autopilot at approximately one-half second after a step stick displacement.

Long Period Response:

The long period response of the sample helicopter is very nearly the same with a tip path plane rate autopilot and with a fuselage rate autopilot since the low values of longitudinal flapping rate, $\dot{\beta}_{1s}$, occurring during these oscillations make the $K_{\beta_{1s}}$ feedback relatively unimportant. It is shown in Section 4.5 that the period of the long period mode is made longer and the oscillations are made less unstable with an increase in the magnitude of the K_θ feedback. However, the long period instability cannot be eliminated by a zero time K_θ rate feedback.

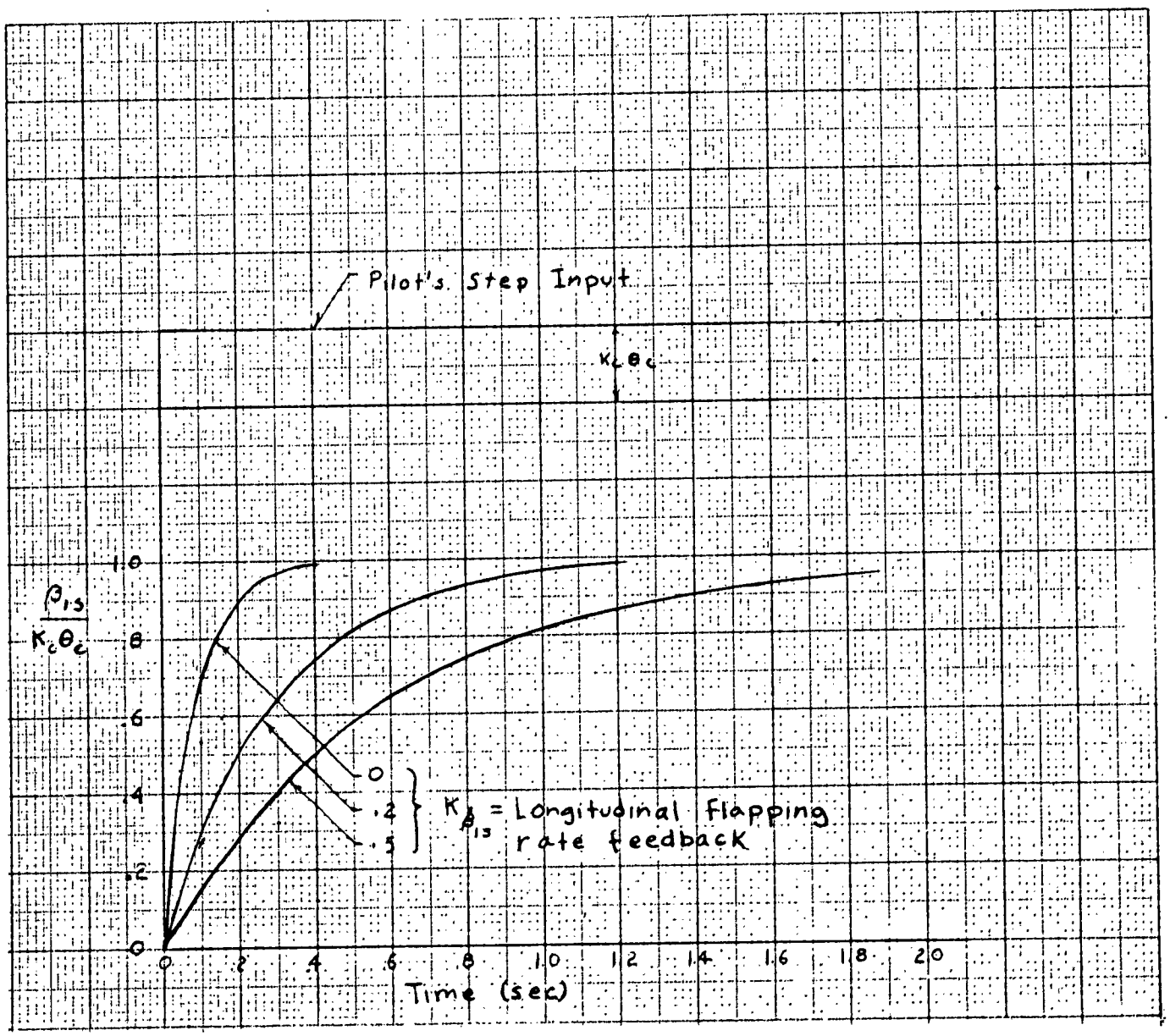

FIG. 45. VARIATION OF BLADE RESPONSE WITH FLAPPING RATE FEEDBACK (FUSELAGE FIXED)

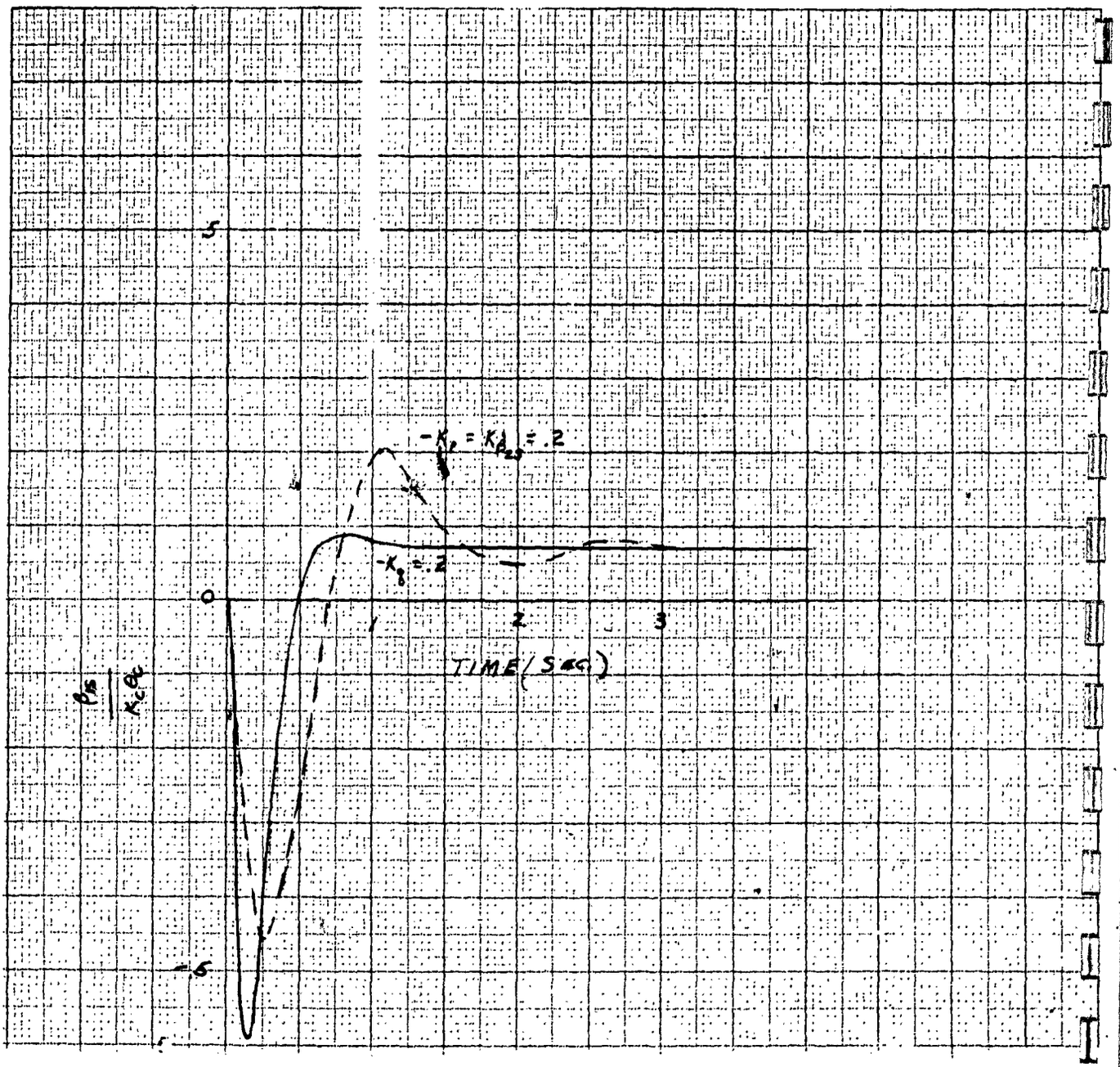

FIG. 46. COMPARISON OF TIP PATH PLANE TRANSIENTS OBTAINED WITH FUSELAGE RATE AND TIP PATH PLANE RATE AUTOPILOTS; HOVERING

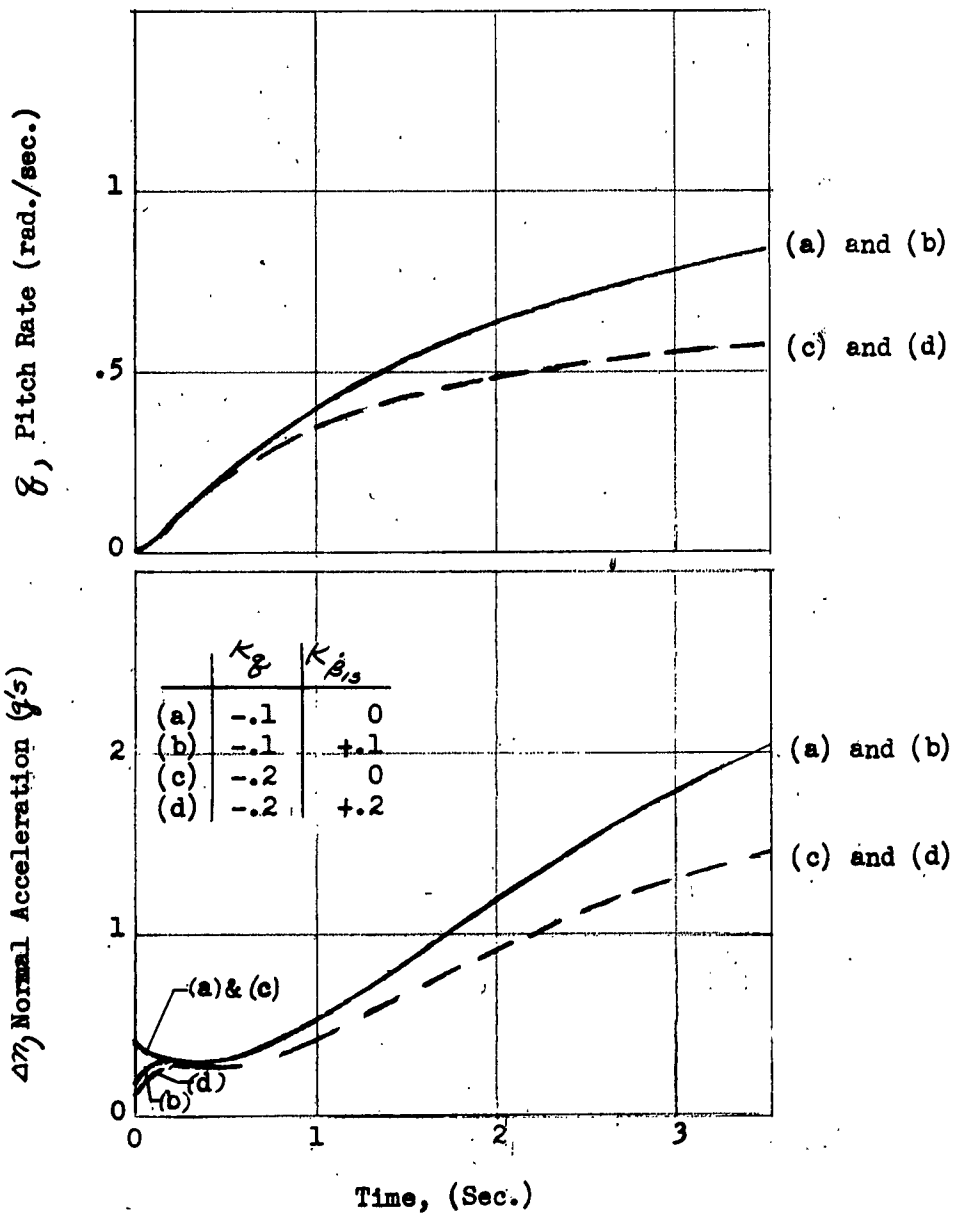

FIG. 47. COMPARISON OF TIP PATH PLANE RATE AND FUSELAGE RATE AUTOPILOTS; INITIAL RESPONSE TO CYCLIC PITCH STEP AT $\mu_0 = .2$

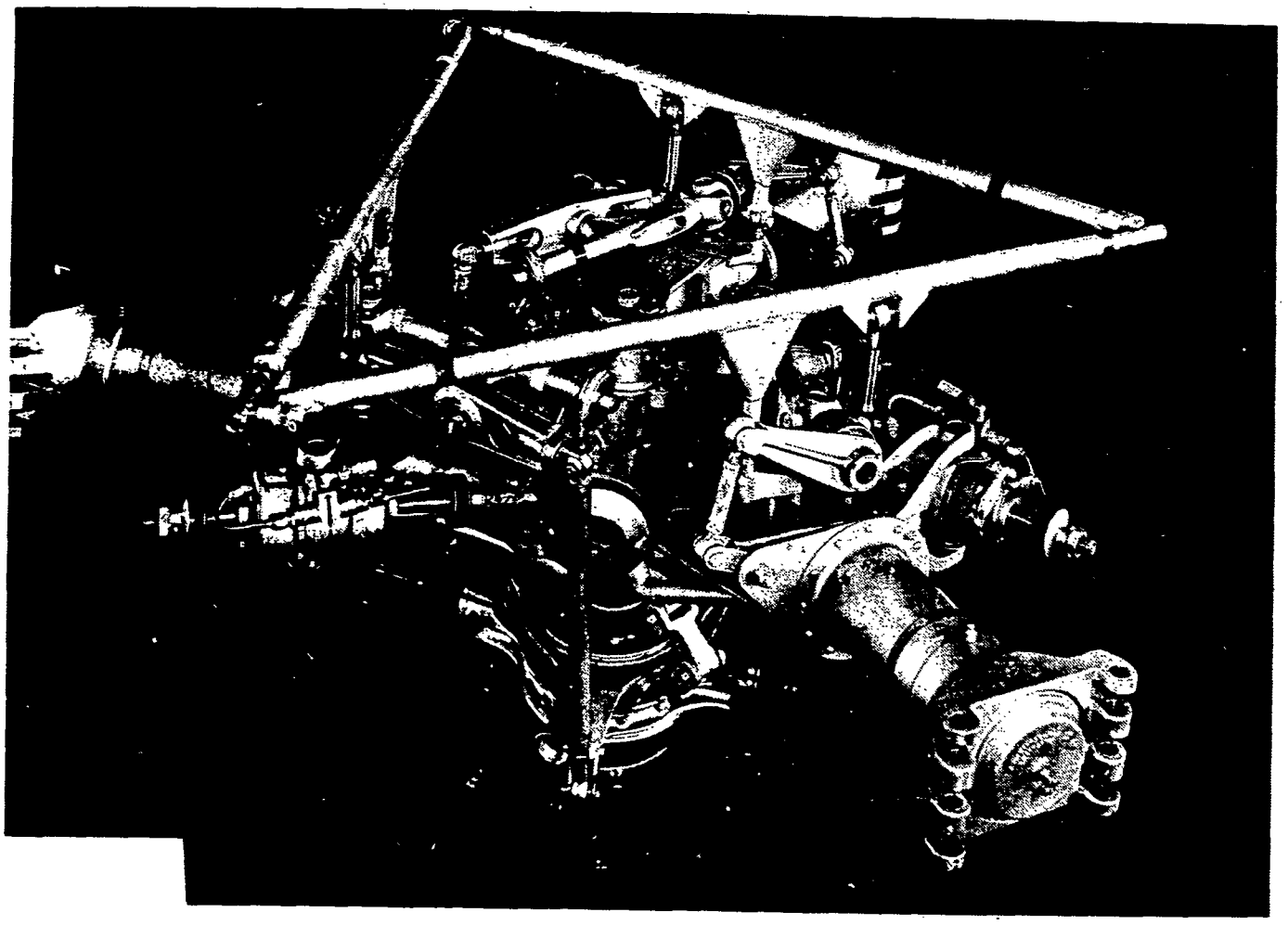

FIG. 48. BIASED CYCLIC CONTROL SYSTEM APPLIED TO H-5 ROTOR HEAD
(Figure taken from Ref. 12)

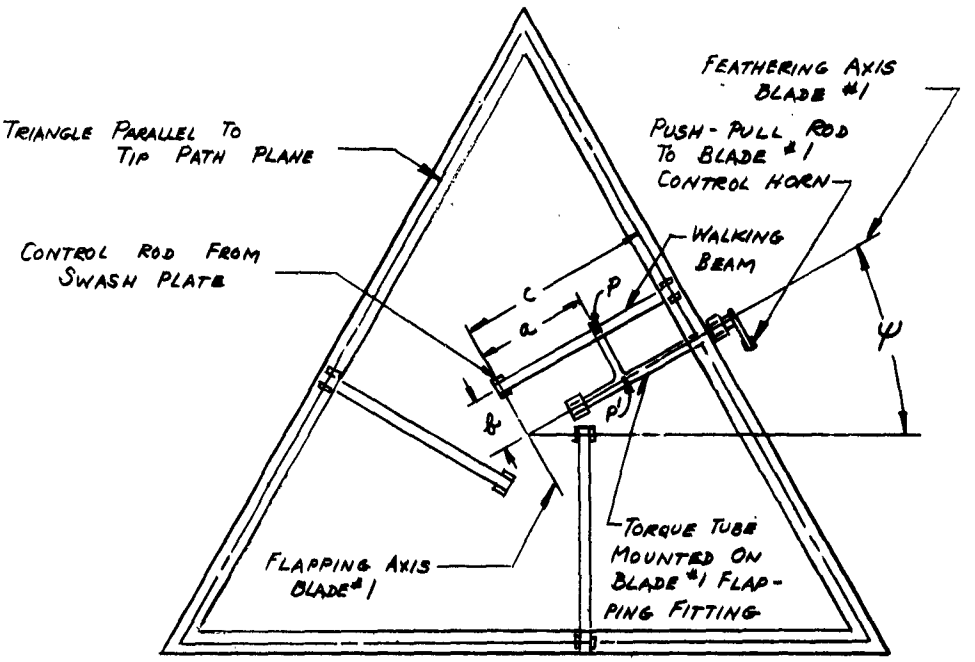

FIG. 49. SCHEMATIC DIAGRAM OF BIASED CYCLIC CONTROL STABILIZER

5.6 Biased Cyclic Control System

(a) Representation by Generalized Autopilot Equations

Cyclic due to autopilot feedbacks:

$$\theta_{1A} = K_{\beta_{1S}} \beta_{1S}$$

Cyclic due to pilot's stick motion:

$$\theta_{1D} = K_D \theta_c$$

(b) Description of Mechanism

Figure 48 is a photograph of a biased cyclic control system for the H-5 helicopter which was described in Ref. 12 and Fig. 49 presents a schematic diagram for the same mechanism. The reference triangle shown is pivoted to the flapping fittings of the three blades in such a manner that it establishes a plane which is parallel to the tip path plane. This attachment is not shown on Fig. 49. The H-5 control system incorporates a torque tube mounted on the flapping fitting of each blade for the purpose of carrying the control input outboard beyond the cyclic pitch change bearings to the blade horn. It can be seen that when the biased cyclic control stabilizer is used the rotation

of the torque tube for each blade depends on the position of the reference triangle as well as on the motion of the control rod from the swash plate. One end of the walking beam shown is pivoted to the reference triangle and the other end is pivoted to the control rod from the swash plate. Point ρ on the walking beam is a ball joint pivot and a difference in vertical motion of points, ρ and ρ' produces a proportional pitch change of Blade #1. Since the reference triangle remains parallel to the tip path plane, this stabilizing device produces a cyclic pitch feedback proportional to the tilt of the tip path plane relative to the shaft (see Part A). The longitudinal and lateral feedback constants introduced by the device are equal in magnitude.

(c) Description of How Device Affects Stability and Control Characteristics

It is shown in Section 3.2 that the influence of a device giving a flapping feedback can be conveniently studied using an effective autopilot equation which does not include blade flapping explicitly but introduces the effect of the flapping feedbacks by using effective feedback constants for the other variables. Another way of looking at the action of a flapping feedback is that it modifies the characteristics of the basic rotor. An increment in rotor tilt produces a proportional increment in cyclic pitch which, in turn, causes aerodynamic forces that modify the rotor tilt. Thus the principal result of the biased cyclic control device is an amplification or attenuation of tip path plane tilt.

The longitudinal flapping equation (B.67, p. 8) takes the following form for hovering using expressions for the derivatives which are given in Part A.

$$\frac{16}{\gamma\Omega}\dot{\beta}_{1s} + \beta_{1s} = -\theta_1 + \left[\frac{16}{\gamma\Omega} + \frac{\mu}{\Omega R}\left(\frac{2}{3}\theta_0 - 2\lambda_0\right)\right]q - \frac{1}{\Omega R}\left(\frac{2}{3}\theta_0 - 2\lambda_0\right)v$$

Substituting for $\theta_1 = \theta_{1A} + \theta_{1B}$ the expressions for the longitudinal cyclic obtained with the biased cyclic system gives

$$\underbrace{\frac{1}{(1+K_{B_{1s}})}}_{\text{Ampl. of rotor time lag}}\underbrace{\frac{16}{\gamma\Omega}\dot{\beta}_{1s} + \beta_{1s}}_{\text{Total rotor tilt relative to shaft}} = \underbrace{\frac{1}{(1+K_{A_{1s}})}}_{\text{Ampl. factor}}\left\{\underbrace{(-K_B\theta_c)}_{\text{Fwd. tilt due to swash plate tilt}} + \underbrace{\left[\frac{16}{\gamma\Omega} + \frac{\mu}{\Omega R}\left(\frac{2}{3}\theta_0 - 2\lambda_0\right)\right]q}_{\text{Forward tilt due to aft pitching velocity } (q)} - \underbrace{\frac{1}{\Omega R}\left(\frac{2}{3}\theta_0 - 2\lambda_0\right)v}_{\text{Aft tilt due to speed increment}}\right\}$$

The above equation is arranged in the same form as the longitudinal flapping equation of the unstabilized helicopter and clearly shows how all of the terms which determine the total tilt are multiplied by $1/(1+K_{A_{1s}})$. This factor is an amplification factor in the useful range of $K_{A_{1s}}$'s for the biased cyclic system which is between 0 and -1. In forward flight the unstable variation of the tip path plane with normal velocity is also amplified. The increase in the tip path plane deflection for a given swash plate deflection could be objectionable in ground runups. However, the same tip path plane tilt for a given stick motion could be maintained by changing the ratio of swash

plate angle to stick deflection (K_D). The forward tilting of the tip path plane due to an aft pitching velocity of the fuselage is increased and has the beneficial effect of increasing the damping in pitch of the helicopter.

Since the control power and rotor damping are primarily due to tilting of the tip path plane relative to the shaft they are affected in approximately the same way by changes in feedback gain. However, when K_D is reduced as mentioned above the control power remains constant and the sensitivity referred to the pilot's stick is reduced.

The third term on the right-hand side of the equation is the aft rotor tilt due to an increment in forward velocity. Its amplification is responsible for an increase in the speed stability of the helicopter in the range of useful gains.

It is interesting to note that in some respects the use of a biased cyclic pitch device is equivalent to using blade flapping hinge offset. In both cases the moments about the c.g. of the helicopter produced by the rotor are greater than would exist without these modifications. The moment amplification in the case of the biased cyclic system is due to a greater tip path plane tilt as a result of cyclic pitch amplification which results in a corresponding tilt of the thrust vector relative to the shaft. In the case of the offset hinge rotor, the amplification is produced by the centrifugal force couple applied to the shaft when the tip path plane tilts relative to the shaft. Although the addition of offset hinges increases the moments on the helicopter, it does not appreciably affect the rate of blade response. On the other hand, the time lag in rotor response due to gyroscopic forces is amplified by the biased cyclic system for feedback gains between $K_{\theta_{1s}} = 0$ and -1. The amplification factor becomes infinite at $K_{\theta_{1s}} = -1$ and at negative values of $K_{\theta_{1s}}$ less than -1 there is a divergent increase in β_{1s} in response to a swash plate deflection.

Initial response characteristics can be improved in hovering with the biased cyclic system since it increases the damping in pitch and roll. However, at high feedback gains the rotor position becomes almost independent of the fuselage motion and a short period oscillatory mode can occur similar to the one described for the stabilizer bar. The prediction of changes produced by the biased cyclic system in the initial response in forward flight is complicated by the increased instability with angle of attack and the increased damping in pitch which oppose each other. The modification of the long period characteristics by the biased cyclic system is also obscured from the intuitive point of view because of its opposing effects on the damping in pitch and speed stability derivatives.

(d) Effects of Biased Cyclic Control on Stability and Control Characteristics of the Sample Helicopter

Initial Response in Hovering Flight:

The effects of the biased cyclic stabilizing mechanism on the initial pitch and roll responses in hovering are illustrated in Fig.50. Time histories are shown for several values of the feedback constant, $K_{\theta_{1s}}$, and the related control gear ratio. The linkage ratio, K_D, is reduced as $K_{\theta_{1s}}$ increases negatively in order to eliminate the possibility of excessive flapping angles.

The case of $K_{\theta_{1s}} = -.5$ and $K_D = .5$ affords a good compromise between desired pitch and roll responses. If the feedback were made more negative the roll response would become objectionably oscillatory and if the feedback were made more positive, the pitch rate response time would increase. As a consequence of the linkage ratio reduction and increased damping, the sensitivity for this case is reduced to approximately half that of the unstabilized helicopter. While the pitch response time of approximately three seconds which is obtained is an improvement over that of the unstabilized helicopter it is still too great.

Initial Response in Forward Flight:

Figure 51 shows initial pitch and normal acceleration response characteristics which might be obtained with the biased cyclic system at $\mu_o = .2$. As pointed out previously, the damping in pitch is increased but an increase in normal velocity instability is also obtained. The net effect is some improvement in maneuver stability and initial forward flight response characteristics. However, at gains as high as $K_{\theta_{1s}} = -.8$ the pitch rate approaches an equilibrium value very slowly and the normal acceleration curves do not become concave downward until after two seconds.

Long Period Response:

Figures 52 and 53 present long period responses obtained for several values of $K_{\theta_{1s}}$ at two values of μ_o. The increments in the speed stability and damping in pitch obtained with the biased cyclic system have opposing effects on the frequency of the long period mode, as mentioned previously, but a net decrease in the period is obtained with more negative gains. It is also found that the stability of the long period oscillation is improved as $K_{\theta_{1s}}$ becomes more negative. These trends are also found using the root locus plot on p. 55 and effective feedback constants computing from the relations given in Section 3.2.

Feedbacks gains of $K_{\theta_{1s}} = -.8$ and lower would probably not be suitable on the basis of initial response characteristics. However, at this feedback the long period response is still quite divergent.

At feedback gains less than $K_{\theta_{1s}} = -.8$ the short period mode becomes very oscillatory. When $K_{\theta_{1s}}$ approaches -1 a neutrally stable short period oscillation is evident in the record. The short period mode of oscillation

involves very little tip path plane motion as evidenced by the fact that the high frequency component in the β_s trace of Fig. 52 is negligible. The period of this mode was computed from the approximate formula,

$$T = 2\pi \sqrt{\frac{I}{W h + \frac{1}{2} \Omega^2 n m_e e d}}$$

which neglects aerodynamic forces. A computed period of 3.3 sec. was obtained which is in fair agreement with the high frequency obtained in the computer solutions.

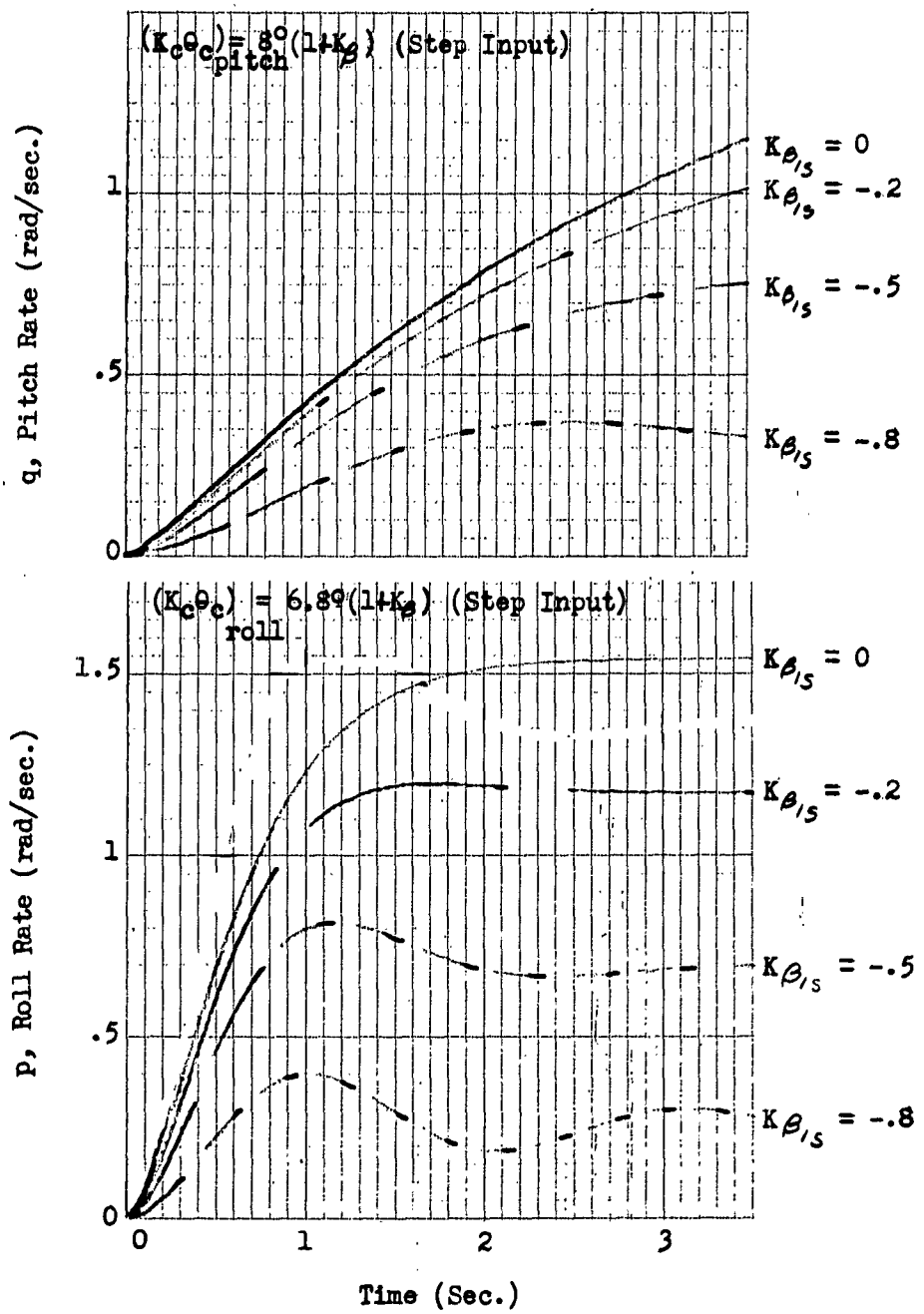

FIG. 50 BIASED CYCLIC CONTROL SYSTEM; INITIAL RESPONSES TO LONGITUDINAL AND LATERAL CYCLIC PITCH STEPS; HOVERING

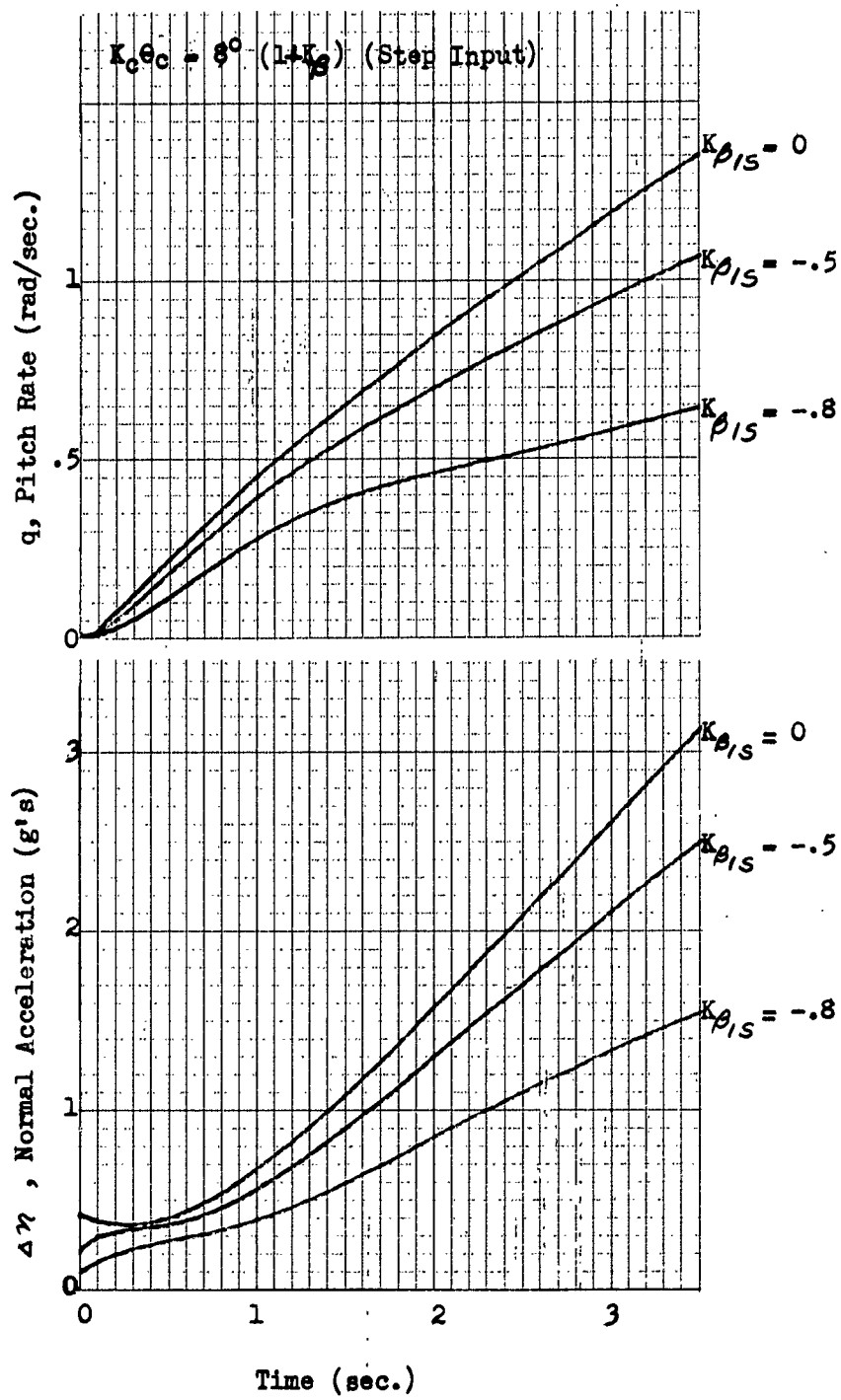

FIG. 51 BIASED CYCLIC CONTROL SYSTEM; INITIAL RESPONSE TO LONGITUDINAL CYCLIC STEP INPUTS; $\mu_o = .2$

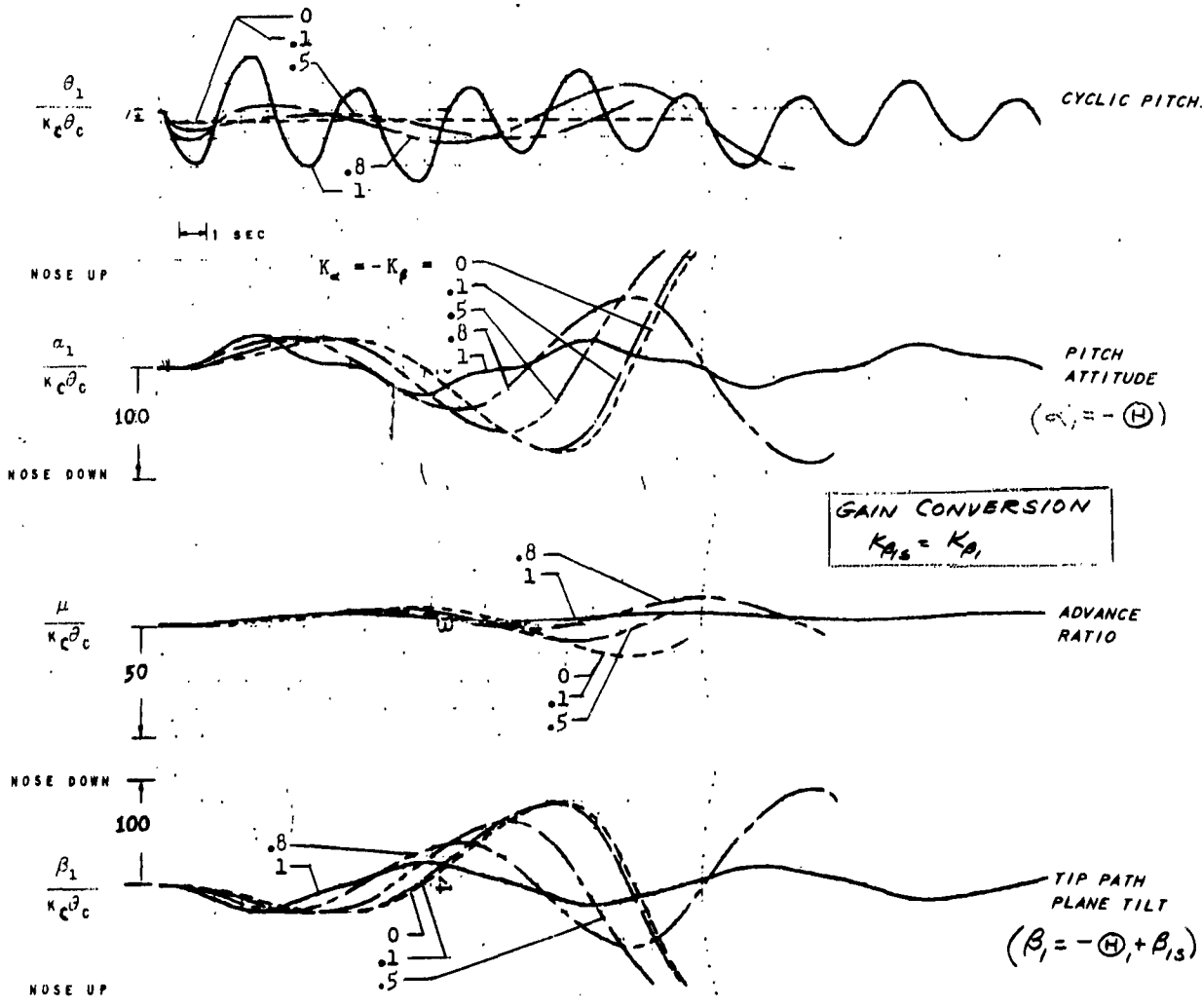

FIG. 52. BIASED CYCLIC CONTROL SYSTEM; HOVERING

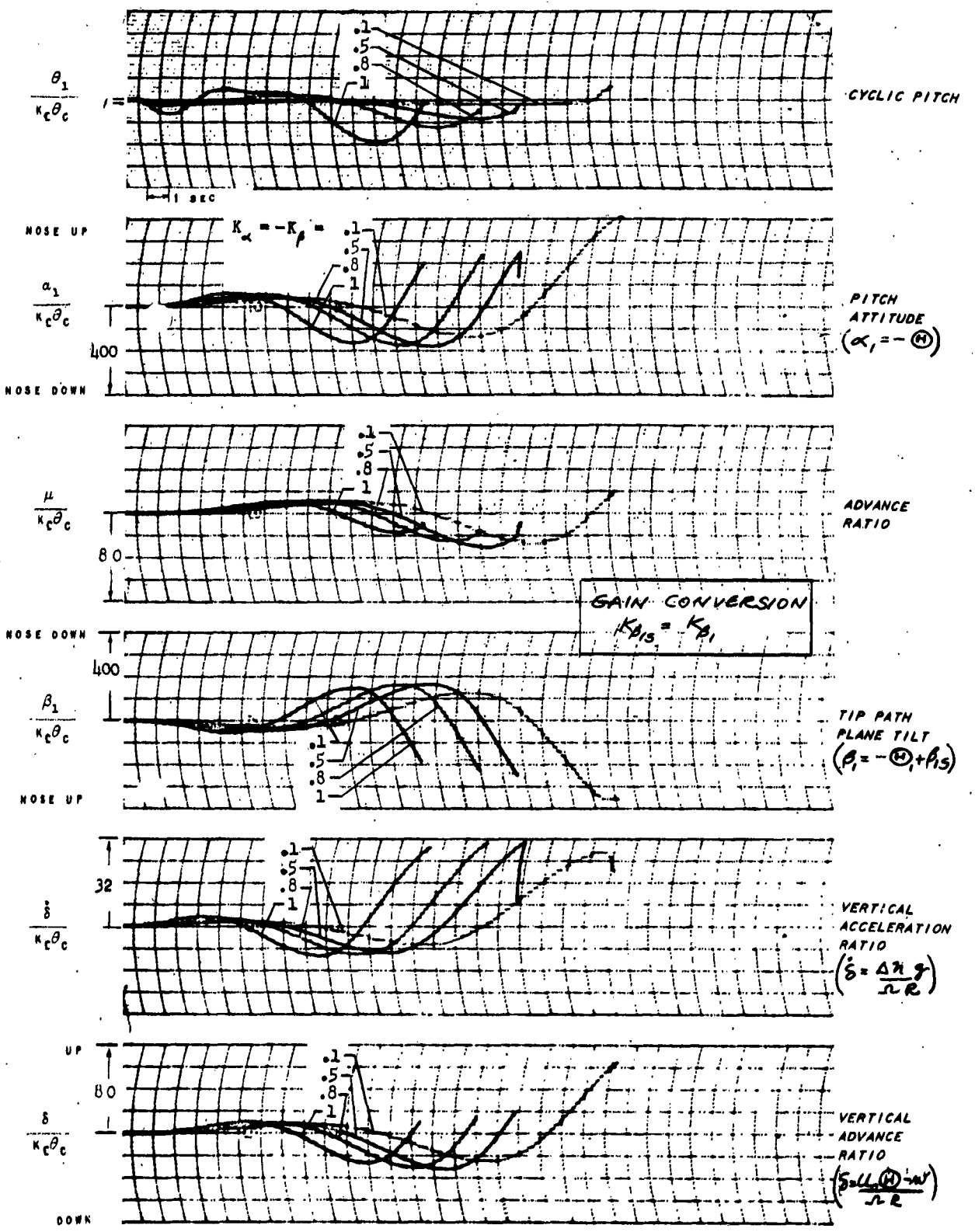

FIG. 53 .BIASED CYCLIC CONTROL SYSTEM ; $\mu_o = .2$

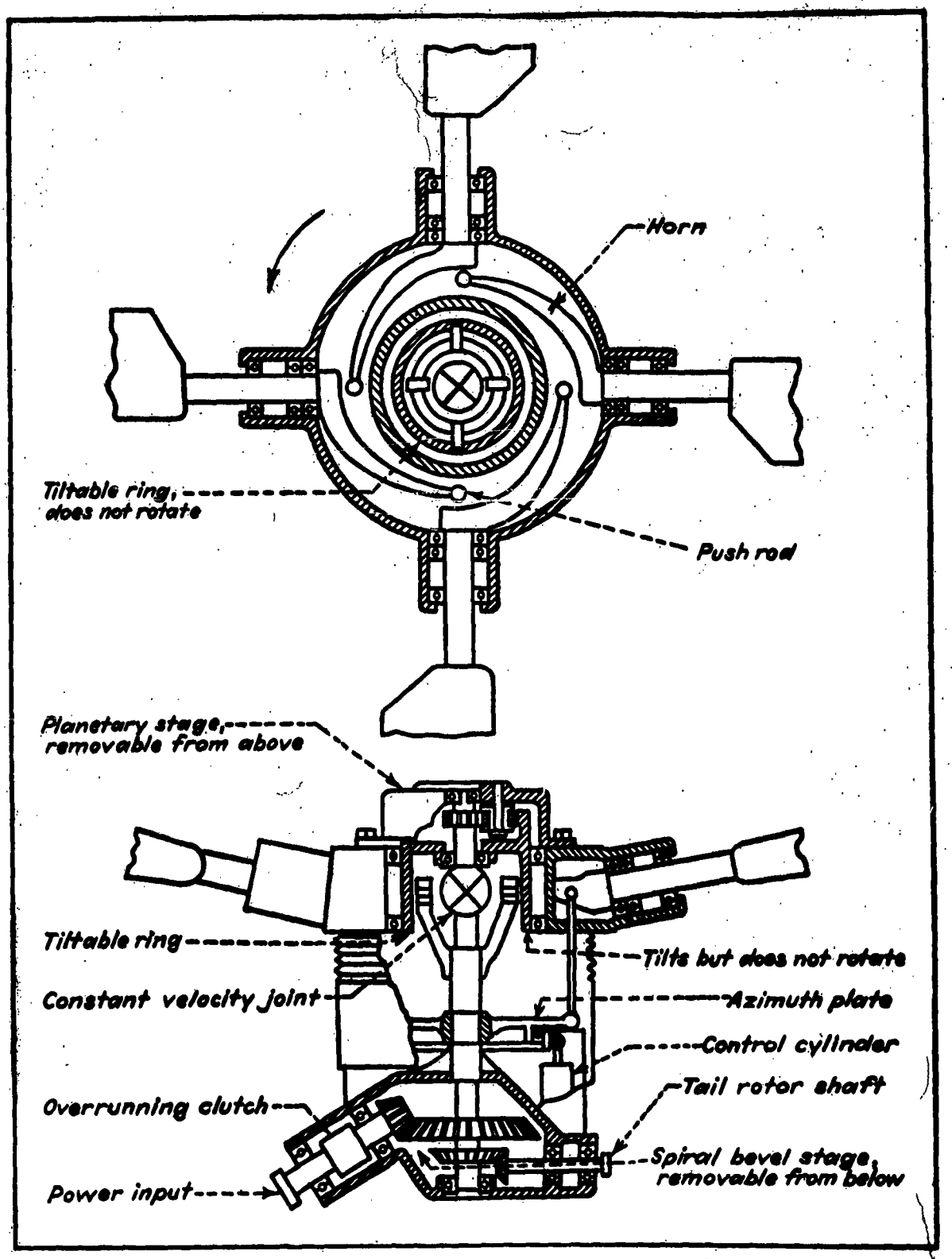

Fig 54 Schematic representation of Doman-Frasier rotor head.
(Taken from Ref. 13)

5.7 Doman-Frasier Rotor Head

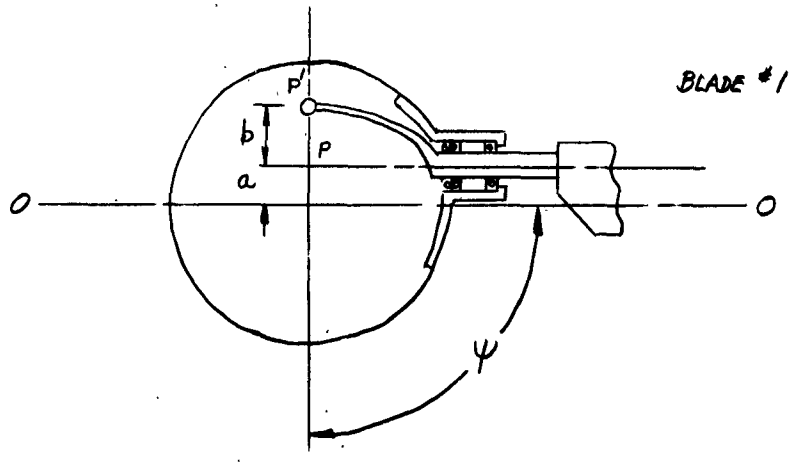

FIG. 55. DIAGRAM SHOWING BLADE CHORDWISE OFFSET

Description of Mechanism:

Figure 54 shows a schematic representation of the Doman-Frasier rotor head taken from Ref. 13. No flapping hinges are provided in this system and the rotor plane of rotation is tilted by tilting the entire hub on which all four blades are mounted. The plane perpendicular to the axis of symmetry of the hub can be assumed parallel to the tip path plane neglecting blade bending.

Figure 54 gives a good over-all picture of the head mechanism but does not show the chordwise offset of the individual blades used in some Doman designs. Figure 55 indicates this offset which introduces a cyclic pitch feedback when the rotor hub tilts relative to the mast. When Blade #1 is in the cross-wind position, as indicated on Fig. 55 , a forward tilting of the tip path plane and rotor hub would cause point P to move into the paper. Since point P' is restrained from moving by the push pull rod from the swash plate, the pitch of Blade #1 would be increased. Consequently, there is a cyclic pitch variation which is proportional to the tilt of the tip path plane relative to a plane perpendicular to the shaft axis (see Part A).

Description of How Device Affects Stability and Control Characteristics:

The cyclic pitch feedbacks of the Doman head and the biased cyclic system are of the same type, and both devices affect the stability and control characteristics of the helicopter in the same manner. Consequently, the discussion previously given for the biased cyclic system is applicable to the Doman Head.

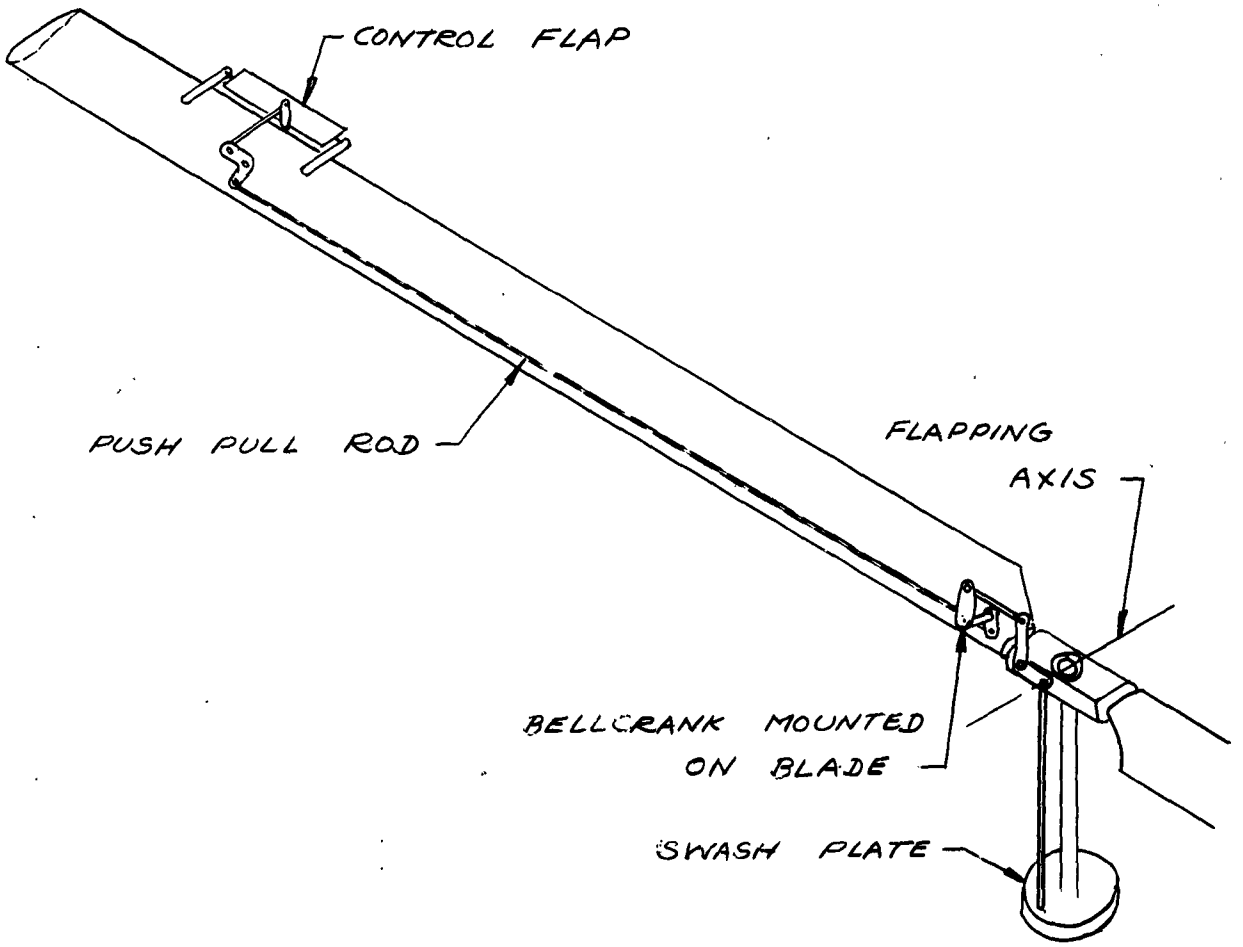

FIG. 56 SCHEMATIC DIAGRAM OF SERVO CONTROL FLAP

5.8 Aerodynamic Servo Control Flap (Kaman)

(a) Representation by Generalized Autopilot Equations

Cyclic due to autopilot feedbacks:

$$\theta_{1A} = K_u U + K_q q + K_w W + K_{\dot{\beta}_{1S}} \dot{\beta}_{1S} + K_{\beta_{1S}} \beta_{1S}$$

Cyclic due to pilot's stick motion:

$$\theta_{1A} = K_c \theta_c$$

(b) General Description

Several helicopter designs (e.g., Kaman helicopters) have used servo control flaps mounted on the blades for rotor control. Figure 56 shows a schematic diagram of the type of servo flap configuration considered in this report. No pitch change bearings are provided at the blade root and pitch change is obtained by structural twisting of the blades. The pilot controls the deflection of the control flap which in turn produces a moment changing the twist of the blades. Cyclic or collective blade pitch changes can be

obtained by applying constant or cyclically varying control flap angles. A possible actuating mechanism is shown for connecting the swash plate to the control flap which incorporates a bell crank mounted at the root of the blade to avoid mechanical coupling with flapping motion. Other root arrangements might be employed to introduce coupling with flapping motion intentionally.

(c) Description of How Device Affects Stability and Control Characteristics

The origins of the cyclic feedbacks obtained with the aerodynamic servo control flap are much the same as those of the swash plate spring-damper device. In both cases motion of the helicopter results in blade pitching moments which produce cyclic pitch changes. It is assumed in discussing the swash plate damper device that the blade rigidity is so high that blade pitching moments would produce negligible structural blade twist. Since the cyclic feedback with the swash plate spring damper is entirely due to the swash plate deflections produced by the applied moments, different longitudinal and lateral feedbacks can be obtained by using different longitudinal and lateral swash plate restraints. On the other hand, the longitudinal and lateral feedbacks of the control flap device are the same, both depending on the torsional rigidity of the blade.

If the blade is dynamically unbalanced because of the addition of the servo flap or overbalanced by compensating ballast weight, the Coriolis forces associated with a pitching velocity of the tip path plane twist the blade cyclically. This is essentially the same effect discussed for the swash plate spring damper on p.110 and is accounted for by the K_{β} and K_{β_3} feedbacks in the generalized autopilot equation. A forward blade c.g. gives a negative K_{β} which tends to increase the damping of the helicopter in pitch and roll. The flapping rate feedback $K_{\dot{\beta}_3}$ due to overbalance is positive for a forward c.g. location and slows down the initial response of the blade to control movement (see p. 109).

In the case of the swash-plate spring damper device the initial blade response could be improved by dampers which introduced a delay before the Coriolis forces could move the swash plate to a new position. There is no practical method for obtaining similar damping with the servo control flap. Tests of a servo flap configuration which were reported in Ref. 14 showed the change in blade twist due to changes in flap angle were almost instantaneous. The small time lag in change of blade twist which does exist is to a large extent determined by the torsional frequency of the rotor blades. Since the torsional frequencies of rotor blades are very high, in general, the time lag (ℓ) in the generalized autopilot representation of the control flap can be taken to be zero.

Apparently it has been the practice to mass balance the blades in some applications of control flaps. In this case, the twisting moments due to Coriolis forces would be eliminated, but K_{β_3}, K_w, and K_v feedbacks would still exist because of the aerodynamic forces acting on the control flap.

It will be remembered that when the tip path plane of a rotor with a flapping hinge tilts relative to the shaft a corresponding cyclic pitch relative to the tip path plane results.

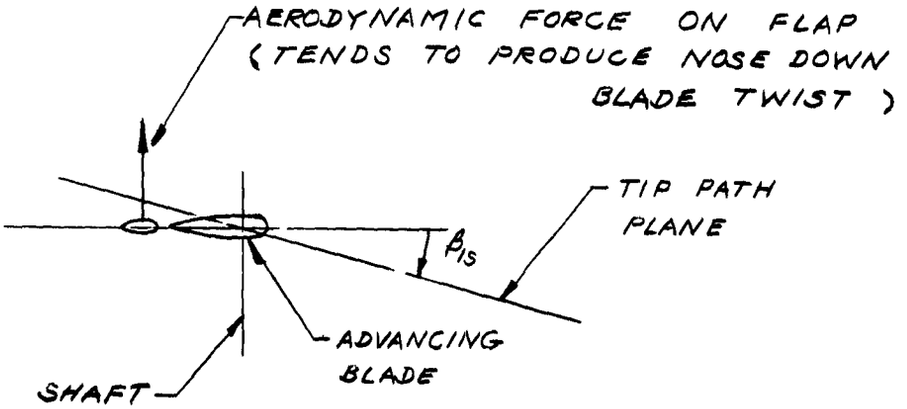

FIG. 57. FLAP FORCE DUE TO ROTOR TILT
(COLLECTIVE PITCH ASSUMED ZERO)

Cyclic aerodynamic forces act on the control flap under these conditions which produce twisting moments that alter the cyclic pitch. For a positive β_{1s} as indicated in Fig. 57, nose down moments act on the advancing blade which reach a maximum at $\psi = 90^{\circ}$ while nose up moments act on the retreating blade with greatest magnitude at $\psi = 270^{\circ}$. It can be seen that the flapping feedback constant $K_{\beta_{1s}}$ is negative since the flap force shown on the advancing blade tends to produce a negative cyclic pitch change. A feedback of this type amplifies the normal rotor tilt as explained on p.114 for the biased cyclic device and an increase in damping in pitch and roll of the helicopter is obtained even when the blades are mass balanced.

The explanation of the normal velocity feedback obtained with the control flap is essentially the same as the one given in Section 5.9 for the swash plate damper device in conjunction with a blade offset between the aerodynamic center and the blade feathering axis. An increase in normal velocity (w) and fuselage angle of attack produces a maximum lift increment on the blade and control flap at an azimuth angle $\psi = 90^{\circ}$ and a minimum increment at $\psi = 270^{\circ}$. Since the flap is aft of the blade elastic axis a nose down blade twist is obtained at $\psi = 90^{\circ}$ and a nose up twist at $\psi = 270^{\circ}$. This cyclic pitch feedback due to the normal velocity is negative and tends to reduce the normal velocity instability of the helicopter.

(d) Effect of an Aerodynamic Servo Flap on the Stability and Control Characteristics of the Sample Helicopter

Initial Response in Hovering Flight:

The study of the effect of a servo flap on the initial response characteristics of the sample helicopter in hovering flight consists in determining the effect of feedbacks which are proportional to the rate of tilting of the tip path plane relative to fixed axes and the flapping of the rotor relative to the shaft. Thus the case considered might be thought of as the combination of a biased cyclic system which gives a flapping feedback and an autopilot which senses the rate of tip path plane tilting relative to fixed axes. In fact, almost identical initial responses can be obtained with any of these devices individually or in combination. The relationships between the aerodynamic servo control flap, biased cyclic, and tip path plane rate feedback systems can be seen most easily from the effective feedback form of the generalized autopilot equation discussed in which blade flapping is expressed in terms of the other variables. This equation reduces to the following for the aerodynamic servo control flap:

$$\theta_1 = K'_u U + K'_w W + K_q q + K'_{\dot{\beta}_{1s}} \dot{\beta}_{1s} + \left[\frac{K_c \theta_c}{1 + K_{\beta_{1s}} (\beta_{1s})_{\theta_1}} \right]$$

The last term gives the steady cyclic pitch which the pilot can apply and includes the amplification due to a flapping feedback. In cases where $K_{\beta_{1s}}$ is different from zero, it has been assumed that the linkage ratio K_c has been changed in the required manner so that cyclic pitch limits are not exceeded with full stick deflections.

In finding initial response characteristics in hovering flight K'_u and K'_w need not be considered. The remaining feedback constants K'_q and $K'_{\dot{\beta}_{1s}}$ can be expressed as follows for the sample helicopter: (See Section 3.1 and 3.2.)

$$K'_q = \frac{K_q + .096 K_{\beta_{1s}}}{1 + K_{\beta_{1s}}}$$

$$K'_{\dot{\beta}_{1s}} = \frac{-K_q - \lambda K_u - .091 K_{\beta_{1s}}}{1 + K_{\beta_{1s}}}$$

It is found that the effective feedback constants K'_q and $K'_{\dot{\beta}_{1s}}$ are opposite in sign but very nearly equal in magnitude*. As a result, essentially the same effective feedback constants and helicopter responses can be obtained with different combinations of pitching rate feedback, K_q, and flapping feedback $K_{\beta_{1s}}$.

*The λK_u term in the numerator of $K'_{\dot{\beta}_{1s}}$ is ordinarily small. It is due to the difference in magnitude of the K_q and $K_{\dot{\beta}_{1s}}$ feedbacks caused by the linear velocity induced at the rotor by an angular velocity about the c.g. of the helicopter.

It follows from the preceding discussion that the effect of an aerodynamic servo control flap on the initial response characteristics of the sample helicopter can be found by proper interpretation of the responses presented for the biased cyclic and tip path plane rate feedback systems. However, in order to make it possible to study the effect of changes in $K_{\dot{\beta}}$ and $K_{\beta_{FS}}$ directly a family of initial response time histories is presented on Fig. 58. It was assumed that $K_{\beta_{FS}} = K_{\dot{\beta}}$ in obtaining the computer solutions which are presented on this figure.

Initial Response in Forward Flight:

Figure 59 presents time histories showing the influence of an aerodynamic servo control flap on the pull up characteristics of the sample helicopter at $\mu_o = .2$. Responses are shown for three different $K_{\dot{\beta}}$'s corresponding to three values of blade chordwise balance. The control flap configuration which is considered gives a flapping feedback constant $K_{\beta_{FS}} = -.5$ and a normal velocity feedback $K_W = -.00037$ rad./(ft./sec.). It is shown in Part A that the ratio of the flapping and normal velocity feedbacks provided by the servo flap depends on the flaps spanwise location as follows,

$$\frac{K_W}{K_{\beta_{FS}}} = \frac{\mu_o (R/R_F)^2}{\Omega R \left[1 - \frac{1}{4}\mu_o^2 (R/R_F)^2\right]}$$

where R_F is the radius of the servo flap. The results shown on Fig. 59 were based on a tab at 75% of the blade radius.

It is assumed that at zero time the pilot instantaneously applies full aft stick displacement which produces a swash plate tilt of $K_c \theta_c = 4^\circ$. This is only 50% of the swash plate deflection of the unstabilized helicopter since the linkage ratio is reduced to avoid excessive flapping due to the negative flapping feedback constant. Consequently, the initial load factor increment at zero time due to the increase in swash plate angle of attack is only one-half as large with the aerodynamic servo control flap as obtained with the unstabilized helicopter. However, there is a rapid increase in cyclic pitch due to the flapping feedback when the tip path plane tilts to a new position as evidenced by the rapid normal acceleration build up in the first .2 sec. Although the normal acceleration time histories for the servo flap case level off at .2 sec., they do not show a dip which might make the pilot think the maximum acceleration had been reached.

It will be noted in the first one-half second that the pitching rate responses obtained with the servo flap are displaced slightly relative to the curve for the unstabilized helicopter. This displacement results from the lower initial cyclic pitch and the slower blade response which is obtained when there is an effective tip path plane rate feedback constant. After about one-half sec., the effect of the increased damping in pitch obtained with the servo flap becomes apparent in the pitch rate responses causing them to level off more rapidly. Also, it is found that the increased damping in pitch causes the normal acceleration time histories for the servo flap to become concave downward before two seconds.

Although the assumed servo flap configuration has a negative normal velocity feedback, $K_w = -.00037$, the effective normal velocity feedback, K'_w, is positive. The explanation for this sign change is that the negative flapping feedback, which causes the unstable variation of tip path plane tilt with normal velocity and angle of attack to be amplified, contributes a large positive increment to the effective normal velocity feedback. Figure 60 was prepared to show the magnitudes of the changes produced by the effective normal velocity feedback by comparing the initial responses for the aerodynamic servo control flap, biased cyclic, and tip path plane rate feedback systems. The feedback constants for the different devices considered on Fig. 60 are tabulated below.

FEEDBACK CONSTANTS FIG. 60

				Effective Constants	
	$K_{\beta_{1s}}$	$K_\theta = -K_{\beta_{1s}}$	K_w	$K'_\theta \approx -K'_{\beta_{1s}}$	K'_w
Tip Path Plane Rate	0	-.1	0	-.1	0
Biased Cyclic	-.5	0	0	-.1	.0009
Servo Flap	-.5	0	-.00037	-.1	.0001

It can be seen that the three devices introduce the same effective pitching rate feedback constant ($K'_\theta = -.1$). They also all introduce approximately the same flapping rate feedback constant ($K_{\beta_{1s}} \approx .1$). As a result, approximately the same cyclic feedback is obtained with each of these devices for a given tilting rate of the tip path plane.

The biased cyclic introduces a large positive effective normal velocity feedback due to its negative flapping feedback ($K_{\beta_{1s}} = -.5$). A much lower effective normal velocity feedback is obtained with the servo flap, and the effective normal velocity feedback of the tip path plane rate device is zero. The responses for the different devices shown on Fig. 60 indicate the time histories become more divergent as the normal velocity instability of the helicopter is made larger by increasing K'_w. The normal velocity feedback of the aerodynamic servo flap becomes more negative as the flap is moved inboard as indicated on p. 128. If it were feasible to use a more inboard flap location than 75% blade radius the normal velocity feedback might be made sufficiently negative to eliminate the normal velocity instability of the helicopter.

Long Period Response:

Figures 61, 62 , and 63 present responses showing the long period characteristics of the sample helicopter when stabilized by an aerodynamic servo control flap. The flap configuration considered on Fig. 61 and Fig. 62 gives a zero forward speed feedback and equal pitching and flapping rate feedbacks ($K_\theta = -K_{\beta_{1s}} = -.1$). Time histories are presented on these figures for flapping feedbacks of $K_{\beta_{1s}} = -.6, -.8$, and -1.

Figure 58 indicates that a fairly good compromise in parameters from the initial response standpoint is obtained by selecting $K_{\beta_{1s}} = -.5$ and $K_\theta = -K_{\beta_{1s}} = -.1$. The curve for $K_{\beta_{1s}} = -.6$ on Fig.61 corresponds to a configuration which is fairly close to the above mentioned configuration of Fig. 58, but the $K_{\beta_{1s}} = -.8$ and -1 configurations of Fig.61 would be undesirable from the initial response standpoint.

The effective feedbacks corresponding to the $K_{\beta_{1s}} = -.6$, $K_\theta = -.1$ case are:

Hovering:

$$K'_\theta = -.394$$
$$K'_u = .001158$$

$\mu_o = .2$:

$$K'_\theta = -.499$$
$$K'_u = .00101$$
$$K'_w = .001415$$

Effective speed and normal velocity feedbacks are present due to the flapping feedback.

Since the long period oscillations on Fig. 61 are not far from neutral stability, it might be expected that the approximate expressions for the long period mode given on p. 23 would be applicable. Substituting numerical value into these expressions gives:

Hovering:

$P \approx$ 16.6 sec.

$\mu_o = .2$:

$P \approx$ 15.8 sec.

The computed periods are found to be nearly the same in hovering and forward flight and are within 12% of those obtained from the analogue solution. A somewhat more divergent long period response is obtained in forward flight.

Figure 63 indicates the result of selecting an initial servo flap angle which would produce a negative speed feedback. The negative speed feedback in combination with the flapping feedback gives an approximately zero effective speed feedback for the case considered. As might be expected, a considerable lengthening of the oscillation periods is obtained compared to those of Fig. 61 but little change in the damping of the long mode is found. These results again show that stabilization with feasible K'_θ and K'_u feedbacks can at best make long mode oscillation approximately neutrally stable.

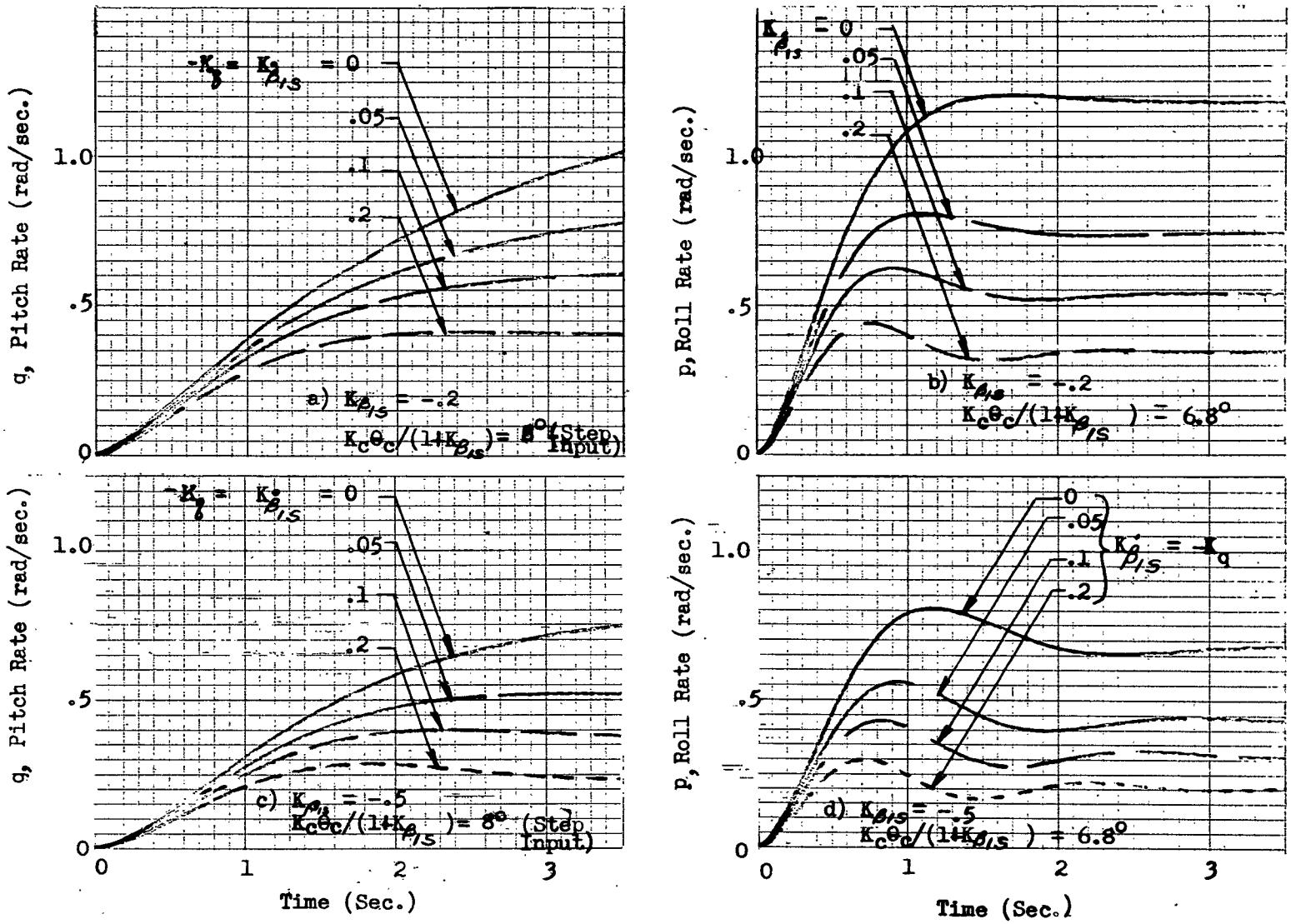

FIG. 58. AERODYNAMIC SERVO CONTROL FLAP; INITIAL RESPONSES TO LONGITUDINAL AND LATERAL STEP INPUTS; HOVERING

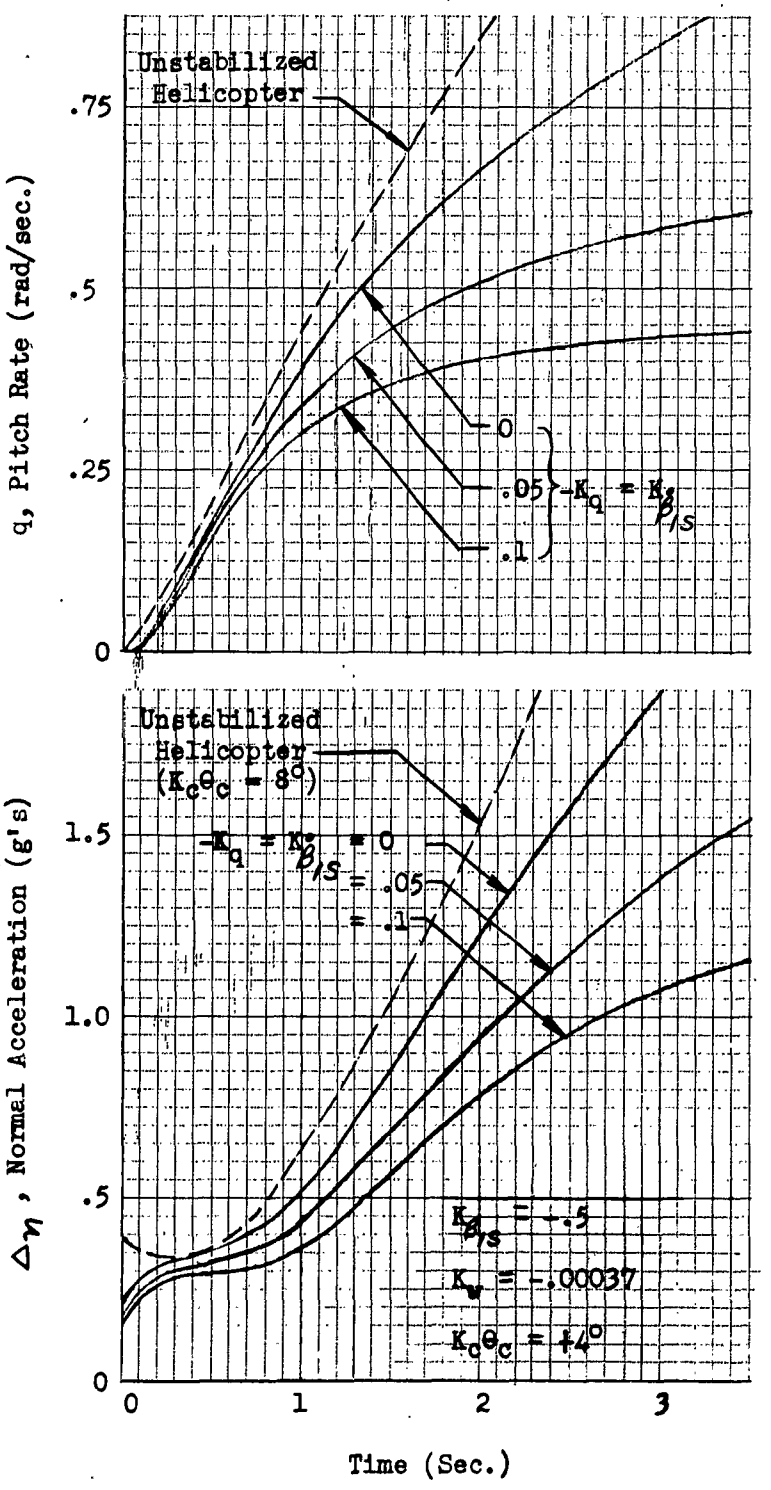

FIG. 59. AERODYNAMIC SERVO CONTROL FLAP; INITIAL RESPONSES TO CYCLIC PITCH STEPS; $\mu_o = .2$

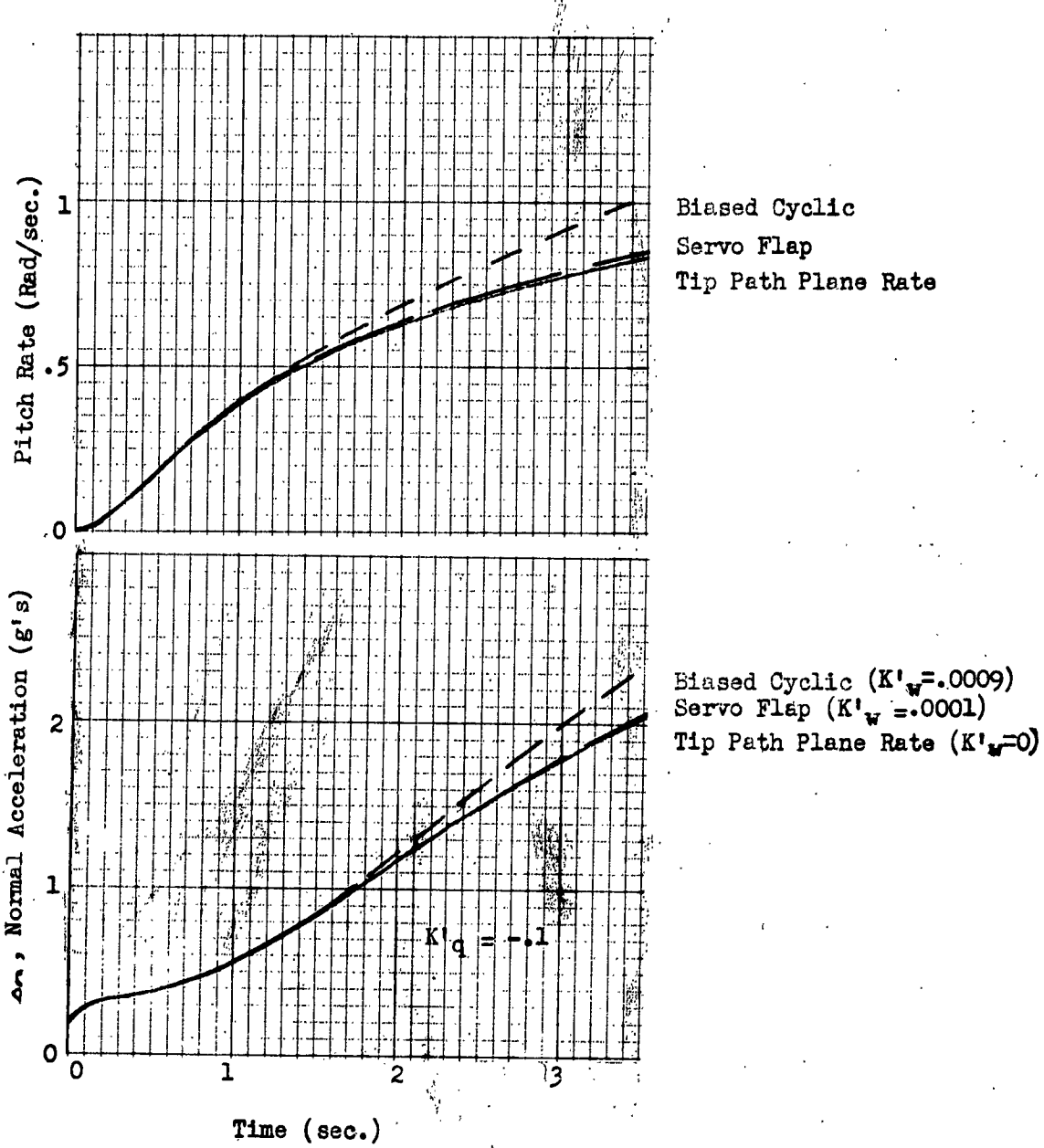

FIG. 60. COMPARISON OF AERODYNAMIC SERVO CONTROL FLAP, BIASED CYCLIC AND TIP PATH PLANE RATE FEEDBACK SYSTEMS; INITIAL RESPONSES TO CYCLIC PITCH STEPS; μ_o = .2.

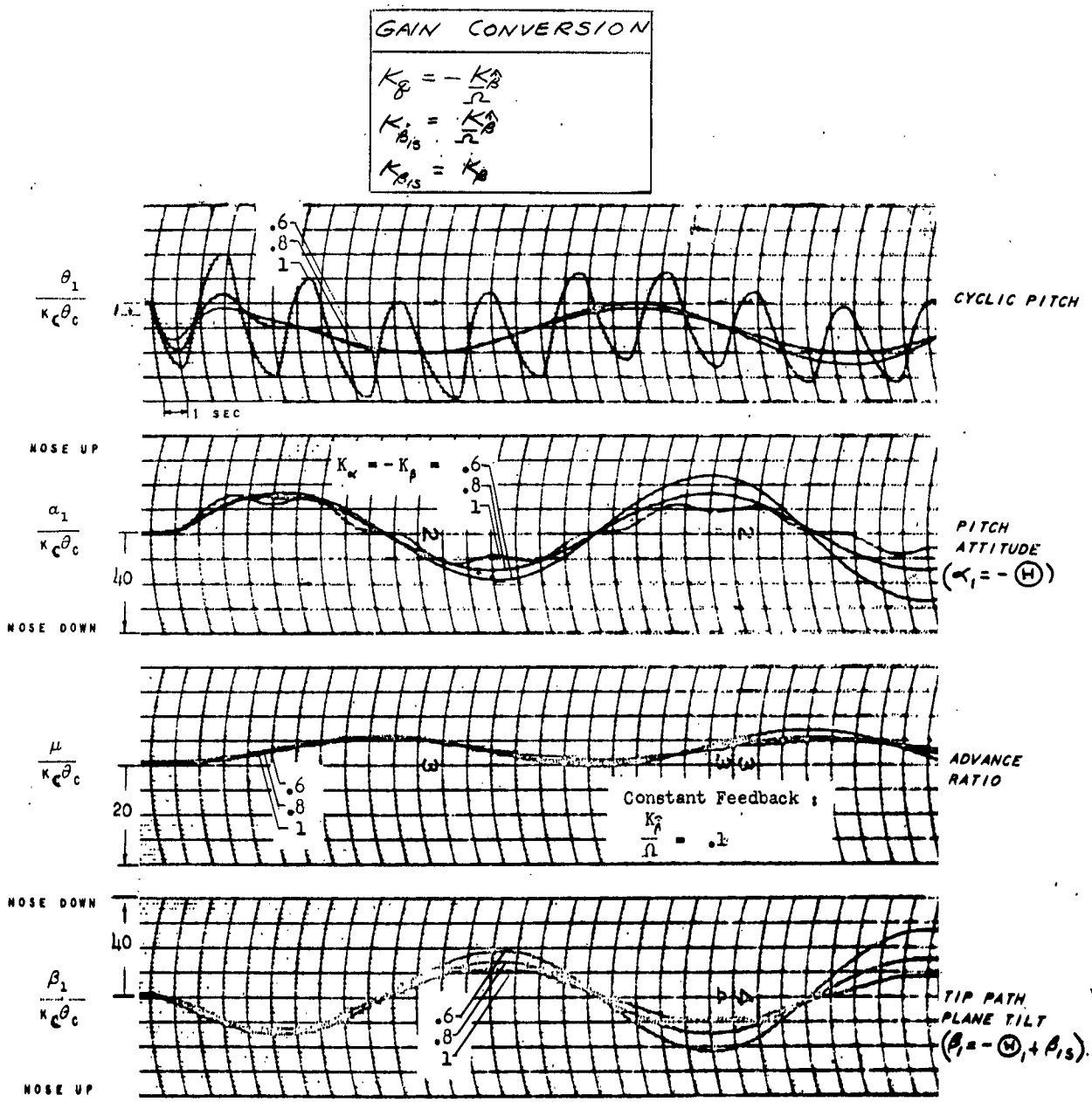

FIG.61. AERODYNAMIC SERVO CONTROL FLAP ; HOVERING

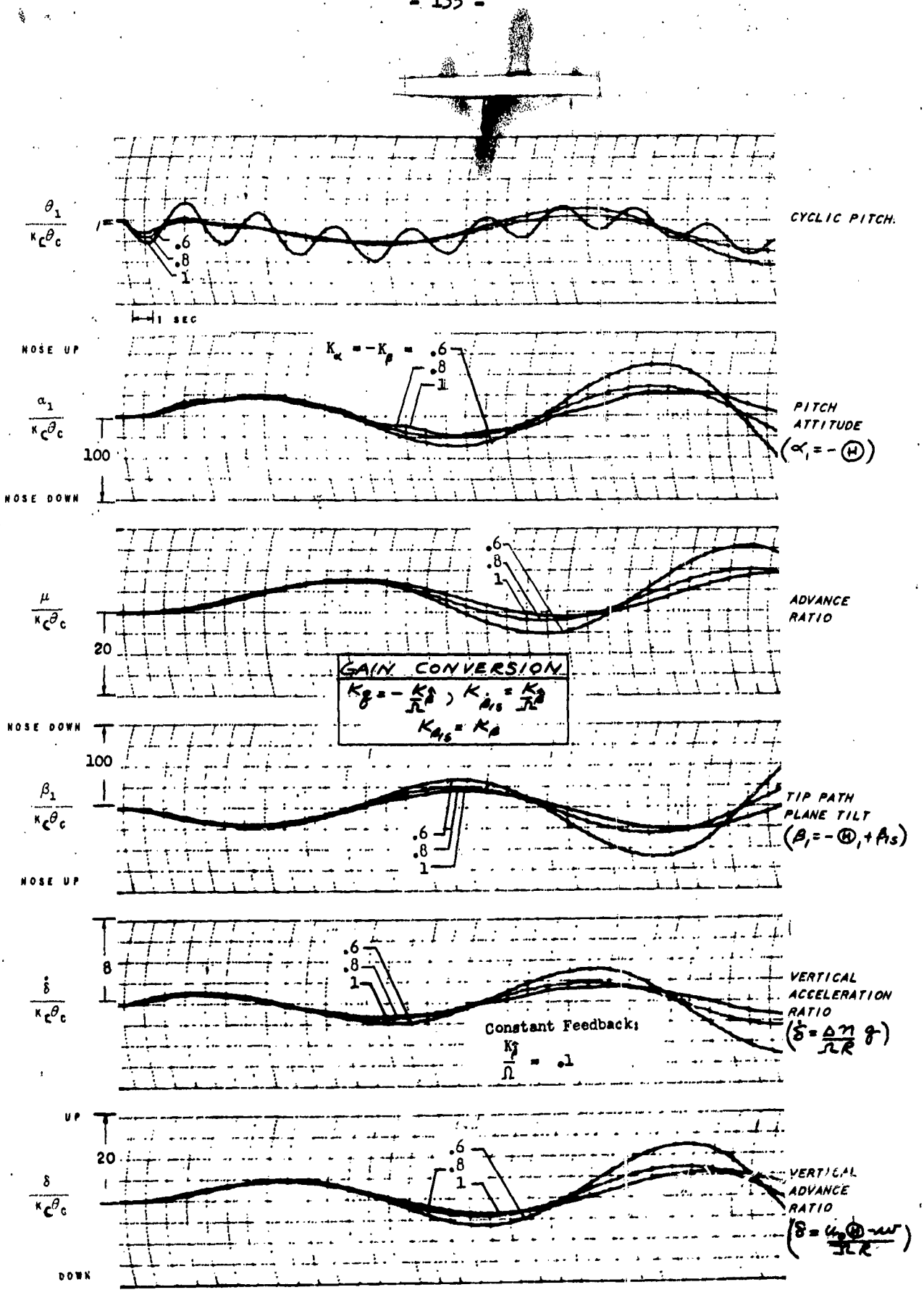

FIG. 62. AERODYNAMIC SERVO CONTROL FLAP ; $\mu_0 = .2$

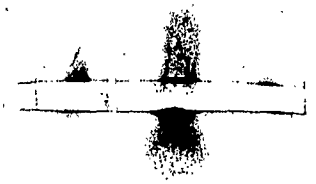

GAIN CONVERSION
$K_{\theta_1} = -\left(\frac{K_\beta}{\Omega} + .0136\, K_\mu\right)$
$K_{\dot\beta_{1S}} = K_\delta$; $K_{\beta_{1S}} = K_\beta$
$K_U = \frac{K_\mu}{490}$

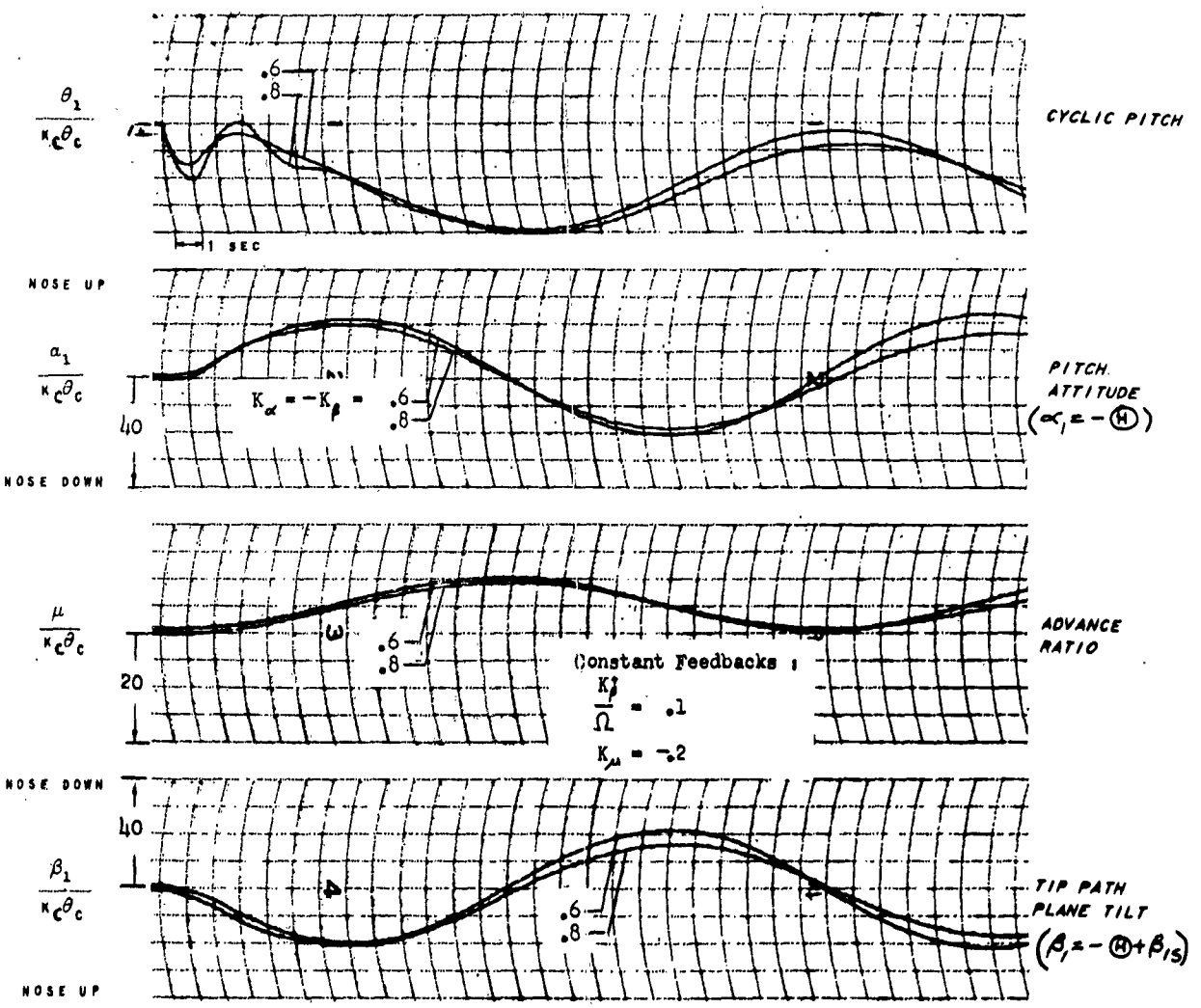

FIG. 63. AERODYNAMIC SERVO CONTROL FLAP ; HOVERING

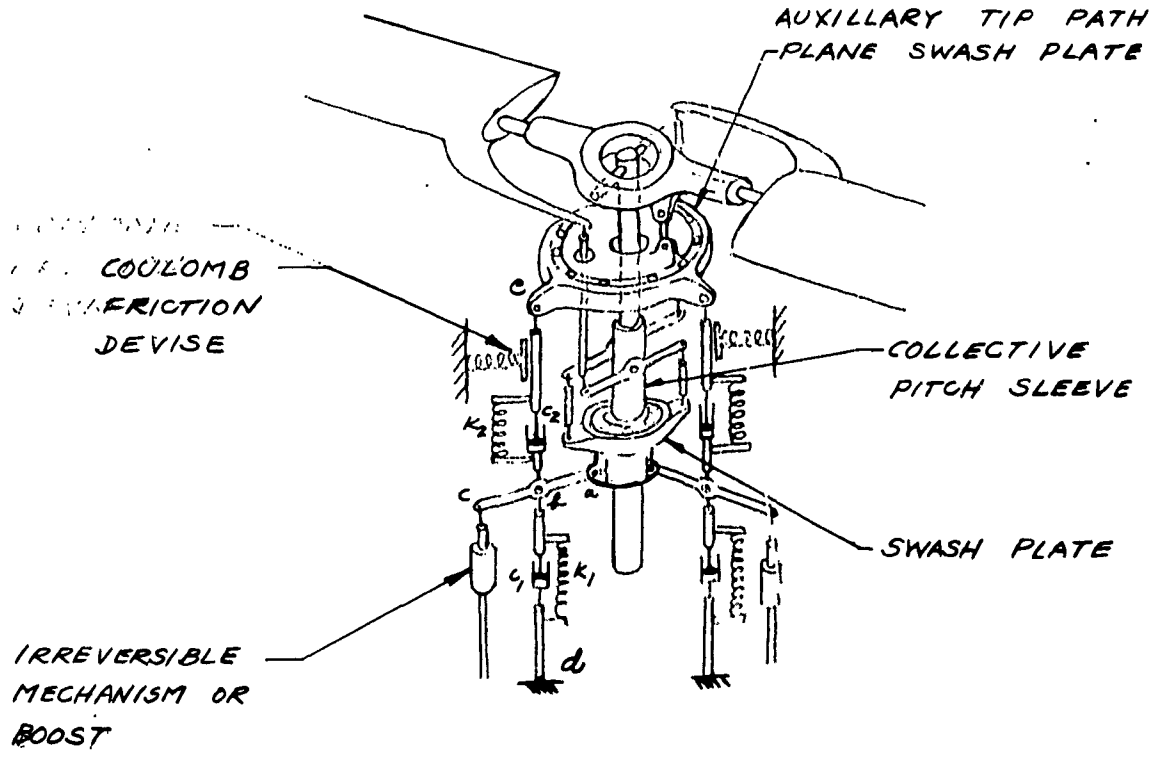

FIG. 64. SCHEMATIC DIAGRAM OF A SWASH PLATE SPRING DAMPER STABILIZING DEVICE

5.9 Swash-Plate Spring-Damper Stabilizing Mechanism

(a) Representation by Generalized Autopilot Equations

Cyclic due to autopilot feedbacks:

$$\ell \dot{\theta}_{1A} + \theta_{1A} = K_u U + K_w W + K_\theta \theta + K_{\beta_{1S}} \dot{\beta}_{1S} + K_{\beta_{1S}} \beta_{1S}$$

Cyclic due to direct mechanical linkage to stick:

$$\theta_{1D} = K_D \theta_c$$

Cyclic due to aerodynamic forces resulting from stick deflection:

$$\ell \dot{\theta}_{1L} + \theta_{1L} = K_L \theta_c$$

(b) General Description

In early flight tests of helicopters it was found that control characteristics were influenced by the chordwise balance of the rotor blades. Hohenemser included the effect of chordwise balance on blade torsion in discussing control in an early paper (Ref. 15) and also considered balance in Ref. 16. However, it is believed Miller (Ref. 17 and 18) presented the first complete analysis of the possibility of utilizing blade dynamic overbalance and aerodynamic unbalance in combination with spring and viscous restraints in the control system to produce desired helicopter stability and control characteristics. The present discussion of a swash-plate spring-damper system is limited to the type discussed by Miller in Ref. 18.

A schematic diagram of a spring damper system which incorporates the two sets of springs and dampers considered by Miller is shown on Figure 64 . This diagram is not intended to suggest a practical configuration for this device but merely to aid in visualizing its operation.

The general description will be confined to the longitudinal components which are labeled on the diagram since the lateral system operates in a similar manner. The basic principal of operation of this device is that forces fed back from the rotor through the linkage system cause the swash-plate to deflect in such a manner that stabilization results. The swash plate assembly which is shown is mounted on a universal joint which cannot move vertically relative to the fuselage, and collective pitch is changed by sliding the collective pitch sleeve up or down. The collective pitch is actuated through an irreversible mechanism and is not affected by the spring-damper system.

The total longitudinal tilt of the swash-plate is proportional to the movement of point a and results from the combined movements of points b and c. The motion of point c is proportional to the fore and aft stick motion of the pilot. A boost or irreversible mechanism is required in the cyclic control system to avoid transmitting the forces produced by unbalancing the blades to the control stick.

The motion of point b is due to deflections of the spring-damper system. Spring K_1 and damper C_1, the spring and damper elements usually envisaged for a device of this type are connected in parallel to the fuselage at point d. The addition of spring K_2 and damper C_2 in parallel was suggested in Ref. 18 to improve the performance of the system. It was proposed that the motion of point e be made proportional to the tilt of the rotor tip path plane relative to the shaft. Presumably this motion might be obtained by the use of an auxiliary tip path plane swash-plate, if no simpler mechanical arrangement could be devised. The tip path plane swash-plate might be mounted to the shaft by a universal joint. In the two blade rotor case of Fig. 64 it would probably be necessary to restrain such an auxiliary swash-plate by sufficient coulomb friction to prevent it being moved by the forces applied by spring K_2 and damper C_2. However, the larger forces due to rotor flapping would be able to overcome the coulomb friction and cause the auxiliary swash-plate to assume a position parallel to the tip path plane.

(c) Description of How Device Affects Stability and Control Characteristics

The previous discussion has been concerned with the kinematics of the swash-plate spring damper stabilizing device, and blade pitching moments which are responsible for the swash-plate deflections have not been discussed. Blade pitching moments occur when the blade c.g. and aerodynamic center are not on the feathering axis or when blade camber is used.

The gyroscopic properties of rotor blades have been referred to previously in discussing the damping of rotors and control rotors. A somewhat more careful consideration of this phenomenon is necessary to understand how blade unbalance influences blade pitching moments. It is convenient to explain these gyroscopic effects in terms of Coriolis forces acting perpendicular to the tip path plane. Figure 65 indicates these Coriolis forces for the case when the tip path plane has a forward tilting velocity. The Coriolis forces are zero at azimuth angle zero and act upward on the advancing blade reaching a maximum when the blade is in the cross wind position. They then gradually decrease in magnitude with azimuth angle becoming zero at an azimuth angle of 180 degrees. The Coriolis forces on the retreating blade act downward for this condition and have their greatest magnitude at an azimuth angle of 270 degrees. It is not difficult to determine the direction of these forces by considering the motion as follows. When a blade element is at an azimuth angle of 45 degrees it has an upward velocity due to the tilting of the tip path plane. However, when the blade element reaches an azimuth angle of 90° and is on the tilting axis its vertical velocity is zero. The mass element tends to retain the vertical velocity it had at azimuth angle 45 degrees and exerts the upward force indicated. Similar reasoning can be used to determine the direction of action of the Coriolis forces at other azimuth positions.

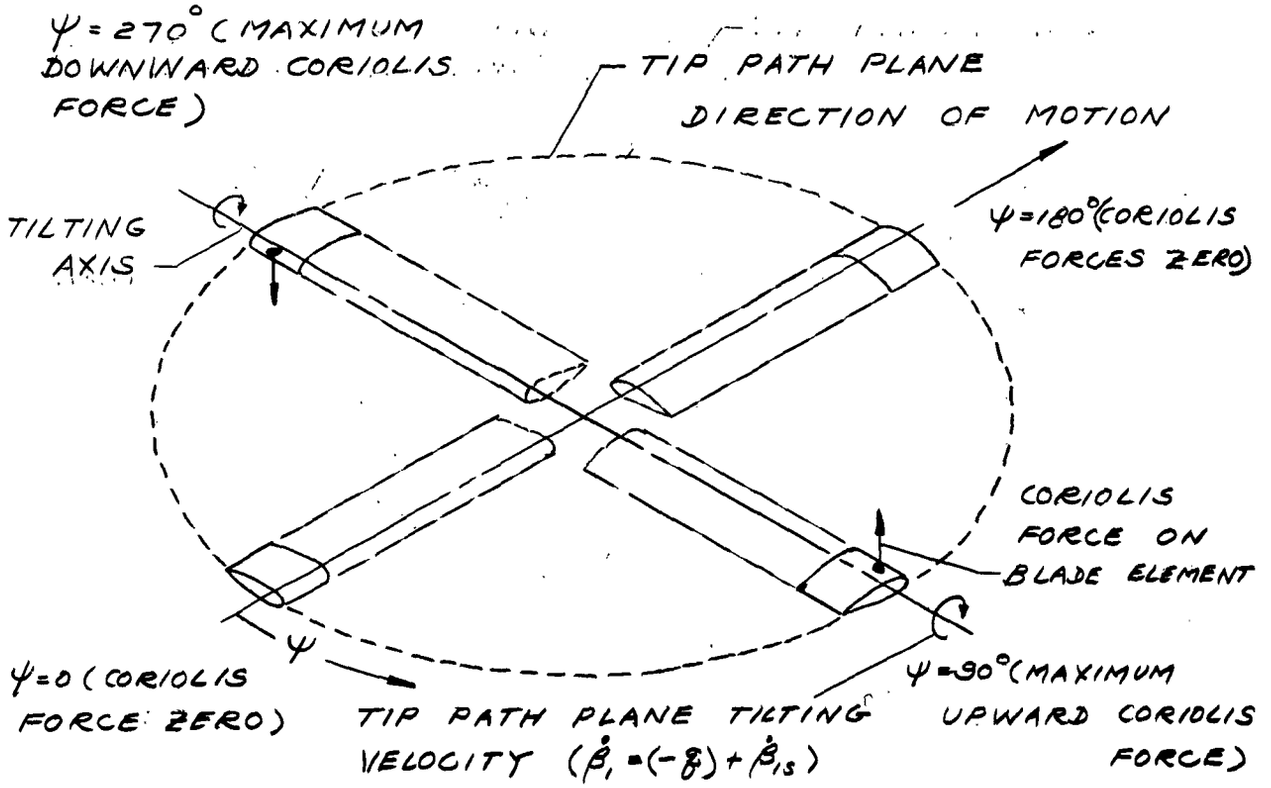

FIG. 65. CORIOLIS FORCES ON BLADE ELEMENT DUE TO FORWARD TILTING VELOCITY OF TIP PATH PLANE

On Figure 65 the c.g. of the blade section is shown to be forward of the blade feathering axis. The Coriolis forces, acting at the c.g., tend to increase the blade pitch at azimuth angle 90 degrees and decrease the blade pitch at azimuth angle 270 degrees, and a corresponding cyclic pitch occurs when the swash-plate is not rigidly restrained. $\dot{\beta}_1$, the forward tilting velocity of the tip path plane referred to fixed axes is in general due to the sum of $(-\dot{\beta})$, the forward pitching velocity of the fuselage and $\dot{\beta}_{1s}$, the tilting velocity of the tip path plane relative to the shaft (i.e. the rate of change of longitudinal flapping). Coriolis forces are primarily responsible for the $K_{\dot{\beta}}$ feedback in the autopilot equation for the swash-plate spring damper and are entirely responsible for the $K_{\dot{\beta}_{1s}}$ feedback when damper C_1 is not present. A forward blade c.g. location as indicated in Figure 65 results in a negative $K_{\dot{\beta}}$ feedback and a positive $K_{\dot{\beta}_{1s}}$ feedback.

The negative $K_{\dot{\beta}}$ feedback increases the damping in pitch of the helicopter as in the case of the Bell Stabilizer bar. If the fuselage had a constant forward pitching velocity $(-\dot{\beta})$, the cyclic feedback $(-\dot{\beta}K_{\dot{\beta}})$ would be positive, making the swash-plate tilt aft relative to the fuselage. The corresponding aft tilt of the tip path plane and thrust vector would produce the desired pitching moment tending to damp the forward pitching velocity of the fuselage.

It should be pointed out that the swash-plate spring-damper mechanism, like the tip path plane rate autopilot can appreciably change the rotor response to a cyclic input applied by the pilot when the helicopter fuselage does not move. This results from the gyroscopic feedback, $K_{\dot{\beta}_{1s}}$, being proportional to the tilting velocity of the tip path plane rather than the rolling or pitch rate of the fuselage as discussed in preceding sections. When the swash-plate is given a forward increment the new equilibrium position of the tip path plane is tilted forward by the same amount whether or not there is a $K_{\dot{\beta}_{1s}}$ feedback. However, the addition of the $K_{\dot{\beta}_{1s}}$ feedback reduces the forward swash-plate tilt while an equilibrium state is being established and thus makes it take longer for a new equilibrium position to be achieved. The rapidity of the blade response is considerably affected by swash-plate damper c_1 . Damper c_1 introduces a time lag ℓ before the blade pitching moments can move the swash-plate to a new position and thus reduces the effectiveness of the $K_{\dot{\beta}_{1s}}$ feedback.

Another application of the swash-plate spring-damper mechanism suggested in Ref. 18 is the control of long period dynamic oscillations by modifying the speed derivative of the helicopter. A speed feedback K_u might be obtained by using cambered rotor blades which tend to decrease blade pitch. Since the moments due to camber are greater on the advancing blade they tend to produce a cyclic pitch which would make the tip path plane tilt forward with an increment in speed partially compensating for the inherent aft tilting of a rotor due to forward speed.

An aerodynamic parameter affecting the feedback constants obtained with the swash-plate spring-damper is the chordwise location of the blade aerodynamic center relative to the blade pitching axis. When the fuselage pitch angle is increased in forward flight increasing the fuselage angle of attack (α_F) and normal velocity (w), there is an increase in rotor lift. The lift increment on the advancing blade is greater than the increment on the retreating blade tending to cause the rotor tip path plane to tilt further aft than in a similar hovering condition. This effect results in the normal velocity instability of the helicopter as previously discussed. However, the increased lift on the advancing blade in the $\psi = 90^\circ$ position produces a nosedown pitching moment increment about the blade feathering axis when the aerodynamic center is aft of the feathering axis, while the decreased lift in the $\psi = 270^\circ$ position produces a nose-up increment in blade pitching moment. These moments produce a cyclic pitch feedback when a swash-plate spring-damper is used which tends to make the tip path plane tip forward and reduce the instability. This effect is accounted for by the K_w feedback in the autopilot equation.

The displacement of the aerodynamic center relative to the feathering axis also affects the speed feedback (K_u) and longitudinal flapping feedback ($K_{\beta_{1s}}$) provided by the swash-plate spring-damper.

Miller's investigation indicated that it was difficult to avoid short period oscillations in the response of the helicopter studied in Ref. (18) when stabilized by a swash-plate spring damper system consisting of spring K_1 and damper c_1 alone. In order to eliminate these transient oscillations, he

suggested introducing spring K_2 and damper C_2 which apply moments to the swash-plate which are proportional to the longitudinal flapping and flapping rate relative to the fuselage. The magnitudes of the $K_{\beta_{1s}}$ and $K_{\dot{\beta}_{1s}}$ feedback constants in the generalized autopilot representation of this device could then be adjusted by changes in K_2 and C_2 without affecting the K_q or K_w feedbacks. He found if possible to obtain well damped short period oscillations in spite of a long autopilot time lag by use of a negative $K_{\dot{\beta}_{1s}}$ feedback.

The spring-damper system which has been discussed offers a number of advantages. One is the fact that different degrees of stabilization could be provided in pitch and roll. However, there are a number of practical difficulties which must be overcome to make such a system a reality. Chief among these are the elimination of unwanted friction in the control system, providing suitable swash-plate damping, and designing a system which is free of flutter and vibration difficulties.

(d) Effect of Basic System ($K_2 = C_2 = 0$) on the Stability and Control Characteristics of the Sample Helicopter

This sub-section considers how the stability and control characteristics of the sample helicopter are affected by the basic swash-plate spring-damper mechanism which does not include spring, K_2, damper C_2, nor the auxiliary tip path plane swash-plate shown on Figure 64. The longitudinal autopilot parameters which are affected by the basic system and the relationships existing between them are as follows:

ℓ — can be adjusted independently by changing swash-plate damper (C_1)

K_u — can be adjusted independently by using blade camber

$K_q = -K_{\dot{\beta}_{1s}} - \ell K_u \approx -K_{\dot{\beta}_{1s}}$ — K_q and $K_{\dot{\beta}_{1s}}$ are approximately equal in magnitude differing only because of the linear velocity at the rotor due to pitching about the c.g. They can be adjusted by changing the blade mass balance.

$\frac{K_w}{K_{A_{1s}}} = \frac{\mu_0}{\lambda R(\frac{1}{3} - \frac{1}{4}\mu_0^2)}$ — Both K_w and $K_{\beta_{1s}}$ are proportional to the offset (χ_1) between the blade aerodynamic center and the feathering axis.

Initial Response in Hovering Flight ($\ell = 0$):

If very stiff swash-plate restraining springs were used and the swash-plate damping were kept to a minimum, it should be possible to make the generalized autopilot time lag negligible as in the case of the servo flap. This would probably require using a strap-type blade retention to reduce the bearing loads due to centrifugal force. In hovering flight the same feedbacks might be obtained with a negligible time lag swash plate spring-damper device as with the servo flap. Thus the initial responses for this case can be studied by referring to the responses presented for the servo flap in Section (5.8). The responses presented

for the tip path plane rate autopilot are also applicable to the negligible time lag spring-damper when there is no aerodynamic offset and $K_{\beta_{1S}}$ feedback.

Separate curves are not presented showing the effect of a negligible time lag swash-plate spring damper on initial longitudinal response characteristics in forward flight. However, the shape of the response curves for the spring-damper device can be inferred from those presented for the aerodynamic servo control flap and the tip path plane rate autopilot.

Curves (b) and (d) on Figure 47 are applicable when there are no $K_{\beta_{1S}}$ and K_W feedbacks which would result from aerodynamic offset. A negative K_W feedback tending to reduce the normal velocity instability of the helicopter is obtained by offsetting the blade aerodynamic center aft of the feathering axis. For example a configuration with an aerodynamic offset which gives a flapping feedback, $K_{\beta_{1S}} = -.5$ would have the following effective normal velocity and pitching rate feedbacks:

$$\text{FOR} \begin{cases} \mu_0 = .2 \\ K_{\beta_{1S}} = -.5 \\ K_q = 0 \end{cases}$$

$$K_W / K_{\beta_{1S}} = .00126$$

$$K'_W = \frac{K_W - .000831 K_{\beta_{1S}}}{1 + 1.08 K_{\beta_{1S}}} = -.00046$$

$$K'_q = \frac{K_q + .0958 K_{\beta_{1S}}}{1 + 1.08 K_{\beta_{1S}}} = -.10$$

Referring to Fig. 60 p133 it can be concluded that the response obtained with a swash plate spring damper configuration giving a feedback $K'_W = -.00046$ would tend to level off slightly faster than the responses for the servo flap and the tip path plane rate autopilot.

Initial Response (Appreciable Time Lags):

In discussing how initial response characteristics are affected by a swash-plate spring-damper mechanism with an appreciable time lag, it is assumed that the aerodynamic offset (χ_A) is zero. Both $K_{\beta_{1S}}$ and K_W are zero when χ_A is zero and the generalized autopilot equation for the basic swash-plate spring-damper system reduces to:

$$l \dot{\theta}_{1A} + \theta_{1A} = K_u u + K_q q + K_{\dot{\beta}_{1S}} \dot{\beta}_{1S}$$

The neglect of the K_w feedback should not seriously reduce the potentialities indicated for the device since it is shown to have a relatively small effect on initial response characteristics in the preceding discussion.

It is not necessary to consider the K_v feedback in discussing the initial response and the remaining control equation for the swash-plate spring-damper with time lag only differs from the generalized autopilot equation for the Bell Stabilizer Bar in the presence of a tip path plane rate feedback. Fig. 66 shows how the initial hovering response characteristics of the sample helicopter are modified by a swash-plate spring-damper stabilizer with a one sec. time lag. For comparison one curve is presented with $K_{\dot{\beta}_{1/3}}$ equal to zero which corresponds to a Bell Stabilizer Bar configuration. It is found that the responses obtained for the swash-plate spring-damper with time lag and the Bell Stabilizer Bar are almost identical.

A very oscillatory roll response is obtained with the swash-plate spring-damper device when there is a large time lag as in the case of the stabilizer bar. However, different longitudinal and lateral autopilot constants can be used with the swash-plate spring-damper making it possible to select optimum values of the time lag for both longitudinal and lateral responses.

Fig. 67 shows how initial response characteristics at $\mu_o = .2$ are modified by a swash-plate spring-damper device for the same feedbacks used for the hovering case on Fig. 66 . These responses are very similar to those which would be obtained with the Bell Stabilizer Bar at the same time lag and pitching rate feedback. It will be noted that there is no reduction in the normal acceleration at zero time due to the $K_{\dot{\beta}_{1/3}}$ feedback as was found on Fig. 47 . When there is an appreciable time lag the feedback is no longer effective in reducing the initial dip in the normal acceleration curve.

Long Period Response:

The long period responses which can be obtained with the basic swash-plate spring-damper device are similar to those with the aerodynamic servo control flap when the time lag is small and are similar to those with the Bell Stabilizer Bar when appreciable autopilot time lags are present. Thus it can be seen from an inspection of the time histories presented in sections 5.3 and 5.8 that the inherent long period instability of the helicopter can be reduced by the basic swash-plate damper system but good damping of the long period mode is not obtained with feedback parameters which are suitable for improving the initial response.

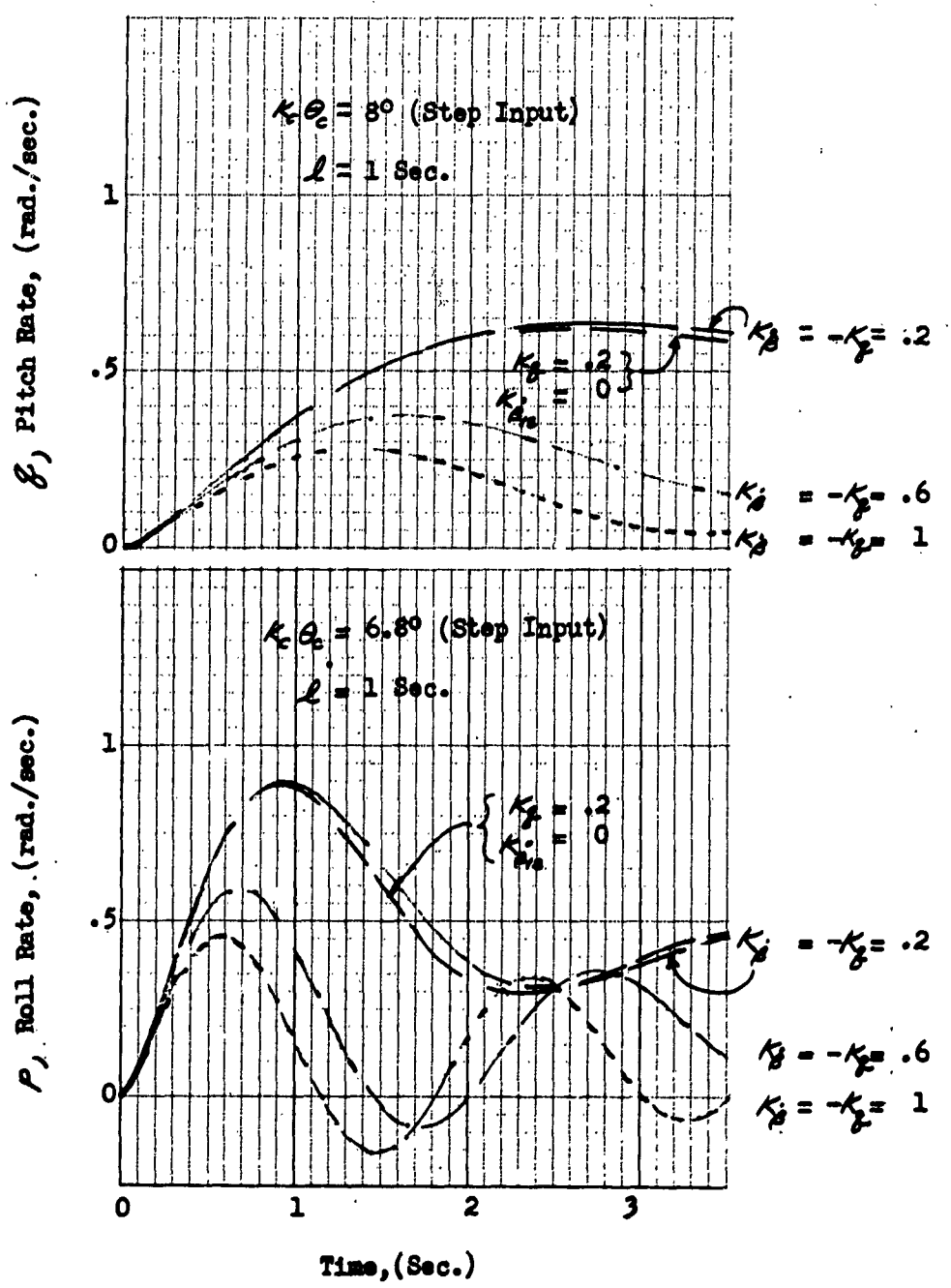

FIG. 66. SWASH PLATE SPRING DAMPER; INITIAL RESPONSES TO LONGITUDINAL AND LATERAL STEP INPUTS IN HOVERING FLIGHT

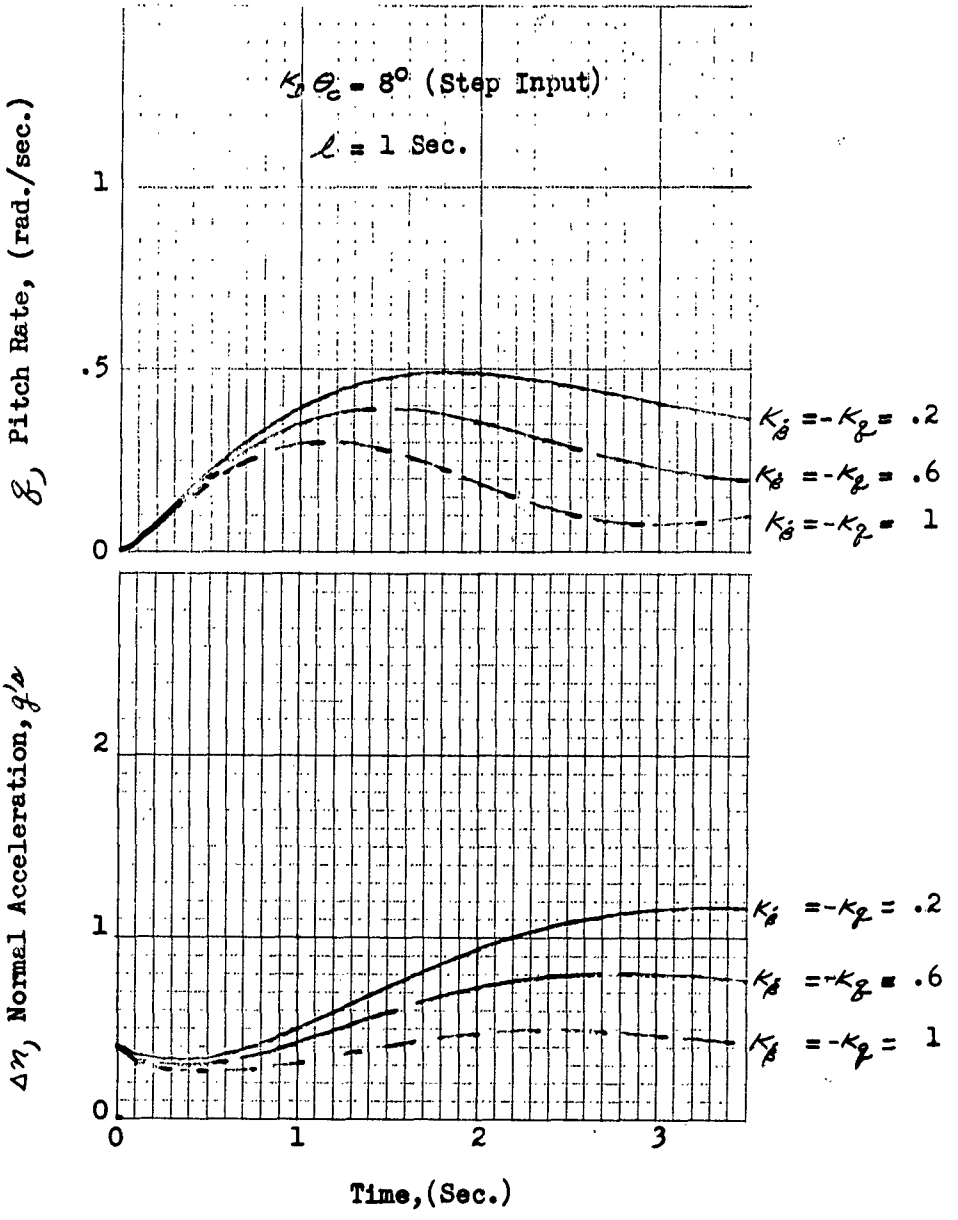

FIG. 67. SWASH PLATE SPRING-DAMPER DEVICE; INITIAL RESPONSE TO LONGITUDINAL CYCLIC PITCH STEP AT μ_o = .2

DISCUSSION OF INDIVIDUAL DEVICES - GROUP IV

The devices classified in Group IV are only effective in forward flight and their principal characteristic is to eliminate the unstable pitching moment variation of the helicopter with normal velocity and fuselage angle of attack. The devices considered in Group IV are the fixed horizontal tail, floating vane stabilizer, and pitch cone coupling linkage and are discussed in sections 5.10, 5.11 and 5.12 respectively.

5.10 Fixed Horizontal Tail

(a) Representation of Device

The fixed horizontal tail is represented by changing the appropriate helicopter stability derivatives (see Part A, Appendix A). It is assumed that the tail forces are small compared to the rotor thrust and only moment changes are significant.

In the space-fixed axis system:

$$\Delta m_\mu = 2 K_t \left[\alpha_{1_0} + (\alpha_i)_t + \frac{(V_i)_{TAIL}}{2\mu_0 \Omega_0 R} \right] \mu_0$$

$$\Delta m_\alpha = K_t \mu_0^2$$

$$\Delta m_\beta = K_t \mu_0$$

$$\Delta m_{\hat{z}} = K_t \left(\frac{l_t}{R} \right) \mu_0$$

$$K_t = \frac{\rho S_t l_t R^2}{2 I} \left(\frac{d C_L}{d \alpha} \right)_t = \text{tail effectiveness}$$

In the moving axis system:

$$\Delta \bar{M}_u = U_0 \rho S_t l_t \left(\frac{d C_L}{d \alpha} \right)_t \left[- \Theta_0 + (\alpha_i)_t + \frac{(V_i)_{TAIL}}{2 U_0} \right]$$

$$\Delta \bar{M}_w = - \frac{U_0 \rho S_t l_t}{2} \left(\frac{d C_L}{d \alpha} \right)_t$$

$$\Delta \bar{M}_q = - \frac{U_0 \rho S_t (l_t)^2}{2} \left(\frac{d C_L}{d \alpha} \right)_t$$

(b) Description of Mechanism

The application of the fixed horizontal tail to the helicopter is, of course, similar to the use of horizontal tails on fixed wing aircraft. The tail on a helicopter encounters high angles of attack in some flight conditions and there has been a tendency to use low aspect ratio or dart configurations to avoid tail stall. Both fixed and movable tails have been employed. (For example Ref.19 presents flight test results obtained with fixed and movable tails linked to the control stick)

Only the longitudinal stability is considered in the present study although mounting additional vertical surfaces would improve lateral characteristics.

(c) Description of How Fixed Tail Affects Stability and Control Characteristics

Since the tail of a helicopter is in general aft of the c.g. the tail forces produced by changes in fuselage angle of attack and normal velocity are in a direction to reduce the angle of attack to zero. Also pitching velocity about the c.g. causes a tail angle of attack increment which gives rise to pitching moments tending to damp the motion. Thus stabilizing increments are added to both the normal velocity and damping in pitch derivatives and these changes do not depend on the tail incidence.

Tail loads are affected by increments in forward speed because of the corresponding changes in dynamic pressure and downwash angle at the tail. The magnitude and the sign of the moment derivative increment, ΔM_u, can be adjusted by changing the tail incidence angle $(\epsilon_i)_t$.

Since the stabilizing moments on the tail are proportional to the initial velocity, U_o, it is evident that this device is ineffective in hovering to the degree of approximation used here.

(d) Effect of Fixed Tail on Stability and Control Characteristics of the Sample Helicopter

It is assumed in the study that the fixed tail added to the sample helicopter is as far aft on the fuselage as possible (i.e. $l_{c/R} \approx 1$). This location gives the maximum increase in damping in pitch for a given increase in normal velocity stability.

Initial Response in Forward Flight:

The destabilizing normal velocity derivative of the helicopter is reduced as K_t increases and becomes zero at $K_t = .0154$. Since the damping in pitch also becomes larger with this change the maneuver stability is increased, and improved initial response characteristics would be expected.

Fig. 68 shows initial response time histories of the sample helicopter with a fixed tail for several values of tail effectiveness. A marked improvement in the form of the responses is noted as K_t increases. In particular the pitch rate response times are reduced and the normal acceleration becomes concave downward at an earlier time. At a tail effectiveness $K_t = .05$ the initial response is seen to become oscillatory. The pitch rate response time at $K_t = .05$ is about 1.5 seconds and the equilibrium pitch rate is approximately .6 rad/sec. A further decrease of the response time is possible with increased tail effectiveness but the pitch rate would also be decreased and the oscillatory nature of the responses might be objectionable. The time histories shown on Fig. 68 were obtained assuming a fixed tail configuration. If a configuration were assumed with a movable tail linked to the control stick similar time histories would be obtained but of increased amplitude. The addition of the tail linkage would not improve the damping in pitch but would make it possible to obtain higher maximum angular velocities for the same response times.

Long Period Response in Forward Flight:

The modifications of long period response characteristics which result from changes in tail effectiveness are shown on Fig. 69. These time histories were obtained assuming an initial effective tail angle of

$$\left[\alpha_{i0} + (\alpha_i)_t + (V_i)_{TAIL}/2\mu_0\Omega R\right] = .1 \text{ rad.}$$

which gives a positive increase in the speed stability derivative. In many cases smaller effective tail angles would be used and would result in smaller speed stability derivatives and longer oscillation periods.

The long period mode becomes marginally stable at $K_t = .05$. This value of the tail effectiveness corresponds to increasing the quasi-static damping in pitch by 60%, the speed stability 170%, and making the angle of attack stability derivative positive and numerically three times greater than that of the basic helicopter. Assuming that a low aspect ratio tail is used such that the lift curve slope is 2 it would be necessary to have a tail area of over 21 square feet to obtain $K_t = .05$.

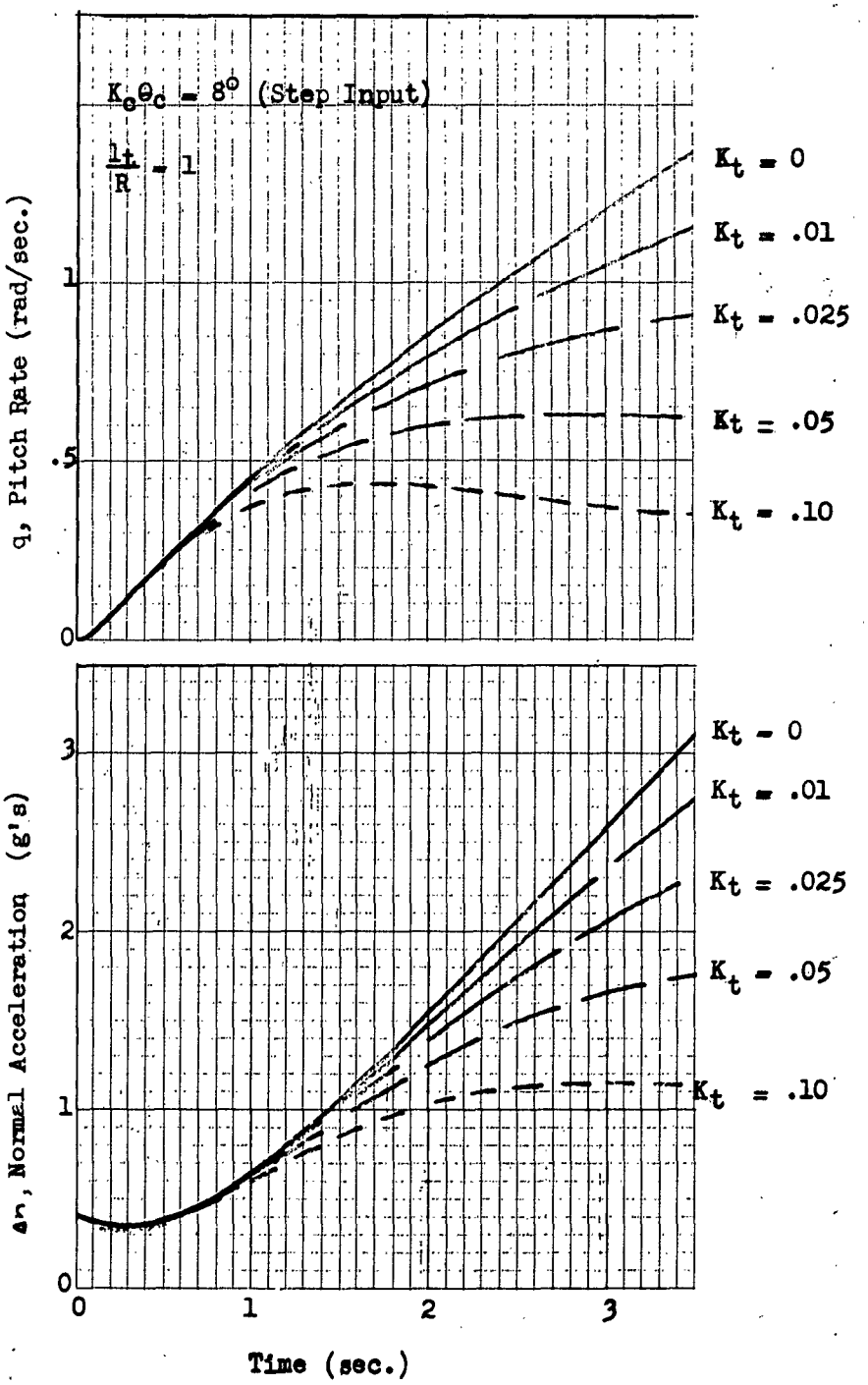

FIG. 68 FIXED HORIZONTAL TAIL. INITIAL RESPONSES TO LONGITUDINAL CYCLIC PITCH STEP; $\mu_o = .2$

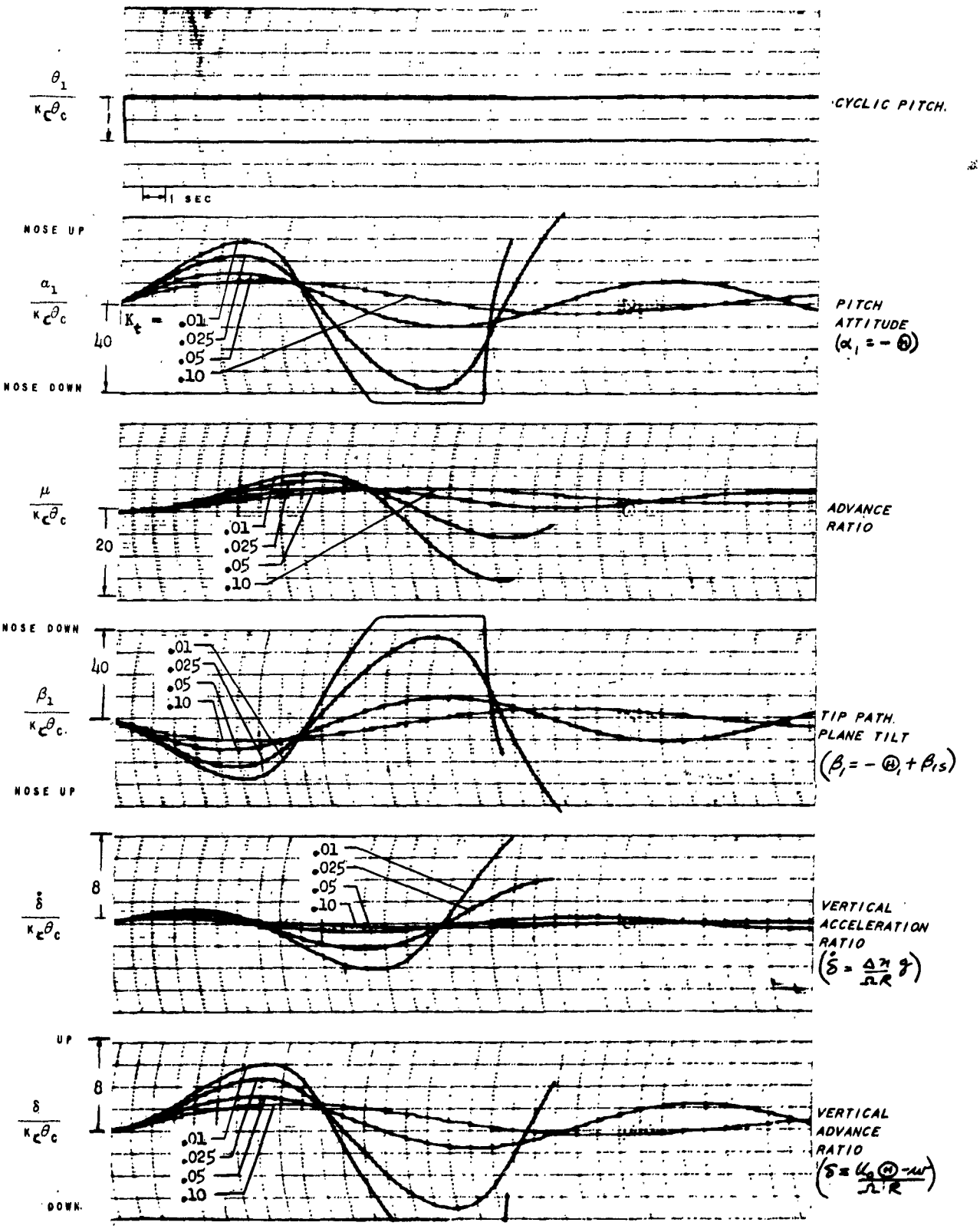

FIG. 69. FIXED HORIZONTAL TAIL ; $\mu_0 = .2$

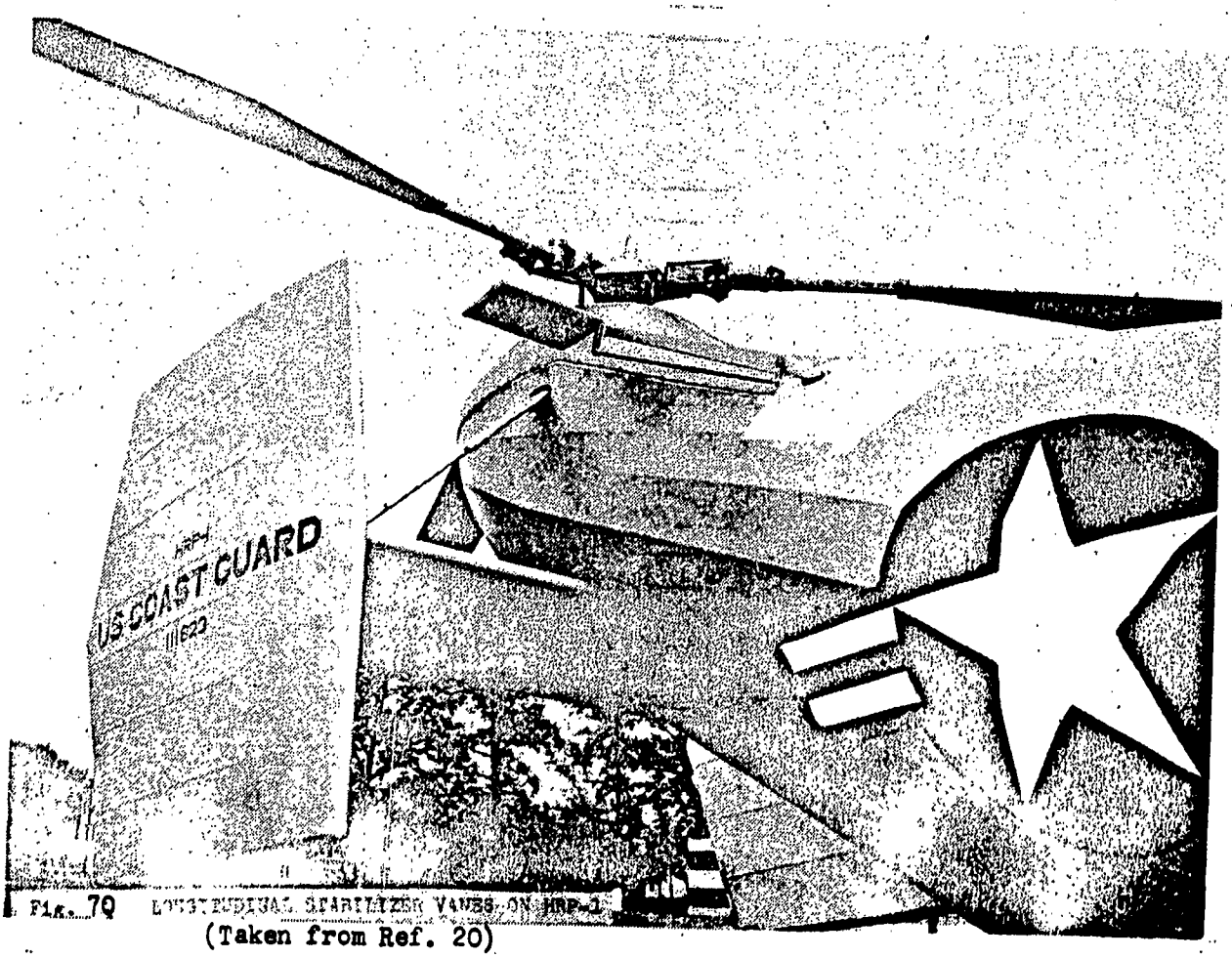

Fig. 79 LONGITUDINAL STABILIZER VANES ON HRP-1
(Taken from Ref. 20)

5.11 Floating Vane Stabilizer (Erickson)

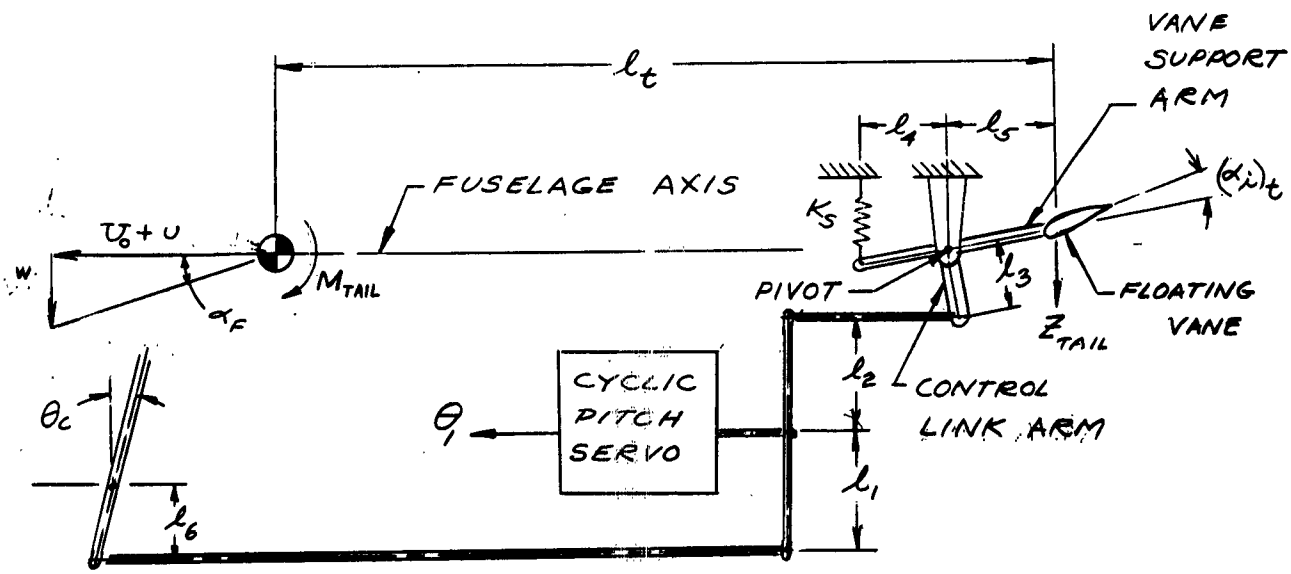

FIG. 71. SCHEMATIC DIAGRAM OF FLOATING TAIL STABILIZER

(a) Representation by Generalized Autopilot Equation

Cyclic pitch due to autopilot feedbacks:

$$l\dot{\theta}_{1A} + \theta_{1A} = K_u U + K_q q + K_w W$$

where

$$K_q = \frac{l_t}{R}\,(R K_w)$$

Cyclic pitch due to pilot's stick motion:

$$\theta_{1D} = K_c \theta_c$$

(b) Description of Mechanism

In 1947 the Coast Guard Rotary Wing Development Unit under the direction of Captain Frank Erickson conducted tests of a Sikorsky HOS-1 helicopter with a set of stabilizing airfoils mounted to the lower swash plate. Since the action of these airfoils on the cyclic pitch was found to have a beneficial effect on stability, further development of floating stabilizer configurations was undertaken. Ref. 20 discusses different devices of this type to provide longitudinal and lateral stability for the stick fixed and stick free cases.

Fig. 70 is a photograph taken from Ref.20 showing an installation in which the floating vane is not mounted on the swash plate but is pivoted on the fuselage. A floating vane of this type was selected for simulation in the present study and Fig.71 shows a schematic diagram of a possible associated control system.

Motion of the floating vane relative to the fuselage causes the cyclic pitch to change and the use of the mixing link shown permits cyclic pitch changes to originate at both the stick and the stabilizer. Obviously the character of the stabilization can be varied by changing the linkage ratios, "tail length", or tail effectiveness. When the device is used in conjunction with a boost system (as shown) the position of the floating stabilizer is not influenced by blade pitching moments and a vane linkage system can be designed which will have a short time lag.

(c) Description of How Device Affects Stability and Control Characteristics

The floating vane stabilizer is only intended to provide stability in forward flight and is ineffective to a first order of approximation in hovering. When the helicopter is disturbed from a trim condition in forward flight the direction and/or magnitude of the airflow at the floating vane is changed resulting in incremental aerodynamic forces on the vane. These force increments cause the vane support arm to rotate until the aerodynamic force moment and restraining spring force moment are in equilibrium. The rotation of the control link arm actuates the cyclic pitch servo which introduces a cyclic pitch tending to restore the helicopter to the trim condition.

The angle of attack change at the vane is primarily due to a change in normal velocity but a pitching velocity also changes the tail airflow angle when the vane is displaced from the c.g. Thus the floating vane provides K_w and K_q feedbacks which effectively change the normal velocity stability and damping in pitch derivatives of the helicopter. Both of these changes are in the direction to increase the maneuver stability of the helicopter. Care must be taken in the selection of a location for the floating tail in order that changes in the rotor downwash in different flight conditions and maneuvers will not have an adverse effect on its operation.

Fig. 71 indicates that the floating airfoil is at an incidence angle relative to its support arm and this incidence angle can be varied in flight. If the angle of attack of the floating tail is not zero in a trim condition there is a cyclic pitch feedback (K_u) when the speed is changed due to the corresponding change in tail load. The speed stability characteristics of the helicopter can be adjusted by changing the floating vane trim angle.

It should be noted that the forces on the floating airfoil are transmitted to the fuselage and produce direct moments about the c.g. like a fixed tail as well as causing cyclic pitch feedbacks. The importance of these direct moments can be minimized if desired by use of a small floating tail.

(d) Effect of Stabilizing Device on the Stability and Control Characteristics of the Sample Helicopter

The computer studies of the response characteristics of the sample helicopter with this device were limited to the case of a small floating vane which would not apply appreciable moments directly to the fuselage. In the present study tail locations at the c.g. ($\frac{l_t}{R} = 0$) and at the aft end of the tail boom ($\frac{l_t}{R} = 1$) were arbitrarily considered although the selection of the tail length for a particular configuration would be influenced by such considerations as the fuselage shape, rotor height, downwash distribution, etc. The speed feedback (K_u) was assumed zero in order to limit the number of parameters although it was realized that more desirable long period responses might be obtained by adjusting this variable.

Initial Response in Forward Flight:

Initial responses of the sample helicopter with a floating vane stabilizer are shown on Figs. 72 and 73 . Time histories are presented on Fig. 72 for a series of normal velocity feedbacks and zero pitching rate feedback (i.e. the vane is assumed located at the c.g.). Both the pitching rate curves and normal acceleration curves are nearly identical with those of the unstabilized helicopter for the first second but level off more rapidly when the normal velocity feedback begins to have an effect. The normal acceleration time histories become concave downward in less than two seconds for feedback constants less than $K_w = -.001$. The pitch rate response time is reduced as K_w becomes more negative but the associated restoring moments cause the short period response to become oscillatory. At a feedback gain of $K_w = -.0051$ the short period oscillations have reached an objectionable magnitude.

The effect of putting the vane at the rear of the fuselage is to introduce a damping in pitch feedback. Comparison of Figs. 72 and 73 shows that the increased damping reduces the response times and amplitudes slightly. It can be seen that a feedback between $K_w = -.00204$ and $-.005$ would give initial pitch rate response characteristics in forward flight which come close to meeting the acceptable requirements of Table 4 (i.e. an equilibrium pitching rate of .5 rad/sec and a response time of one sec.)

Long Period Response:

Fig. 74 shows long period responses obtained with a pure normal velocity feedback which might be obtained with the floating tail located at the c.g. It will be noted that the long period mode becomes more stable as the magnitude of the gain is increased and there is also a large increase in its period of oscillation. At a gain of $K_w = -.0051$ the previously discussed undesirable short period oscillation becomes apparent in the responses. Fig. 75 shows the effect of variation in gain when the floating tail is located at the end of the tail boom. Although there is a small rate feedback in this case the long period responses for the same normal velocity feedbacks are almost the same as shown on Fig. 74. It must be concluded that the damping in pitch obtained with the

floating tail is of secondary importance in the long period responses. Nevertheless, it can be seen the damping in pitch obtained at the aft tail location reduces the high frequency response.

The large increase in the period of long period oscillations is in accordance with the following approximate formula which was discussed in section 2.2.

$$T_o \approx 2\pi \sqrt{\frac{-\bar{M}_g + \frac{W}{g} V \frac{\bar{M}_w}{\bar{Z}_w}}{g \bar{M}_v}}$$

For example using the data in Appendix A to compute the required derivatives for the case,

$$\mu_o = .2$$

$$K_w = -.00204$$

$$K_g = -.05$$

one obtains

$$T_o = 23.2 \text{ sec.}$$

The period of 23.2 seconds computed by this approximate formula is in fair agreement with the 26 sec. period obtained in the computer solution, and it is found that the term involving the normal velocity stability (i.e. $\bar{M}_w$) has an important effect on the period.

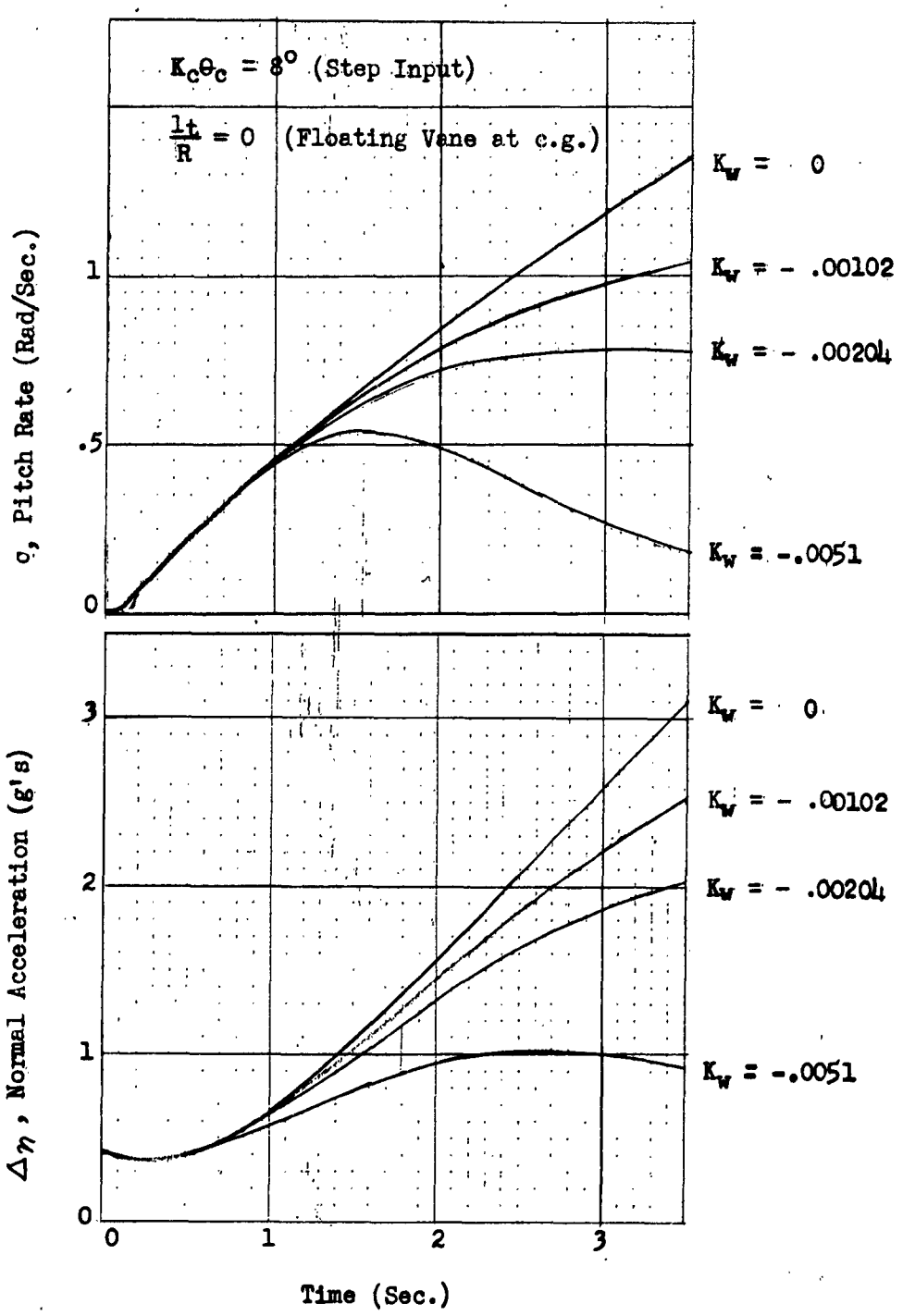

FIG. 72. FLOATING VANE STABILIZER; INITIAL RESPONSES TO LONGITUDINAL CYCLIC STEP INPUTS; $\mu_o = .2$

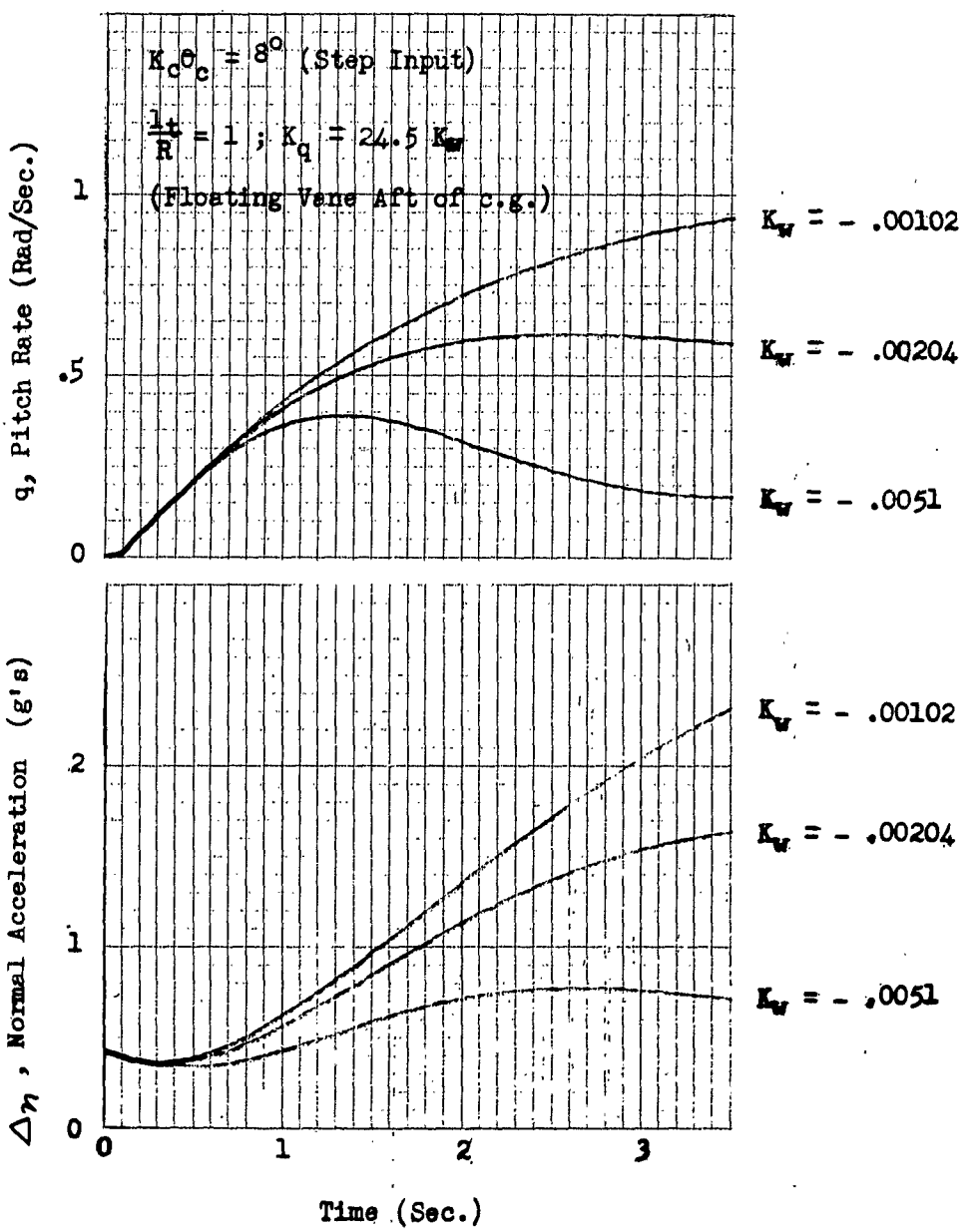

FIG. 73. FLOATING VANE STABILIZER; INITIAL RESPONSES TO LONGITUDINAL CYCLIC STEP INPUTS; $\mu_o = .2$

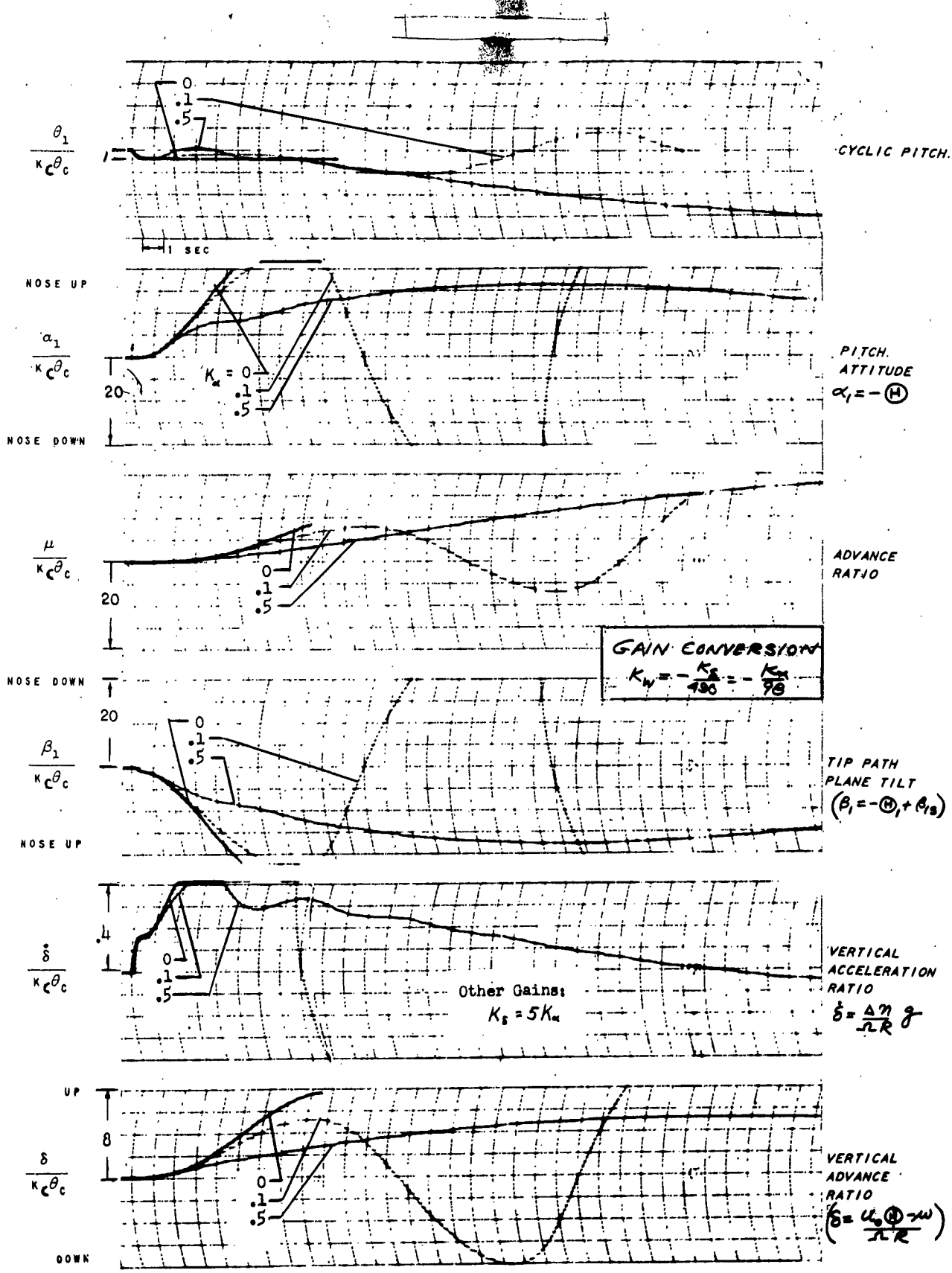

FIG. 74. FLOATING VANE STABILIZER; $\mu_e = .2$; $\frac{h_s}{R} = 0$.

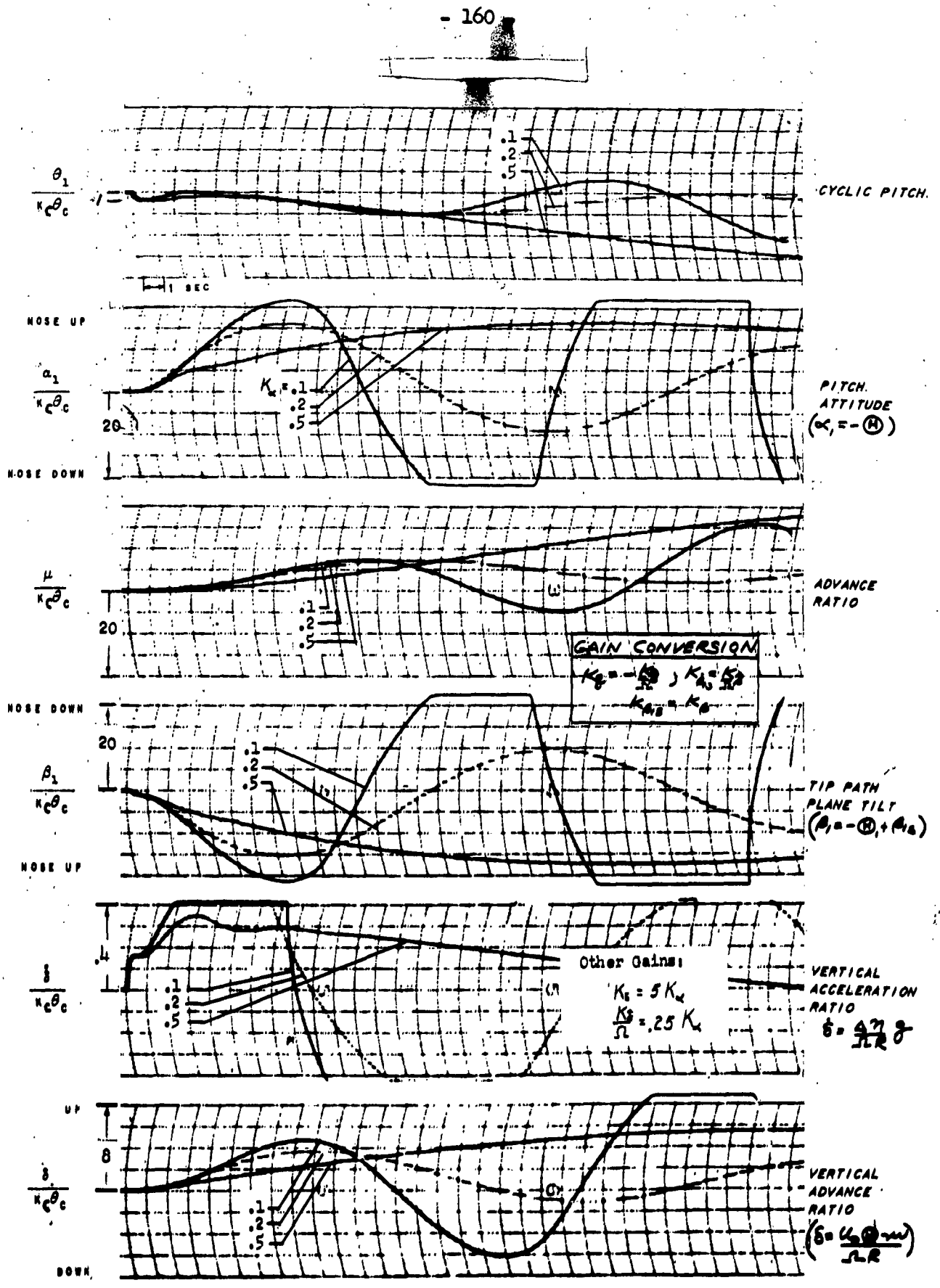

FIG. 75. FLOATING VANE STABILIZER; $\mu_o = .2$; $\frac{h_f}{R} = 1$

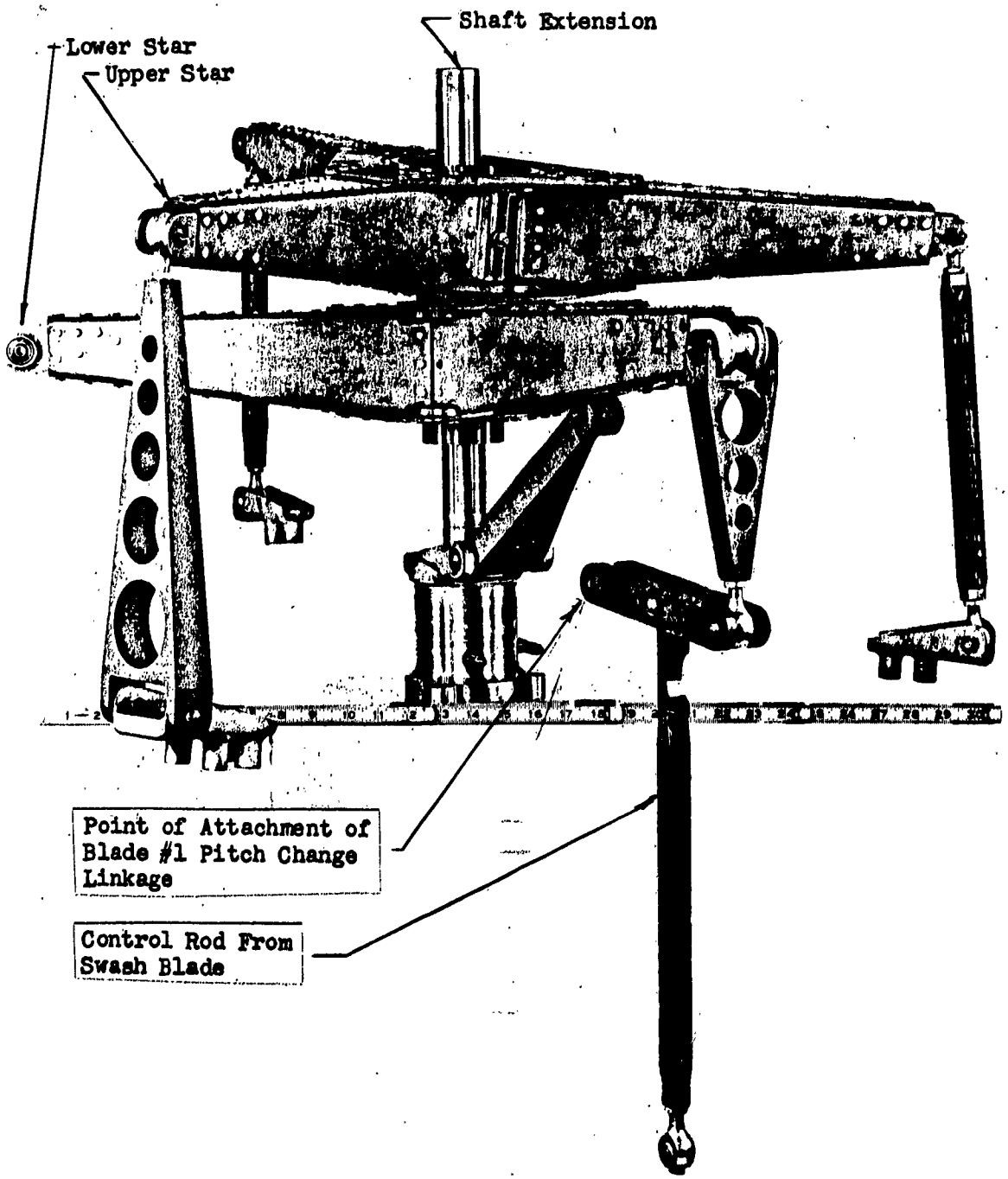

FIG. 76 . PITCH-CONE MECHANISM USED TO MODIFY H-5 HELICOPTER

5.12 Pitch-Cone Coupling Stabilizing Mechanism

(a) Description of Mechanism:

Ref. 21 studied the stability characteristics of a type of rotor in which the collective pitch angle is kinematically coupled with the coning angle. Fig. 76 shows a photograph of a mechanism producing such a coupling which was used to modify an H-5 helicopter in evaluation tests of the coupling effect (Ref. 22). The principle of the pitch-cone coupling can be readily seen from the Fig. 76 mechanism, but a simpler device would be provided on a helicopter originally designed to have pitch-cone coupling.

When this mechanism is used the pitch of each blade depends on the vertical position of the lower star as well as the motion of the control rods from the swash plate. The lower star can slide up and down on the shaft extension but cannot tilt relative to the shaft, and thus its motion can only change collective pitch. The vertical motion of the lower star is determined by the upper star shown in the photograph. The upper star is free to tilt about a swivel bearing mounted on the extension of the housing of the lower star. It is attached to the three blades by links outboard of their flapping hinges. Since the upper star can tilt relative to the shaft, it remains parallel to the tip path plane. A tilt of the tip path plane and upper star will not produce vertical motion of the lower star and change the collective pitch. However, if the blade coning changes, the upper star will move vertically on the shaft and corresponding collective pitch changes result.

There are only two parameters to be adjusted with this device. They are the ratio of changes in collective pitch to change in coning angle and the initial collective pitch angle when the coning is zero. In this report the initial collective pitch angle is chosen in such a manner that the trim conditions at $\mu = .2$ are the same as if there were no pitch cone linkage.

(b) Description of How Device Affects Stability and Control Characteristics:

The primary purpose of using pitch-cone coupling is to obtain a stable variation of pitching moment with fuselage angle of attack and thus to avoid dangerous build ups in pitch attitude and normal acceleration following a cyclic input by the pilot. Another advantage of this device cited in Ref. 21 is the elimination of collective pitch adjustment in going into autorotation.

It can be readily seen that pitch-cone coupling tends to reduce the load factors occurring in pull-up maneuvers. As the load factor increases the rotor coning angle increases which in turn lowers the collective pitch angle. The rotor thrust is reduced by the decrease in collective pitch and a lower load factor is obtained than would exist without pitch-cone coupling. In general it might be said the pitch-cone rotor acts in such a manner as to prevent sudden changes in rotor thrust. This effect minimizes the effects of gusts and helps prevent inadvertent induction of blade stall in high speed flight. Pilot's comment included in Ref. 22 pointed out that the landing and take-off characteristics of the test helicopter were improved by the addition of pitch-cone coupling. This improvement was attributed to the fact that sudden accelerations were avoided when the pilot moved the collective pitch stick.

The previous discussion has emphasized the decrease in load factor in a pullup maneuver when pitch-cone coupling is used. In addition, the decrease in collective pitch influences the angle which the rotor tip path plane makes with respect to the shaft. The aft tilt of a rotor in forward flight is proportional to the collective pitch angle. Consequently, the decrease in collective pitch angle obtained in a pull-up maneuver with a configuration incorporating pitch-cone coupling results in a decrease in the aft rotor tilt due to forward velocity. In other words the rotor tip path plane and thrust are tilted forward tending to restore the helicopter to its original position. In Ref. 23 it was pointed out that an accurate determination of the effects of a pitch-cone linkage on static stability must consider how rotor drag forces affect pitching moments about the c.g. as well as the moment increments due to changes in the magnitude and direction of the thrust vector. Moments from both sources are included in the equations of motion presented in Part A.

The effect of pitch-cone coupling on the speed derivatives of the helicopter is more difficult to see from a physical standpoint than on the normal velocity derivatives. It can be shown that in forward flight the combination of cyclic pitch and differences in velocity on the advancing and retreating blades tends to reduce blade coning. When the speed is increased the coning decreases and the pitch cone linkage in turn increases the collective pitch. A greater aft tilt of the rotor with forward speed results than would otherwise occur due to the greater collective pitch angle. Since this tilt is in a direction opposing the motion it represents increased speed stability.

The addition of the pitch-cone coupling does not influence the gyroscopic action of the rotor and the damping in pitch and roll of the helicopter are unchanged. Since the speed stability is increased and the damping in pitch and roll are unchanged, it would be expected that the addition of a pitch-cone-linkage to a helicopter would raise the frequency of long period dynamic oscillations.

Ref. 21 showed that considerable difference exists between the characteristics of constant speed and constant torque rotors with pitch-cone coupling. Both cases can be analyzed by the equations presented in Part A.

(c) Effect of Pitch-Cone Coupling on the Stability and Control Characteristics of the Sample Helicopter:

The effect of a pitch-cone linkage on the stability and control characteristics of the sample helicopter was investigated using the equations of motion derived in Part A. The computer simulation was done assuming constant rotor rpm, and the equations used included blade longitudinal flapping as a separate degree of freedom. However, for discussion purposes it is more convenient to consider the quasi-static equations in which the blade degree of freedom has been eliminated. Table 8 presents a comparison of the more significant quasi-static derivatives for different pitch-cone ratios.

TABLE 8

tan δ_3 = Pitch-Cone Ratio	Vertical Damping	Vertical Control Force	Speed Stab.	Damping in Pitch	Normal Velocity Stability	Control Power
	$-\bar{Z}'_w$	$-\bar{Z}'_{\theta_1}$	$\bar{M}'_u$	$-\bar{M}'_q$	$-\bar{M}'_w$	$\bar{M}'_{\theta_1}$
	lbs / (ft/sec)	lbs / (rad)	ft lbs / (ft/sec)	ft lbs / (rad/sec)	ft lbs / rad	ft lbs / rad
0	162	15900	44.0	+5094	-37.8	61140
1.5	94	9260	46.1	+5094	- 4.1	57600
2.7	51	4960	47.7	+5094	+17.7	54600

It will be noted that going from a pitch-cone ratio of 0 to 2.7 results in large changes in the vertical damping, vertical force due to control movement, and normal velocity derivatives. Smaller changes are noted in the speed stability and control power while the change in damping in pitch with the blade pitch-cone ratio is found to be negligible.

Fig. 77 compares the responses in a pull-up obtained with the unstabilized helicopter of Appendix A and the same helicopter stabilized with a pitch-cone mechanism of ratio 2.7. The differences in the responses are about what would be expected on the basis of the derivative changes of Table 8 . Referring to the δ trace it can be seen that the initial jump in acceleration has been reduced with pitch-cone feedback although the same swash plate motion is applied by the pilot. The initial acceleration jump with the unstabilized helicopter for an 8° cyclic pitch movement is approximately .4 g. Reduction in the collective pitch angle with the upward coning of the blades reduces the initial acceleration to about .1 g's for the pitch-cone ratio case.

Although the normal velocity and angle of attack stability changes from unstable to stable as the pitch-cone ratio goes from 0 to 2.7, the degree of stability attained is small. The magnitudes of the pitching moments arising from $\bar{M}'_w$ derivative are small compared to those due to control application, damping in pitch, and speed stability. Since the damping in pitch and the speed stability are not greatly changed at a pitch cone ratio of 2.7 it is not surprising that the period of the long period mode is approximately the same for the two curves on Fig. 77 . There is, nevertheless, a significant improvement in the damping of the long period mode oscillations although they remain unstable.

Fig. 78 is for the same case shown on Fig. 77 but an extended time scale and higher recorder gains are used making it more convenient for studying

initial response characteristics. It is found that the typical helicopter stabilized by a pitch-cone feedback of 2.7 is marginal according to the NACA normal acceleration response criteria. The normal acceleration ($\ddot{z}$ trace) just starts to become concave downward at 2 sec. after a step input. It will be noted that the normal acceleration curve at times less than 2 sec. is of a desirable shape without any deceptive dips.

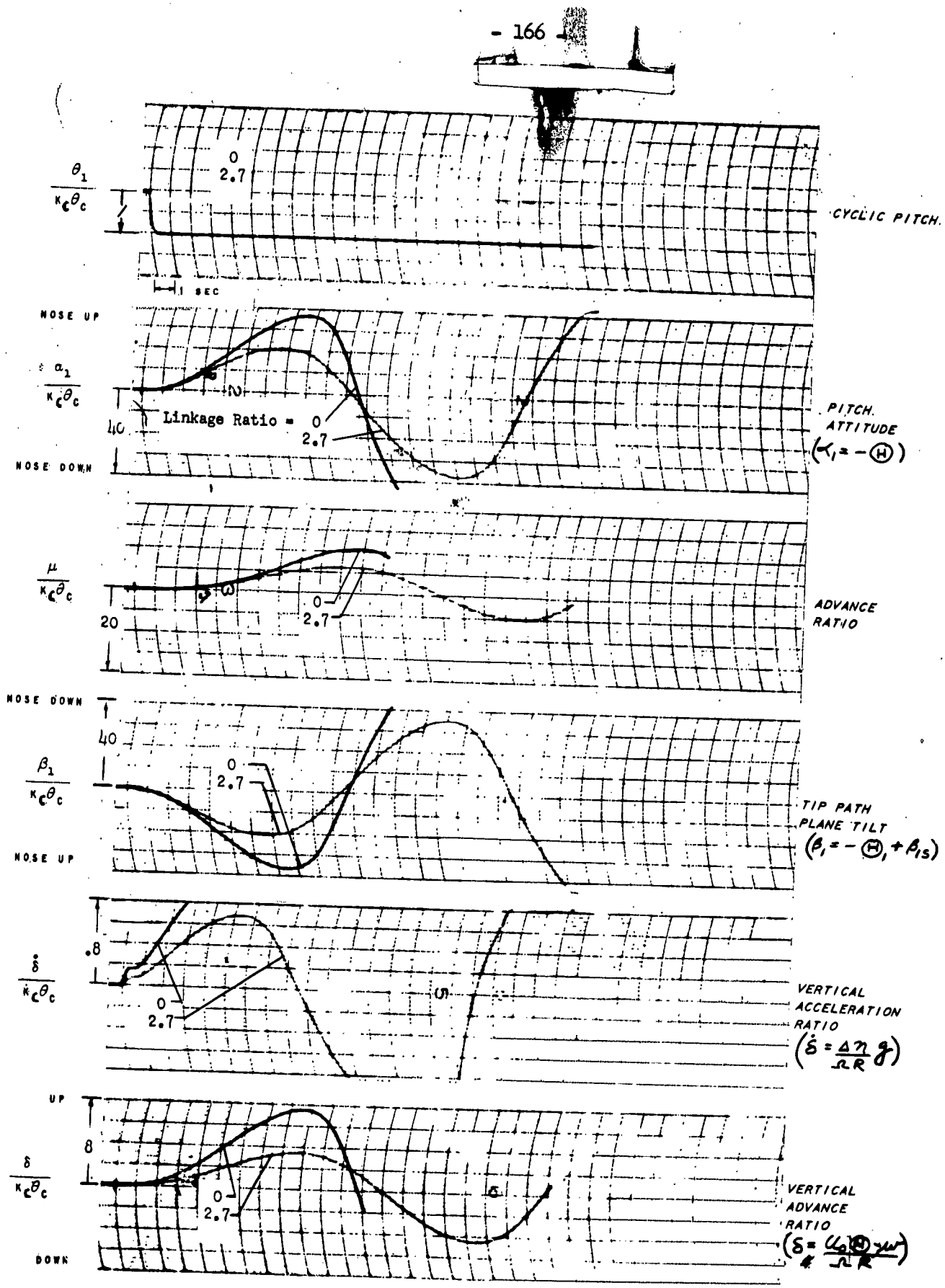

FIG. 77 . PITCH-CONE COUPLING; $\mu_o = .2$

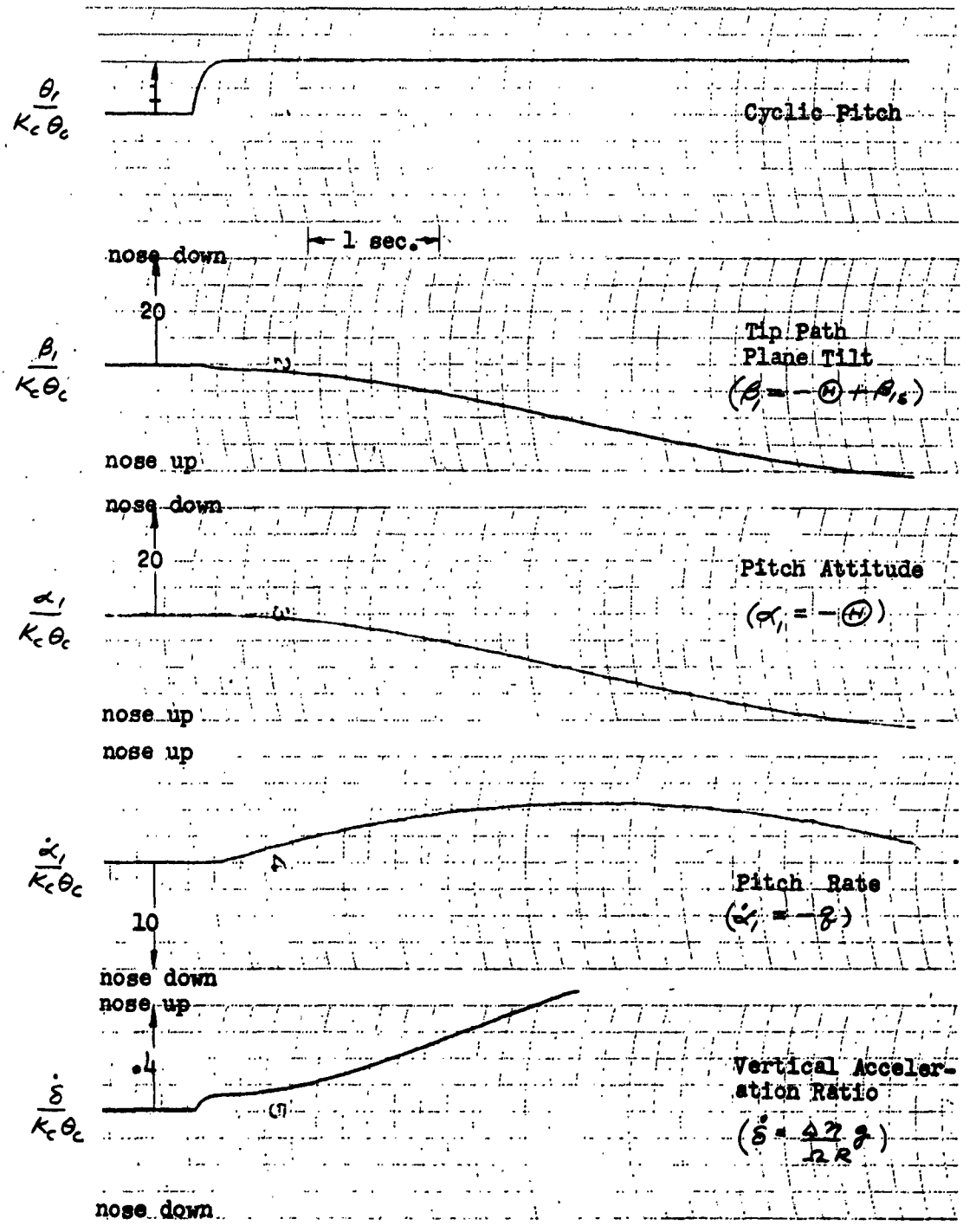

FIG. 78 . PITCH-CONE STABILIZER; INITIAL LONGITUDINAL RESPONSES; $\mu_o = .2$; PITCH-CONE RATIO= 2.7

REFERENCES

1. Amer, K. B. Method for Studying Helicopter Longitudinal Maneuver Stability NACA TN 3022 October 1953

2. Gustafson, F. B., Amer, K. B., Haig, C. R. and Reeder, J. R. Longitudinal Flying Qualities of Several Single-Rotor Helicopters in Forward Flight NACA TN 1983 November 1949

3. Carter Jr., E. S. An Analysis of the Helicopter Transfer Function to Predict Achievable Handling Characteristics of the Stabilized Helicopter Proceedings of the 8th Annual Forum, A. H. S. 16 May 1952

4. Military Specification, Helicopter Flying Qualities, Requirements for MIL-H-8501 5 November 1952

5. Kelley, B. Helicopter Stability with Young's Lifting Rotor Written: March 1945 S.A.E. Journal December 1945

6. Reeder, J. P., and Whitten, J. B. Some Effects of Varying the Damping in Pitch and Roll on the Flying Qualities of a Small Single-Rotor Helicopter NACA TN 2459 Written: 26 September 1951

7. Stuart III, J. The Helicopter Control Rotor Rotating Wing Aircraft Session, 16th Annual Meeting, I.A.S., New York, January 26-29, 1948, I.A.S. Fairchild Preprint Number 110

8. Jacoby, D. R. Experimental and Theoretical Investigation of the Hiller Rotormatic Control - Final Report United Helicopters, Inc. Report 150.5 April 4, 1949

9. Meyers, D. N., Vanderlip, E. G., and Halpert, P. Helicopter Stability and Automatic Control Aeronautical Engineering Review July 1951

10. Kendall, D. E. Automatic Control of Helicopters Tenth Annual Forum of American Helicopter Society, Proceedings of 25 May 1954

11. Sissingh, G. J. Automatic Stabilization of Helicopters Journal of Helicopter Association of G. B., v. 2, No. 3 23 October 1948

12. Bensen, I. B. Biased Cyclic Control for H-5 Helicopter General Electric Report No. R50GL174 1 June 1950

13. Montgomery, G. N. Unique Rotor Affords New Safety Aviation Week 26 January 1948

14. Carpenter, P. J., and Paulnock, R. S. Hovering and Low-Speed Performance and Control Characteristics of an Aerodynamic Servocontrolled Helicopter Rotor System as Determined on the Langley Helicopter Tower NACA TN 2086 May 1950

15. Hohenemser, K. Theory of Helicopter Control in Hovering Flight A.M.C. Translation No. F-TS-1006-RE 1946

16. Hohenemser, K. Contribution to the Problem of Helicopter Stability Fourth Annual Forum of American Helicopter Society, Proceedings of 22 April 1948

17. Miller, R. H. Helicopter Control and Stability in Hovering Flight Journal Aeronautical Sciences, p. 453 August 1948

18. Miller, R. H. A Method for Improving the Inherent Stability and Control Characteristics of Helicopters Journal of the Aeronautical Sciences, Vol. 17, No. 6 June 1950

19. Gustafson, F. B. Desirable Longitudinal Flying Qualities for Helicopters and Means to Achieve Them Aero Engineering Review, p. 27 June 1951

20. Erickson, F. A., and Spratt, G. A New Approach to Helicopter Stability Proceedings of the 9th Annual Forum A.H.S. May 1953

21. Hohenemser, K. A Type of Lifting Rotor with Inherent Stability Journal of Aeronautical Sciences September 1950

22. Vary, V. V., and Eggert, W. W. Cornell Rotor Stabilizer W.A.D.C. Technical Note WCT 53-16 March 1953

23. Miller, R. H. Lecture Notes on the Automatic Stabilization and Control of Helicopters MIT Course No. 16.51 July 1951

NOMENCLATURE

Configuration

r blade station

R blade radius

c blade chord

h distance of hub above c.g.

l_t distance between c.g. and tail

n number of blades

S disc area

S_t horizontal tail area

σ rotor solidity

$(\alpha_i)_t$ angle of tail with respect to fuselage centerline (plus for down tail load)

W gross weight

m mass of helicopter

m_b mass of one blade

γ blade inertia number $= \frac{\rho a c R^4}{I_b}$

$I_b = \int_e^R r^2 dm$, blade moment of inertia

I helicopter pitching inertia about c.g. (assuming rotor mass concentrated at hub)

Aerodynamic

$\left(\frac{\partial C_L}{\partial \alpha}\right)_t$ tail lift curve slope

a rotor blade section lift curve slope

T thrust

L lift

M pitching moment about c.g. (positive aft)

X $X_R + X_F$ = total horizontal force (positive aft)

Z vertical force (positive down)

$\bar{X}$ force along $\bar{x}$ axis

$\bar{Z}$ force along $\bar{z}$ axis

$\lambda_0 = \mu_0 \beta_{10} + \frac{V_{i_0}}{\Omega_0 R}$ = initial inflow relative to tip plane (+ down)

Ω rotor rotational speed

Nomenclature Used in Discussion of Stability Equations

x horizontal displacement of rotor hub from space fixed origin

y lateral displacement of rotor hub from space fixed origin

z vertical displacement of rotor hub from space fixed origin

$\left.\begin{matrix}\bar{x}\\ \bar{z}\end{matrix}\right\}$ axes moving with the helicopter

ψ azimuth angle of blade (measured from aft position)

$\alpha_\psi = \alpha_1 \cos\psi + \alpha_2 \sin\psi$, attitude angle of fuselage relative to horizontal plane

α_1 longitudinal component of attitude angle

α_2 lateral component of attitude angle

α_f angle of attack of fuselage = $-\alpha_1 + \frac{\bar{w}}{\mu} = \frac{w}{U_0}$

(α_{i_t}) angle of tail surface relative to fuselage conterline (plus for down tail load)

$\beta_\psi = \beta_0 + \beta_1 \cos\psi + \beta_2 \sin\psi$, blade flapping at azimuth relative to horizontal plane

β_0 coning angle

β_1 longitudinal tilt of tip path plane relative to horizontal plane

β_2 lateral tilt of tip path plane relative to horizontal plane

$\beta_{s\psi} = \beta_0 + \beta_{1s} \cos\psi + \beta_{2s} \sin\psi$, blade flapping at azimuth relative to shaft

Δn normal acceleration increment

$\theta_\psi = \theta_0 + \theta_1 \sin\psi + \theta_2 \cos\psi$, pitch angle of blade at azimuth ψ relative to shaft

θ_0 collective pitch angle

θ_1 longitudinal cyclic pitch angle

θ_2 lateral cyclic pitch angle

$\bar{\theta}_0$ collective pitch angle controlled directly by pilot's collective pitch stick

Θ attitude angle of fuselage (angle between longitudinal axis of fuselage and horizontal plane) $= -\alpha_1$

V_t induced velocity at rotor

$(V_i)_t$ induced velocity at tail due to rotor

$\mu = \frac{\dot{x}}{\Omega_0 R}$, rotor advance ratio

$\delta = \frac{\dot{z}}{\Omega_0 R}$, rotor vertical advance ratio

u velocity component in horizontal plane relative to blade section

u_p vertical velocity component relative to blade section

u_0 initial velocity along $\bar{x}$ axis

u perturbation velocity along $\bar{x}$ axis

w perturbation velocity along $\bar{z}$ axis

q pitching velocity $(= \dot{\Theta} = -\dot{\alpha}_1)$

a' angle between thrust vector and a line $\perp$ to swash plate

Stability Derivatives

Dimensionless stability derivatives referred to horizontal and vertical axes (origin at hub, blade flapping degree of freedom included):

$$x_\mu, x_{\alpha_1}, x_{\dot{\alpha}_1}, x_\delta, x_{\dot{\beta}_1}, x_{\beta_1}, x_{\theta_1}, z_\mu, z_{\alpha_1}, z_\delta, z_{\dot{\beta}_1}, z_{\beta_1}, z_{\theta_1}$$
$$m_\mu, m_{\alpha_1}, m_{\dot{\alpha}_1}, m_\delta, m_{\dot{\beta}_1}, m_{\beta_1}, m_{\theta_1}, \beta_{\mu_1}, \beta_{\alpha_1}, \beta_{\delta_1}, \beta_{\dot{\beta}_1}, \beta_{\theta_1}$$

Dimensionless quasi-static stability derivatives referred to horizontal and vertical axes (origin at hub, blade flapping degree of freedom eliminated):

$$x'_\mu \;,\; x'_{\alpha_1} \;,\; x'_{\dot{\alpha}_1} \;,\; x'_\delta \;,\; x'_{\dot{\beta}_1} \;,\; x'_{\theta_1} \;,\; z'_\mu \;,\; z'_{\dot{\alpha}_1} \;,\; z'_\delta \;,\; z'_{\dot{\beta}_1} \;,\; z'_{\theta_1}$$

$$m'_\mu \;,\; m'_{\alpha_1} \;,\; m'_{\dot{\alpha}_1} \;,\; m'_\delta \;,\; m'_{\dot{\beta}_1} \;,\; m'_{\theta_1}$$

Dimensional stability derivatives referred to moving axes (origin at c.g., blade flapping degree of freedom included):

$$\bar{X}_u \;,\; \bar{X}_w \;,\; \bar{X}_q \;,\; \bar{X}_{\dot{\beta}_{1s}} \;,\; \bar{X}_{\beta_{1s}} \;,\; \bar{X}_{\theta_1} \;,\; \bar{Z}_u \;,\; \bar{Z}_w \;,\; \bar{Z}_q \;,\; \bar{Z}_{\dot{\beta}_{1s}} \;,\; \bar{Z}_{\beta_{1s}} \;,\; \bar{Z}_{\theta_1}$$

$$\bar{M}_u \;,\; \bar{M}_w \;,\; \bar{M}_q \;,\; \bar{M}_{\dot{\beta}_{1s}} \;,\; \bar{M}_{\beta_{1s}} \;,\; \bar{M}_{\theta_1} \;,\; (\beta_{1s})_u \;,\; (\beta_{1s})_w \;,\; (\beta_{1s})_q \;,\; (\beta_{1s})_{\dot{\beta}_{1s}} \;,\; (\beta_{1s})_{\theta_1}$$

Dimensional quasi-static stability derivatives referred to moving axes (origin at c.g., blade flapping degree of freedom eliminated):

$$\bar{X}'_u \;,\; \bar{X}'_w \;,\; \bar{X}'_q \;,\; \bar{X}'_{\dot{\theta}_1} \;,\; \bar{X}'_{\theta_1} \;,\; \bar{Z}'_u \;,\; \bar{Z}'_w \;,\; \bar{Z}'_q \;,\; \bar{Z}'_{\dot{\theta}_1} \;,\; \bar{Z}'_{\theta_1}$$

$$\bar{M}'_u \;\; \bar{M}'_w \;\; \bar{M}'_q \;\; \bar{M}'_{\dot{\theta}_1} \;\; \bar{M}'_{\theta_1}$$

Dimensional quasi-static derivatives (origin at c.g., flapping and swash plate degrees of freedom eliminated)

$$\bar{\bar{X}}_u \;,\; \bar{\bar{X}}_w \;,\; \bar{\bar{X}}_q \;,\; \bar{\bar{X}}_\Theta \;,\; \bar{\bar{X}}_{\theta_1} \;,\; \bar{\bar{Z}}_u \;,\; \bar{\bar{Z}}_w \;,\; \bar{\bar{Z}}_q \;,\; \bar{\bar{Z}}_\Theta \;,\; \bar{\bar{Z}}_{\theta_1} \;,\; \bar{\bar{M}}_u \;,\; \bar{\bar{M}}_w \;,\; \bar{\bar{M}}_q \;,\; \bar{\bar{M}}_\Theta \;,\; \bar{\bar{M}}_{\theta_1}$$

Autopilot Symbols

Dimensionless generalized autopilot feedback constants referred to horizontal and vertical axes:

$$K_{\dot{\mu}} \;,\; K_\mu \;,\; K_{\dot{\alpha}_1} \;,\; K_{\dot{\alpha}_1} \;,\; K_{\alpha_1} \;,\; K_q \;,\; K_\delta \;,\; K_{\dot{\beta}_1} \;,\; K_{\beta_1}$$

Dimensionless quasi-static generalized autopilot constants referred to horizontal and vertical axes:

$$K'_\mu \;,\; K'_{\dot{\alpha}_1} \;,\; K'_{\alpha_1} \;,\; K'_\delta$$

Dimensional generalized autopilot feedback constants referred to moving axes:

$$K_u \;,\; K_w \;,\; K_q \;,\; K_\Theta \;,\; K_{\dot{\beta}_{1s}} \;,\; K_{\beta_{1s}}$$

Dimensional quasi-static generalized autopilot feedback constants referred to moving axes:

$$K'_u \;,\; K'_w \;,\; K'_q \;,\; K'_\Theta \;,\; K'_{\theta_1}$$

ℓ autopilot time lag

ℓ_L input system time lag

ℓ' quasi-static autopilot time lag

θ_c pilot's control input

$K_c\theta_c$ direct cyclic input due to pilot

$K_L\theta_c$ portion of cyclic input due to pilot which is affected by a time lag

$K_c = K_L + K_D$

$\theta_1 = \theta_{1A} + \theta_{1D} + \theta_{1L}$ = instantaneous longitudinal cyclic pitch at blade

θ_{1A} cyclic pitch due to autopilot feedbacks

θ_{1D} cyclic pitch due to direct pilot input

θ_{1L} cyclic pitch due to portion of pilot's cyclic pitch input which is affected by a time lag

Miscellaneous Symbols

$\Delta = \frac{d}{\Omega dt}$

Ω_o, etc. (subscript o indicates initial value)

$\Delta\mu$, etc. (Δ represents incremental value)

ρ density of air

τ $\frac{\rho a n c R^2}{m}$

g acceleration due to gravity

s d/dt or symbol in Laplace transform

APPENDIX A

Parameters of Sample Helicopter

The sample helicopter selected for stability studies was the Sikorsky XHO3S-2 as modified for stability tests at C.A.L.. Fig. 13 is a three view diagram showing the dimensions of the aircraft. The physical characteristics used to describe the aircraft were in part obtained from manufacturers data and in part based on tests performed at C.A.L..

The tabulated basic trim conditions and stability derivatives were computed in accordance with the theoretical expressions developed in Part A (Case A.1) with the assumptions of no tip losses, constant rotor speed, a lift curve slope of 5.5 per radian, and no tail surfaces.

FIG. 79. MODEL XHO3S-2 HELICOPTER
THREE VIEW DIAGRAM

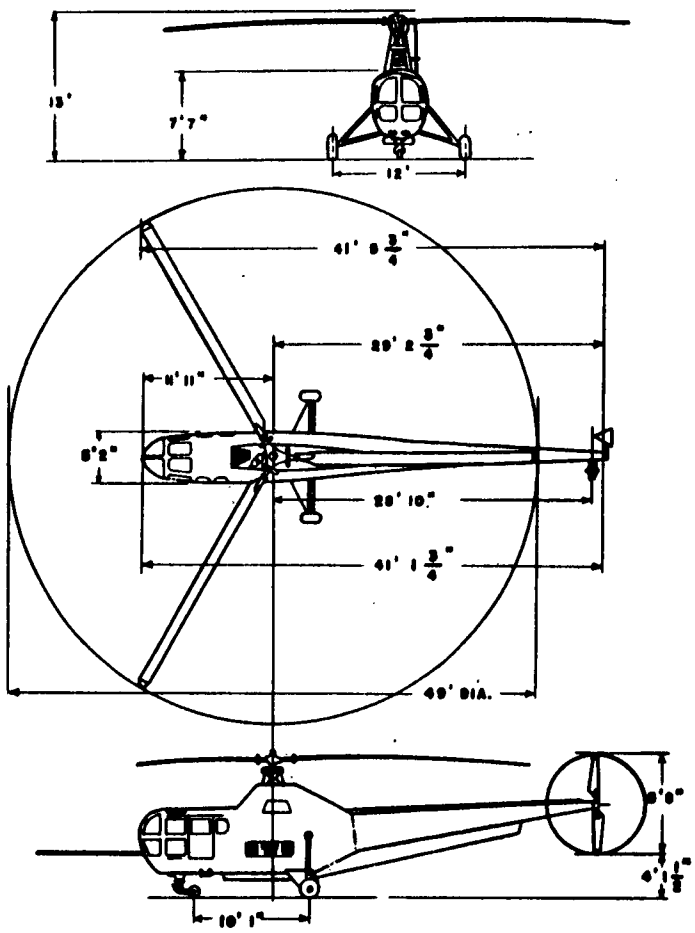

Physical Constants

Main Rotor

Radius, R	24.5 ft.
Blade Chord, c	1.37 ft.
Disc Area, S	1890 ft.^{2}
Rotational speed, Ω	20 rad./sec.
Number of blades, n	3
Mass per blade, m_b	4.2 slugs
Flapping Hinge Offset, e	.75 ft.
Inertia Number, γ	8.82
Distance to blade c.g., d	11.5 ft.
Solidity, σ	.052
Distance from c.g. to rotor hub, h	6.65 ft.

General

Gross Weight, W	5500 lbs.
Pitching Inertia about c.g., I	15000 slugs ft.^{2}
Rolling Inertia about c.g. I_r	3000 slugs ft.^{2}

Aerodynamic Constants

Main Rotor

Lift curve slope, a	5.5/rad.
Profile drag coefficient, C_{D_o}	.012

Fuselage

Equivalent flat plate area, f	18 ft.^{2}
Fuselage moment coefficients	0

Trim Conditions

μ_o	θ_0	λ_o	β_0	β_{1c}	$(\theta_{20}-\beta_{20})$	α_{1c}	θ_{1c}
0	.180	.051	.123	0	0	0	0
.2	.146	.023	.115	.050	.030	.042	-.072

Stability Derivatives for Equations Referred to Horizontal-Vertical Axes (Blade degree of freedom included)

	$\mu_o = 0$	$\mu_o = .2$
X_μ	.000849	.001900
X_δ	0	.002205
X_{α_1}	-.001211	-.000075
X_{β_1}	-.002068	-.002680
$X_{\dot{\beta}_1}$	0	.000036
X_{θ_1}	.001211	.000075
$X_{\dot{\alpha}}$	0	-.000325
Z_μ	UNCOUPLED	.002660
Z_δ		.047500
Z_α		.009500
Z_{β_1}		0
$Z_{\dot{\beta}_1}$		0
Z_{θ_1}		-.009500
m_μ	.001579	.001095
m_δ	0	.000398
m_α	.007484	.008700
m_{β_1}	-.007484	-.008621
$m_{\dot{\beta}_1}$	0	.000066
m_{θ_1}	.002252	.000880

	$\mu_o = 0$	$\mu_o = .2$
$\beta_{1\mu}$	-.378	-.290
$\beta_{1\delta}$	0	.407
$\beta_{1\alpha_1}$	1.000	1.080
$\beta_{1\hat{\beta}}$	-1.814	-1.849
$\beta_{1\theta_1}$	-1.000	-1.080

Quasi-Static Stability Derivatives for Equations Referred to Horizontal-Vertical Axes (Blade degree of freedom eliminated)

	$\mu_o = 0$	$\mu_o = .2$
X'_μ	.001631	.002677
X'_δ	0	.001114
X'_{α_1}	-.003279	-.002970
$X'_{\hat{\alpha}_1}$	.003750	.004991
X'_{θ_1}	.003279	.002970
$X'_{\hat{\theta}_1}$	-.003750	-.004666
Z'_μ		.002660
Z'_δ		.047500
Z'_{α_1}		.009500
$Z'_{\hat{\alpha}}$	UNCOUPLED	0
Z'_{θ_1}		-.0095
$Z'_{\hat{\theta}_1}$		0
m'_μ	.004409	.003595
m'_δ	0	-.003085
m'_{α_1}	0	-.000617
$m'_{\hat{\alpha}_1}$	.013580	.016006
m'_{θ_1}	.009736	.010190
$m'_{\hat{\theta}_1}$	-.013580	-.016006

Stability Derivatives for Equations Referred to Moving Axes (Blade degree of freedom included)

	$\mu_o = 0$	$\mu_o = .2$
$\bar{X}_u$	-2.900	-6.492
$\bar{X}_w$	0	7.532
$\bar{X}_q$	19.25	46.08
$\bar{X}_{\beta_{1s}}$	3462	4486
$\bar{X}_{\dot{\beta}_{1s}}$	0	-3.011
$\bar{X}_{\theta_1}$	-2026	-125.5
$\bar{Z}_u$	UNCOUPLED	9.088
$\bar{Z}_w$		-162.3
$\bar{Z}_q$		-61.75
$\bar{Z}_{\beta_{1s}}$		0
$\bar{Z}_{\dot{\beta}_{1s}}$		0
Z_{θ_1}		-15900
$\bar{M}_u$	19.34	13.41
$\bar{M}_w$	0	-4.872
$\bar{M}_q$	-128.4	-108.81
$\bar{M}_{\beta_{1s}}$	-44904	-51726
$\bar{M}_{\dot{\beta}_{1s}}$	0	19.8
$\bar{M}_{\theta_1}$	13512	5280
$(\beta_{1s})_u$	-.000772	-.000592
$(\beta_{1s})_w$	0	-.000831
$(\beta_{1s})_q$	.09582	.09638
$(\beta_{1s})_{\dot{\beta}_{1s}}$	-.0907	-.0925
$(\beta_{1s})_{\theta_1}$	-1.000	-1.08

Effective and Quasi-Static Stability Derivatives for Equations Referred to Moving Axes (Blade equation eliminated)

	$\mu_o = 0$	$\mu_o = .2$
$\bar{X}'_u$	-5.57	-9.14
$\bar{X}'_w$	0	3.806
$\bar{X}'_q$	350.8	451.1
$\bar{X}'_{\theta_1} = -\bar{X}'_{\beta_{1s}}$	313.7	417.5
$\bar{X}'_{\theta_1}$	-5485	-4970
$\bar{Z}'_u$		9.08
$\bar{Z}'_w$		-162.3
$\bar{Z}'_q$		-60.4
$\bar{Z}'_{\dot{\theta}_1} = -\bar{Z}'_{\dot{\beta}_{1s}}$	UNCOUPLED	0
$\bar{Z}'_{\theta_1}$		-15900
$\bar{M}'_u$	54.0	44.02
$\bar{M}'_w$	0	37.80
$\bar{M}'_q$	-4433	-5094.
$\bar{M}'_{\dot{\theta}_1} = -\bar{M}'_{\dot{\beta}_{1s}}$	-4074	-4800
$\bar{M}'_{\theta_1}$	58416	61140

Equivalent Helicopter Derivatives

		$\mu_o = 0$	$\mu_o = .2$
$\bar{\bar{X}}_u$	$\bar{\bar{X}}_u' + \bar{\bar{X}}_{\theta_1}' K_u'$	$-5.57 - 5485 K_u'$	$-9.14 \quad -4970 K_u'$
$\bar{\bar{X}}_w$	$\bar{\bar{X}}_w' + \bar{\bar{X}}_{\theta_1}' K_w'$	0	$3.806 \quad -4970 K_w'$
$\bar{\bar{X}}_q$	$\bar{\bar{X}}_q' + \bar{\bar{X}}_{\theta_1}' K_q'$	$350.8 - 5485 K_q'$	$451.1 \quad -4970 K_q'$
$\bar{\bar{X}}_{\textcircled{M}}$	$\bar{\bar{X}}_{\theta_1}' K_{\textcircled{M}}'$	$-5485 K_{\textcircled{M}}'$	$-4970 K_{\textcircled{M}}'$
$\bar{\bar{X}}_{\theta_1}$		$-5485/(1 + K_{\beta_{1s}})$	$-4970/(1+1.08 K_{\beta_{1s}})$
$\bar{\bar{Z}}_u$	$\bar{\bar{Z}}_u' + \bar{\bar{Z}}_{\theta_1}' K_u'$		$9.08 \quad -15900 K_u'$
$\bar{\bar{Z}}_w$	$\bar{\bar{Z}}_w' + \bar{\bar{Z}}_{\theta_1}' K_w'$		$-162.3 \quad -15900 K_w'$
$\bar{\bar{Z}}_q$	$\bar{\bar{Z}}_q' + \bar{\bar{Z}}_{\theta_1}' K_q'$	UNCOUPLED	$-60.4 \quad -15900 K_q'$
$\bar{\bar{Z}}_{\textcircled{M}}$	$\bar{\bar{Z}}_{\theta_1}' K_{\textcircled{M}}'$		$-15900 K_{\textcircled{M}}'$
$\bar{\bar{Z}}_{\theta_1}$			$-15900/(1+1.08 K_{\beta_{1s}})$
$\bar{M}_u$	$\bar{M}_u' + \bar{M}_{\theta_1}' K_u'$	$54 + 58416 K_u'$	$44.02 + 61140 K_u'$
$\bar{M}_w$	$\bar{M}_w' + \bar{M}_{\theta_1}' K_w'$	0	$37.80 + 61140 K_w'$
$\bar{M}_q$	$\bar{M}_q' + \bar{M}_{\theta_1}' K_q'$	$-4433 + 58416 K_q'$	$-5094 + 61140 K_q'$
$\bar{M}_{\textcircled{M}}$	$\bar{M}_{\theta_1}' K_{\textcircled{M}}'$	$58416 K_{\textcircled{M}}'$	$61140 K_{\textcircled{M}}'$
$\bar{M}_{\theta_1}$		$58416/(1 + K_{\beta_{1s}})$	$61140/(1 + 1.08 K_{\beta_{1s}})$
$\bar{I}$	$I - \bar{M}_{\dot{\theta}_1}' K_q$	$15000 + 4074 K_q'$	$15000 + 4800 K_q'$